Development of an Adverse Outcome Pathway for 5α-reductase Inhibition: Environmental Implications for Endocrine Disruption

Dissertation

zur Erlangung des Grades

des Doktors der Naturwissenschaften

der Naturwissenschaftlich-Technischen Fakultäten

der Universität des Saarlandes

von

Hyunki Cho

Saarbrücken

2025

Tag des Kolloquiums:	24.09.2025
Dekan:	Prof. Dr.-Ing. Dirk Bähre
Berichterstatter:	Prof. Dr. Markus R. Meyer
	Prof. Dr. Alexandra K. Kiemer
Akad. Mitglied:	Dr. Yuliya Silina
Vorsitz:	Prof. Dr. Marc Schneider

Die vorliegende Arbeit wurde von August 2020 bis March 2025 unter Anleitung von Herrn Prof. Dr. Markus R. Meyer am KIST Europe Forschungsgesellschaft mbH angefertigt.

Summary

With the rising use of hair loss treatments, concerns have increased about environmental exposure to 5α-reductase (SRD5A) inhibitors such as finasteride and dutasteride, classified as endocrine-disrupting chemicals (EDCs). To assess their risks, this study applied the Adverse Outcome Pathway (AOP) framework in vertebrate and invertebrate models. A sensitive LC-MS/MS assay was developed to evaluate SRD5A inhibition in human and fish cell lines, providing species-specific insights. In zebrafish embryos, inhibition caused hormonal disruptions, including reductions in dihydrotestosterone (DHT) and 17β-estradiol, underscoring DHT's role in estrogenic signaling. In H295R cells, GC-MS/MS-based profiling of 17 steroid hormones revealed systemic disruptions across progestins, glucocorticoids, mineralocorticoids, and androgens, extending beyond OECD TG 456 assays. To enhance ecological relevance, Daphnia magna was studied; genomic data suggested an SRD5A-like enzyme involved in ecdysteroidogenesis. Finasteride exposure impaired reproduction, affected ecdysteroid-related gene expression, and altered lipid metabolism. These findings connect molecular initiating events to adverse outcomes across species, advancing robust AOPs for regulatory toxicology. This work highlights the systemic and environmental risks of SRD5A inhibitors and supports sustainable chemical management to protect ecosystems and human health.

Zusammenfassung

Mit der zunehmenden Nutzung von Haarwuchsmitteln wächst die Sorge über Umweltbelastungen durch 5α-Reduktase-(SRD5A)-Inhibitoren wie Finasterid und Dutasterid, die als endokrine Disruptoren (EDCs) gelten. Zur Risikobewertung wurde das Adverse Outcome Pathway (AOP)-Konzept in Wirbeltier- und Wirbellosenmodellen angewendet. Ein sensitiver LC-MS/MS-Assay ermöglichte die Analyse der SRD5A-Hemmung in menschlichen und Fischzelllinien und lieferte artspezifische Einblicke. In Zebrafischembryonen führte die Hemmung zu Hormonstörungen, darunter verringerte Spiegel von Dihydrotestosteron (DHT) und 17β-Östradiol, was die Rolle von DHT in östrogener Signalgebung verdeutlichte. In H295R-Zellen zeigte das GC-MS/MS-Profiling von 17 Steroidhormonen systemische Störungen über Gestagene, Glukokortikoide, Mineralokortikoide und Androgene hinaus und erweiterte damit bestehende OECD-TG-456-Ansätze. Zur ökologischen Relevanz wurde Daphnia magna untersucht; genomische Daten deuten auf ein SRD5A-ähnliches Enzym in der Ecdysteroidogenese hin. Eine Exposition gegenüber Finasterid beeinträchtigte die Reproduktion, veränderte den Lipidstoffwechsel und beeinflusste ecdysteroidassoziierte Genexpression. Die Ergebnisse verknüpfen molekulare Initiierungsereignisse mit nachteiligen Wirkungen über Spezies hinweg und fördern robuste AOPs für die regulatorische Toxikologie. Damit werden die systemischen und ökologischen Risiken von SRD5A-Inhibitoren hervorgehoben und Grundlagen für nachhaltiges Chemikalienmanagement geschaffen.

Graphical Abstract

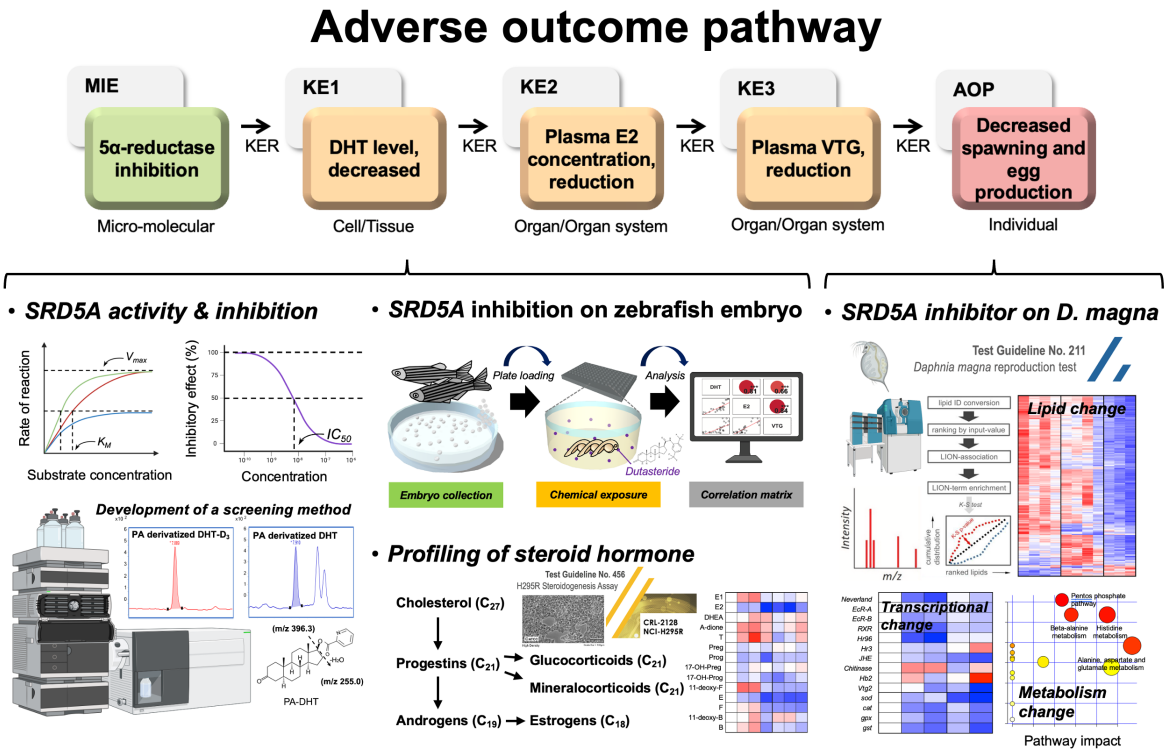

Acknowledgments

I sincerely appreciate Prof. Dr. Markus R. Meyer, Prof. Dr. Alexandra K. Kiemer, and Dr. Chang Seon Ryu for their invaluable support and scientific discussions during my work on this thesis. I would also like to thank Dr. Young Jun Kim, Dr. Youngsam Kim, Dr. Indong Jun, and Dr. Juyong Yoon for their contributions, discussions, and advice on the published papers.

I am grateful to Dr. Chang Gyun Park, Dr. Younghun Seo, Mr. Seoung Gun Bang, Dr. Matthias Altmeyer, Mr. Carsten Brill, Dr. Baeckkyoung Sung, Mr. Karim Md Adnan, and Dr. Soochoel Choi for their assistance in performing experiments and for their valuable advice.

Lastly, I would like to thank all KIST members and my university for their support and insightful discussions.

Vorveröffentlichungen aus dieser Dissertation

Teile dieser Arbeit wurden vorab mit Genehmigung der Naturwissenschaftlich-Technischen Fakultäten, vertreten durch den Mentor der Arbeit, in folgenden Beiträgen veröffentlicht oder sind derzeit in Vorbereitung der Veröffentlichung.

Publications

Bereits veröffentlichte Publikationen (mit offenem Zugang):

1. **Cho, H.**; Jun, I.; Adnan, K.M.; Park, C.G.; Lee, S.A.; Yoon, J.; Ryu, C.S.; Kim, Y.J. Effects of 5α-reductase inhibition by dutasteride on reproductive gene expression and hormonal responses in zebrafish embryos. *Comp. Biochem. Physiol. C Toxicol. Pharmacol.* **2024**, 287, 110048. doi:10.1016/j.cbpc.2024.110048.
2. **Cho, H.**; Sung, S.E.; Jang, G.; Esterhuizen, M.; Ryu, C.S.; Kim, Y.; Kim, Y.J. Adverse effects of the 5-alpha-reductase inhibitor finasteride on Daphnia magna: Endocrine system and lipid metabolism disruption. *Ecotoxicol. Environ. Saf.* **2024**, 281, 116606. doi:10.1016/j.ecoenv.2024.116606.
3. Kim, D.[†]; **Cho, H.**[†]; Eggers, R.; Kim, S.K.; Ryu, C.S.; Kim, Y.J. Development of a Liquid Chromatography/Mass Spectrometry-Based Inhibition Assay for the Screening of Steroid 5-α Reductase in Human and Fish Cell Lines. *Molecules* **2021**, 26, doi:10.3390/molecules26040893. ([†], These authors equally contributed to this work)

Publikationen in Vorbereitung der Veröffentlichung:

1. Cho, H.; Jun, I.; Kim, Y.J.; Ryu, C.S. Impact of 5α-reductase inhibitors on steroidogenesis: A GC-MS/MS-Based profiling approach in H295R Cells (A case of study with the SRD5A inhibition and steroid hormone profiling).

Weitere Publikationen, die nicht Teil dieser Arbeit sind:

1. **Cho, H.K.**; Park, C.G.; Lim, H.B. Construction of a Synergy Combination Model for Turmeric (Curcuma longa L.) and Black Pepper (Piper nigrum L.) Extracts: Enhanced Anticancer Activity against A549 and NCI-H292 Human Lung Cancer Cells. *Curr. Issues Mol. Biol.* **2024**, 46, 5551-5560. doi:10.3390/cimb46060332.
2. Park, C.G.; Adnan, K.M.; **Cho, H.**; Ryu, C.S.; Yoon, J.; Kim, Y.J. A combined in vitro-in silico method for assessing the androgenic activities of bisphenol A and its analogues. *Toxicol. In Vitro* **2024**, 98, 105838. doi:10.1016/j.tiv.2024.105838.
3. Lee, S.-A.; Ryu, C.S.; Park, C.G.; **Cho, H.**; Jun, I.; Park, C.-B.; Esterhuizen, M.; Kim, Y.J. Investigating the endocrine disruption effects of four disinfection byproducts on zebrafish estrogen receptor-α. *Front. mar. sci.* **2023**, 10, doi:10.3389/fmars.2023.1306130.

4. Jun, I. [†]; **Cho, H.** [†]; Amos, S.E.; Choi, Y.; Choi, Y.S.; Ryu, C.S.; Lee, S.A.; Han, D.W.; Han, H.S.; Yang, J.H.; et al. Thyroid-Friendly Soft Materials as 3D Cell Culture Tool for Stimulating Thyroid Cell Function. *Small* **2023**, 19, e2300236. doi:10.1002/smll.202300236. ([†], These authors equally contributed to this work)

5. **Cho, H.**; Kim, Y.J.; Chae, J.W.; Meyer, M.R.; Kim, S.K.; Ryu, C.S. In vitro metabolic characterization of the SARS-CoV-2 papain-like protease inhibitors GRL0617 and HY-17542. *Front. Pharmacol.* **2023**, 14, 1067408. doi:10.3389/fphar.2023.1067408.

6. **Cho, H.**; Ryu, C.S.; Lee, S.A.; Adeli, Z.; Meupea, B.T.; Kim, Y.; Kim, Y.J. Endocrine-disrupting potential and toxicological effect of para-phenylphenol on Daphnia magna. *Ecotoxicol. Environ. Saf.* **2022**, 243, 113965. doi:10.1016/j.ecoenv.2022.113965.

7. **Cho, H.**; Seol, Y.; Baik, S.; Sung, B.; Ryu, C.S.; Kim, Y.J. Mono(2-ethylhexyl) phthalate modulates lipid accumulation and reproductive signaling in Daphnia magna. *Environ. Sci. Pollut. Res.* 2022, 29, 55639-55650. doi:10.1007/s11356-022-19701-1.

8. **Cho, H.**; Choi, I.; Kim, S.K.; Baik, S.; Ryu, C.S. LC-MS-based assay of granisetron 7-hydroxylation activity for the evaluation of CYP1A1 induction from diesel particulate matter-exposed hepatic and respiratory cell lines. *Food Chem. Toxicol*. **2022**, 161, 112829. doi:10.1016/j.fct.2022.112829.

Conference Contributions (Posters and Oral Presentations)

1. Poster presentation, **Cho, H.**, Ryu, C.S., Kang, M.K. Granisetron 7-hydroxylation assay for the specific hepatic and extrahepatic CYP1A1 activity measurement. *The 25th International Symposium on Microsomes and Drug Oxidations (MDO)*, Prague, 2024.

2. Poster presentation, **Cho, H.**, Park, C.G., Ryu, C.S., Kim, Y.J. *In vitro* assessment of thyroid peroxidase and thyroid hormone receptor-disrupting activities. The 14th BioDectors conference 2024, Amsterdam, 2024.

3. Poster presentation, **Cho, H.**, Ryu, C.S., Lee, S.A., Kim, Y., Kim, Y.J. Reproductive toxicity study of para-phenylphenol on Daphnia Magna*, EKC2022,* Marseille, 2022.

4. Poster presentation, Hirn-Derksen, B., Ryu C.S., **Cho, H.**, Kim, J.Y., Hempel, G. Development of a dynamic pharmacokinetic model to predict disposition of Dutasteride in zebrafish embryos. *Population Approach Group Europe 2022 (PAGE)*, Ljubljana, 2022.

5. Poster presentation, Ryu, C.S., **Cho, H.**, Seol, Y., Chae, J.W., Kim, W.K., Baek, S.H., Jung, Y.S., Kim, S.K., Kim, Y.J. Evaluation of mono(2-ethylhexyl) phthalate metabolites, lipid accumulation and reproductive signaling in *daphnia magna. The 37th Annual meeting of KSOT/KEMS*, Gangneung, 2021.

6. Oral presentation, Ryu, C.S., **Cho, H.**. *In vitro* metabolic characterization of GRL0617 and HY-17542, SARS-CoV-2. *EKC2021*, Essen, 2021.

7. Oral presentation, **Cho, H.**, Kim, S.K., Baik, S., Ryu, C.S., LC-MS-based assay of granisetron 7-hydroxylation activity for the evaluation of CYP1A1 induction from diesel particulate matter-exposed hepatic and respiratory cell lines. *EKC2021*, Essen, 2021.

8. Poster presentation, Moon, H.K., **Cho, H.**, Ryu, C.S., Chae, J.W. Development of physiologically based pharmacokinetcs model of bisphenol S in zebrafish. *2021 Fall International Convention of PSK*, Jeonju, 2021.

Table of Contents

Chapter 1. Introduction

1.1 Chemical risk assessment and regulation

1.1.1 Introduction to chemical risk and production growth

With the growth of industrial activities, the increasing production of chemical substances has brought significant benefits to modern life. However, the accompanying challenges and adverse effects cannot be overlooked. Recent analyses of global inventories estimate that over 350,000 chemicals have been registered for production and application-a figure significantly higher than previously reported [1]. The identities of many chemicals remain ambiguous, with over 50,000 ambiguously described and more than 70,000 withheld due to confidentiality restrictions. This lack of transparency leaves the potential risks of many chemicals unassessed [2; 1].

1.1.2 Understanding endocrine-disrupting chemicals (EDCs)

Over the past two decades, endocrine-disrupting chemicals (EDCs) have drawn considerable attention from toxicologists, endocrinologists, and public health professionals. These substances interfere with the endocrine system by disrupting the production, secretion, transport, binding, or elimination of natural hormones [3]. EDCs act through mechanisms such as mimicking natural hormones (e.g., bisphenol A's estrogenic activity) [4-6], antagonizing hormonal effects (e.g., atrazine's inhibition of androgen signaling) [7], or altering hormone metabolism [8]. Their molecular diversity-spanning industrial chemicals, pharmaceuticals, and natural compounds-enables simultaneous disruption of multiple endocrine pathways [5]. This is particularly concerning during critical developmental windows (e.g., prenatal and early postnatal stages), where precise hormonal signaling is essential for growth and differentiation [9].

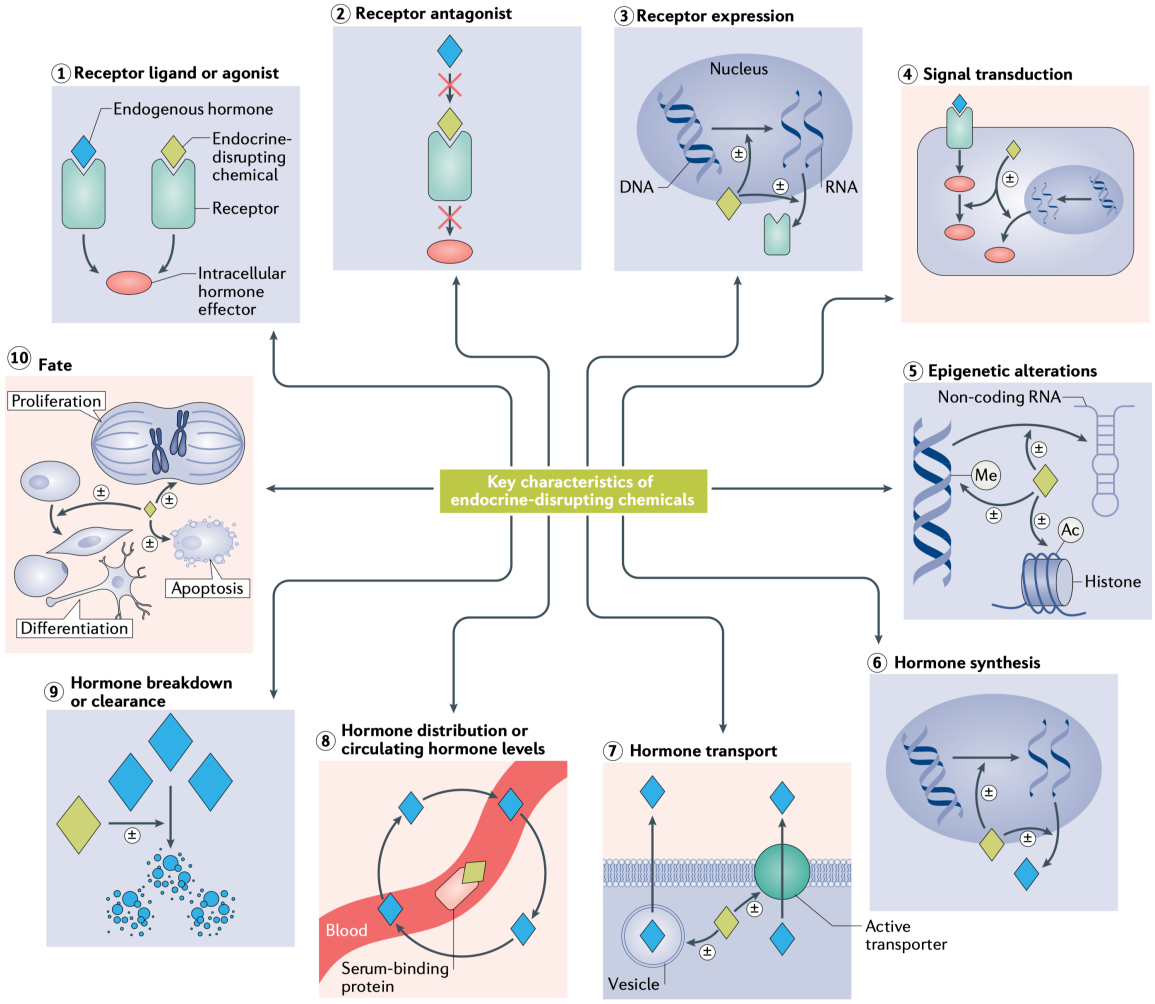

Figure 1.1. Defining attributes of endocrine-disrupting chemicals (EDCs). Arrows highlight the ten distinct key characteristics of endocrine-disrupting chemicals (EDCs), with the ± symbol representing the ability of the EDCs to either enhance or inhibit processes and outcomes. The figure was adapted from La Merrill et al. (2020).

1.1.3 Pathways and ecological impact of EDCs

EDCs enter the environment through industrial effluents, agricultural runoff, and domestic wastewater (Figure 1.2) [10; 2]. Many wastewater treatment plants (WWTPs) fail to completely remove these compounds, allowing them to persist and accumulate in aquatic systems [11]. While some chemicals degrade rapidly, others remain stable, bioaccumulating and exerting toxic effects on aquatic organisms [10]. In vertebrates like zebrafish (*Danio rerio*), EDCs disrupt endocrine processes critical for reproduction and development. For example, synthetic estrogens (e.g., 17α-ethinylestradiol) induce vitellogenin (VTG) production in male zebrafish, causing feminization and impaired reproduction [12; 13]. Similarly, androgen disruptors like flutamide suppress male-specific traits and alter gonadal development [14; 15]. In invertebrates like *Daphnia magna* (*D. magna*), EDCs disrupt molting and reproductive cycles regulated by hormone signaling, leading to altered brood size, molting frequency, and

offspring sex ratios [16-19]. These disruptions threaten individual fitness and population stability, highlighting the risks EDCs pose to aquatic biodiversity and ecosystem health [20].

Figure 1.2. Emerging contaminants, which are newly identified synthetic or naturally occurring chemicals or biological agents, enter the environment through various pathways, including industrial discharges, agricultural runoff, and wastewater effluents. Once released, these contaminants undergo transformation processes such as degradation, volatilization, and bioaccumulation, which influence their distribution across environmental compartments, including aquatic systems, soils, and the atmosphere. These processes ultimately determine their persistence and impact on ecosystems. The figure was adapted from Wang et al. (2024).

1.1.4 Regulatory frameworks for chemical risk assessment

To mitigate the risks, regulatory frameworks such as the European Union's REACH (Registration, Evaluation, Authorization, and Restriction of Chemicals) (https://environment.ec.europa.eu/topics-/chemicals/reach-regulation_en) have been established. These frameworks aim to ensure safe chemical production, use, and disposal while minimizing environmental impact. Comprehensive risk assessments integrate hazard identification, exposure assessment, and risk characterization to evaluate chemical effects on ecosystems and human populations [22; 23]. However, the complexity of environmental exposures and the vast number of uncharacterized chemicals necessitate continuous advancements in regulatory strategies.

1.2 Adverse outcome pathway (AOP) framework

1.2.1 Overview of the AOP concept

The adverse outcome pathway (AOP) framework has emerged as a critical tool for advancing chemical risk assessment [24; 25]. An AOP systematically links a molecular initiating event (MIE)-the initial interaction of a chemical with a biological target-to an adverse outcome (AO) observable at the individual or population level (Figure 1.3). By organizing biological information into interconnected key events (KEs), AOPs integrate diverse data (e.g., molecular assays, organism-level studies) into a transparent, mechanistic framework [26].

AOPs are chemically agnostic, focusing on biological pathways rather than specific chemicals, which makes them broadly applicable across stressors and species [24; 27]. This versatility makes them powerful tools in environmental and regulatory toxicology For instance, an AOP outlining hormone receptor disruption leading to reproductive failure can apply to diverse endocrine-disrupting chemicals (EDCs) [28; 29]. This flexibility enhances the utility of AOPs in regulatory toxicology by enabling predictive, efficient, and mechanism-based chemical evaluations, ultimately supporting the development of targeted testing strategies.

The development of an AOP involves comprehensive integration of knowledge from multiple sources, including *in vivo* experiments, *in vitro* assays, and computational modeling [30]. This integrative approach ensures that each AOP component is supported by robust and reproducible evidence [24]. Transparency is central to AOP development, with all supporting data meticulously documented in platforms such as the AOP-Wiki (Available from http://aopwiki.org), a global repository for collaboratively developed AOPs [31; 25]. The open-access nature of the AOP-Wiki fosters international collaboration, enabling researchers to continuously refine AOPs. This iterative process enhances their scientific credibility and regulatory relevance, ensuring adaptability to advances in toxicology and evolving regulatory requirements. Moreover, the standardized format of AOPs promotes their adoption in chemical safety evaluations, bridging data gaps and guiding the development of mechanism-based testing strategies.

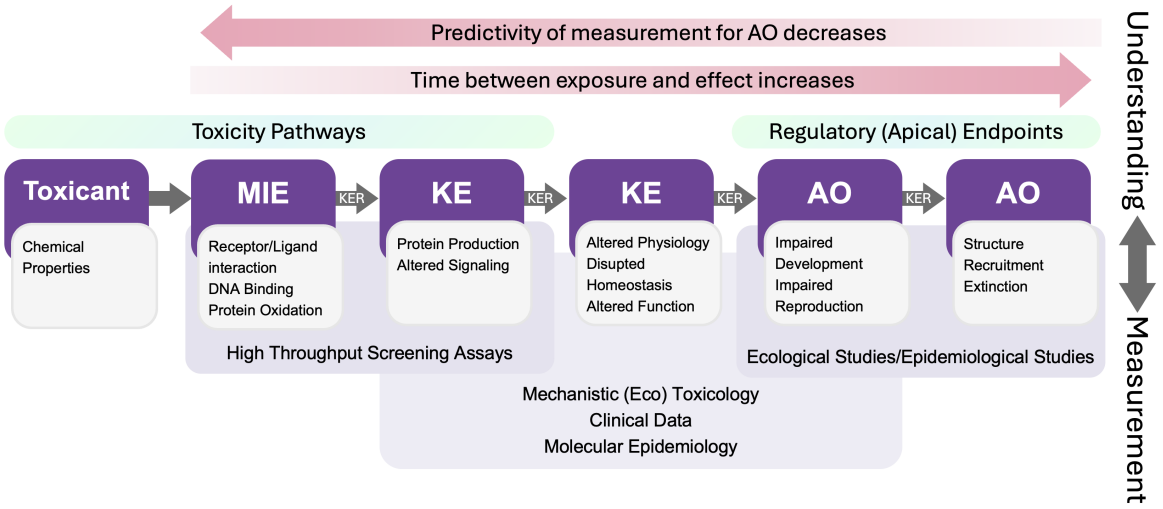

Figure 1.3. Schematic illustration of the AOP framework linking different levels of data streams to outcomes relevant for supporting regulatory decision-making for chemical safety assessment. The figure was adapted from Ankley and Edwards (2018) with partially modifications.

1.2.2 Quantitative AOPs (qAOPs)

Quantitative AOPs (qAOPs) represent an advancement in the AOP framework by incorporating quantitative data to define dose-response relationships and thresholds between key events [32; 25; 33]. While traditional AOPs provide a qualitative understanding of the biological mechanisms underlying chemical toxicity, qAOPs enhance this framework by enabling the prediction of adverse outcomes under specific exposure scenarios. Through the integration of experimental data and mathematical modeling, qAOPs quantify the relationships between KEs, offering a more precise and predictive tool for risk assessment [34]. Techniques such as Bayesian networks are commonly employed to address uncertainties and variability in biological responses, while regression modeling serves as a mechanistic approach to quantitatively link KEs along the AOP (Figure 1.4) [34]. For instance, linear or nonlinear regression models can characterize dose-response relationships or temporal changes between upstream molecular events and downstream outcomes. These models enable the integration of quantitative data to identify thresholds or tipping points that trigger adverse outcomes. By bridging the gap between mechanistic understanding and practical risk assessments, qAOPs enhance the utility of AOPs in regulatory toxicology and environmental monitoring.

The development of qAOPs involves systematically mapping quantitative linkages between upstream and downstream events. For example, a decrease in plasma 17β-estradiol (E2) concentration (KE) can be mathematically modeled to predict downstream effects, such as reductions in plasma VTG concentration, cumulative fecundity, and spawning, ultimately culminating in a decreased population growth rate (AO) [35]. These quantitative relationships are critical for establishing thresholds where a specific level of an upstream KE elicits a defined change in the downstream KE. This approach is particularly valuable for identifying critical dose levels that inform safe exposure limits. Additionally, qAOPs contribute to

regulatory decision-making by enabling probabilistic modeling of chemical effects, thereby providing a robust framework for chemical safety evaluations.

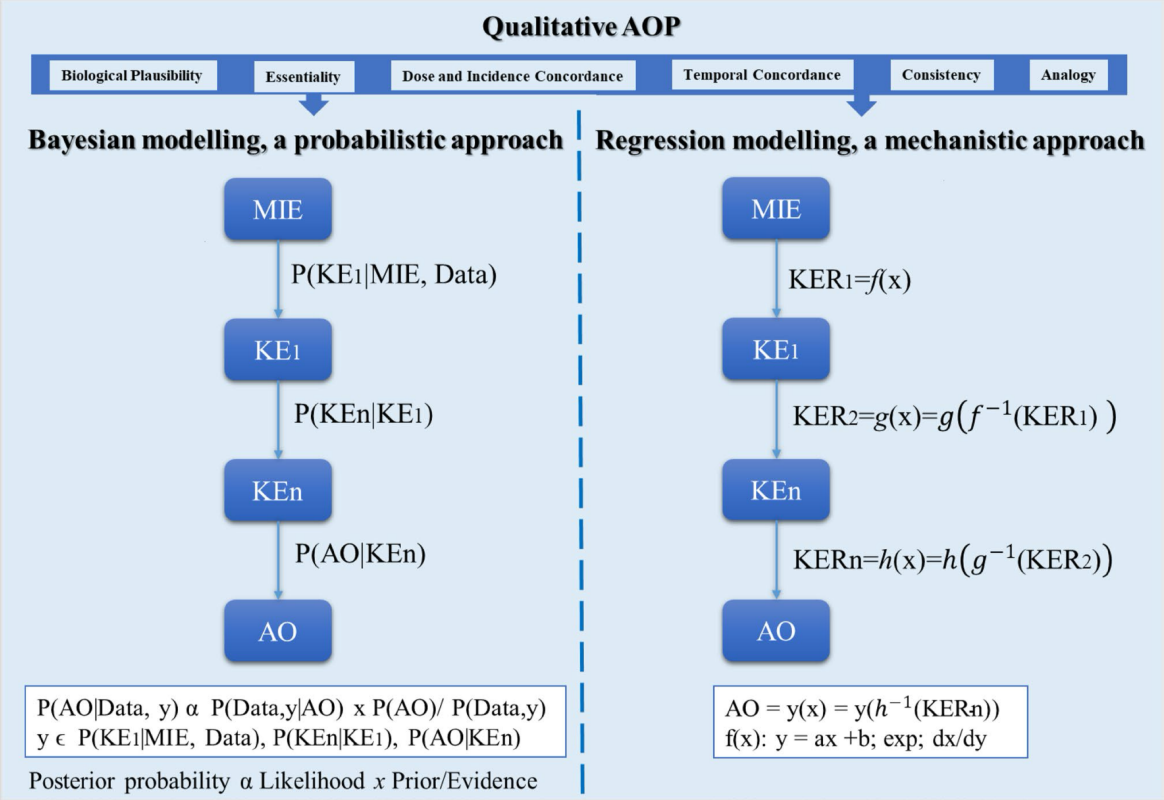

Figure 1.4. Conceptual depiction of various types of qAOP models. qAOPs serve an informative role in prioritizing and computationally modeling the AO of interest and can be further quantified using a weight-of-evidence approach. Probabilistic modeling often employs Bayes' theorem, as outlined below. Mechanistic qAOP models incorporate mathematical functions, such as linear regressions, to describe key relationships. The figure was adapted from Spinu et al. (2020).

1.2.3 AOP networks

AOP networks extend the AOP framework by connecting multiple AOPs that share common KEs or AOs, reflecting the complexity of biological systems and chemical interactions. Unlike single, linear AOPs, networks capture interconnected pathways through which individual events can exert a wide range of effects [36]. This network-based approach is especially valuable for evaluating cumulative and combined chemical exposures, as it accounts for interactions between pathways and identifies critical nodes within the system. For example, in reproductive toxicity, an AOP network available in the AOP-Wiki might connect multiple MIEs, such as 5α-reductase (SRD5A) inhibition, estrogen receptor antagonism, aromatase inhibition, or androgen receptor agonism, to common downstream events like decreased plasma E2 levels and reduced VTG synthesis (Figure 1.5). These interconnected pathways converge on AOs, such as reduced fecundity or population declines in aquatic organisms. Shared KEs, like decreased

VTG production or reduced plasma E2 levels, serve as pivotal nodes that link various events to reproductive dysfunction. Recognizing these shared events is crucial for identifying regulatory intervention points and evaluating the cumulative effects of chemical mixtures. As a result, AOP networks hold significant promise in guiding the development of assays with varying specificity, designed to target either distinct MIEs or clusters of mechanistically related MIEs.

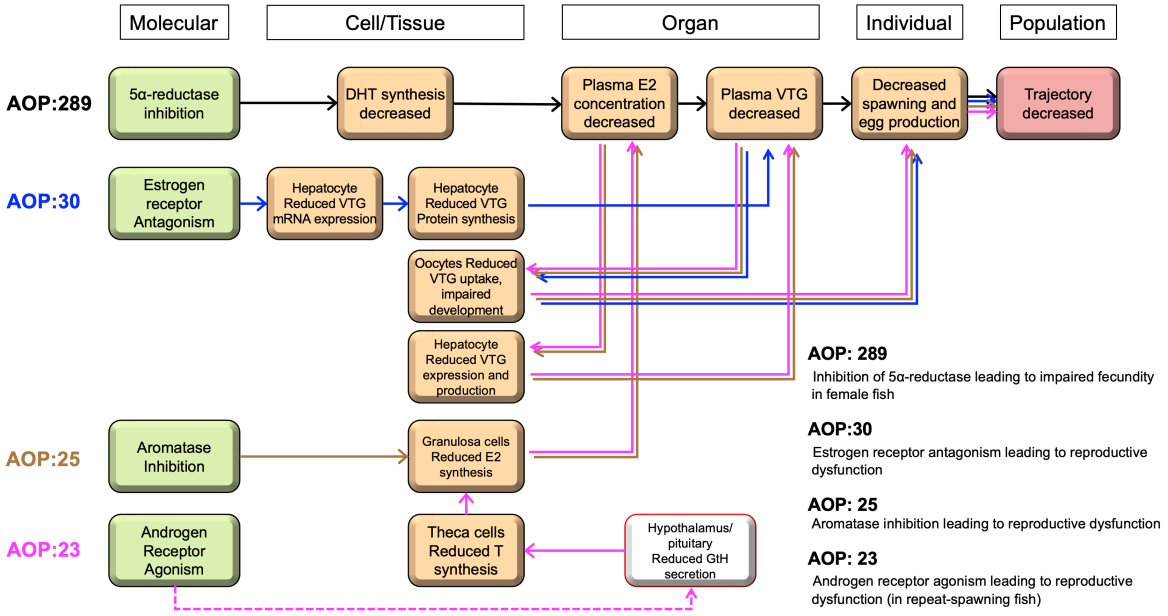

Figure 1.5. An example of an AOP network illustrating four reproductive toxicity-related signaling pathways. Green boxes denote MIEs, orange boxes represent KEs, and the red box indicates the AO. Each arrow color corresponds to a specific AOP pathway. Abbreviations: DHT, dihydrotestosterone; E2, 17β-estradiol; VTG, vitellogenin; T, testosterone; GtH, gonadotropin hormone. Data retrieved from the AOP-Wiki (Available from http://aopwiki.org).

1.2.4 Application of AOPs in Integrated Approaches to Testing and Assessment (IATA)

Integrated Approaches to Testing and Assessment (IATA) are pragmatic and science-driven frameworks for chemical hazard and risk characterization, combining the integrated analysis of existing data in a weight-of-evidence assessment and the generation of new information through targeted testing strategies [25]. AOPs can play a vital role in IATA by acting as blueprints that bridge the gap between *in vitro*, *in silico*, and *in vivo* testing based on existing information (Figure 1.6). The structured nature of AOPs allows the mapping of mechanistic data to AOs, providing a systematic framework to interpret results from high-throughput screening or cell-based assays [25]. For instance, molecular perturbations observed in *in vitro* systems can be linked to KEs in an AOP, facilitating predictions of organismal and population-level impacts. This capability not only reduces the need for extensive *in vivo* testing but also improves the accuracy and efficiency of hazard identification and risk characterization. Moreover, various evidence associated with KEs, including those from qAOPs, demonstrate high levels of reliability and specificity. These insights can guide the development of test methods and defined approaches applicable within

regulatory contexts [37]. Thus, AOPs are integral to the functionality and success of IATA, providing the mechanistic backbone that links diverse data sources to adverse outcomes. Their ability to streamline testing, reduce animal use, and enhance predictive power makes AOPs important in regulatory context.

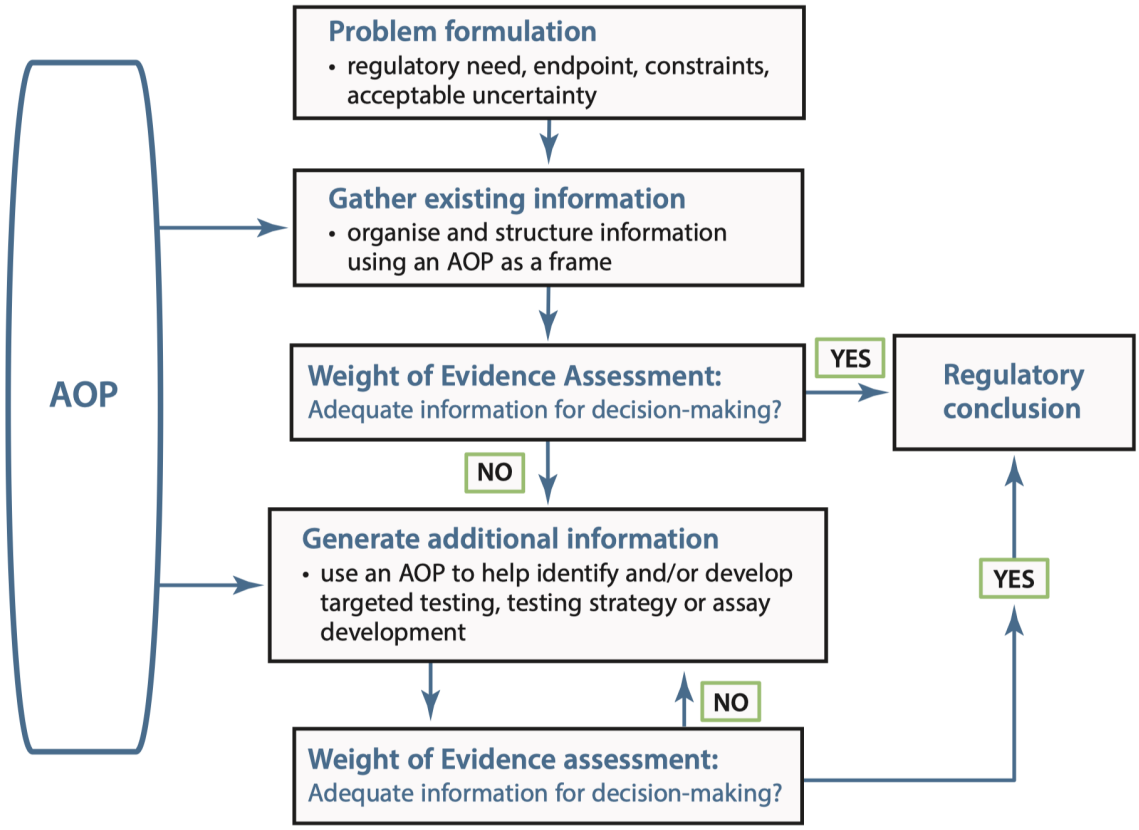

Figure 1.6. AOPs can support a framework to develop IATA in decision context. The figure adapted from OECD. (2017).

1.3 Steroid signaling pathways

1.3.1 Steroidogenesis in vertebrates: reproductive functions

Steroidogenesis involves the conversion of cholesterol into biologically active steroid hormones, including progestins, corticosteroids, androgens, and estrogens (Figure 1.7) [38]. These hormones act as potent signaling molecules, influencing a wide range of physiological functions by binding to receptor molecules that function as transcription factors, thereby regulating gene expression. Androgens, such as testosterone, are primarily synthesized in the testes of males and to a lesser extent in females [39]. In males, androgens drive critical reproductive processes such as spermatogenesis, the development and maintenance of secondary sexual characteristics, and spawning behaviors. Additionally, in male teleost fish, androgens regulate accessory reproductive structures like breeding tubercles and specialized

spawning coloration, enhancing reproductive fitness [40; 41]. In females, androgens contribute to ovarian follicle development, highlighting their roles beyond male-specific functions [42]. Estrogens, particularly 17β-estradiol (E2), are synthesized from testosterone through the action of aromatase, encoded by the cyp19a gene, and play vital roles in female reproductive processes. E2 regulates vitellogenesis by stimulating the liver to produce vitellogenin, a precursor of egg yolk proteins essential for oocyte growth and maturation [43]. Additionally, estrogens synchronize ovulation and spawning, ensuring successful fertilization and embryonic development [44]. Beyond their direct roles in reproduction, estrogens maintain ovarian tissue integrity, modulate lipid metabolism to meet energy demands during reproduction, and influence spawning-associated behaviors [45; 46]. Disruptions in steroidogenesis, whether in hormone synthesis or signaling, can impair reproductive success, leading to reduced gamete quality, altered secondary sexual characteristics, and disrupted spawning cycles. The tightly regulated synthesis of androgens and estrogens underpins reproductive health, collectively driving key processes such as gametogenesis, secondary sexual development, and spawning.

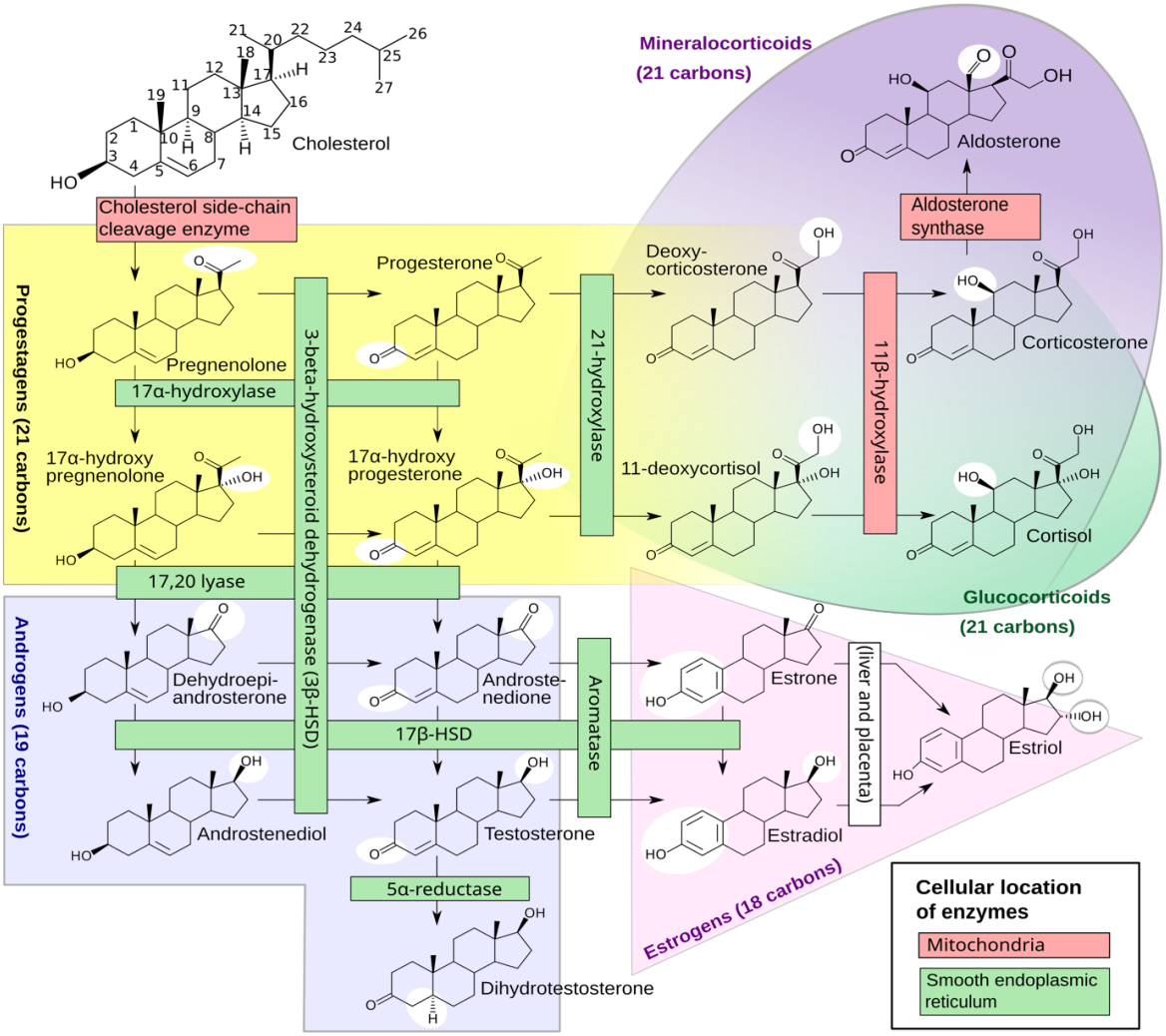

Figure 1.7. Overview of the biosynthetic reaction of steroid hormones. The figure adapted from Häggström and Richfield (2014).

1.3.2 Ecdysteroidogenesis in invertebrates: Pathways and reproductive regulation

Ecdysteroidogenesis is the process by which ecdysteroids, the primary steroid hormones in invertebrates, are synthesized (Figure 1.8). These hormones are essential for molting and metamorphosis. Unlike vertebrates, invertebrates cannot synthesize cholesterol *de novo* and instead rely on dietary sterols as precursors [48]. Cholesterol is first converted to 7-dehydrocholesterol by the enzyme neverland, encoded by the neverland gene. It is further transformed into ecdysone in the prothoracic gland through the action of cytochrome P450 enzymes encoded by the Halloween genes, including *spook* (*Cyp307a1*), *phantom* (*Cyp306a1*), *disembodied* (*Cyp302a1*), and *shadow* (*Cyp315a1*). Ecdysone is then converted into 20-hydroxyecdysone (20E), the biologically active form of ecdysteroids, by the enzyme encoded by *shade* (*Cyp314a1*) [49; 50]. However, the precise intermediate steps from 7-dehydrocholesterol to 5β-ketodiol remain unclear due to the instability of intermediates in the prothoracic gland [51; 52].

Ecdysteroids, particularly 20E, are crucial regulators of molting and metamorphosis in insects. They exert their effects by interacting with nuclear receptor complexes. At the molecular level, 20E binds to the ecdysteroid receptor (EcR), which forms a heterodimer with ultraspiracle (USP), the invertebrate homolog of the mammalian retinoid X receptor (RXR) [53]. This 20E-EcR-USP complex acts as a transcriptional regulator by binding to ecdysone response elements in the promoters of target genes, thereby modulating gene expression to drive development and reproduction [49; 54]. Downstream signaling pathways regulated by 20E influence oogenesis and embryonic development through nuclear receptors such as E75 and HR3, which coordinate these critical stages [55-57]. The 20E signaling cascade involves the sequential activation of early, early-late, and late genes, underscoring its role as a developmental switch [56]. Despite significant advancements, further research is required to elucidate the biological signals governing ecdysteroid biosynthesis and the molecular pathways that synchronize molting and reproduction, ensuring a comprehensive understanding of these intricate processes.

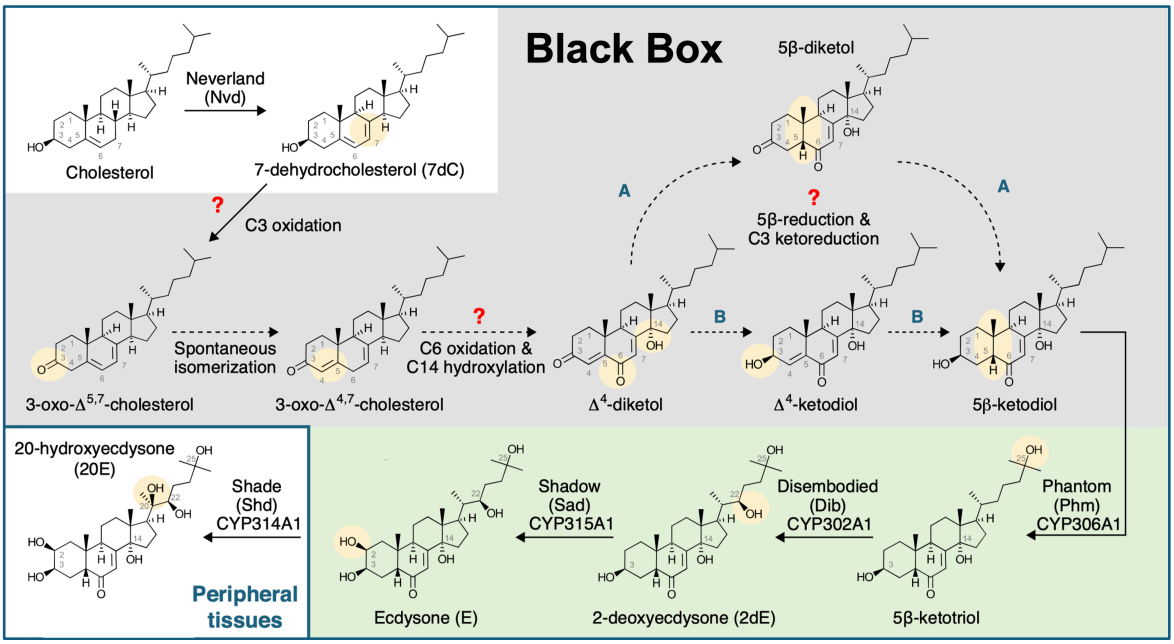

Figure 1.8. Overview of the ecdysteroid biosynthetic reaction. The figure adapted from Pan et al. (2021).

1.4 Steroid 5α-reductase

1.4.1 5α-reductase in steroid biosynthetic pathway: function in vertebrates and potential in invertebrate

Steroid 5α-reductase (SRD5A; 3-oxo-5α-steroid 4-dehydrogenase) is a critical enzyme in the steroidogenesis pathway, catalyzing the conversion of testosterone to dihydrotestosterone (DHT), a potent androgen essential for reproductive and developmental processes in vertebrates (Figure 1.9). DHT exhibits a higher affinity for androgen receptors (ARs) compared to testosterone, thereby amplifying its regulatory effects on target tissues [59]. Additionally, 5α-reductase enzymes are involved in degradative pathways, facilitating the reduction of circulating C21 steroids for urinary excretion [38]. Three isozymes of SRD5A have been identified in vertebrates: SRD5A1, SRD5A2, and SRD5A3, each with distinct tissue distributions and functional roles [60]. SRD5A1 is primarily expressed in non-androgenic tissues such as the liver, kidneys, scalp, brain, and skin, while SRD5A2 is predominantly active in the prostate and reproductive tissues, playing a crucial role in male sexual development and the maintenance of secondary sexual characteristics. SRD5A3, more recently identified, has a ubiquitous expression profile. Recent databases, including NCBI Genome Assembly (ASM2063170v1.1; accessed from https://www.ncbi.nlm.nih.gov/datasets/genome/GCF_020631705.1), UniProt (A0A0P5T180; accessed from https://www.uniprot.org/uniprotkb/A0A0P5T180/entry), and KEGG (T07514: 116924669; accessed from https://www.kegg.jp/entry/dmk:116924669), have documented a gene in *D. magna* encoding a protein with functional similarity to vertebrate steroid 5α-reductase (SRD5A). Annotated as 3-oxo-5α-steroid 4-dehydrogenase, this gene suggests that invertebrates like *D. magna* may possess an enzyme with a comparable role to SRD5A in vertebrates, particularly in ecdysteroidogenesis.

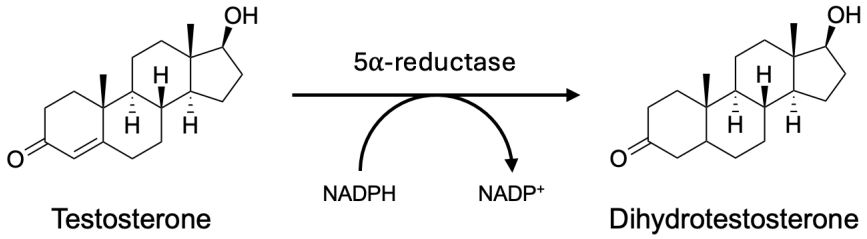

Figure 1.8. Conversion of testosterone to dihydrotestosterone by 5α-reductase.

1.4.2 5α-reductase inhibitors: Clinical applications and environmental concerns

Inhibitors of 5α-reductase, such as finasteride and dutasteride, act through competitive inhibition by binding to the active site of 5α-reductase, preventing the conversion of testosterone to DHT and thereby reducing androgenic activity in target tissues [61]. These inhibitors are widely prescribed to treat benign prostatic hyperplasia and androgenetic alopecia, conditions increasingly prevalent due to aging populations and rising stress levels [62; 63]. Hair loss, particularly androgenetic alopecia, affects a significant portion of the population and is closely linked to elevated levels of DHT [64]. By reducing DHT levels, these drugs mitigate hair follicle miniaturization, a key factor in the progression of hair loss. Finasteride, marketed as Propecia for hair loss and benign prostatic hyperplasia, selectively inhibits SRD5A2, the isozyme predominantly active in reproductive tissues. Dutasteride, marketed as Avodart, inhibits both SRD5A1 and SRD5A2, offering higher potency and suitability for severe cases of hair loss and prostate enlargement. According to Korean market sales data from 2018, finasteride generated sales of 67.2 billion won, while dutasteride reached 51.8 billion won. Driven by the growing demand to address hair loss problems, the market for these drugs continues to expand globally, including in Korea. (Figure 1.9) [62; 63].

While effective clinically, the widespread use of finasteride and dutasteride raises environmental concerns due to their persistence and potential long-term ecological impacts. Dutasteride, in particular, exhibits high potency and an extended biological half-life of up to 5 weeks [61]. Finasteride has been detected in domestic sewage treatment plants and surface waters in Sweden at concentrations of 0.01 and 0.02 μg/L, respectively [65; 66]. These compounds, when inadequately removed during wastewater treatment, can accumulate in aquatic environments, potentially disrupting hormone signaling in aquatic organisms. Studies have indicated that endocrine-disrupting compounds, including finasteride and dutasteride, may impair reproduction and alter population dynamics in sensitive species [67]. The persistence and potential bioaccumulation of these drugs in aquatic ecosystems underscore the need for robust chemical risk assessment strategies to mitigate their environmental impact.

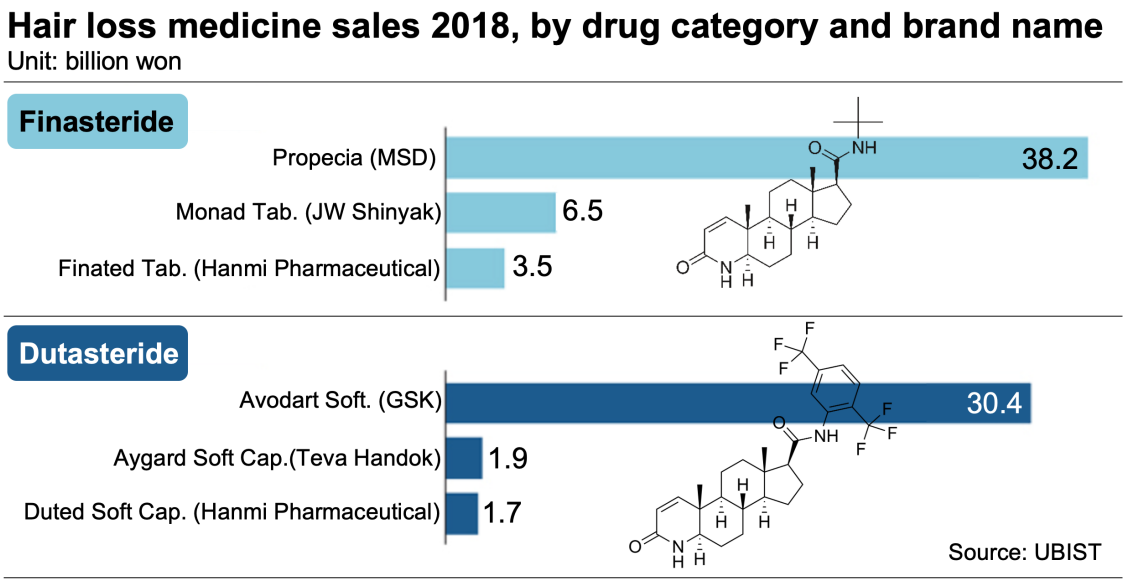

Figure 1.9. Market Sales of Finasteride and Dutasteride in South Korea in 2018. Data was accessed from Korea JoongAng Daily (Available from https://koreajoongangdaily.joins.com/2019/04/01/industry-/Baldness-battle-heats-up-as-new-pill-is-offered/3061309.html, acceded on 06 January 2025).

1.5 Test models

1.5.1 Cell lines

The HEK293 cell line, derived from human embryonic kidney cells, is a versatile system widely used for transient transfection studies [68]. In 5α-reductase (SRD5A) research, HEK293 cells can be engineered to overexpress specific SRD5A isozymes (e.g., SRD5A1, SRD5A2, or SRD5A3), allowing researchers to study the enzymatic conversion of testosterone to dihydrotestosterone (DHT) in a controlled environment. This model facilitates evaluating the effects of inhibitors such as finasteride and dutasteride, as well as investigating isozyme-specific differences in inhibitor sensitivity, substrate specificity, and tissue expression profiles. The ease of genetic manipulation and compatibility with high-throughput assays make HEK293 cells invaluable in SRD5A studies.

The H295R cell line, derived from human adrenocortical carcinoma, provides a robust model for investigating steroidogenesis and endocrine disruption [69]. This cell line synthesizes a broad range of steroid hormones, including androgens, estrogens, glucocorticoids, and mineralocorticoids. It is particularly useful for assessing how EDCs and pharmaceutical inhibitors impact the steroidogenic pathway by quantifying hormone levels such as testosterone and estradiol. The H295R steroidogenesis assay, outlined in OECD. (2023), is a cornerstone of regulatory toxicology, providing insights into the mechanisms by which chemicals disrupt steroidogenic pathways.

1.5.2 Zebrafish (*Danio rerio*) embryo

The zebrafish (*Danio rerio*) model has become a staple for whole-organism studies examining the developmental and reproductive effects of chemical exposure [70]. Zebrafish embryos offer unique advantages, such as rapid development, optical transparency, and genetic similarity to humans [71]. Moreover, they are classified as non-animal testing models up to 120 hours post-fertilization [72]. Zebrafish embryo assays, as detailed in OECD Test Guideline 236, are widely used to assess developmental toxicity and endocrine disruption [73]. Their high correlation with toxicity findings in adult fish supports their utility in early-tier risk assessments [74-76]. Furthermore, zebrafish embryos are instrumental in studying teratogenicity and endocrine-disrupting effects. For example, exposure to EDCs has been shown to impair gonadal development and disrupt sexual differentiation, demonstrating their value in evaluating reproductive toxicity [77; 13].

1.5.3 *Daphnia magna*

D. magna, a freshwater crustacean, is a keystone species in aquatic ecosystems and an essential invertebrate model in ecotoxicology [78]. Its sensitivity to various pollutants, including EDCs, makes it ideal for monitoring and assessing chemical impacts on freshwater ecosystems [79; 80]. The reproductive system of *D. magna* is highly responsive to endocrine disruption, with molting and reproductive cycles regulated by ecdysteroids and juvenile hormones [81]. Additional advantages include its high sensitivity to environmental changes, short life cycle, and low maintenance costs [82]. Studies have demonstrated that D. magna responds to vertebrate hormones, provides cross-reactive endpoints, and offers valuable insights into comparative ecdysteroid and steroid signaling systems [83-86; 49]. These attributes establish *D. magna* as a robust model for investigating endocrine disruption, with broader applications in toxicology and ecology.

1.6 Bibliography

1. Wang, Z.; Walker, G.W.; Muir, D.C.G., Nagatani-Yoshida, K. Toward a Global Understanding of Chemical Pollution: A First Comprehensive Analysis of National and Regional Chemical Inventories. *Environ. Sci. Technol.* **2020**, 54, 2575-2584. doi:10.1021/acs.est.9b06379.
2. Naidu, R.; Biswas, B.; Willett, I.R.; Cribb, J.; Kumar Singh, B.; Paul Nathanail, C.; Coulon, F.; Semple, K.T.; Jones, K.C.; Barclay, A.; et al. Chemical pollution: A growing peril and potential catastrophic risk to humanity. *Environ. Int.* **2021**, 156, 106616. doi:10.1016/j.envint.2021.106616.
3. Beronius, A., Vandenberg, L.N. Using systematic reviews for hazard and risk assessment of endocrine disrupting chemicals. *Rev. Endocr. Metab. Disord.* **2015**, 16, 273-287. doi:10.1007/s11154-016-9334-7.
4. Gore, A.C.; Chappell, V.A.; Fenton, S.E.; Flaws, J.A.; Nadal, A.; Prins, G.S.; Toppari, J., Zoeller, R.T. EDC-2: The Endocrine Society's Second Scientific Statement on Endocrine-Disrupting Chemicals. *Endocr. Rev.* **2015**, 36, E1-e150. doi:10.1210/er.2015-1010.
5. La Merrill, M.A.; Vandenberg, L.N.; Smith, M.T.; Goodson, W.; Browne, P.; Patisaul, H.B.; Guyton, K.Z.;

Kortenkamp, A.; Cogliano, V.J.; Woodruff, T.J.; et al. Consensus on the key characteristics of endocrine-disrupting chemicals as a basis for hazard identification. *Nat. Rev. Endocrinol.* **2020**, 16, 45-57. doi:10.1038/s41574-019-0273-8.

6. Mahalingam, S.; Ther, L.; Gao, L.; Wang, W.; Ziv-Gal, A., Flaws, J.A. The effects of in utero bisphenol A exposure on ovarian follicle numbers and steroidogenesis in the F1 and F2 generations of mice. *Reprod. Toxicol.* **2017**, 74, 150-157. doi:10.1016/j.reprotox.2017.09.013.
7. Hayes, T.B.; Anderson, L.L.; Beasley, V.R.; de Solla, S.R.; Iguchi, T.; Ingraham, H.; Kestemont, P.; Kniewald, J.; Kniewald, Z.; Langlois, V.S.; et al. Demasculinization and feminization of male gonads by atrazine: Consistent effects across vertebrate classes. *J. Steroid. Biochem. Molec. Biol.* **2011**, 127, 64-73. doi:doi.org/10.1016/j.jsbmb.2011.03.015.
8. Diamanti-Kandarakis, E.; Bourguignon, J.P.; Giudice, L.C.; Hauser, R.; Prins, G.S.; Soto, A.M.; Zoeller, R.T., Gore, A.C. Endocrine-disrupting chemicals: an Endocrine Society scientific statement. *Endocr. Rev.* **2009**, 30, 293-342. doi:10.1210/er.2009-0002.
9. Patisaul, H.B., Adewale, H.B. Long-term effects of environmental endocrine disruptors on reproductive physiology and behavior. *Front. Behav. Neurosci.* **2009**, 3, 10. doi:10.3389/neuro.08.010.2009.
10. Heys, K.A.; Shore, R.F.; Pereira, M.G.; Jones, K.C., Martin, F.L. Risk assessment of environmental mixture effects. *RSC Adv.* **2016**, 6, 47844-47857. doi:10.1039/C6RA05406D.
11. Ortiz-Villanueva, E.; Jaumot, J.; Martínez, R.; Navarro-Martín, L.; Piña, B., Tauler, R. Assessment of endocrine disruptors effects on zebrafish (Danio rerio) embryos by untargeted LC-HRMS metabolomic analysis. *Sci. Total Environ.* **2018**, 635, 156-166. doi:10.1016/j.scitotenv.2018.03.369.
12. Chikae, M.; Ikeda, R.; Hasan, Q.; Morita, Y., Tamiya, E. Effect of alkylphenols on adult male medaka: plasma vitellogenin goes up to the level of estrous female. *Environ. Toxicol. Pharmacol.* **2003**, 15, 33-36. doi:10.1016/j.etap.2003.08.005.
13. Segner, H. Zebrafish (Danio rerio) as a model organism for investigating endocrine disruption. *Comp. Biochem. Physiol. C Toxicol. Pharmacol.* **2009**, 149, 187-195. doi:10.1016/j.cbpc.2008.10.099.
14. Milsk, R.; Cavallin, J.E.; Durhan, E.J.; Jensen, K.M.; Kahl, M.D.; Makynen, E.A.; Martinović-Weigelt, D.; Mueller, N.; Schroeder, A.; Villeneuve, D.L.; et al. A study of temporal effects of the model anti-androgen flutamide on components of the hypothalamic-pituitary-gonadal axis in adult fathead minnows. *Aquat. Toxicol.* **2016**, 180, 164-172. doi:10.1016/j.aquatox.2016.09.021.
15. Wheeler, J.R.; Segner, H.; Weltje, L., Hutchinson, T.H. Interpretation of sexual secondary characteristics (SSCs) in regulatory testing for endocrine activity in fish. *Chemosphere* **2020**, 240, 124943. doi:10.1016/j.chemosphere.2019.124943.
16. Dang, Z.; Cheng, Y.; Chen, H.M.; Cui, Y.; Yin, H.H.; Traas, T.; Montforts, M., Vermeire, T. Evaluation of the Daphnia magna reproduction test for detecting endocrine disruptors. *Chemosphere* **2012**, 88, 514-523. doi:10.1016/j.chemosphere.2012.03.012.
17. Fuertes, I.; Jordão, R.; Piña, B., Barata, C. Time-dependent transcriptomic responses of Daphnia magna exposed to metabolic disruptors that enhanced storage lipid accumulation. *Environ. Pollut.* **2019**, 249, 99-108. doi:10.1016/j.envpol.2019.02.102.
18. Mu, X.; Rider, C.V.; Hwang, G.S.; Hoy, H., LeBlanc, G.A. Covert signal disruption: anti-ecdysteroidal activity of bisphenol A involves cross talk between signaling pathways. *Environ. Toxicol. Chem.* **2005**,

24, 146-152. doi:10.1897/04-063r.1.

19. Oda, S.; Tatarazako, N.; Watanabe, H.; Morita, M., Iguchi, T. Production of male neonates in Daphnia magna (Cladocera, Crustacea) exposed to juvenile hormones and their analogs. *Chemosphere* **2005**, 61, 1168-1174. doi:10.1016/j.chemosphere.2005.02.075.
20. Sumpter, J.P., Johnson, A.C. Lessons from endocrine disruption and their application to other issues concerning trace organics in the aquatic environment. *Environ. Sci. Technol.* **2005**, 39, 4321-4332. doi:10.1021/es048504a.
21. Wang, F.; Xiang, L.; Sze-Yin Leung, K.; Elsner, M.; Zhang, Y.; Guo, Y.; Pan, B.; Sun, H.; An, T.; Ying, G.; et al. Emerging contaminants: A One Health perspective. *The Innovation* **2024**, 5, 100612. doi:10.1016/j.xinn.2024.100612.
22. Agency, E.C. New approach methodologies in regulatory science – Proceedings of a scientific workshop – Helsinki, 19-20 April 2016. *European Chemicals Agency* **2016**. doi:10.2823/543644.
23. Agency, E.C. Report on the European Chemicals Agency's "New approach methodologies workshop: towards an animal free regulatory system for industrial chemicals" (31 May – 1 June 2023, Helsinki, Finland). *European Chemicals Agency* **2023**. doi:10.2823/7494.
24. Ankley, G.T.; Bennett, R.S.; Erickson, R.J.; Hoff, D.J.; Hornung, M.W.; Johnson, R.D.; Mount, D.R.; Nichols, J.W.; Russom, C.L.; Schmieder, P.K.; et al. Adverse outcome pathways: a conceptual framework to support ecotoxicology research and risk assessment. *Environ. Toxicol. Chem.* **2010**, 29, 730-741. doi:10.1002/etc.34.
25. OECD. Guidance Document for the Use of Adverse Outcome Pathways in Developing Integrated Approaches to Testing and Assessment (IATA), OECD Series on Testing and Assessment, No. 260. *OECD Publishing* **2017**, Paris. doi:10.1787/44bb06c1-en.
26. Ankley, G.T., Edwards, S.W. The Adverse Outcome Pathway: A Multifaceted Framework Supporting 21(st) Century Toxicology. *Curr. Opin. Toxicol.* **2018**, 9, 1-7. doi:10.1016/j.cotox.2018.03.004.
27. Villeneuve, D.L.; Crump, D.; Garcia-Reyero, N.; Hecker, M.; Hutchinson, T.H.; LaLone, C.A.; Landesmann, B.; Lettieri, T.; Munn, S.; Nepelska, M.; et al. Adverse outcome pathway (AOP) development I: strategies and principles. *Toxicol. Sci.* **2014**, 142, 312-320. doi:10.1093/toxsci/kfu199.
28. AOP-Wiki Androgen receptor agonism leading to reproductive dysfunction (in repeat-spawning fish). *Society for Advancement of AOPs [Online]*, April 29, 2023, Available from: https://aopwiki.org/aops/23.
29. AOP-Wiki Estrogen receptor antagonism leading to reproductive dysfunction. *Society for Advancement of AOPs [Online]*, April 29, 2023, Available from: https://aopwiki.org/aops/30.
30. Groh, K.J.; Carvalho, R.N.; Chipman, J.K.; Denslow, N.D.; Halder, M.; Murphy, C.A.; Roelofs, D.; Rolaki, A.; Schirmer, K., Watanabe, K.H. Development and application of the adverse outcome pathway framework for understanding and predicting chronic toxicity: I. Challenges and research needs in ecotoxicology. *Chemosphere* **2015**, 120, 764-777. doi:10.1016/j.chemosphere.2014.09.068.
31. Leist, M.; Ghallab, A.; Graepel, R.; Marchan, R.; Hassan, R.; Bennekou, S.H.; Limonciel, A.; Vinken, M.; Schildknecht, S.; Waldmann, T.; et al. Adverse outcome pathways: opportunities, limitations and open questions. *Arch. Toxicol.* **2017**, 91, 3477-3505. doi:10.1007/s00204-017-2045-3.
32. Conolly, R.B.; Ankley, G.T.; Cheng, W.; Mayo, M.L.; Miller, D.H.; Perkins, E.J.; Villeneuve, D.L., Watanabe, K.H. Quantitative Adverse Outcome Pathways and Their Application to Predictive Toxicology.

Environ. Sci. Technol. **2017**, 51, 4661-4672. doi:10.1021/acs.est.6b06230.

33. Villeneuve, D.L.; Crump, D.; Garcia-Reyero, N.; Hecker, M.; Hutchinson, T.H.; LaLone, C.A.; Landesmann, B.; Lettieri, T.; Munn, S.; Nepelska, M.; et al. Adverse outcome pathway development II: best practices. *Toxicol. Sci.* **2014**, 142, 321-330. doi:10.1093/toxsci/kfu200.
34. Spinu, N.; Cronin, M.T.D.; Enoch, S.J.; Madden, J.C., Worth, A.P. Quantitative adverse outcome pathway (qAOP) models for toxicity prediction. *Arch. Toxicol.* **2020**, 94, 1497-1510. doi:10.1007/s00204-020-02774-7.
35. AOP-Wiki Inhibition of 5α-reductase leading to impaired fecundity in female fish. *Society for Advancement of AOPs [Online]*, April 29, 2023, Available from: https://aopwiki.org/aops/289.
36. Knapen, D.; Vergauwen, L.; Villeneuve, D.L., Ankley, G.T. The potential of AOP networks for reproductive and developmental toxicity assay development. *Reprod. Toxicol.* **2015**, 56, 52-55. doi:10.1016/j.reprotox.2015.04.003.
37. Tollefsen, K.E.; Scholz, S.; Cronin, M.T.; Edwards, S.W.; de Knecht, J.; Crofton, K.; Garcia-Reyero, N.; Hartung, T.; Worth, A., Patlewicz, G. Applying Adverse Outcome Pathways (AOPs) to support Integrated Approaches to Testing and Assessment (IATA). *Regul. Toxicol. Pharmacol.* **2014**, 70, 629-640. doi:10.1016/j.yrtph.2014.09.009.
38. Miller, W.L., Auchus, R.J. The molecular biology, biochemistry, and physiology of human steroidogenesis and its disorders. *Endocr. Rev.* **2011**, 32, 81-151. doi:10.1210/er.2010-0013.
39. Borg, B. Androgens in teleost fishes. *Comp. Biochem. Physiol. C, Pharmacol. Toxicol. Endocrinol.* **1994**, 109, 219-245. doi:doi.org/10.1016/0742-8413(94)00063-G.
40. Kodric-Brown, A. Sexual Dichromatism and Temporary Color Changes in the Reproduction of Fishes1. *Am. Zool.* **1998**, 38, 70-81. doi:10.1093/icb/38.1.70.
41. McMillan, S.C.; Xu, Z.T.; Zhang, J.; Teh, C.; Korzh, V.; Trudeau, V.L., Akimenko, M.A. Regeneration of breeding tubercles on zebrafish pectoral fins requires androgens and two waves of revascularization. *Development* **2013**, 140, 4323-4334. doi:10.1242/dev.095992.
42. Gervásio, C.G.; Bernuci, M.P.; Silva-de-Sá, M.F., Rosa, E.S.A.C. The role of androgen hormones in early follicular development. *ISRN Obstet. Gynecol.* **2014**, 2014, 818010. doi:10.1155/2014/818010.
43. Sullivan, C.V., Yilmaz, O. Vitellogenesis and Yolk Proteins, Fish, In *Encyclopedia of Reproduction (Second Edition)*, Skinner, M.K., Academic Press, Oxford, 2018, 266-277, doi:doi: 10.1016/B978-0-12-809633-8.20567-0.
44. Segner, H. Chapter 86 - Reproductive and developmental toxicity in fishes, In *Reproductive and Developmental Toxicology*, Gupta, R.C., Academic Press, San Diego, 2011, 1145-1166, doi:doi: 10.1016/B978-0-12-382032-7.10086-4.
45. Munakata, A., Kobayashi, M. Endocrine control of sexual behavior in teleost fish. *Gen. Comp. Endocrinol.* **2010**, 165, 456-468. doi:10.1016/j.ygcen.2009.04.011.
46. Sun, S.X.; Wu, J.L.; Lv, H.B.; Zhang, H.Y.; Zhang, J.; Limbu, S.M.; Qiao, F.; Chen, L.Q.; Yang, Y.; Zhang, M.L.; et al. Environmental estrogen exposure converts lipid metabolism in male fish to a female pattern mediated by AMPK and mTOR signaling pathways. *J. Hazard. Mater.* **2020**, 394, 122537. doi:10.1016/j.jhazmat.2020.122537.
47. Häggström, M., Richfield, D. Diagram of the pathways of human steroidogenesis. *WikiJournal of*

Medicine **2014**, 1. doi:10.15347/wjm/2014.005.

48. Clark, A.J., Bloch, K. The Absence of Sterol Synthesis in Insects. *J. Biol. Chem.* **1959**, 234, 2578-2582. doi:10.1016/S0021-9258(18)69741-8.
49. Miyakawa, H.; Sato, T.; Song, Y.; Tollefsen, K.E., Iguchi, T. Ecdysteroid and juvenile hormone biosynthesis, receptors and their signaling in the freshwater microcrustacean Daphnia. *J. Steroid Biochem. Mol. Biol.* **2018**, 184, 62-68. doi:10.1016/j.jsbmb.2017.12.006.
50. Rewitz, K.F.; O'Connor, M.B., Gilbert, L.I. Molecular evolution of the insect Halloween family of cytochrome P450s: phylogeny, gene organization and functional conservation. *Insect Biochem. Mol. Biol.* **2007**, 37, 741-753. doi:10.1016/j.ibmb.2007.02.012.
51. Gilbert, L.I.; Rybczynski, R., Warren, J.T. Control and biochemical nature of the ecdysteroidogenic pathway. *Annu. Rev. Entomol.* **2002**, 47, 883-916. doi:10.1146/annurev.ento.47.091201.145302.
52. Niwa, R., Niwa, Y.S. Enzymes for ecdysteroid biosynthesis: their biological functions in insects and beyond. *Biosci. Biotechnol. Biochem.* **2014**, 78, 1283-1292. doi:10.1080/09168451.2014.942250.
53. Bonneton, F., Laudet, V. 6 - Evolution of Nuclear Receptors in Insects, In *Insect Endocrinology*, Gilbert, L.I., Academic Press, San Diego, 2012, 219-252, doi:doi.org/10.1016/B978-0-12-384749-2.10006-8.
54. Thomas, H.E.; Stunnenberg, H.G., Stewart, A.F. Heterodimerization of the Drosophila ecdysone receptor with retinoid X receptor and ultraspiracle. *Nature* **1993**, 362, 471-475. doi:10.1038/362471a0.
55. Bialecki, M.; Shilton, A.; Fichtenberg, C.; Segraves, W.A., Thummel, C.S. Loss of the ecdysteroid-inducible E75A orphan nuclear receptor uncouples molting from metamorphosis in Drosophila. *Dev. Cell* **2002**, 3, 209-220. doi:10.1016/s1534-5807(02)00204-6.
56. Hannas, B.R., LeBlanc, G.A. Expression and ecdysteroid responsiveness of the nuclear receptors HR3 and E75 in the crustacean Daphnia magna. *Mol. Cell. Endocrinol.* **2010**, 315, 208-218. doi:10.1016/j.mce.2009.07.013.
57. Su, Y.; Guo, Q.; Gong, J.; Cheng, Y., Wu, X. Functional expression patterns of four ecdysteroid receptor isoforms indicate their different functions during vitellogenesis of Chinese mitten crab, Eriocheir sinensis. *Comp. Biochem. Physiol. A Mol. Integr. Physiol.* **2020**, 248, 110754. doi:10.1016/j.cbpa.2020.110754.
58. Pan, X.; Connacher, R.P., O'Connor, M.B. Control of the insect metamorphic transition by ecdysteroid production and secretion. *Curr. Opin. Insect Sci.* **2021**, 43, 11-20. doi:10.1016/j.cois.2020.09.004.
59. Park, C.G.; Adnan, K.M.; Cho, H.; Ryu, C.S.; Yoon, J., Kim, Y.J. A combined in vitro-in silico method for assessing the androgenic activities of bisphenol A and its analogues. *Toxicol. In Vitro* **2024**, 98, 105838. doi:10.1016/j.tiv.2024.105838.
60. Langlois, V.S.; Zhang, D.; Cooke, G.M., Trudeau, V.L. Evolution of steroid-5alpha-reductases and comparison of their function with 5beta-reductase. *Gen. Comp. Endocrinol.* **2010**, 166, 489-497. doi:10.1016/j.ygcen.2009.08.004.
61. Nickel, J.C. Comparison of clinical trials with finasteride and dutasteride. *Rev. Urol.* **2004**, 6 Suppl 9, S31-39.
62. Sharma, R. Dutasteride Market Research Report 2032. *[Online]*, December 19, 2024, Available from: https://dataintelo.com/report/dutasteride-market-report.
63. Singh, S., Deshmukh, R. Finasteride Market Size, Share, Competitive Landscape and Trend Analysis Report by Application (Benign Prostatic Hyperplasia (BPH), Male pattern baldness), by Type (Branded ,

Generic), by Distribution Channel (Hospital Pharmacies, Online Providers, Drug Stores and Retail Pharmacies): Global Opportunity Analysis and Industry Forecast, 2021-2031. *[Online]*, February 04, 2023, Available from: https://www.alliedmarketresearch.com/finasteride-market-A14012.

64. York, K.; Meah, N.; Bhoyrul, B., Sinclair, R. A review of the treatment of male pattern hair loss. *Expert Opin. Pharmacother.* **2020**, 21, 603-612. doi:10.1080/14656566.2020.1721463.
65. Health and Medical Care Administration, R.S. Finasteride. *[Online]*, December 27, 2023, Available from: https://janusinfo.se/beslutsstod/lakemedelochmiljo/pharmaceuticalsandenvironment/databaseenven/finasteride.5.30a7505616a041a09b062df5.html#:~:text=Finasteride%20has%20been%20detected%20in,purified%20wastewater%20nationally%20in%20Sweden.
66. Vieno, N.; Hallgren, P.; Wallberg, P.; Pyhälä, M., Zandaryaa, S. Emerging pollutants in water series, 1, *Pharmaceuticals in the aquatic environment of the Baltic Sea region: a status report*, UNESCO, Paris, 2017, ISBN 978-92-3-100213-7.
67. Fent, K.; Weston, A.A., Caminada, D. Ecotoxicology of human pharmaceuticals. *Aquat. Toxicol.* **2006**, 76, 122-159. doi:10.1016/j.aquatox.2005.09.009.
68. Pulix, M.; Lukashchuk, V.; Smith, D.C., Dickson, A.J. Molecular characterization of HEK293 cells as emerging versatile cell factories. *Curr. Opin. Biotechnol.* **2021**, 71, 18-24. doi:10.1016/j.copbio.2021.05.001.
69. OECD. Test No. 456: H295R Steroidogenesis Assay, OECD Guidelines for the Testing of Chemicals, Section 4. *OECD Publishing* **2023**, Paris. doi:10.1787/9789264122642-en.
70. Nikam, V.S.; Singh, D.; Takawale, R., Ghante, M.R. Zebrafish: An emerging whole-organism screening tool in safety pharmacology. *Indian J. Pharmacol.* **2020**, 52, 505-513. doi:10.4103/ijp.IJP_482_19.
71. Howe, K.; Clark, M.D.; Torroja, C.F.; Torrance, J.; Berthelot, C.; Muffato, M.; Collins, J.E.; Humphray, S.; McLaren, K.; Matthews, L.; et al. The zebrafish reference genome sequence and its relationship to the human genome. *Nature* **2013**, 496, 498-503. doi:10.1038/nature12111.
72. Strähle, U.; Scholz, S.; Geisler, R.; Greiner, P.; Hollert, H.; Rastegar, S.; Schumacher, A.; Selderslaghs, I.; Weiss, C.; Witters, H.; et al. Zebrafish embryos as an alternative to animal experiments--a commentary on the definition of the onset of protected life stages in animal welfare regulations. *Reprod. Toxicol.* **2012**, 33, 128-132. doi:10.1016/j.reprotox.2011.06.121.
73. OECD. Test No. 236: Fish Embryo Acute Toxicity (FET) Test, OECD Guidelines for the Testing of Chemicals, Section 2. **2013**. doi:doi.org/10.1787/9789264203709-en.
74. Birke, A., Scholz, S. Zebrafish embryo and acute fish toxicity test show similar sensitivity for narcotic compounds. *Altex* **2019**, 36, 131-135. doi:10.14573/altex.1808101.
75. Busquet, F.; Strecker, R.; Rawlings, J.M.; Belanger, S.E.; Braunbeck, T.; Carr, G.J.; Cenijn, P.; Fochtman, P.; Gourmelon, A.; Hübler, N.; et al. OECD validation study to assess intra- and inter-laboratory reproducibility of the zebrafish embryo toxicity test for acute aquatic toxicity testing. *Regul. Toxicol. Pharmacol.* **2014**, 69, 496-511. doi:10.1016/j.yrtph.2014.05.018.
76. Lammer, E.; Carr, G.J.; Wendler, K.; Rawlings, J.M.; Belanger, S.E., Braunbeck, T. Is the fish embryo toxicity test (FET) with the zebrafish (Danio rerio) a potential alternative for the fish acute toxicity test? *Comp. Biochem. Physiol. C Toxicol. Pharmacol.* **2009**, 149, 196-209. doi:10.1016/j.cbpc.2008.11.006.
77. Santos, D.; Luzio, A., Coimbra, A.M. Zebrafish sex differentiation and gonad development: A review on

the impact of environmental factors. *Aquat. Toxicol.* **2017**, 191, 141-163. doi:10.1016/j.aquatox.2017.08.005.

78. Ebert, D., *Ecology, Epidemiology, and Evolution of Parasitism in Daphnia [Internet]*, Bethesda (MD): National Center for Biotechnology Information (US), 2005, Available from: http://www.ncbi.nlm.nih.gov/entrez/query.fcgi?db=Books.
79. Guilhermino, L.; Diamantino, T.; Silva, M.C., Soares, A.M. Acute toxicity test with Daphnia magna: an alternative to mammals in the prescreening of chemical toxicity? *Ecotoxicol. Environ. Saf.* **2000**, 46, 357-362. doi:10.1006/eesa.2000.1916.
80. Tkaczyk, A.; Bownik, A.; Dudka, J.; Kowal, K., Ślaska, B. Daphnia magna model in the toxicity assessment of pharmaceuticals: A review. *Sci. Total Environ.* **2021**, 763, 143038. doi:10.1016/j.scitotenv.2020.143038.
81. Mu, X., Leblanc, G.A. Cross communication between signaling pathways: juvenoid hormones modulate ecdysteroid activity in a crustacean. *J. Exp. Zool. A Comp. Exp. Biol.* **2004**, 301, 793-801. doi:10.1002/jez.a.104.
82. Kang, Y.; Yan, X.; Li, L.; Zhang, Q.; Zeng, L., Luo, J. Daphnia magna may serve as a powerful tool in screening endocrine disruption chemicals (EDCs). *Environ. Sci. Technol.* **2014**, 48, 881-882. doi:10.1021/es405379p.
83. Alla, L.N.R.; Monshi, M.; Siddiqua, Z.; Shields, J.; Alame, K.; Wahls, A.; Akemann, C.; Meyer, D.; Crofts, E.J.; Saad, F.; et al. Detection of endocrine disrupting chemicals in Danio rerio and Daphnia pulex: Step-one, behavioral screen. *Chemosphere* **2021**, 271, 129442. doi:10.1016/j.chemosphere.2020.129442.
84. Cho, H.; Ryu, C.S.; Lee, S.A.; Adeli, Z.; Meupea, B.T.; Kim, Y., Kim, Y.J. Endocrine-disrupting potential and toxicological effect of para-phenylphenol on Daphnia magna. *Ecotoxicol. Environ. Saf.* **2022**, 243, 113965. doi:10.1016/j.ecoenv.2022.113965.
85. Colbourne, J.K.; Pfrender, M.E.; Gilbert, D.; Thomas, W.K.; Tucker, A.; Oakley, T.H.; Tokishita, S.; Aerts, A.; Arnold, G.J.; Basu, M.K.; et al. The ecoresponsive genome of Daphnia pulex. *Science* **2011**, 331, 555-561. doi:10.1126/science.1197761.
86. Kashian, D.R., Dodson, S.I. Effects of vertebrate hormones on development and sex determination in Daphnia magna. *Environ. Toxicol. Chem.* **2004**, 23, 1282-1288. doi:10.1897/03-372.

Chapter 2. Aim and structure of the thesis

Motivation

SRD5A inhibitors, such as dutasteride and finasteride, have gained significant prominence as therapeutic agents for the treatment of androgenetic alopecia and benign prostatic hyperplasia, driven by the growing demand for effective hair loss solutions. While widely used, their extensive usage and persistence in the environment have raised concerns about potential environmental impacts, particularly on aquatic ecosystems. As these compounds enter waterways, they may disrupt hormonal systems in aquatic species, posing serious risks to biodiversity and environmental stability. Traditionally, SRD5A has been studied for its androgenic function, primarily its role in converting testosterone to DHT, a potent androgen essential for regulating various physiological processes. However, recent studies suggest that DHT may also play an estrogenic role, as its reduction has been associated with decreased E2 levels, which, in turn, impact VTG production—a critical factor in reproductive function. Despite these findings, the mechanistic link between decreased DHT and reduced E2 levels remains poorly understood, warranting further exploration. Adding to these concerns, recent genomic studies have identified SRD5A-like genes in *D. magna*, a keystone species in freshwater ecosystems, raising the possibility that SRD5A inhibitors, which persist in aquatic environments, may similarly disrupt hormonal processes in invertebrates. Such disruptions could have cascading effects on aquatic food webs, underscoring the need to investigate the environmental implications of SRD5A inhibition. Leveraging the AOP framework, which systematically links molecular-level changes to population-level effects, the inclusion of *D. magna* as a target species will expand the scope of regulatory toxicology and enhance chemical risk assessments. By addressing these knowledge gaps, this research aims to contribute to the development of a robust AOP framework for SRD5A inhibitors and their environmental impacts.

Structure of the Thesis

After the introduction, the thesis is organized into four main chapters. The first chapter presents the development and application of a screening assay for SRD5A activity to evaluate the potency of inhibitors across species. This study has been published in *Molecules*. The second chapter explores the effects of SRD5A inhibition on reproduction-related pathways in zebrafish embryos and was published in *Comparative Biochemistry and Physiology Part C: Toxicology & Pharmacology*. The third chapter focuses on steroid hormone profiling to investigate the effects of SRD5A inhibition, with the study currently being prepared for publication. The fourth chapter examines the effects of SRD5A inhibitors on reproductive changes in *D. magna*, specifically through lipid alterations, and was published in *Ecotoxicology and Environmental Safety*. Finally, the thesis concludes with a summary and discussion of the overall findings. The published papers in their original formats are included in the appendix.

Chapter 3. Screening of SRD5A activity and inhibition

Contribution

As accepted in: Kim, D.†; **Cho, H.**†; Eggers, R.; Kim, S.K.; Ryu, C.S.; Kim, Y.J. Development of a Liquid Chromatography/Mass Spectrometry-Based Inhibition Assay for the Screening of Steroid 5-α Reductase in Human and Fish Cell Lines. *Molecules* 2021, 26, doi:10.3390/molecules26040893. (†, These authors equally contributed to this work).

Authorship contributions

Chang Seon Ryu, Sang Kyum Kim, And Young Jun Kim conceived and designed the experiments; Dahye Kim, **Hyunki Cho**, and Ruth Eggers performed the experiments, and analyzed the data; Dahye Kim, **Hyunki Cho**, and Chang Seon Ryu wrote the paper; Sang Kyum Kim, Chang Seon Ryu, and Young Jun Kim reviewed and edited the entire manuscript. All authors have read and agreed to the published version of the manuscript.

Relation to the thesis

To evaluate SRD5A activity and the inhibitory effects of SRD5A inhibitors, a screening method utilizing liquid chromatography-tandem mass spectrometry (LC-MS/MS) was developed. To overcome sensitivity issue in detecting DHT via LC-MS/MS, a picolinic acid derivatization method was applied. SRD5A activity was assessed in both human and fish models, with enzymatic activity parameters analyzed through Km and Vmax values using the Michaelis-Menten equation. Additionally, finasteride and dutasteride were tested as SRD5A inhibitors, and their inhibitory effects were compared through co-treatment with testosterone to determine IC_{50} values.

In this chapter, the relationship between SRD5A inhibition (MIE) and reduced DHT levels (KE) was investigated using multiple models. Quantitative, dose-dependent data on SRD5A activity and inhibition were obtained to identify species-specific differences in enzymatic responses to finasteride and dutasteride. These findings enhance our understanding of the mechanistic link between MIE and KE, providing foundational data for the development of AOPs related to SRD5A inhibition. Additionally, the comparative analysis of SRD5A inhibition in human and fish models offers robust quantitative evidence to support AOP applications and inform chemical risk assessments across species.

3.1 Abstract

SRD5A is responsible for the reduction of steroids to 5α reduced metabolites, such as the reduction of testosterone to DHT. A new AOP for SRD5A inhibition to reduce female reproduction in fish (AOP 289) is under development to clarify the antiestrogenic effects of SRD5A inhibitors in female fish. A sensitive method for the DHT analysis using chemical derivatization and liquid chromatography–tandem mass spectrometry was developed. A cell-based SRD5A inhibition assay that utilizes human cell lines, fish cell lines, and a transient overexpression system, was developed. The measured IC_{50} values of two well-known SRD5A inhibitors, finasteride and dutasteride, were comparable in the different systems. The IC_{50} of dutasteride in the fish cell lines was higher than that in the human cell lines. In addition, finasteride showed a higher IC_{50} against the RTG-2 cell line. These results demonstrated that SRD5A inhibition could differ in terms of structural characteristics among species. The assay has high sensitivity and reproducibility and is suitable for the application in SRD5A inhibition screening for various EDCs. Future studies will continue to evaluate the quantitative inhibition of SRD5A by EDCs to compare the endocrine-disrupting pathway in different species.

Keywords: SRD5A; dihydrotestosterone; *in vitro*; dutasteride; finasteride; AOP

3.2 Introduction

SRD5A is a membrane-bound protein that is responsible for reducing steroids such as testosterone, progesterone, and androstenedione to 5α reduced metabolites such as DHT, 5α-dihydroprogesterone (DHP) and androstanedione, respectively. There are three isoforms of SRD5A in humans: SRD5A1, SRD5A2, and SRD5A3. SRD5A1, and SRD5A2 have functionality for 5α reduction of steroids in humans. DHT is a more potent androgen than testosterone and has a function in androgen receptor activation [1-3]. The regulation of SRD5A is important for the treatment of benign prostate hyperplasia and prostate cancer, and SRD5A inhibitors have also been used for the treatment of baldness [4-6].

SRD5A inhibition was suggested as a new MIE in the AOP 289 [7]. AOP 289, which is entitled 'Inhibition of 5α-reductase leading to impaired fecundity in female fish', describes the effects of SRD5A on reducing estradiol and further decreasing egg production via vitellogenin reduction. SRD5A is expressed in both sexes, and DHT is involved in E2 level regulation [8]. Even though a lower expression of SRD5A was detected in females, its inhibition reduced the fecundity of fish and affected several aspects of reproductive endocrine functions in both sexes of fathead minnows [9]. For the development of a quantitative AOP for SRD5A inhibition, a quantitative structure–activity relationship is required for EDC evaluation. Several methods have been described for screening the pharmacological aspects of 5AR inhibitors, but experimental data are limited in fishes for screening for endocrine disruption.

In practice, SRD5A inhibition studies are traditionally conducted using radioactive substrates with thin layer chromatography or high-performance liquid chromatography (HPLC) detection[10; 11]. A native substrate method without radiolabeled isotopes that utilizes a spectrophotometric method [12] and a

HPLC-UV detection method was also developed [13]. However, these methods have not been extensively applied due to their limitations, which include safety issues with radiometric assays and low sensitivity. The liquid chromatography-tandem mass spectrometry (LC-MS/MS) method can be used for high-throughput screening (HTS) techniques, and combinational chemistry during drug discovery and development has led to a tremendous increase in the number of compounds to be evaluated for potential SRD5A inhibition [14; 15]. Recently, sensitive chemical derivatization methods for DHT detection in LC-MS/MS were developed [16].

In the present study, using this chemical derivatization technique, a cell incubation method was developed, and the metabolites of the substrates were determined in a single assay using LC-MS/MS for HTS of 5AR inhibition. LNCaP clone FGC (LNCaP) and DU145 cells that express the SRD5A1 gene, SW-13 cells that express the SRD5A1 and SRD5A2 genes, and HEK-293 cells with transient overexpression of human and zebrafish SRD5A isozymes were compared to establish the enzyme inhibition method. In addition, to understand species differences in 5AR between fish and humans, the inhibition of SRD5A was compared in the SRD5A -expressing zebrafish liver cells (ZFL) and rainbow trout gonad cell lines (RTG-2).

3.3 Materials and Methods

3.3.1 Chemicals and reagents

Fetal bovine serum (FBS), Leibowitz's L-15 medium, the Roswell Park Memorial Institute (RPMI) 1640 medium, Ham's F12 medium, Eagle's minimal essential medium (EMEM), Dulbecco's modified Eagle's medium (DMEM), the Opti-MEM medium, a penicillin/streptomycin solution and trypsin were obtained from GIBCO (Grand Island, NY, USA). Trout serum was purchased from Caisson Laboratories (Smithfield, VA, USA). Mouse epidermal growth factor (EGF) and HEPES were purchased from Thermo Fisher Scientific (Waltham, MA, USA). Sodium bicarbonate, bovine insulin, DHT, DHT-D3 solution, methyl-tertiary-butyl ether (MTBE), triethylamine (TEA), tetrahydrofuran (THF), 2-picolinic acid (PA), 4-(dimethylamino) pyridine (DMAP), 2-methyl-6-nitrobenzoic anhydride (MNBA), and acetic acid were purchased from Sigma-Aldrich (St. Louis, MO, USA), and HPLC grade formic acid was purchased from Fisher Scientific (Pittsburgh, PA, USA). MS-grade methanol and water were obtained from VWR (Westchester, NY, USA). The stock solution and internal standard were prepared in methanol. The derivatization reagent was prepared by dissolving 25.0 mg of PA, 10.0 mg of DMAP, and 20.0 mg of MNBA in 1 mL of THF [17] and vortexing. Then, the mixture was left at room temperature for at least 5 min before the sample pretreatment.

3.3.2 Cell culture

HEK-293, LNCaP, DU-145, SW-13, and ZFL cell lines were obtained from the American Type Culture

Collection (ATCC; Manassas, VA, USA) and cultured according to their instructions. The HEK-293 cells were cultured in a high-glucose DMEM that contained 10% FBS, 100 units/mL penicillin, and 100 µg/mL streptomycin. The DU-145 cells were cultured in EMEM that contained 10% FBS, 100 units/mL penicillin, and 100 µg/mL streptomycin. The LNCaP cells were cultured in RPMI 1640 that contained 10% FBS, 100 units/mL penicillin, and 100 µg/mL streptomycin at 37 °C in 5% CO_2. SW-13 cells were cultured in Leibovitz's L-15 medium with 10% FBS at 37 °C without CO_2. ZFL cells were cultured in a complete medium that was composed of 50% L-15, 35% DMEM medium, and 15% F12 medium that contained 0.15 g/mL sodium bicarbonate, 15 mM HEPES, 0.01 mg/mL bovine insulin, 50 ng/mL mouse EGF, 5% FBS, and 0.5% trout serum at 28 °C without CO_2. RTG-2 cells were obtained from Prof. Kristin Schirmer (EAWAG, Switzerland) and cultured in the L-15 medium with 5% FBS, 100 units/mL penicillin, and 100 µg/mL streptomycin at 20 °C without CO_2.

3.3.3 Transient overexpression

Human and zebrafish SRD5A isozymes (hSRD5As and zfSRD5As) expression vectors were purchased from GenScript (Cat. #OHu02727D, pcDNA3.1+/C-(K)-DYK-SRD5A1; Cat. # OHu18065D, pcDNA3.1+/C-(K)-DYK-SRD5A2; Cat. #ODa35277, pcDNA3.1 + /C-(K)-DYK-srd5a1; Cat. #ODa35277; pcDNA3.1 + /C-(K)-DYK-srd5a2a, Cat. #ODa35087, pcDNA3.1 + /C-(K)-DYK-srd5a2b; Cat. #ODa00115, pcDNA3.1 + /C-(K)-DYK-srd5a3). Transient overexpression was induced using transfection of cDNA with lipofectamine 3000 reagents (Thermo Fisher Scientific). HEK-293 cells were seeded in 24-well plates at a density of 1.0×10^5 cells per well and incubated at 37 °C in an atmosphere of 5% CO_2. After overnight culture, 500 ng of cDNA and 0.75 µL of the Lipofectamine 3000 reagent were diluted in the Opti-MEM medium and incubated for 15 min for DNA-lipid complex formation. The DNA-lipid complex was added to the wells and incubated for 6 h. After incubation, the sample-treated medium was changed to the complete culture medium and incubated for 18 h.

3.3.4 Cell culture assay application

All cells were seeded on a 24-well plate. The seeding densities of the DU-145, LNCaP, and SW-13 cells were 0.5×10^5 cells per well. The ZFL and RTG-2 cells were seeded at densities of 1.0×10^5 cells and 2.0×10^5 cells, respectively. After overnight culture, the culture media was aspirated from each well and treated with testosterone that was diluted in the complete medium for 3 h and 6 h. In the case of transiently transfected HEK-293 cells, the testosterone treatment was applied after transient overexpression under the same conditions as other cell lines. The treated media were collected from each well and centrifuged at 3000 × g for 5 min at 4 °C. The supernatants were stored at −80 °C until needed. A selective SRD5A2 inhibitor, namely, finasteride, and a dual inhibitor of SRD5A1 and SRD5A2, namely, dutasteride, were used as inhibitors of SRD5A. The seeding conditions of all cells were the same as those previously described. After overnight culture, the culture medium was aspirated, and the cells were cotreated with a

medium that contained testosterone and inhibitors for 3 h. The medium was collected from each well and centrifuged at 3000 × g for 5 min at 4 ◦ C. The supernatants were stored at −80 ◦ C until analysis.

3.3.5 qRT-PCR

The total RNA was isolated using a column-based kit (Qiagen, Valencia, CA, USA). cDNA was synthesized from 500 ng of the total RNA using a high-capacity RNA-to-cDNA kit (Applied Biosystems, Foster City, CA, USA) according to the manufacturer's instructions. qRT-PCR assays were conducted using a TaqMan gene expression assay on a 7500 FAST real-time PCR system (Applied Biosystems). Reaction cycles were performed as follows: initial denaturation for 2 min at 5 °C, 40 cycles of amplication at 95 °C for 3 sec, and 60 °C for 30 sec. The TaqMan assay ID is as follows (Gene, assay ID): RPLO0, Hs00420895_gH; SRD5A1, Hs00165843_m1; SRD5A2, Hs00165843_m1. Relative gene expression levels were calculated using the $2^{-\Delta\Delta Ct}$ method [18].

3.3.6 Sample preparation

A method that was modified by Abe et al. (2009) was used for DHT extraction from the samples. Each sample, which included the calibration, quality control (QC), and assay medium, was placed in 1.5 mL PP tubes and spiked with a 0.5 ng/mL DHT-D3 internal standard prior to extraction. All sample tubes were vortexed for 5 s, and the samples were extracted using a liquid-liquid extraction (LLE) method via the addition of 600 µL of MTBE. The samples were vortexed and centrifuged at 4500 × g rpm for 5 min, and the organic phase was transferred into glass tubes. The extraction step was repeated once, and the organic phase extracts were dried under a stream of nitrogen. After the samples were dried, 100 µL of the derivatization reagent and 100 µL of TEA were added for DHT derivatization. The samples were vortexed and incubated at room temperature, and 1 mL of 10% acetic acid was added to stop the reaction after 30 min of incubation. The LLE step, which was conducted before the derivatization step, was repeated twice. The organic phase extracts were collected, dried under a stream of nitrogen, and reconstituted in 50 µL of 80% methanol that contained 0.1% formic acid for LC-MS/MS analysis.

3.3.7 Instrumental conditions

The extracts were analyzed for DHT via ultra-performance LC-MS/MS (Agilent 1200/6460C QQQMSD coupled Jet Stream technology electrospray ion (ESI) source; Agilent Technologies, Santa Clara, CA, USA). To separate the analytes, a Kinetex XB-C18 column (2.1 mm × 150 mm, 2.6 µm) that was fitted with a ZORBAX Eclipse Plus C18 guard column (2.1 mm × 5 mm, 1.8 µm) was used. The mobile phase solvents were 0.1% formic acid and methanol, with a flow rate of 300 µL/min for 14 min and a sample injection volume of 10 µL. The gradient started at 5% methanol, was increased to 90% with a 3 min ramp, and was maintained until 5 min. Then, the ramp was increased to 95% methanol until 13 min. At 13.1

min, the ramp was decreased to 5% methanol, which was maintained until 14 min. Mass spectrometry was conducted in the positive ion electrospray mode and multiple reaction mode (MRM) to identify and quantify DHT. The MRM transitions are 396.3 > 255.0 and 273.0 for PA-derivatized DHT and 399.3 > 258.0 and 276.0 for DHT-D3, respectively. The optimized MS conditions are as follows: gas temperature of 350 °C, gas flow of 10 L/min, nebulizer gas pressure of 45 psi, sheath gas temperature of 350 °C, sheath gas flow of 11 L/min, capillary voltage of 3500 V, nozzle voltage of 500 V, and collision energies of 16 V for DHT and 14 V for DHT-D3.

3.3.8 Calibration curve and LLOQ

A linear calibration curve was established using a standard solution that consisted of a concentration series of 0.1, 0.5, 1, 5, 10, 50, 100, 500, and 1000 nM DHT with 5 ng/mL DHT-D3. The calibrators for DHT were prepared in an assay medium with a blank (which contained only 5 ng/mL DHT-D3). To evaluate the linearity of the calibration curve, a 1/x weighting linear regression was used. The LLOQ was defined as the lowest concentration of the calibrators at which the signal sensitivity was 3-fold higher than those of the corresponding blank samples.

3.3.9 Accuracy and precision

The accuracy and precision of the method were evaluated using intra- and interday QC samples. Five replicates each of low QC, medium QC, and high QC samples were prepared by spiking into standard solutions of DHT and DHT-D3 in an assay medium. Their concentrations are 5, 50, and 500 nM, respectively, which represent 100% DHT accuracy of each QC set. The method accuracy was evaluated based on the recoveries (%) that were calculated for each QC spiking level. The precision of the method was expressed as the coefficient of variation (CV, %). CV was determined by dividing the relative standard deviations of the QC samples by the average DHT concentration of the QC samples. The interday accuracy and precision were determined via three parallel analyses of three sets of QC samples (low, medium, and high). The intraday accuracy and precision were determined via analysis of five replicate samples of each QC set for 3 consecutive days.

3.3.10 Data analysis

The LC-MS/MS data were analyzed with the MassHunter quantitative analysis software (Agilent). The DHT inhibition in the presence of inhibitors was expressed as a percentage of the corresponding control value. Each point was expressed as the mean ± S.D. A sigmoid-shaped curve was fitted to the data, and the enzyme kinetic module and inhibition parameter IC_{50} were calculated by fitting the Hill equation to the data using nonlinear regression (least-squares best fit modeling) of the plot of the percent control

activity vs. concentration of the test inhibitor using GraphPad Prism 8 (GraphPad Software Inc., San Diego, CA, USA). Control samples (without the inhibitor) were assayed in each analytical run. The amount of metabolite in each sample (relative to the control samples) was plotted vs. the inhibitor concentration.

3.4 Results

3.4.1 Method validation

3.4.1.1 Linearity of the calibration curve and LLOQ

The 1/x weighted linear regression calibration curve for DHT was obtained by plotting the MRM peak area ratio (analyte/IS) versus the concentration over the working range 0.01–1000 nM for the assay media. The 1/x weighted linear correlation coefficient (R^2) for DHT exceeded 0.995. The LLOQ of this method for DHT was 0.05 nM. Chromatograms of 2-PA-derivatized DHT and DHT-d3 are presented in Figure 3.1.

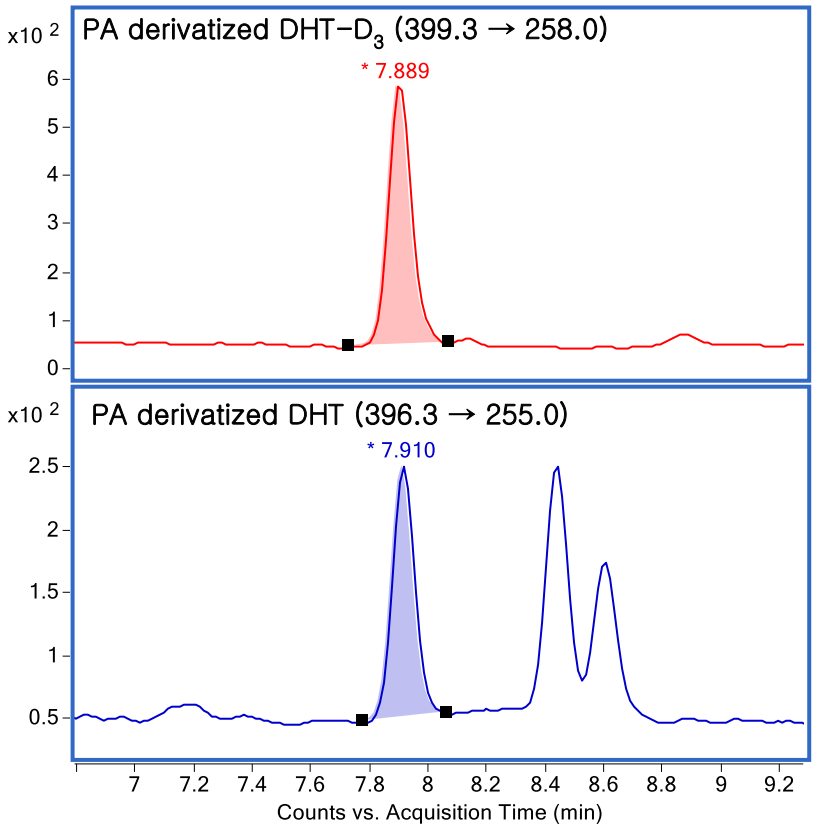

Figure 3.1 Chromatograms of PA-derivatized DHT and DHT-D3.

3.4.1.2 Accuracy and precision

The method accuracy and precision that were determined using the low QC, medium QC and high QC samples are presented in Table 3.1. The inter day accuracies for the low, medium, and high QC samples were 102.3, 104.0, and 95.0%, respectively, and the intraday accuracies for the low, medium, and high QC samples were 101, 98.9, and 95.5%, respectively. The interday precisions were 1.3% for low QC, 0.7% for medium QC, and 1.6% for high QC, and the intraday precisions were 0.9% for low QC, 2.5% for medium QC, and 1.3% for high QC. Acceptable method accuracies and precisions on the QC samples were obtained.

Table 3.1 The method accuracy and precision (*n*=5).

	Low QC	Med QC	High QC
CV % - inter day[a]	1.3	0.7	1.6
CV % - intra day[b]	0.9	2.5	1.3
Accuracy % - inter day	102.3	104.0	95.0
Accuracy % - intra day	101.0	98.9	95.5

[a], Coefficient of variation within days; [b], Coefficient of variation between 3 consecutive days.

3.4.2 Assay application in human cell lines

The gene expression levels of SRD5A1 and SRD5A2 in LNCaP, DU-145, and SW-13 cells are presented in Figure S3.1. All cell lines showed SRD5A1 expression, but SRD5A2 expression was identified only for SW-13 cells. For the calculation of K_M, testosterone treatment was applied in increments of 0 to 10 μM in the LNCaP and DU-145 cells and in increments of 0 to 50 μM in the SW-13 cells for 3 h. The *de novo* synthesized DHT levels were measured (Figure 3.2). The calculated values of V_{max} and K_M are presented in Table 3.2. The V_{max} value of the DU-145 cells was 34.00 pmol/h, which exceeded those of the other two cell lines. Based on the calculated K_M value as the substrate concentration, inhibition assays were conducted by treating the cells with a selective SRD5A2 inhibitor, namely, finasteride, and a dual SRD5A1 and SRD5A2 inhibitor, namely, dutasteride (Figure 3.3). The IC_{50} value of each inhibitor was calculated and is presented in Table 3.

Table 3.2. V_{max} and K_M value at each cell lines.

		V_{max} (pmol h^{-1}; CI*)	K_M (μM; CI*)
Human cell lines	LNCaP	17.40 (15.46-20.32)	15.10 (12.35-19.25)
	DU-145	34.00 (29.97-40.70)	9.15 (7.01-12.81)
	SW-13	13.23 (12.52-14.01)	19.42 (17.16-21.88)
hSRD5A overexpression lines	hSRD5A1	3.86 (3.54-4.21)	2.29 (1.70-3.09)
	hSRD5A2	9.89 (8.93-10.92)	0.36 (0.18-0.65)
Fish cell lines	ZFL	52.49 (48.09-57.10)	0.46 (0.31-0.68)
	RTG-2	5.89 (5.35-6.47)	1.12 (0.78-1.61)
zfSRD5A overexpression lines	zfSRD5A1	24.48 (21.65-28.41)	35.24 (28.35-45.06)
	zfSRD5A2a	11.54 (8.61-18.56)	25.88 (17.20-46.99)
	zfSRD5A2b	5.79 (5.56-6.04)	12.40 (11.23-13.72)
	zfSRD5A3	8.66 (8.13-9.28)	22.53 (19.82-25.78)

*, The values in parentheses are 95% confidence intervals (CI).

Table 3.3. IC_{50} values of finasteride and dutasteride in each cell lines.

		IC_{50} value	
		Finasteride (nM; 95% CI*)	Dutasteride (nM; 95% CI*)
Human cell lines	LNCaP	251.0 (197.1-314.7)	1.26 (1.02-1.57)
	DU-145	308.5 (217.0-415.5)	3.83 (3.10-4.78)
	SW-13	213.5 (180.2-250.7)	4.75 (4.26-5.32)
hSRD5A overexpression lines	hSRD5A1	341.1 (270.1-429.0)	1.37 (0.86-2.17)
	hSRD5A2	69.8 (33.3-133.1)	1.19 (0.96-1.47)
Fish cell lines	ZFL	142.4 (121.5-165.7)	7.33 (5.49-10.13)
	RTG-2	2667 (2394-2952)	13.19 (10.73-16.54)
zfSRD5A overexpression lines	zfSRD5A1	2154 (1663-2943)	28.85 (19.79-44.08)
	zfSRD5A2a	298.9 (266.6-335.6)	43.17 (36.81-50.93)
	zfSRD5A2b	112.0 (65.8-142.1)	2.76 (2.15-3.52)
	zfSRD5A3	303.3 (269.0-342.7)	10.84 (9.21-12.91)

*, The values in parentheses are 95% confidence intervals (CI).

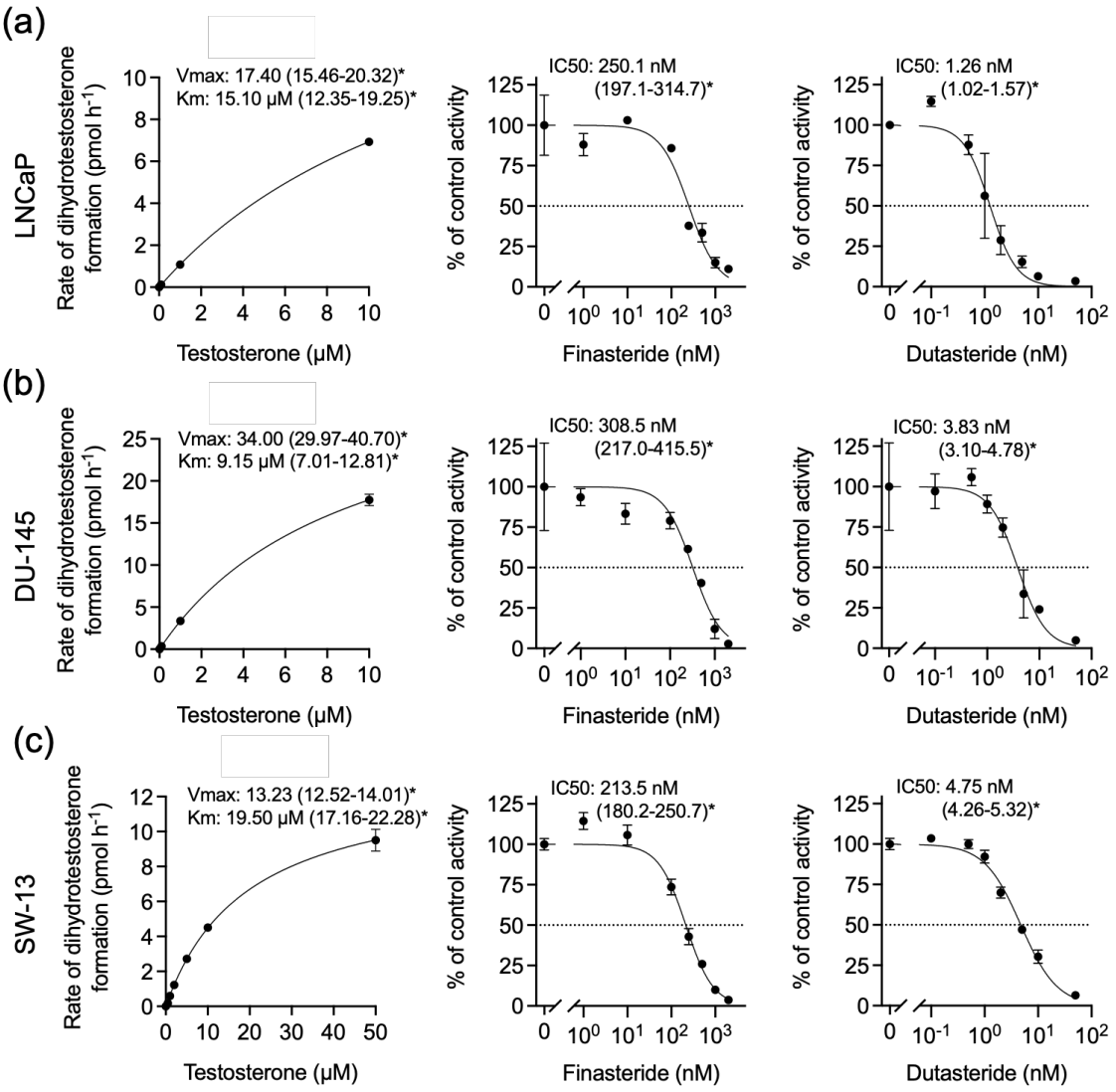

Figure 3.2 Activity of of SRD5A and inhibitory effects of finasteride and dutasteride on (a) LNCaP, (b) DU-145, and (c) SW-13 cells. The data are expressed as the mean ± standard deviation (SD) of three repeated experiments. *, The values in parentheses are 95% confidence intervals.

3.4.3 Assay application in hSRD5A-overexpressing HEK-293 cells

For the calculation of K_M, testosterone was added in increments of 0 to 50 μM to non-vector- (Figure S3.2) and HEK-293-hSRD5A1 cells and in increments of 0 to 10 μM to HEK-293-hSRD5A2 cells 24 h after transfection. The DHT levels were measured (Figure 3.3). The calculated K_M and V_{max} values are presented in Table 3.2. SRD5A2 showed a higher production rate (V_{max} and K_M were 9.89 and 0.34 μM, respectively) due to the higher affinity of the enzyme for testosterone. Based on the calculated K_M values, inhibition assays were conducted by treating the cells with selective SRD5A2 inhibitor finasteride and the dual SRD5A1 and SRD5A2 inhibitor dutasteride (Figure 3.3). The calculated IC_{50} values were presented in Table 3.3.

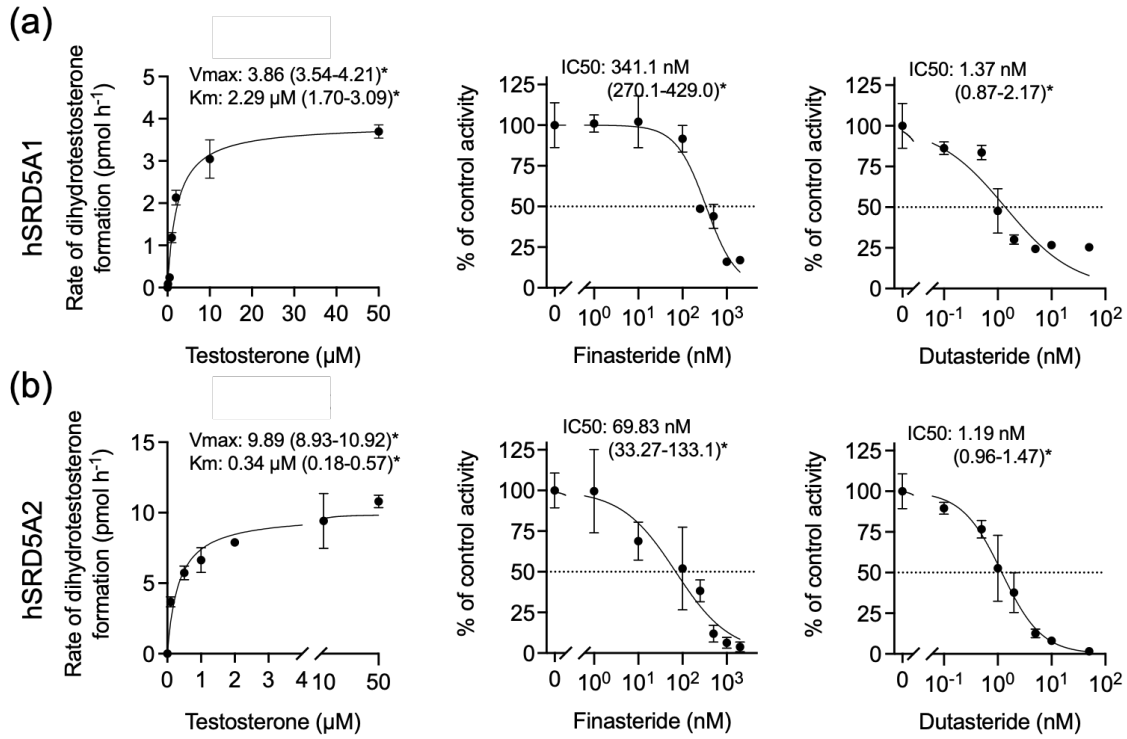

Figure 3.3 Activity of human SRD5Aand inhibitory effects of finasteride and dutasteride on (a) HEK-293-hSRD5A1 and (b) HEK-293-hSRD5A2 cells. The data are expressed as the mean ± standard deviation (SD) of three repeated experiments. *, The values in parentheses are 95% confidence intervals.

3.4.4 Assay application in a fish cell lines

For the calculation of K_M for optimized assay conditions, ZFL and RTG-2 cells were treated with testosterone in increments of 0 to 50 μM. The DHT levels were measured (Figure 3.4). The calculated K_M and V_{max} values are presented in Table 3.2. Based on the calculated K_M values, inhibition assays were conducted (Figure 3.4). Both the RTG-2 and ZFL cells showed lower K_M values than human cell lines. The V_{max} value of the ZFL cells (52.49 pmol/h) substantially exceeded those of the 5AR-overexpressing cell line and the human cell lines (17.40 in LNCaP, 34.00 in DU-145, and 13.23 in SW-13). The IC_{50} value of finasteride in the RTG-2 cells was 2497 nM, which exceeded those of the 5AR-overexpressing cell line and the human cell lines (1.37 in HEK-293-hSRD5A1 and 1.19 in HEK-293-hSRD5A2) (Table 3.3). Furthermore, the IC_{50} values of dutasteride in both fish cell lines exceeded those of the 5AR-overexpressing cell line and the human cell lines.

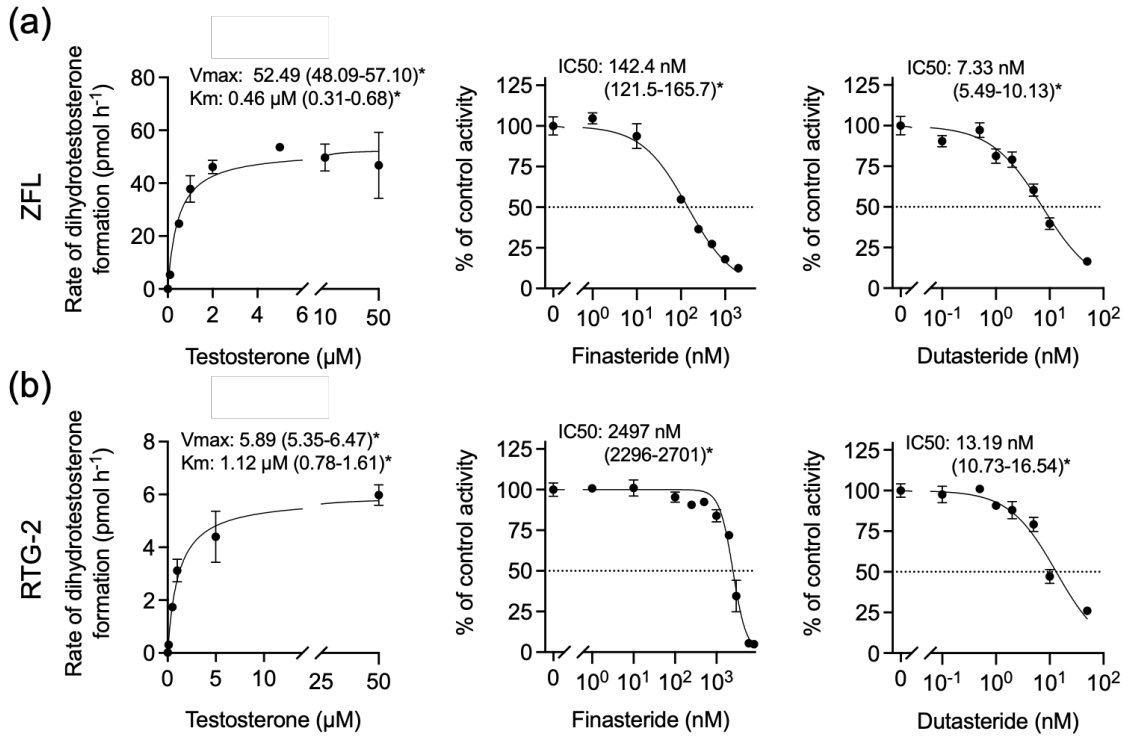

Figure 3.4 Activity of SRD5A and inhibitory effects of finasteride and dutasteride on (a) ZFL and (b) RTG-2 cells. The data are expressed as the mean ± standard deviation (SD) of three repeated experiments. *, The values in parentheses are 95% confidence intervals.

3.4.5 Assay application in zfSRD5A-overexpressing HEK-293 cells

For the calculation of K_M, testosterone was treated to different concentration from 0 to 33.3 μM. DHT levels were measured (Figure. 3.6). The calculated K_M values for the zfSRD5A isoforms (zfSRD5A1, zfSRD5A2a, zfSRD5A2b, and zfSRD5A3) were 35.24, 25.88, 12.40, and 22.53 μM, respectively (Table 3.2). Based on the calculated K_M value, an inhibition assay was conducted by co-treating the cells with different concentrations of finasteride and dutasteride with testosterone (Figure. 3.6). IC_{50} values of finasteride in each isoform (zfSRD5A1, zfSRD5A2a, zfSRD5A2b, and zfSRD5A3) were 2154, 298.9, 112.0, and 303.3 nM, respectively (Table 3.3). IC_{50} values of dutasteride in each isoform (zfSRD5A1, zfSRD5A2a, zfSRD5A2b, and zfSRD5A3) were 28.85, 43.17, 2.76, and 10.84 nM, respectively.

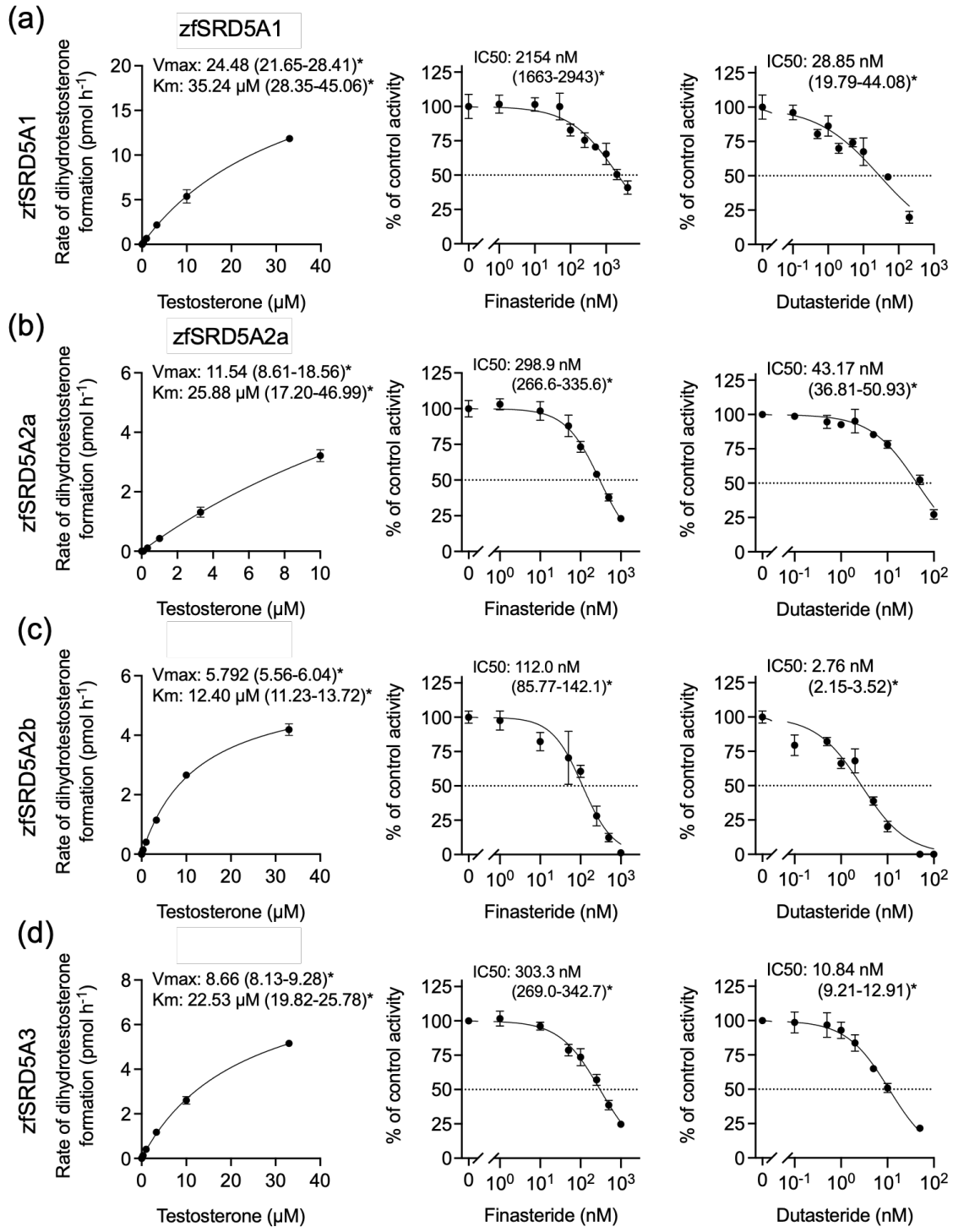

Figure 3.6 Activity of SRD5A and inhibitory effects of finasteride and dutasteride on (a) HEK-293-zfSRD5A1, (b) HEK-293-zfSRD5A2a, (c) HEK-293-zfSRD5A2b, and (d) HEK-293-zfSRD5A23 cells. The data are expressed as the mean ± standard deviation (SD) of three repeated experiments. *, The values in parentheses are 95% confidence intervals.

3.5 Discussion

Fluorinated anhydride acylation methods are widely used for gas chromatography mass spectrometry (GC-MS) for steroid quantification. Similar to the acylation reaction of fluorinated anhydrides and the hydroxyl group of the seventeenth carbon position in the steroid reaction, derivatization using PA showed a higher sensitivity in the detection of 17-OH steroids, such as corticosteroids, in ESI-LC/MS [17]. Recently, LC-MS based quantification methods for androgens such as DHT that utilize various sample sources were developed, and SRD5A inhibition studies were conducted [19; 16; 20-23]. The method in the present study requires an additional derivatization step compared to the direct measurement. However, compared to these reports, the LLOQ of DHT (14.5 pg/mL) in the present study showed higher sensitivity than hydroxylamine hydrochloride derivatization [21] or direct measurement [19; 24] by using LLE after PA derivatization. Also, methods using solid-phase extraction have been developed for the detection of steroids, but these methods are not efficient in time and cost-effective compared with LLE [16; 25; 26]. The present study also used 2 times the LLE step using MTBE after and before derivatization, this process increased the recovery of target compounds from 69 to 74% to 89–108% [16]. The lower limit of quantification of other studies using spectrophotometric method for DHT were from 0.2–10 nM [12; 20; 27], and other studies using radioactive substrates were range of 25 to 250 ng. The comparison study between immunoassay and LC/MS detection of DHT showed that the variation of detection was relatively more significant in immunoassay than in MS systems [28]. Thus, the method in the present study has an advantage for the detection of DHT than other methods.

A cell-based assay has additional factors that need to optimizing assay condition, but it has more reliability to *in vivo* system than purified enzyme or centrifuged fraction. Inhibition of SRD5A reduced the DHT levels in tissues and can affect the androgen receptor (AR) expression [29-31]. Steroids such as androgens, estrogens, and corticosteroids and inhibitors of SRD5A are widely utilized in pharmacological applications, and these chemicals may act as EDCs and substantially impact fish and other species that are exposed to the environment [32; 33]. We compared the SRD5A activities and inhibition rates of SRD5A by finasteride and dutasteride between human cell lines and fish cell lines. The V_{max} and K_M values in human cell lines were the largest in the DU-145 cells (Table 3.2). This result may be related to AR signaling. The LNCaP cell line was AR-positive, whereas the DU-145 cell line was AR-negative. DHT can be metabolized to DHT-glucuronide by the uridine diphosphate-glucuronosyltransferase (UGT) 2B15 and 2B17 enzymes in prostate cells, and these enzymes are modulated by AR [34]. It is possible that the rate of DHT production in AR-negative DU-145 cells exceeds those in other cell lines. The optimal pH of SRD5A1 activity is a broad range from 6.0 to 8.5, and the range for SRD5A2 is from 5.0 to 5.5 [34; 12; 35]. The steroid affinity of SRD5A2 is 10–20 times higher than that of SRD5A1 under optimal conditions [36].

Under transient transfection conditions, the V_{max} values in HEK-293-hSRD5A1 and HEK-293-hSRD5A2 were approximately 2 times and 5 times larger, respectively, than those of the nontransfected HEK-293

cells. The K_M values in HEK-293-hSRD5A1 and HEK-293-hSRD5A2 were approximately 3.3 times and 21 times smaller, respectively. The transfected cell lines did not show a higher V_{max} compared to human cell lines, but the K_M values decreased; hence, we assume that transient conditions can be used for the comparison of specific enzyme inhibition.

Both fish cell lines were more sensitive to testosterone treatment than human cell lines, and the ZFL cells were more sensitive than the RTG-2 cells. Other studies showed that the activity of SRD5A in goldfish (*Carassius auratus*) was high in nonreproductive tissues such as the liver, brain and pituitary tissues, and it was reported that the expression pattern of SRD5A2 in toadfish (*Opsanus tau*) was significantly higher in the liver than in the gonad, in contrast to that in humans [37; 38]. In the case of rainbow trout (*Oncorhynchus mykiss*), SRD5A activity was confirmed in the skin of males and females [39; 40]. Although we did not measure the SRD5A activity in whole tissue cells, our results demonstrated that fish cell lines are more sensitive to testosterone than human cell lines. The results showed a clear difference in steroid metabolism between the human and fish cell lines. In addition, the activity of SRD5A in fish liver cells exceeded that in gonad cells.

The results of the SRD5A inhibition assay demonstrated that dutasteride was more potent than finasteride in all cell lines. This is because dutasteride, which is a SRD5A dual inhibitor, had a higher SRD5A inhibition efficiency, and this tendency was similar to that observed in previous studies [39; 41]. However, all the fish cell lines except ZFL on finasteride showed relatively lower sensitivity than human cell lines, and the IC_{50} value of RTG-2 on finasteride was 14 times larger than those on other cell lines. The IC_{50} values of dutasteride in fish cell lines exceeded those in human cell lines.

Similar to our results, other studies also reported that the activity of inhibitors differs among species. The inhibitory effects of finasteride, which mainly inhibits SRD5A2, were similar among dogs, monkeys, and humans, whereas finasteride inhibited both SRD5A1 and SRD5A2 in rats [42; 43]. In addition, in a comparison of rat and human IC_{50} values comparisons of finasteride using rat SRD5A in prostate microsome were 11 nM, 13 nM, and 237 nM, and IC_{50} values of dutasteride to rat and human SRD5A were in the range of 0.2–7 nM [44-46; 15; 47; 48]. It was suggested that the difference in amino acid sequences may present a differential response to inhibitors [43]. The amino acid sequence identity of SRD5A1 in humans and fish was approximately 50.2–51.7%, and for SRD5A2 the amino acid identity was detected as 42.4–52.3% (Table 3.4). Due to the difference in amino acid sequences, the enzymes may differ structurally, and accordingly, the interactions between the substrate or inhibitor and the enzymes can also differ. This suggests that known EDCs may exert various adverse effects on several species through other interactions; thus, future studies are necessary for identifying differences in the impact of EDCs among species.

Table 4. Percentage of amino acid identity of human, zebrafish and rainbow trout SRD5As.

	Zebrafish SRD5A1	Rainbow trout SRD5A1
Human SRD5A1	51.7	50.2

	Zebrafish		Rainbow trout
	SRD5A2a	SRD5A2b	SRD5Aa
Human SRD5A2	52.3	42.4	50.2

Data was compared with human SRD5As amino acid sequence. The amino acid sequence and percentage of amino acid identity was compared using NCBI's BLAST (http://blast.ncbi.nlm.nih.gov/Blast.cgi) and UniProt (http://www.uniprot.org). The sequences used for analysis are following (species, gene_GenBank GI ID): (Human, SRD5A1_4507201, SRD5A2_39812447); (Zebrafish, srd5a1_11549628, SRD5A2a_6-2955375, SRD5A2b_62202806); (Rainbow trout, SRD5A1_1211289547, SRD5A2a_1211257249).

3.6 Conclusion

The present study established cell-based SRD5A inhibition assay models using quantitative LC-MS/MS analysis. Using this method, all the fish cell lines except the ZFL cell line for finasteride showed significantly higher IC_{50} values for dutasteride and finasteride. This method can be used as a tool for SRD5A inhibitor screening in the early stages of drug discovery. In future studies, the inhibitory potency of chemicals will be evaluated for predicting endocrine disruption via a SRD5A inhibition assay to develop quantitative AOPs for SRD5A inhibition in fishes.

3.7 Acknowledgments

This research was supported by a National Research Council of Science and Technology (NST) grant by the Korean government (MSIP) (No. CAP-17-01-KIST Europe) and the Korea Institute of Science and Technology Europe basic research program (Project no. 12101).

3.8 Bibliography

1. Bruchovsky, N., Wilson, J.D. The conversion of testosterone to 5-alpha-androstan-17-beta-ol-3-one by rat prostate in vivo and in vitro. *J. Biol. Chem.* **1968**, 243, 2012-2021.
2. Langlois, V.S.; Zhang, D.; Cooke, G.M., Trudeau, V.L. Evolution of steroid-5alpha-reductases and comparison of their function with 5beta-reductase. *Gen. Comp. Endocrinol.* **2010**, 166, 489-497. doi:10.1016/j.ygcen.2009.08.004.
3. Russell, D.W., Wilson, J.D. Steroid 5 alpha-reductase: two genes/two enzymes. *Annu. Rev. Biochem.* **1994**, 63, 25-61. doi:10.1146/annurev.bi.63.070194.000325.

4. Diani, A.R.; Mulholland, M.J.; Shull, K.L.; Kubicek, M.F.; Johnson, G.A.; Schostarez, H.J.; Brunden, M.N., Buhl, A.E. Hair growth effects of oral administration of finasteride, a steroid 5 alpha-reductase inhibitor, alone and in combination with topical minoxidil in the balding stumptail macaque. *J. Clin. Endocrinol. Metab.* **1992**, 74, 345-350. doi:10.1210/jcem.74.2.1309834.
5. McConnell, J.D.; Roehrborn, C.G.; Bautista, O.M.; Andriole, G.L., Jr.; Dixon, C.M.; Kusek, J.W.; Lepor, H.; McVary, K.T.; Nyberg, L.M., Jr.; Clarke, H.S.; et al. The long-term effect of doxazosin, finasteride, and combination therapy on the clinical progression of benign prostatic hyperplasia. *N. Engl. J. Med.* **2003**, 349, 2387-2398. doi:10.1056/NEJMoa030656.
6. McConnell, J.D.; Wilson, J.D.; George, F.W.; Geller, J.; Pappas, F., Stoner, E. Finasteride, an inhibitor of 5 alpha-reductase, suppresses prostatic dihydrotestosterone in men with benign prostatic hyperplasia. *J. Clin. Endocrinol. Metab.* **1992**, 74, 505-508. doi:10.1210/jcem.74.3.1371291.
7. AOP-Wiki Inhibition of 5α-reductase leading to impaired fecundity in female fish. *Society for Advancement of AOPs [Online]*, April 29, 2023, Available from: https://aopwiki.org/aops/289.
8. García-García, M.; Sánchez-Hernández, M.; García-Hernández, M.P.; García-Ayala, A., Chaves-Pozo, E. Role of 5α-dihydrotestosterone in testicular development of gilthead seabream following finasteride administration. *J. Steroid Biochem. Mol. Biol.* **2017**, 174, 48-55. doi:10.1016/j.jsbmb.2017.07.024.
9. Margiotta-Casaluci, L.; Courant, F.; Antignac, J.P.; Le Bizec, B., Sumpter, J.P. Identification and quantification of 5α-dihydrotestosterone in the teleost fathead minnow (Pimephales promelas) by gas chromatography-tandem mass spectrometry. *Gen. Comp. Endocrinol.* **2013**, 191, 202-209. doi:10.1016/j.ygcen.2013.06.017.
10. Andersson, S.; Bishop, R.W., Russell, D.W. Expression cloning and regulation of steroid 5 alpha-reductase, an enzyme essential for male sexual differentiation. *J. Biol. Chem.* **1989**, 264, 16249-16255.
11. Raynaud, J.P.; Cousse, H., Martin, P.M. Inhibition of type 1 and type 2 5alpha-reductase activity by free fatty acids, active ingredients of Permixon. *J. Steroid Biochem. Mol. Biol.* **2002**, 82, 233-239. doi:10.1016/s0960-0760(02)00187-5.
12. Iwai, A.; Yoshimura, T.; Wada, K.; Watabe, S.; Sakamoto, Y.; Ito, E., Miura, T. Spectrophotometric method for the assay of steroid 5α-reductase activity of rat liver and prostate microsomes. *Anal Sci* **2013**, 29, 455-459. doi:10.2116/analsci.29.455.
13. Matsuda, H.; Sato, N.; Yamazaki, M.; Naruto, S., Kubo, M. Testosterone 5alpha-reductase inhibitory active constituents from Anemarrhenae Rhizoma. *Biol. Pharm. Bull.* **2001**, 24, 586-587. doi:10.1248/bpb.24.586.
14. Abe, M.; Ito, Y.; Oyunzul, L.; Oki-Fujino, T., Yamada, S. Pharmacologically relevant receptor binding characteristics and 5alpha-reductase inhibitory activity of free Fatty acids contained in saw palmetto extract. *Biol. Pharm. Bull.* **2009**, 32, 646-650. doi:10.1248/bpb.32.646.
15. Mitamura, K.; Narukawa, H.; Mizuguchi, T., Shimada, K. Degradation of Estrogen Conjugates Using Titanium Dioxide as a Photocatalyst. *Anal. Sci.* **2004**, 20, 3-4. doi:10.2116/analsci.20.3.
16. Gorityala, S.; Yang, S.; Montano, M.M., Xu, Y. Simultaneous determination of dihydrotestosterone and its metabolites in mouse sera by LC-MS/MS with chemical derivatization. *J. Chromatogr. B Analyt. Technol. Biomed. Life Sci.* **2018**, 1090, 22-35. doi:10.1016/j.jchromb.2018.05.008.
17. Yamashita, K.; Takahashi, M.; Tsukamoto, S.; Numazawa, M.; Okuyama, M., Honma, S. Use of novel

picolinoyl derivatization for simultaneous quantification of six corticosteroids by liquid chromatography-electrospray ionization tandem mass spectrometry. *J. Chromatogr. A* **2007**, 1173, 120-128. doi:10.1016/j.chroma.2007.10.023.

18. Schmittgen, T.D., Livak, K.J. Analyzing real-time PCR data by the comparative CT method. *Nat. Protoc.* **2008**, 3, 1101-1108. doi:10.1038/nprot.2008.73.
19. Cao, Z.; Lu, Y.; Cong, Y.; Liu, Y.; Li, Y.; Wang, H.; Zhang, Q.; Huang, W.; Liu, J.; Dong, Y.; et al. Simultaneous quantitation of four androgens and 17-hydroxyprogesterone in polycystic ovarian syndrome patients by LC-MS/MS. *J. Clin. Lab. Anal.* **2020**, e23539. doi:10.1002/jcla.23539.
20. Jain, R.; Monthakantirat, O.; Tengamnuay, P., De-Eknamkul, W. Identification of a new plant extract for androgenic alopecia treatment using a non-radioactive human hair dermal papilla cell-based assay. *BMC Complement. Altern. Med.* **2016**, 16, 18. doi:10.1186/s12906-016-1004-5.
21. Srivilai, J.; Rabgay, K.; Khorana, N.; Waranuch, N.; Nuengchamnong, N., Ingkaninan, K. A new label-free screen for steroid 5α-reductase inhibitors using LC-MS. *Steroids* **2016**, 116, 67-75. doi:10.1016/j.steroids.2016.10.007.
22. Tan, J.J.Y.; Pan, J.; Sun, L.; Zhang, J.; Wu, C., Kang, L. Bioactives in Chinese Proprietary Medicine Modulates 5α-Reductase Activity and Gene Expression Associated with Androgenetic Alopecia. *Front. Pharmacol.* **2017**, 8, 194. doi:10.3389/fphar.2017.00194.
23. Wang, D., Zhang, M. Rapid quantitation of testosterone hydroxyl metabolites by ultra-performance liquid chromatography and mass spectrometry. *J. Chromatogr. B Analyt. Technol. Biomed. Life Sci.* **2007**, 855, 290-294. doi:10.1016/j.jchromb.2007.05.022.
24. Nouri, M.Z.; Kroll, K.J.; Webb, M., Denslow, N.D. Quantification of steroid hormones in low volume plasma and tissue homogenates of fish using LC-MS/MS. *Gen. Comp. Endocrinol.* **2020**, 296, 113543. doi:10.1016/j.ygcen.2020.113543.
25. Licea-Perez, H.; Wang, S.; Szapacs, M.E., Yang, E. Development of a highly sensitive and selective UPLC/MS/MS method for the simultaneous determination of testosterone and 5alpha-dihydrotestosterone in human serum to support testosterone replacement therapy for hypogonadism. *Steroids* **2008**, 73, 601-610. doi:10.1016/j.steroids.2008.01.018.
26. Yamashita, K.; Miyashiro, Y.; Maekubo, H.; Okuyama, M.; Honma, S.; Takahashi, M., Numazawa, M. Development of highly sensitive quantification method for testosterone and dihydrotestosterone in human serum and prostate tissue by liquid chromatography-electrospray ionization tandem mass spectrometry. *Steroids* **2009**, 74, 920-926. doi:10.1016/j.steroids.2009.06.007.
27. Koseki, J.; Matsumoto, T.; Matsubara, Y.; Tsuchiya, K.; Mizuhara, Y.; Sekiguchi, K.; Nishimura, H.; Watanabe, J.; Kaneko, A.; Hattori, T.; et al. Inhibition of Rat 5α-Reductase Activity and Testosterone-Induced Sebum Synthesis in Hamster Sebocytes by an Extract of Quercus acutissima Cortex. *Evid. Based Complement. Alternat. Med.* **2015**, 2015, 853846. doi:10.1155/2015/853846.
28. Dorgan, J.F.; Fears, T.R.; McMahon, R.P.; Aronson Friedman, L.; Patterson, B.H., Greenhut, S.F. Measurement of steroid sex hormones in serum: a comparison of radioimmunoassay and mass spectrometry. *Steroids* **2002**, 67, 151-158. doi:10.1016/s0039-128x(01)00147-7.
29. Audet-Walsh, É.; Yee, T.; Tam, I.S., Giguère, V. Inverse Regulation of DHT Synthesis Enzymes 5α-Reductase Types 1 and 2 by the Androgen Receptor in Prostate Cancer. *Endocrinology* **2017**, 158, 1015-

1021. doi:10.1210/en.2016-1926.

30. Bauman, T.M.; Sehgal, P.D.; Johnson, K.A.; Pier, T.; Bruskewitz, R.C.; Ricke, W.A., Huang, W. Finasteride treatment alters tissue specific androgen receptor expression in prostate tissues. *Prostate* **2014**, 74, 923-932. doi:10.1002/pros.22810.
31. Wang, L.G.; Liu, X.M.; Kreis, W., Budman, D.R. Down-regulation of prostate-specific antigen expression by finasteride through inhibition of complex formation between androgen receptor and steroid receptor-binding consensus in the promoter of the PSA gene in LNCaP cells. *Cancer Res.* **1997**, 57, 714-719.
32. Chang, H.; Wan, Y., Hu, J. Determination and source apportionment of five classes of steroid hormones in urban rivers. *Environ. Sci. Technol.* **2009**, 43, 7691-7698. doi:10.1021/es803653j.
33. Schmid, S.; Willi, R.A., Fent, K. Effects of environmental steroid mixtures are regulated by individual steroid receptor signaling. *Aquat. Toxicol.* **2020**, 226, 105562. doi:10.1016/j.aquatox.2020.105562.
34. Bao, B.Y.; Chuang, B.F.; Wang, Q.; Sartor, O.; Balk, S.P.; Brown, M.; Kantoff, P.W., Lee, G.S. Androgen receptor mediates the expression of UDP-glucuronosyltransferase 2 B15 and B17 genes. *Prostate* **2008**, 68, 839-848. doi:10.1002/pros.20749.
35. Span, P.N.; Smals, A.G.; Sweep, C.G., Benraad, T.J. Rat steroid 5 alpha-reductase kinetic characteristics: extreme pH-dependency of the type II isozyme in prostate and epididymis homogenates. *J. Steroid Biochem. Mol. Biol.* **1995**, 54, 185-192. doi:10.1016/0960-0760(95)00125-j.
36. Normington, K., Russell, D.W. Tissue distribution and kinetic characteristics of rat steroid 5 alpha-reductase isozymes. Evidence for distinct physiological functions. *J. Biol. Chem.* **1992**, 267, 19548-19554.
37. Martyniuk, C.J.; Bissegger, S., Langlois, V.S. Current perspectives on the androgen 5 alpha-dihydrotestosterone (DHT) and 5 alpha-reductases in teleost fishes and amphibians. *Gen. Comp. Endocrinol.* **2013**, 194, 264-274. doi:10.1016/j.ygcen.2013.09.019.
38. Pasmanik, M.; Schlinger, B.A., Callard, G.V. In vivo steroid regulation of aromatase and 5 alpha-reductase in goldfish brain and pituitary. *Gen. Comp. Endocrinol.* **1988**, 71, 175-182. doi:10.1016/0016-6480(88)90308-5.
39. Bramson, H.N.; Hermann, D.; Batchelor, K.W.; Lee, F.W.; James, M.K., Frye, S.V. Unique preclinical characteristics of GG745, a potent dual inhibitor of 5AR. *J. Pharmacol. Exp. Ther.* **1997**, 282, 1496-1502.
40. Latz, M., Reinboth, R. Androgen metabolism in the skin of the rainbow trout (Oncorhynchus mykiss). *Fish Physiol. Biochem.* **1993**, 11, 281-286. doi:10.1007/bf00004576.
41. Tian, G.; Mook, R.A., Jr.; Moss, M.L., Frye, S.V. Mechanism of time-dependent inhibition of 5 alpha-reductases by delta 1-4-azasteroids: toward perfection of rates of time-dependent inhibition by using ligand-binding energies. *Biochemistry* **1995**, 34, 13453-13459. doi:10.1021/bi00041a024.
42. Azzolina, B.; Ellsworth, K.; Andersson, S.; Geissler, W.; Bull, H.G., Harris, G.S. Inhibition of rat alpha-reductases by finasteride: evidence for isozyme differences in the mechanism of inhibition. *J. Steroid Biochem. Mol. Biol.* **1997**, 61, 55-64. doi:10.1016/s0960-0760(97)00002-2.
43. Levy, M.A.; Brandt, M.; Sheedy, K.M.; Holt, D.A.; Heaslip, J.I.; Trill, J.J.; Ryan, P.J.; Morris, R.A.; Garrison, L.M., Bergsma, D.J. Cloning, expression and functional characterization of type 1 and type 2 steroid 5 alpha-reductases from Cynomolgus monkey: comparisons with human and rat isoenzymes. *J. Steroid Biochem. Mol. Biol.* **1995**, 52, 307-319. doi:10.1016/0960-0760(94)00183-m.
44. di Salle, E.; Giudici, D.; Radice, A.; Zaccheo, T.; Ornati, G.; Nesi, M.; Panzeri, A.; Délos, S., Martin, P.M.

PNU 157706, a novel dual type I and II 5alpha-reductase inhibitor. *J. Steroid Biochem. Mol. Biol.* **1998**, 64, 179-186. doi:10.1016/s0960-0760(97)00158-1.

45. Häusler, A.; Allegrini, P.R.; Biollaz, M.; Batzl, C.; Scheidegger, E., Bhatnagar, A.S. CGP 53153: a new potent inhibitor of 5alpha-reductase. *J. Steroid Biochem. Mol. Biol.* **1996**, 57, 187-195. doi:10.1016/0960-0760(95)00260-x.
46. Hirosumi, J.; Nakayama, O.; Fagan, T.; Sawada, K.; Chida, N.; Inami, M.; Takahashi, S.; Kojo, H.; Notsu, Y., Okuhara, M. FK143, a novel nonsteroidal inhibitor of steroid 5 alpha-reductase: (1) In vitro effects on human and animal prostatic enzymes. *J. Steroid Biochem. Mol. Biol.* **1995**, 52, 357-363. doi:10.1016/0960-0760(94)00187-q.
47. Mitamura, K.; Ogasawara, C.; Shiozawa, A.; Terayama, E., Shimada, K. Determination method for steroid 5alpha-reductase activity using liquid chromatography/atmospheric pressure chemical ionization-mass spectrometry. *Anal. Sci.* **2005**, 21, 1241-1244. doi:10.2116/analsci.21.1241.
48. Xu, Y.; Dalrymple, S.L.; Becker, R.E.; Denmeade, S.R., Isaacs, J.T. Pharmacologic basis for the enhanced efficacy of dutasteride against prostatic cancers. *Clin. Cancer Res.* **2006**, 12, 4072-4079. doi:10.1158/1078-0432.Ccr-06-0184.

3.9 Supporting information

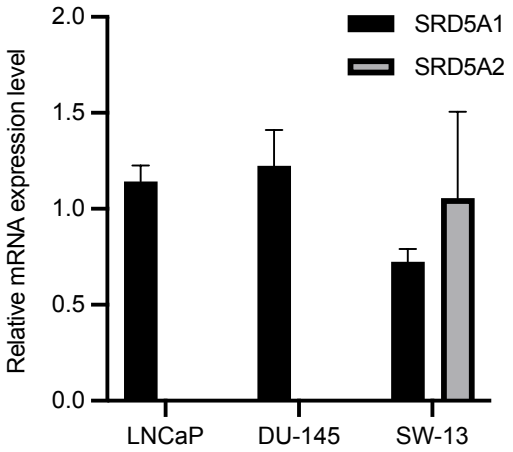

Figure S3.1 Quantitative PCR analysis for measuring the mRNA expression levels of SRD5A1 and SRD5A2 in the LNCaP, DU-145, and SW-13 cell lines. The data are expressed as the mean ± standard deviation (SD) of three repeated experiments.

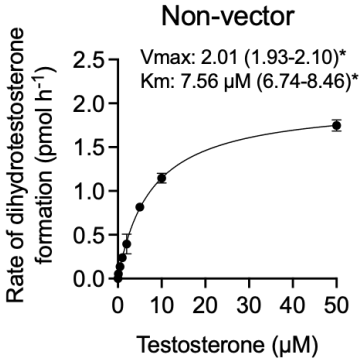

Figure S3.2 Activity of SRD5A on HEK-293 cells. The data are expressed as the mean ± standard deviation (SD) of three repeated experiments. *, The values in parentheses are 95% confidence intervals.

Chapter 4. SRD5A inhibition on zebrafish embryo

Contribution

As accepted in: **Hyunki Cho**[†], Indong Jun[†], Karim Md Adnan, Chang Gyun Park, Sang-Ah Lee, Juyong Yoon, Chang Seon Ryu, and Young Jun Kim, "Effects of 5α-reductase inhibition by dutasteride on reproductive gene expression and hormonal responses in zebrafish embryos" *Comparative Biochemistry and Physiology, Part C* 2025, 287:110048, https://doi.org/10.1016/j.cbpc.2024.110048, ([†], These authors equally contributed to this work).

Authorship contributions

Hyunki Cho: Writing–original draft and review & editing, Validation, Investigation, Formal analysis, Data curation. Indong Jun: Writing–original draft and review & editing, Visualization, Investigation, Data curation. Karim Md Adnan: Writing–review & editing, Visualization, Data curation. Chang Gyun Park: Writing–review & editing, Visualization, Formal analysis, Data curation. Sang-Ah Lee: Writing–review & editing, Visualization, Formal analysis, Data curation. Juyong Yoon: Writing–review & editing, Validation, Data curation. Chang Seon Ryu: Writing–original draft and review & editing, Visualization, Validation, Supervision, Methodology, Conceptualization. Young Jun Kim: Writing–review & editing, Supervision, Project administration, Funding acquisition.

Relation to the thesis

Chapter 4 explores the impact of SRD5A inhibition on zebrafish embryos, providing critical quantitative data on the downstream effects of decreased DHT levels caused by dutasteride exposure. While the precise mechanisms linking reduced DHT to decreased E2 levels remain unclear, this chapter demonstrates the quantitative relationships between DHT, E2, and VTG levels. Notably, molecular docking analyses suggest that the effects of dutasteride may operate independently of androgen or estrogen receptor interactions, emphasizing the importance of DHT in reproductive signaling.

This chapter contributes to the thesis by supporting the development of an AOP for SRD5A inhibition (AOP 289) through dose-dependent, quantitative data on key biomarkers associated with reproductive impairment. While the mechanistic link between DHT reduction and decreased E2 levels remains unresolved, the findings indicate the potential role of alternative synthetic pathways of DHT, underscoring the complexity of SRD5A inhibition and its broader implications.

4.1 Abstract

Steroid 5α-reductase (SRD5A) is a crucial enzyme involved in steroid metabolism, primarily converting testosterone to dihydrotestosterone (DHT). Dutasteride, an inhibitor of SRD5A types 1 and 2, is widely used for treating benign prostatic hyperplasia. An adverse outcome pathway (AOP) has been documented wherein SRD5A inhibition decreases DHT synthesis, leading to reduced levels of 17β-estradiol (E2) and vitellogenin (VTG), subsequently impairing fecundity in fish (AOP 289). However, the molecular and cellular mechanisms underlying these effects remain poorly understood. In this study, we assessed the impact of SRD5A inhibition on zebrafish embryos (Danio rerio). Exposure to dutasteride resulted in decreased DHT, E2, and VTG levels, showing a positive correlation. Dutasteride also downregulated the expression of reproduction-related genes (*srd5a2*, *cyp19a1*, *esr1*, *esr2a*, *esr2b*, and *vtg*), with interrelated reductions observed across these levels. Docking studies suggested that dutasteride's effects may operate independently of androgen receptor (AR) and estrogen receptor (ER) interactions. Furthermore, co-exposure of dutasteride (0.5 or 2 μM) with 0.5 μM DHT revealed gene expression levels comparable to the control group. These findings underscore DHT's pivotal role in modulating estrogenic function and the interplay between estrogenic and androgenic responses in vertebrates. Our proposed AOP model offers insights into mechanistic gaps, thereby enhancing current understanding and bridging knowledge disparities.

Keywords: 5α-reductase; Dutasteride; dihydrotestosterone; Reproductive toxicity; Zebrafish embryo; Adverse outcome pathway

4.2 Introduction

Dihydrotestosterone (DHT) is recognized as a potent androgen found in various classes of vertebrates, including mammals, birds, reptiles, and amphibians [1]. DHT is converted from testosterone (T) by steroid 5α-reductase (SRD5A). Although 11-ketotestosterone (11KT) is generally considered the major androgen in teleosts, DHT also plays a role in development of the male reproductive organs and is involved in the transition from the mitotic to the meiotic stage of spermatogenesis [2-5]. Exposure to DHT (200 ng/L) in male juvenile fathead minnows (*Pimephales promelas*) induces spermatogenesis, whereas, in females, it disrupts ovarian development and functions, leading to the development of spermatogenic tissue [5]. Additionally, studies have reported that exposure to SRD5A inhibitors in teleost fish results in histological alterations of the ovary, decreased proportion of vitellogenic oocytes, and fluctuations in the expression levels of reproduction-related genes and serum steroid hormone levels[3; 4]. These findings suggest a key regulatory role of DHT in reproduction of teleost fishes.

Given the importance of understanding biological mechanisms, zebrafish (*Danio rerio*) serves as an ideal sentinel for assessing aquatic toxicity across vertebrates and has become a popular model system in aquatic ecotoxicology [6; 7]. Many studies have demonstrated that the zebrafish model offers excellent versatility for applications ranging from acute systemic toxicity to chronic toxicity, teratogenicity, and

endocrine disruption [8-10]. The OECD Test Guideline 236, an acute toxicity test for fish embryos, has facilitated the use of fish embryos in toxicity studies due to advantages such as reduced ethical concerns compared to tests on adult fish, lower costs, and faster results [11].

In recent years, regulatory toxicology has embraced the 3Rs concept (replacement, reduction, and refinement of animal experiments) [12] to develop alternative approaches to conventional vertebrate toxicity testing. Understanding toxicological effects and accumulating toxicity data are essential to support this approach. Adverse outcome pathways (AOPs) provide highly structured conceptual frameworks for describing toxicological processes [13]. AOPs organize knowledge about the progression of toxicity from molecular initiating events (MIEs) through subsequent key events (KEs) to adverse outcomes (AOs), providing mechanistic evidence to predict potential hazards by linking events across different organismal levels. Current AOP formulations have focused on initiating or early-stage events of toxicological responses for their cost- and time-efficient applications [13; 14]. Particularly, AOPs are crucial for transitioning from animal testing to mechanistic-based toxicity assessments using *in vivo* and *in vitro* models.

Building on the AOP-Wiki related to impaired fecundity in fish, we organized the present study using AOP 289, which is currently under development [15]. AOP 289 describes that inhibition of SRD5A (as the MIE) decreases DHT synthesis, sequentially leading to decreased plasma 17β-estradiol (E2) and vitellogenin (VTG) levels, reduced spawning and egg production in zebrafish, and ultimately decreased population levels as the AO. However, a detailed understanding at the molecular level, particularly elucidating the anti-estrogen effects of SRD5A inhibition in fish, is currently lacking. This study aimed to understand the transition from MIE to KEs by evaluating estrogenic effects following SRD5A inhibition in zebrafish embryos. Dutasteride, an inhibitor of SRD5A1 and 2, was used as the MIE, and the relationships between each KE were evaluated at the level of reproductive factors and gene expression. These results can help fill knowledge gaps in AOPs regarding the biological mechanisms of SRD5A inhibition in zebrafish embryos.

4.3 Materials and methods

4.3.1 Chemicals and reagents

Dutasteride (CAS No. 164656-23-9), DHT (CAS No. 521-18-6), and T (CAS No. 58-22-0) were purchased from Sigma-Aldrich (Steinheim, Germany). The stock solutions of dutasteride, T, and DHT were dissolved in dimethyl sulfoxide (DMSO) at 20, 100, and 100 mM, respectively. The solvent was limited to 0.01 % DMSO (*v*/*v*) or less in the zebrafish embryo experiment. All the other chemicals were of analytical grade.

4.3.2 Zebrafish maintenance

Adult wild-type zebrafish were obtained from the European Zebrafish Resource Center (EZRC; Karlsruhe, Germany). Fish maintenance, breeding conditions, and egg production were performed under internationally accepted standards in an aerated aquarium system (temperature 28.0 ± 0.5 °C and 16/8 h dark/light cycle) with E3 medium (5 mM sodium chloride, 0.17 mM potassium chloride, 0.33 mM calcium chloride, 0.33 mM magnesium sulfate, and 0.01 % methylene blue). The fish were fed a commercial flake diet (JBL, Germany) supplemented with freshly hatched brine shrimp (Artemia).

4.3.3 Maximum tolerated concentration (MTC)

Zebrafish eggs were collected approximately 60 min after natural mating and rinsed in E3 medium. Unfertilized or injured eggs were discarded. To determine the MTC, fertilized eggs were randomly selected and carefully distributed in a 6-well plate, filled with 6 mL of different concentrations of dutasteride (0.005, 0.05, 0.1, 0.5, 1, and 2 μM) or negative (E3 medium containing 0.01 % DMSO). The test was performed in a climate chamber at 28.0 ± 0.5 °C and 16/8 h dark/light cycle until 120 h post-fertilization (hpf). No food or aeration was provided during the experiment. Embryonic development was assessed at 24, 48, 72, 96, and 120 hpf using a stereomicroscope (SteREO Discovery V8; Carl Zeiss, Zena, Germany). The distinction between normal and abnormal embryo development in terms of phenotypic changes (i.e. skeletal deformity) was established according to the descriptions of zebrafish development reported by [16]. In addition, survival (egg coagulation, somite formation, and heartbeat) and hatching rates were observed and reported.

4.3.4 Exposure experimental procedures on zebrafish embryo

4.3.4.1 Dutasteride exposure

A schematic diagram of the study is presented in Figure 4.1. Zebrafish embryos were placed into 1 L aquarium filled E3 medium and maintained at 28.0 ± 0.5 °C and 16/8 h dark/light cycle until 72 hpf. 20 zebrafish embryos were then placed into each well of 6-well plates filled with 10 mL of each exposure medium, negative control (0.01 % DMSO), and dutasteride (0.005, 0.05, 0.5, and 2 μM), and incubated until 120 hpf. The test solution was changed daily to prevent concentration by uptake and bioaccumulation of the compound in zebrafish embryos.

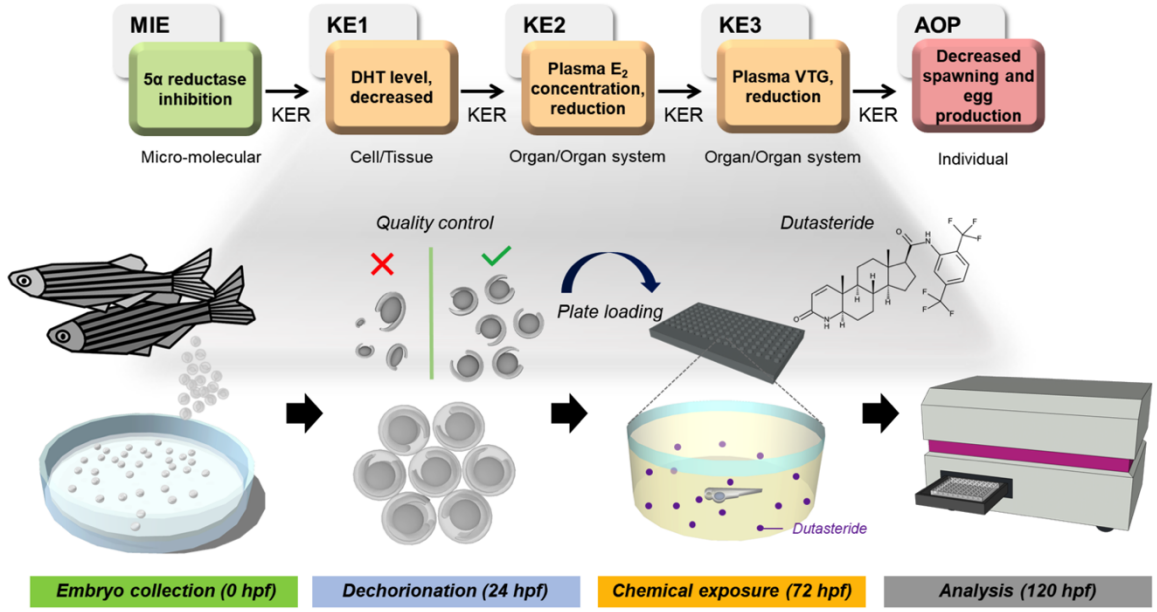

Figure 4.1. AOP 289 and schematic diagram representing the assessment of zebrafish embryos exposed to dutasteride. Fertilized eggs were collected and maintained on a 16 h light/8 h dark cycle at 28 °C ± 0.5 °C and unfertilized eggs were separated. Dutasteride was exposed to zebrafish embryos at 72 h post fertilization (hpf). The embryos were collected at 120 hpf and utilized for subsequent assays.

4.3.4.2 Steroid hormone extraction and measurement

DHT and E2 levels were measured using ELISA kits (Cat. #KA1886; Abnova, Heidelberg, Germany; Cat. #501890; Cayman, Hamburg, Germany). 200 embryos from 10 wells were collected into a tube for steroid hormone extraction according to the manufacturer's instructions. The embryos were washed with distilled water and dried under a stream of nitrogen. Methanol (1 mL) was added to each tube, and embryos were homogenized using the TissueLyser bead LT (Qiagen, Hilden, Germany). After centrifugation at 10,000 ×*g* and 4 °C for 10 min, the supernatant was dried under a nitrogen stream. The extracted steroids were reconstituted with 500 uL of the assay buffer supplied in the kit. The samples were stored at −80 °C until analysis. Each tube was considered a sample, and at least five replicate samples from each condition were prepared from independent cultures ($n \geq 5$). Measurement was performed by a Spark multimode microplate reader (Tecan, Männedorf, Switzerland) at the absorbance of 450 nm. The protein concentration for normalization was determined using the BCA protein assay (Thermo Scientific, Karlsruhe, Germany).

4.3.4.3 VTG measurement

VTG levels were measured using an ELISA kit (Cat. #10004995; Cayman) according to the manufacturer's instructions. 200 embryos from 10 wells were collected into a tube and washed with

distilled water. Cold RIPA buffer was added to each tube and the samples were homogenized by vortexing for 2 min. The homogenates were centrifuged at 14,000 ×*g* and 4 °C for 10 min. Finally, the supernatants were transferred to new tubes and were stored at −80 °C until analysis. Each tube was considered a sample, and at least five replicate samples from each condition were prepared from independent cultures ($n \geq 5$). Measurement was performed by a Spark multimode microplate reader (Tecan) at the absorbance of 492 nm. The protein concentration for normalization was determined using the BCA protein assay (Thermo Scientific).

4.3.4.4 mRNA expression level measurement

40 embryos from 2 wells were collected into a tube and washed with distilled water. The TRIzol reagent (Invitrogen, Carlsbad, CA, USA) was added to each tube and homogenized with beads. Total RNA was isolated using a column-based kit (cat. #74136; Qiagen). cDNA was synthesized from 500 ng of total RNA using a High-Capacity RNA-to-cDNA Kit (Applied Biosystems, Waltham, MA, USA) according to the manufacturer's instructions. qRT-PCR assays were performed using a TaqMan™ Fast Advanced Master Mix and a Fast SYBR™ Green Master Mix on a 7500 FAST real-time PCR system (Applied Biosystems). The PCR reaction cycles for the SYBR Green assay were as follows: initial denaturation at 95 °C for 20 s, followed by 40 amplification cycles of 95 °C for 3 s and 60 °C for 30 s. For the TaqMan assay, the reaction cycles were: initial denaturation at 90 °C for 20 s, followed by 40 amplification cycles of 95 °C for 3 s and 60 °C for 30 s. Relative mRNA expression of *srd5a2* (Dr03128500_m1; Thermo Scientific), *cyp19a1* (PPZ00217A; Qiagen), *esr1* (Dr03093579_m1; Thermo Scientific), *esr2a* (Dr03074408_m1; Thermo Scientific), *esr2b* (Dr03150586_m1; Thermo Scientific), and *vtg2* (PPZ10052A; Qiagen) was calculated using $2^{-\Delta\Delta Ct}$ method with the endogenous control *eef1a1la* (Dr03432748_m1; Thermo Scientific) and *g6pd* (PPZ12949A; Qiagen) for normalization [17]. Each tube was considered a sample, and at least four replicate samples from each condition were prepared from independent cultures ($n \geq 4$).

4.3.5 Homology modeling and molecular docking

For the preparations of zebrafish estrogen receptor alpha (zfERα) and zebrafish androgen receptor (zfAR), we downloaded the crystal structures of human ER (hER) and AR (hAR) (Protein Data Bank [PDB] code: 2YJA for hERα and 2 AM9 for hAR) were downloaded from the PDB (http://www.rcsb.org/) and used as template structures. MODELLER 9.25 (https://salilab.org/modeller/9.25/release.html) was used to generate homology models of zfER and zfAR. MODELLER uses a comparative modeling approach to compare the sequence alignment quality of the target protein sequence with that of one or more known template 1protein structures [18]. Ten models were generated for both the zfER and zfAR protein sequences, among which only one structure with the lowest discrete optimized protein energy (DOPE)

score was selected as the target receptor for molecular docking experiments [19]. For the molecular docking process, crystallographic water molecules were removed from the crystal structures, and charges and hydrogen atoms were added. The ligand structures were prepared from the PubChem database (ligand, PubChem CID: E2, 5757; DHT, 10635; dutasteride, 6918296). Each structure was saved in SDF format, and the geometry was optimized using the MM2 method of energy minimization. Eventually, the prepared files were converted to PDB format using Discovery Studio Visualizer 2016 (Accelrys Software). The ligand structures were applied to AutoDock 4.2 (Scripps Research Institute, California). Docking simulations and visualizations were performed using CDOCKER [20] and AutoDock 4.2 [21] software. Standard docking was performed using flexible ligands docked onto rigid proteins. We performed five independent runs per ligand and used grid conditions of 40, 40, and 40 points in the x-, y-, and z-directions, respectively, with grid spacing of 1.0 Å. An energy map was constructed using a distance-dependent function of the dielectric constant. All other parameters were set to default values. Docking sites were calculated based on their ranking and binding free energies. The docked positions were analyzed for hydrogen bonding and hydrophobic, van der Waals, and halogen interactions using Discovery Studio Visualizer 2019.

4.3.6 Construction of ARE receptor cell line and response activity

HEK293 cells were used as transfection hosts and maintained in DMEM containing 10 % FBS at 37 °C and 5 % CO_2 condition. HEK293-ARE-zfAR cells were constructed using lentiviral transduction for androgen receptor element (ARE, CS-GS241B-mCHER-Lv207-01; Labomics S.A., Nivelles, Belgium) [22] and the PiggyBac transposon system for zfAR (pPB-Puro-CAG > zAR; VectorBuilder Inc., Chicago, IL, USA), according to the manufacturer's instructions. After that, HEK293-ARE-zfAR cells were then maintained in a complete medium with hygromycin (10 μg/mL) and puromycin (2 μg/mL). For the measurement of ARE-zfAR response activity, HEK293-ARE-zfAR cells were seeded on black 96 well plates at a density of 1.0×10^5 cells/mL in an androgen-free medium containing charcoal-stripped FBS. After 24 h, each well was treated with DHT, flutamide as an antagonist [23], or dutasteride for 48 h. Fluorescence intensity was measured using a Spark multimode microplate reader (Tecan) at excitation and emission wavelengths of 485 and 528 nm for eGFP and 590 and 645 nm for mCherry signals, respectively.

4.3.7 Statistical analysis

All results were obtained from at least three independent experiments. Data are expressed as the mean ± standard deviation. Statistical differences in each group were determined by one-way analysis of variance (ANOVA) followed by Tukey's honestly significant difference test using GraphPad Prism software (version 9.5.1; GraphPad Software, San Diego, CA, USA). Correlation analysis was performed using the

"psych" package in R to investigate the relationship between each group (https://cran.r-project.org/web/packages/psych/psych.pdf). Before calculating each correlation coefficient, the dataset was subjected to the Shapiro-Wilk test using the basic function in the R open-source software. All test groups followed a Gaussian distribution ($p > 0.05$).

4.4 Results

4.4.1 MTC and toxicity of dutasteride in zebrafish embryos

The survival and hatching rate of zebrafish embryos exposed to dutasteride (0.005, 0.05, 0.1, 0.5, 1, and 2 μM) were evaluated. Due to the low solubility of dutasteride, the highest concentration was 2 μM. Up to 2 μM dutasteride exposure, no morphologic abnormalities were observed (Figure 4.2A). There was no difference in the survival rate up to 2 μM exposure compared to the control (Figure 4.2B). The hatching rate was similar to the survival rate (Figure 4.2C). Up to 2 μM exposure, the hatching rates were approximately 75 % at 72 hpf and >90 % hatching rate at 96 hpf.

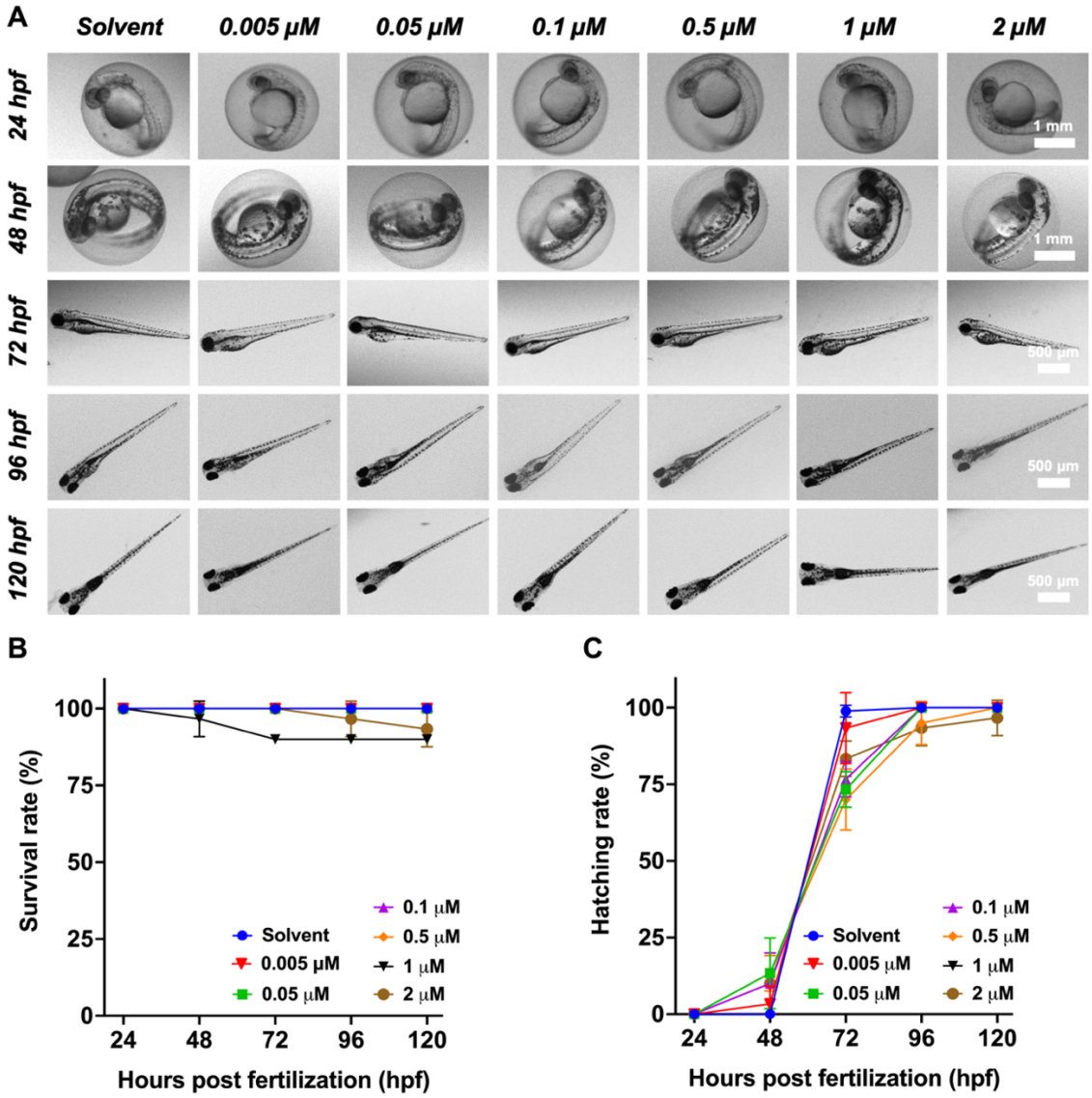

Figure. 4.2. MTC and toxic effects of dutasteride exposure in zebrafish embryos at various developmental stages. Phenotypes, mortality, and hatching rate were measured from 1 to 120 hpf. (A) Representative images of the embryos. (B) The survival rate and (C) the hatching rate in zebrafish embryos exposed to dutasteride (n = 20). Data are expressed as mean ± SD.

4.4.2 Measurement of DHT, E2, and VTG levels

The exposure of zebrafish embryos to dutasteride significantly decreased DHT, E2, and VTG levels in a concentration-dependent manner. Significant decreases in DHT, E2 and VTG levels were observed at 0.05, 0.005, and 0.005 μM dutasteride exposure, respectively (Figure 4.3A-C). A correlation analysis between DHT, E2, and VTG levels in each group was performed (Figure 4.3D). The analysis involved the Pearson's correlation coefficient between individual expression levels and a scatter plot of each dataset. Strong positive correlations were observed between DHT-VTG (r_p = 0.81, ***p < 0.001) and E2-VTG (r_p = 0.84, ***p < 0.001). The correlation coefficient between the DHT and VTG was 0.66 (***p < 0.001).

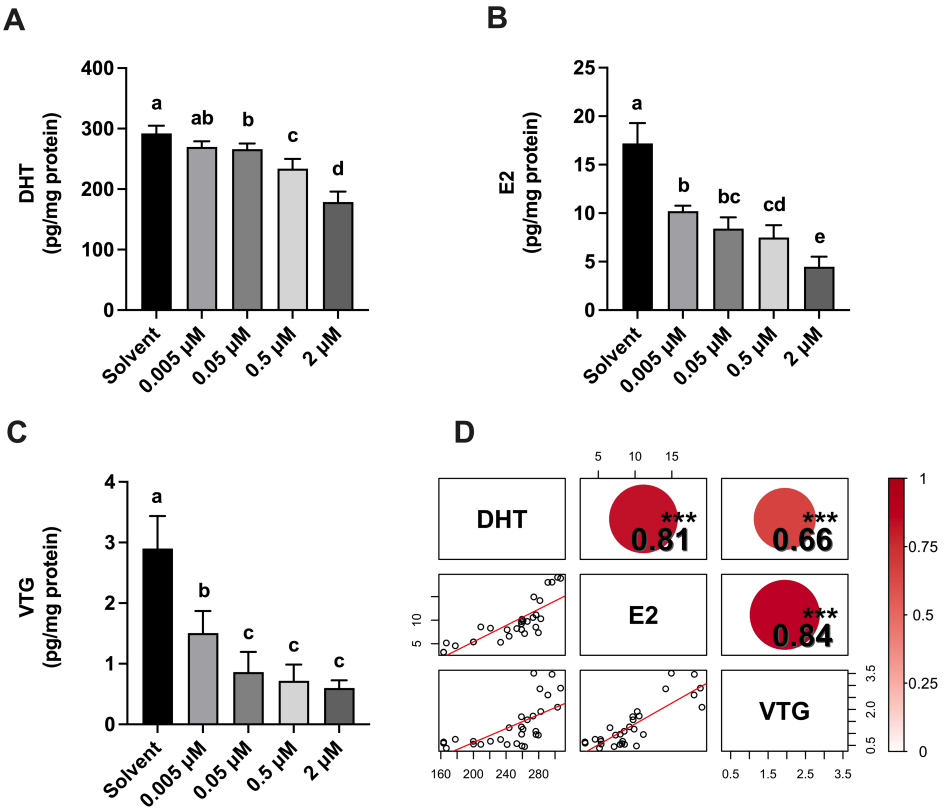

Figure 4.3. The level of steroid hormones (DHT and E2) and VTG in zebrafish embryos exposed to dutasteride from 72 to 120 hpf. (A) DHT, (B) E2, and (C) VTG levels were measured by ELISA ($n \geq 5$). Data are expressed as mean ± SD. Different letter for a single substance indicates a significant difference at $p < 0.05$, according to ANOVA with Tukey's multiple comparison tests. (D) Correlation matrix between DHT, E2, and VTG levels. The upper displays Pearson's correlation coefficients (r_p). The color intensity indicates the strength of the correlation. The lower displays scatter plots of each data set with linear regression lines.

4.4.3 Gene expression level of zebrafish embryos exposed to dutasteride

To investigate changes at the molecular level caused by dutasteride exposure, the expression levels of reproductive-related genes (*srd5a2*, *cyp19a1*, *esr1*, *esr2a*, *esr2b*, and *vtg*) were measured (Figure 4.4A-F). The expression levels of *srd5a2* decreased from 0.05 μM and *cyp19a1* decreased in a concentration-dependent manner after 0.005 μM exposure (Figure 4.4A-B). Among the three subtype genes encoding ER, the expression level of *esr1* was significantly decreased after 0.005 μM dutasteride exposure, *esr2a* was decreased after dutasteride 2 μM exposure, *esr2b* was decreased after 0.5 and 2 μM dutasteride exposure (Figure 4.4C-E). The expression level of *vtg* decreased in a concentration-dependent manner after 0.05 to 2 μM exposure (Figure 4.4F). To verify the correlation between reproductive factors and gene expression levels, a correlation analysis between the expression levels of each group was performed (Figure 4.4G). The analysis involved Pearson's correlation coefficient between individual expression levels and a scatter plot of each dataset. The strong positive correlations >0.7 were shown at the *srd5a2-esr1* (***$p < 0.001$), *-esr2b* (***$p < 0.001$), and *-vtg* (***$p < 0.001$), *cyp19a1-esr1* (***$p < 0.001$), *-vtg* (***$p < 0.001$), *esr1-esr2b* (***$p < 0.001$), and *-vtg* (***$p < 0.001$), *esr2a-esr2b* (***$p < 0.001$), and *esr2b-vtg* (***$p < 0.001$). The correlation coefficient for the other groups ranged from 0.48 to 0.68, indicating a moderate positive correlation (***$p < 0.001$).

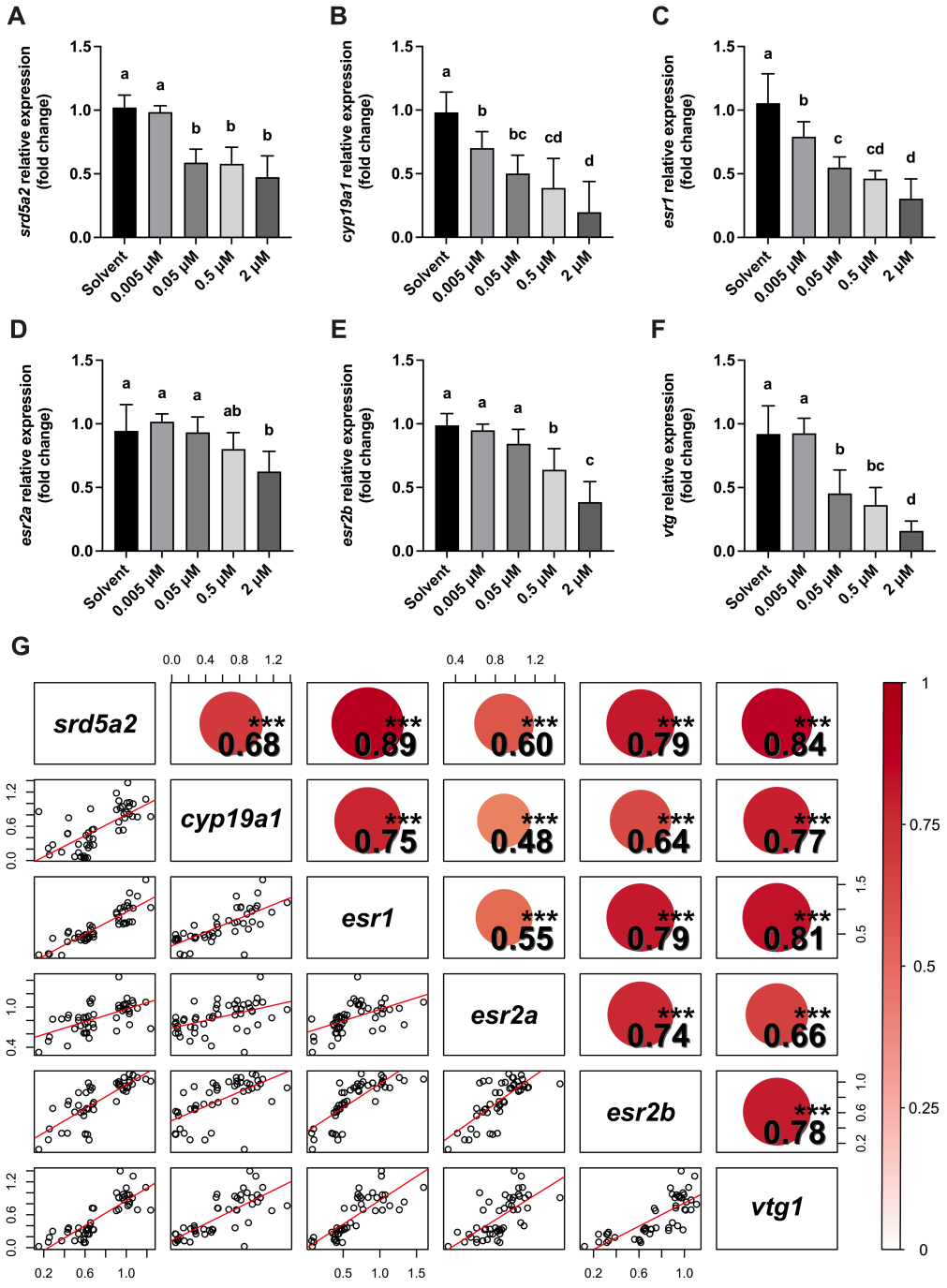

Figure. 4.4. Relative expression levels of genes in zebrafish embryos exposed to dutasteride from 72 to 120 hpf. The expression levels of (A) *srd5a2*, (B) *cyp19a1* (C) *esr1*, (D) *esr2a*, (E) *esr2b*, (C), and (F) *vtg* were quantified by RT-qPCR ($n \geq 5$). Data are expressed as mean ± SD. Different letter for a single substance indicates a significant difference at $p < 0.05$, according to ANOVA with Tukey's multiple comparison tests. (G) Correlation matrix between gene expression levels. The upper triangle displays Pearson's correlation coefficients (r_p). The color intensity indicates the strength of the correlation. Lower triangle displays scatter plots of each data set with linear regression lines.

4.4.4 Molecular docking for zfER and zfAR with dutasteride and response activity of ARE-zfAR

Docking simulations between the receptors and chemicals revealed multiple docking poses for each ligand-binding site. The best pose for each docking simulation is shown in Figure 4.5A, and the number of interactions and binding free energies are listed in Table S4. For zfERα, the docking complex with E2 showed 20 interactions, including 3 hydrogen bonds, 10 hydrophobic interactions, and 7 Van der Waals interactions. The binding free energies were −10.6 (Vina) and −49.8 (CDOCKER) Kcal/mol, respectively. Dutasteride was docked to zfERα, revealing a binding affinity of −9.8 (Vina) and −56.4 (CDOCKER) Kcal/mol, along with 2 hydrogen bonds, 3 hydrophobic interactions, 9 van der Waals interactions, and 1 halogen interaction. In zfAR, the docking complex with DHT exhibited 22 interactions, including 3 hydrogen bonds, 7 hydrophobic interactions, and 12 van der Waals interactions, with a binding free energy of −9.6 (Vina) and −43.2 (CDOCKER) kcal/mol. The docking of dutasteride to zfAR showed a binding affinity of −9.8 (Vina) and −86.07 (CDOCKER) Kcal/mol, accompanied by 1 hydrogen bond, 8 hydrophobic interactions, 9 van der Waals interactions, and 2 halogen interactions.

ARE-zfAR response activity was measured to confirm the molecular docking results. The mCherry fluorescent signal activity showed a dose-dependent increase in the ARE reporter response following treatment with DHT (Figure 4.5B-C). Treatment with flutamide, an AR antagonist, resulted in a dose-dependent decrease in the mCherry signal (Figure 4.5C). Dutasteride did not significantly decrease the mCherry signal up to the maximum concentration (50 nM).

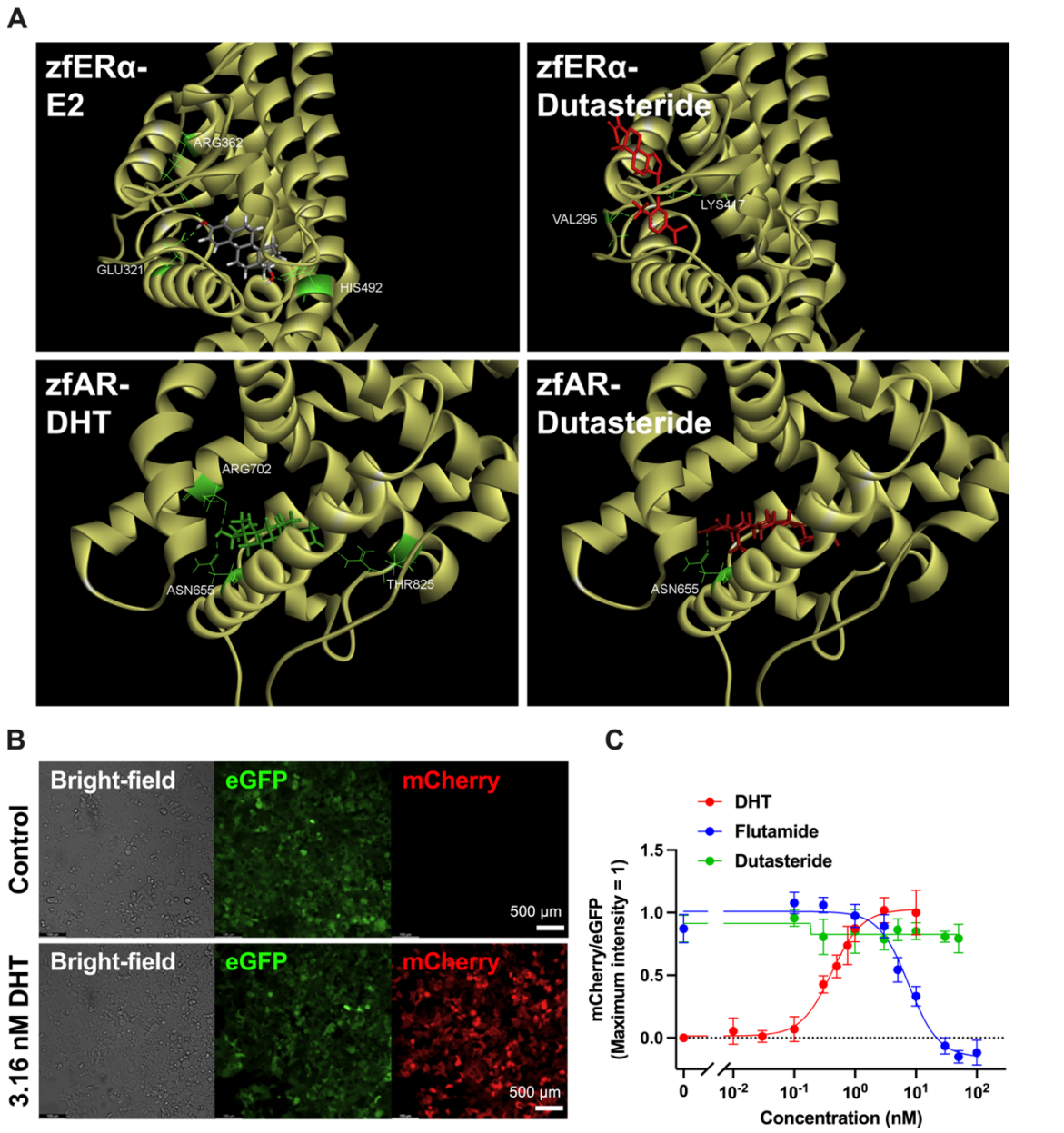

Figure. 4.5. Representative molecular docking images of (A) E2 and dutasteride with zfERα and DHT and dutasteride with zfAR. The green color indicates the residues interacting with ligands via hydrogen bonds. (B) Fluorescence image on HEK293-ARE-zfAR treated to 0.1 % DMSO (control) and 3.16 nM DHT. (C) ARE-zfAR response activities to DHT, flutamide, and dutasteride. Data are expressed as mean ± SD ($n \geq 4$).

4.4.5 Gene expression level of zrbrafish embryos co-exposed to dutasteride and/or DHT

It was necessary to determine whether the change in molecular signaling under reduced DHT concentrations in zebrafish embryos could be restored by SRD5A inhibition. This study investigated the effect of DHT treatment on reproduction-related gene expression in the presence and absence of dutasteride. DHT exposure was at a concentration of 0.5 μM, and the exposure concentration of dutasteride was selected at 0.5 and 2 μM, based on previous experiments that demonstrated a significant reduction in expression levels. The exposure to 0.5 μM DHT significantly increased the expression levels of *srd5a2*, *cyp19a1*, *esr1*, *esr2a*, *esr2b*, and *vtg* in comparison to the control (Figure 4.6). In contrast to the findings presented in Figure 4.6 A-F, which indicate a reduction in gene expression, the levels of *srd5a2*, *cyp19a1*, *esr1*, *esr2a*, *esr2b*, and *vtg* expression in the DHT with dutasteride co-exposure group were not significantly different from those in the control group (Figure 4.6).

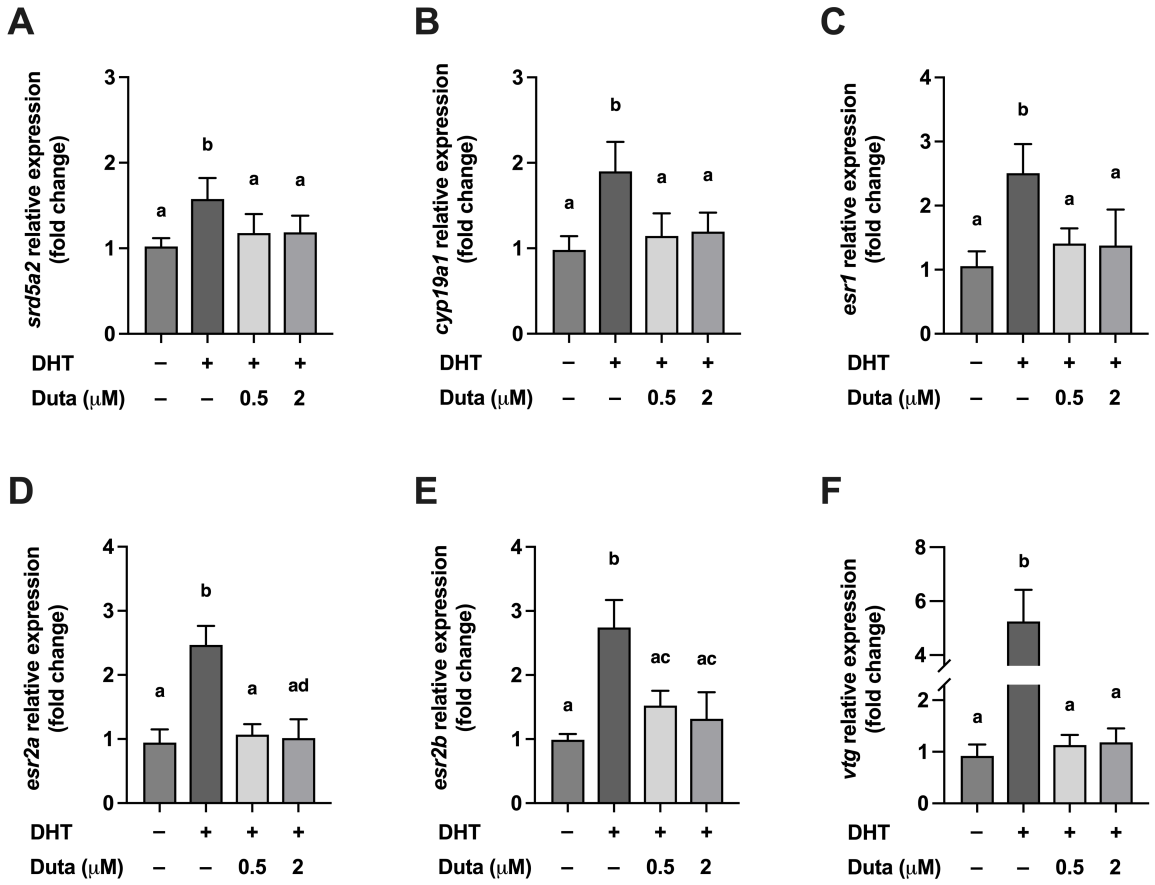

Figure. 4.6. Relative expression levels of genes in zebrafish embryos exposed dutasteride and/or 0.5 μM DHT from 72 to 120 hpf. The expression levels of (A) *srd5a2*, (B) *cyp19a1*(C) *esr1*, (D) *esr2a*, (E) *esr2b*, (C), and (F) *vtg* were quantified by RT-qPCR ($n \geq 4$). Data are expressed as mean ± SD. A different letter for single substance indicates a significant difference at the $p < 0.05$, according to ANOVA with Tukey's multiple comparison tests.

4.5 Discussion

Previously, we developed an AOP that demonstrated that SRD5A inhibitors led to impaired fecundity in female fish [15]. In this AOP, inhibition of SRD5A was identified as the MIE. This inhibition results in decreased expression of DHT (KE1), which subsequently downregulates androgen signaling. Downregulation of androgen signaling leads to decreased E2 (KE2). The reduction in E2 levels caused a decline in VTG protein production (KE3), ultimately leading to decreased fertility (AO) (Figure 4.1). However, the key event relationship (KER) linking decreased DHT and decreased E2 levels remains incompletely understood, and evidence involved in this relationship is needed to clarify the mechanisms. In this study, we investigated a series of pathways involving DHT by measuring the sequential relationship of each KE, such as reproduction-related factors including hormone levels (DHT and E2), VTG levels, and gene expression levels in zebrafish embryos. For the inhibition of SRD5A, dutasteride was employed due to its broad-spectrum inhibition, allowing for a more comprehensive reduction in DHT levels.

The MTC on phenotype image, mortality, and hatching rate confirmed the absence of toxicity, including morphological abnormalities up to 2 μM exposure of dutasteride on zebrafish embryos. SRD5A inhibition is known to decrease DHT levels with a high correlation. This finding is supported by García-García et al. who observed a significant decline in the expression of *srd5a* and DHT in gilthead seabream (*Sparus aurata*) following finasteride exposure. Additionally, our previous study demonstrated the inhibitory effect of dutasteride on zebrafish liver cells, with an IC_{50} value of 7.33 nM [24]. This study confirmed the inhibitory effects of dutasteride on zfSRD5A isoforms (SRD5A1, SRD5A2a, SRD5A2b, and SRD5A3) in a transiently transfected cell line with IC_{50}. The values for the isoforms ranged from 2.76 to 43.17 nM (Figure 3.6), and a concentration-dependent decrease in DHT levels was observed in zebrafish embryos following exposure to up to 2 μM dutasteride (Figure 4.3). However, even exposure to high concentrations of dutasteride which sufficiently inhibited SRD5A, reduced DHT levels by approximately 69 %. This may be attributed to the relatively high basal levels of DHT in the eggs or yolks received from the mother. Alternatively, there are three potential biosynthetic pathways for DHT: the front-door pathway and two back-door pathways [25]. The front-door pathway, a classical pathway, is involved in the conversion of T to DHT. Two non-canonical backdoor pathways are involved in the production of DHT by utilizing intermediate substrates, including progesterone, androsterone, androstanediol, dehydroepiandrosterone, androstenedione, and androstenedione [26]. In humans, clinical deficiency of SRD5A type 2 has been associated with increased expression of enzymes responsible for DHT production via backdoor pathways, as well as enhanced activity of chemical transformation of the relevant steroidogenic enzymes, which involve alternative DHT synthesis pathways [27; 28; 26]. Although the evidence is not yet clear in fish, it has been suggested that the upregulation of alternative signaling pathways compensates for the downregulation of the classic DHT synthesis pathway upon exposure to dutasteride.

Zebrafish embryos hatch approximately 72 h hpf, exhibiting anatomical development and the ability to express genes such as aromatase and ERs, which are crucial for the synthesis of endogenous E2 [29-32].

Similarly, *srd5a* isoforms are expressed at an early stage of development in fathead minnow embryos [1]. With regard to gene regulation, the *srd5a2* regulates prostate genes by establishing a feedback loop [33]. In rats, DHT administration upregulates the expression of SRD5A. This increase in expression enhances transcriptional activity through a feed-forward mechanism in which DHT promotes its own biosynthesis [34]. Conversely, the administration of finasteride in rats resulted in a reduction in DHT levels, which in turn led to the downregulation of SRD5A genes in a DHT-dependent manner [35]. Furthermore, DHT can be converted to 5α-androstane-3β,17β-diol (3βAdiol), an androgen metabolite, through the actions of two key enzymes, 17β-hydroxysteroid dehydrogenase (17β-HSD) and 3β-hydroxysteroid dehydrogenase (3β-HSD) [36]. 3βAdiol may bind to ERβ1 and induce ERE-mediated transcription by recruiting coactivators from ERα and ERβ2 [37; 38].

Ishikawa et al. also suggested the possibility that SRD5A inhibitor could reduce the conversion of DHT into estrogenic steroid like 3βAdiol. Similarly, our finding demonstrated that dutasteride exposure led to the down-regulation of both androgenic and estrogenic factors. Specifically, the positive correlation between DHT and E2 (Figure 4.4D), as well as between *srd5a2* and other reproductive gene expression levels (Figure 4.4G), suggests a potential link between DHT level and estrogenic signalings. This evidence raises the posibility that DHT might function as a source of estrogen or play a role in estrogen signaling [39]. Aromatase (encoded by *cyp19a1a* and *cyp19a1b*, which are specifically expressed in the gonads and brain, respectively) is an important factor in sex differentiation in fish [40]. The *cyp19a1b*promoter contains estrogen and androgen response elements (ERE and ARE) [41]. Several studies have demonstrated that aromatase is positively regulated by estrogen in fish. However, the effects of androgens are poorly understood [42-44]. Some studies have demonstrated that DHT is an effective activator of aromatase expression in zebrafish and stimulated expression of the aromatase gene has been observed following exposure to DHT [45; 41]. This indicates that androgens may regulate aromatase expression in the same manner as estrogens. ERs (encoded by *esr1*, *esr2a*, and *esr2b* in zebrafish) are known to be induced by estrogens, and their activation is highly related to vitellogenesis [46]. Conversely, this implies that ER transcription and, by extension, VTG transcription can be regulated by estrogen. Although studies have suggested that DHT may regulate androgenic and estrogenic signaling, the specific relationship between DHT and estrogenic effects remains challenging to determine.

The molecular docking interactions between zfERα and E2 were consistent with those observed in a previous study [47]. Similarly, our previous work identified hydrogen bond interactions between ASN705, ARG752, and THR877 in the hAR-DHT complex [23]. Furthermore, critical poses of amino acid residues for ligand recognition in the hAR and hERα receptors have been reported in prior studies, highlighting the key roles of residues in the ligand-binding pocket (LBP) in transactivation [48-50]. The previously conducted docking simulations of E2 yielded results consistent with those of the current study [51]. In our study, dutasteride was docked into the LBP of zfERα, though different docking sites were observed compared to the E2-zfERα complex. For zfAR, dutasteride interacted in a position similar to that of DHT near the LBP site. However, assessment of ARE-zfAR response activity indicated that dutasteride did not have an antagonistic effect on zfAR binding (Figure 4.5C). Despite the presence of a hydrogen bond in

the zfAR-dutasteride complex aligning with the zfAR-DHT complex (ASN655, ARG702, and THR825), this suggests that dutasteride does not impact zfAR-DHT binding interactions. These findings imply dutasteride does not act like antagonistic chemicals in zfERα and zfAR, respectively.

The present study demonstrated that dutasteride decreased DHT, E2, and VTG levels in zebrafish embryos, an effect that was independent of interactions with ER and AR as well as the gene expression levels associated with these signals. These findings suggest that dutasteride-induced DHT levels play a crucial role in steroid hormone signaling. This hypothesis is supported by the present results (Figure 4.6). DHT has received little attention in fish owing to its dominant androgens (T and 11-KT) and 12- and 20-fold lower levels of DHT compared to T in male and female fathead minnow, respectively [52; 1]. Nevertheless, despite its low levels, DHT not only exhibits a high affinity for AR binding but also demonstrates unexpected responses to the steroid hormone biosynthetic pathway and androgenic signaling [53; 54]. Previous studies have demonstrated that DHT regulates VTG synthesis by binding to the ER in the liver of black goby (*Gobius niger*). This estrogenic effect is more pronounced in female and E2-treated male hepatocytes than in untreated male hepatocytes [55-57]. Riley et al. (2004) demonstrated that exposure to 5 μM DHT for 48 h in female tilapia (*Oreochromis mossambicus*) hepatocytes increased VTG release, while co-treatment of DHT with tamoxifen inhibited VTG production. These findings provide evidence that DHT may be involved in the estrogenic signaling pathway, suggesting that the level of DHT is important for signaling associated with reproduction. These findings are consistent with the results of the present study, which demonstrated that DHT treatment resulted in increased gene expression levels and that dutasteride treatment with DHT led to the recovery of these levels (Figure 4.6).

4.6 Conclusion

The present study demonstrated that dutasteride inhibited SRD5A activity in zebrafish, resulting in a reduction in E2 and VTG levels, as well as gene expression levels (*srd5a2a*, *cyp19a1*, *esr1*, *esr2a*, *esr2b*, and *vtg*). Furthermore, the inhibitory effect of dutasteride was independent of ER and AR interactions. The positive correlations observed between DHT and -E2 and -VTG, and between *srd5a2* and other genes (*cyp19a1*, *esr1*, *esr2a*, *esr2b*, and *vtg*) suggest a close relationship between them, providing valuable insights into the response-response relationship for the development of quantitative AOP (qAOP) from downstream to upstream key events. The results of the co-treatment experiment with dutasteride and DHT showed that the decreased gene expression levels after exposure to dutasteride recovered to the control level, which proved that DHT is important in reproductive signaling. This finding supports the hypothesis that DHT levels are important for reproductive signaling. Although our results do not provide evidence of a direct relationship between DHT and E2 levels, the estrogenic effect of DHT was indirectly confirmed by molecular docking and gene expression results. These results provide additional evidence to support the development of qAOP. Consequently, further studies are required to identify alternative pathways for DHT synthesis in fish.

4.7 Acknowledgments

This research was supported by the Korea Environmental Industry and Technology Institute through the Core Technology Development Project for Environmental Diseases Prevention and Management (2021003310001), funded by the Korea Ministry of Environment and Bio-cluster Industry Capacity Enhancement Project of Jeonbuk Technopark (JBTP)

4.8 Bibliography

1. Martyniuk, C.J.; Bissegger, S., Langlois, V.S. Reprint of "Current perspectives on the androgen 5 alpha-dihydrotestosterone (DHT) and 5 alpha-reductases in teleost fishes and amphibians". *Gen. Comp. Endocrinol.* **2014**, 203, 10-20. doi:10.1016/j.ygcen.2014.06.011.
2. Effects of 5α-dihydrotestosterone on expression of genes related to steroidogenesis and spermatogenesis during the sex determination and differentiation periods of the pejerrey, Odontesthes bonariensis. *Comp. Biochem. Physiol. A Mol. Integr. Physiol.* **2015**, 182, 1-7. doi:10.1016/j.cbpa.2014.12.003.
3. García-García, M.; Sánchez-Hernández, M.; García-Hernández, M.P.; García-Ayala, A., Chaves-Pozo, E. Role of 5α-dihydrotestosterone in testicular development of gilthead seabream following finasteride administration. *J. Steroid Biochem. Mol. Biol.* **2017**, 174, 48-55. doi:10.1016/j.jsbmb.2017.07.024.
4. Margiotta-Casaluci, L.; Hannah, R.E., Sumpter, J.P. Mode of action of human pharmaceuticals in fish: the effects of the 5-alpha-reductase inhibitor, dutasteride, on reproduction as a case study. *Aquat. Toxicol.* **2013**, 128-129, 113-123. doi:10.1016/j.aquatox.2012.12.003.
5. Margiotta-Casaluci, L., Sumpter, J.P. 5α-Dihydrotestosterone is a potent androgen in the fathead minnow (Pimephales promelas). *Gen. Comp. Endocrinol.* **2011**, 171, 309-318. doi:10.1016/j.ygcen.2011.02.012.
6. McGrath, P., Li, C.Q. Zebrafish: a predictive model for assessing drug-induced toxicity. *Drug Discov. Today* **2008**, 13, 394-401. doi:10.1016/j.drudis.2008.03.002.
7. Spitsbergen, J.M., Kent, M.L. The state of the art of the zebrafish model for toxicology and toxicologic pathology research--advantages and current limitations. *Toxicol. Pathol.* **2003**, 31 Suppl, 62-87. doi:10.1080/01926230390174959.
8. He, J.H.; Gao, J.M.; Huang, C.J., Li, C.Q. Zebrafish models for assessing developmental and reproductive toxicity. *Neurotoxicol. Teratol.* **2014**, 42, 35-42. doi:10.1016/j.ntt.2014.01.006.
9. Selderslaghs, I.W.; Van Rompay, A.R.; De Coen, W., Witters, H.E. Development of a screening assay to identify teratogenic and embryotoxic chemicals using the zebrafish embryo. *Reprod. Toxicol.* **2009**, 28, 308-320. doi:10.1016/j.reprotox.2009.05.004.
10. Volz, D.C.; Belanger, S.; Embry, M.; Padilla, S.; Sanderson, H.; Schirmer, K.; Scholz, S., Villeneuve, D. Adverse outcome pathways during early fish development: a conceptual framework for identification of chemical screening and prioritization strategies. *Toxicol. Sci.* **2011**, 123, 349-358. doi:10.1093/toxsci/kfr185.
11. OECD. Test No. 236: Fish Embryo Acute Toxicity (FET) Test, OECD Guidelines for the Testing of Chemicals, Section 2. **2013**. doi:doi.org/10.1787/9789264203709-en.
12. Bradbury, S.P.; Feijtel, T.C., Van Leeuwen, C.J. Meeting the scientific needs of ecological risk assessment

in a regulatory context. *Environ. Sci. Technol.* **2004**, 38, 463a-470a. doi:10.1021/es040675s.

13. Ankley, G.T.; Bennett, R.S.; Erickson, R.J.; Hoff, D.J.; Hornung, M.W.; Johnson, R.D.; Mount, D.R.; Nichols, J.W.; Russom, C.L.; Schmieder, P.K.; et al. Adverse outcome pathways: a conceptual framework to support ecotoxicology research and risk assessment. *Environ. Toxicol. Chem.* **2010**, 29, 730-741. doi:10.1002/etc.34.
14. Villeneuve, D.L.; Crump, D.; Garcia-Reyero, N.; Hecker, M.; Hutchinson, T.H.; LaLone, C.A.; Landesmann, B.; Lettieri, T.; Munn, S.; Nepelska, M.; et al. Adverse outcome pathway (AOP) development I: strategies and principles. *Toxicol. Sci.* **2014**, 142, 312-320. doi:10.1093/toxsci/kfu199.
15. AOP-Wiki Inhibition of 5α-reductase leading to impaired fecundity in female fish. *Society for Advancement of AOPs [Online]*, April 29, 2023, Available from: https://aopwiki.org/aops/289.
16. Kimmel, C.B.; Ballard, W.W.; Kimmel, S.R.; Ullmann, B., Schilling, T.F. Stages of embryonic development of the zebrafish. *Dev. Dyn.* **1995**, 203, 253-310. doi:10.1002/aja.1002030302.
17. Schmittgen, T.D., Livak, K.J. Analyzing real-time PCR data by the comparative CT method. *Nat. Protoc.* **2008**, 3, 1101-1108. doi:10.1038/nprot.2008.73.
18. Webb, B., Sali, A. Comparative Protein Structure Modeling Using MODELLER. *Curr. Protoc. Bioinformatics* **2016**, 54, 5.6.1-5.6.37. doi:10.1002/cpbi.3.
19. Shen, M.Y., Sali, A. Statistical potential for assessment and prediction of protein structures. *Protein Sci.* **2006**, 15, 2507-2524. doi:10.1110/ps.062416606.
20. Wu, G.; Robertson, D.H.; Brooks, C.L., 3rd, Vieth, M. Detailed analysis of grid-based molecular docking: A case study of CDOCKER-A CHARMm-based MD docking algorithm. *J. Comput. Chem.* **2003**, 24, 1549-1562. doi:10.1002/jcc.10306.
21. Trott, O., Olson, A.J. AutoDock Vina: improving the speed and accuracy of docking with a new scoring function, efficient optimization, and multithreading. *J. Comput. Chem.* **2010**, 31, 455-461. doi:10.1002/jcc.21334.
22. Azeem, W.; Hellem, M.R.; Olsen, J.R.; Hua, Y.; Marvyin, K.; Qu, Y.; Lin, B.; Ke, X.; Øyan, A.M., Kalland, K.H. An androgen response element driven reporter assay for the detection of androgen receptor activity in prostate cells. *PLoS One* **2017**, 12, e0177861. doi:10.1371/journal.pone.0177861.
23. Park, C.G.; Adnan, K.M.; Cho, H.; Ryu, C.S.; Yoon, J., Kim, Y.J. A combined in vitro-in silico method for assessing the androgenic activities of bisphenol A and its analogues. *Toxicol. In Vitro* **2024**, 98, 105838. doi:10.1016/j.tiv.2024.105838.
24. Kim, D.; Cho, H.; Eggers, R.; Kim, S.K.; Ryu, C.S., Kim, Y.J. Development of a Liquid Chromatography/Mass Spectrometry-Based Inhibition Assay for the Screening of Steroid 5-α Reductase in Human and Fish Cell Lines. *Molecules* **2021**, 26. doi:10.3390/molecules26040893.
25. Cai, C.; Chen, S.; Ng, P.; Bubley, G.J.; Nelson, P.S.; Mostaghel, E.A.; Marck, B.; Matsumoto, A.M.; Simon, N.I.; Wang, H.; et al. Intratumoral de novo steroid synthesis activates androgen receptor in castration-resistant prostate cancer and is upregulated by treatment with CYP17A1 inhibitors. *Cancer Res.* **2011**, 71, 6503-6513. doi:10.1158/0008-5472.Can-11-0532.
26. Zhou, J.; Wang, Y.; Wu, D.; Wang, S.; Chen, Z.; Xiang, S., Chan, F.L. Orphan nuclear receptors as regulators of intratumoral androgen biosynthesis in castration-resistant prostate cancer. *Oncogene* **2021**, 40, 2625-2634. doi:10.1038/s41388-021-01737-1.

27. Auchus, R.J. The backdoor pathway to dihydrotestosterone. *Trends Endocrinol. Metab.* **2004**, 15, 432-438. doi:10.1016/j.tem.2004.09.004.
28. Mostaghel, E.A. Beyond T and DHT - novel steroid derivatives capable of wild type androgen receptor activation. *Int. J. Biol. Sci.* **2014**, 10, 602-613. doi:10.7150/ijbs.8844.
29. Cohen, A.; Popowitz, J.; Delbridge-Perry, M.; Rowe, C.J., Connaughton, V.P. The Role of Estrogen and Thyroid Hormones in Zebrafish Visual System Function. *Front. Pharmacol.* **2022**, 13, 837687. doi:10.3389/fphar.2022.837687.
30. Sawyer, S.J.; Gerstner, K.A., Callard, G.V. Real-time PCR analysis of cytochrome P450 aromatase expression in zebrafish: gene specific tissue distribution, sex differences, developmental programming, and estrogen regulation. *Gen. Comp. Endocrinol.* **2006**, 147, 108-117. doi:10.1016/j.ygcen.2005.12.010.
31. Trant, J.M.; Gavasso, S.; Ackers, J.; Chung, B.C., Place, A.R. Developmental expression of cytochrome P450 aromatase genes (CYP19a and CYP19b) in zebrafish fry (Danio rerio). *J. Exp. Zool.* **2001**, 290, 475-483. doi:10.1002/jez.1090.
32. von Hellfeld, R.; Brotzmann, K.; Baumann, L.; Strecker, R., Braunbeck, T. Adverse effects in the fish embryo acute toxicity (FET) test: a catalogue of unspecific morphological changes versus more specific effects in zebrafish (Danio rerio) embryos. *Environ. Sci. Eur.* **2020**, 32, 122. doi:10.1186/s12302-020-00398-3.
33. Zager, M.G., Barton, H.A. A multiscale, mechanism-driven, dynamic model for the effects of 5α-reductase inhibition on prostate maintenance. *PLoS One* **2012**, 7, e44359. doi:10.1371/journal.pone.0044359.
34. Torres, J.M.; Ruiz, E., Ortega, E. Development of a quantitative RT-PCR method to study 5alpha-reductase mRNA isozymes in rat prostate in different androgen status. *Prostate* **2003**, 56, 74-79. doi:10.1002/pros.10221.
35. George, F.W.; Russell, D.W., Wilson, J.D. Feed-forward control of prostate growth: dihydrotestosterone induces expression of its own biosynthetic enzyme, steroid 5 alpha-reductase. *Proc. Natl. Acad. Sci. U. S. A.* **1991**, 88, 8044-8047. doi:10.1073/pnas.88.18.8044.
36. Handa, R.J.; Pak, T.R.; Kudwa, A.E.; Lund, T.D., Hinds, L. An alternate pathway for androgen regulation of brain function: activation of estrogen receptor beta by the metabolite of dihydrotestosterone, 5alpha-androstane-3beta,17beta-diol. *Horm. Behav.* **2008**, 53, 741-752. doi:10.1016/j.yhbeh.2007.09.012.
37. Pak, T.R.; Chung, W.C.; Hinds, L.R., Handa, R.J. Estrogen receptor-beta mediates dihydrotestosterone-induced stimulation of the arginine vasopressin promoter in neuronal cells. *Endocrinology* **2007**, 148, 3371-3382. doi:10.1210/en.2007-0086.
38. Pak, T.R.; Chung, W.C.; Lund, T.D.; Hinds, L.R.; Clay, C.M., Handa, R.J. The androgen metabolite, 5alpha-androstane-3beta, 17beta-diol, is a potent modulator of estrogen receptor-beta1-mediated gene transcription in neuronal cells. *Endocrinology* **2005**, 146, 147-155. doi:10.1210/en.2004-0871.
39. Ishikawa, T.; Glidewell-Kenney, C., Jameson, J.L. Aromatase-independent testosterone conversion into estrogenic steroids is inhibited by a 5 alpha-reductase inhibitor. *J. Steroid Biochem. Mol. Biol.* **2006**, 98, 133-138. doi:10.1016/j.jsbmb.2005.09.004.
40. Chiang, E.F.; Yan, Y.L.; Tong, S.K.; Hsiao, P.H.; Guiguen, Y.; Postlethwait, J., Chung, B.C. Characterization of duplicated zebrafish cyp19 genes. *J. Exp. Zool.* **2001**, 290, 709-714.

doi:10.1002/jez.1121.

41. Mouriec, K.; Gueguen, M.M.; Manuel, C.; Percevault, F.; Thieulant, M.L.; Pakdel, F., Kah, O. Androgens upregulate cyp19a1b (aromatase B) gene expression in the brain of zebrafish (Danio rerio) through estrogen receptors. *Biol. Reprod.* **2009**, 80, 889-896. doi:10.1095/biolreprod.108.073643.
42. Le Page, Y.; Menuet, A.; Kah, O., Pakdel, F. Characterization of a cis-acting element involved in cell-specific expression of the zebrafish brain aromatase gene. *Mol. Reprod. Dev.* **2008**, 75, 1549-1557. doi:10.1002/mrd.20892.
43. Le Page, Y.; Scholze, M.; Kah, O., Pakdel, F. Assessment of xenoestrogens using three distinct estrogen receptors and the zebrafish brain aromatase gene in a highly responsive glial cell system. *Environ. Health Perspect.* **2006**, 114, 752-758. doi:10.1289/ehp.8141.
44. Menuet, A.; Pellegrini, E.; Brion, F.; Gueguen, M.M.; Anglade, I.; Pakdel, F., Kah, O. Expression and estrogen-dependent regulation of the zebrafish brain aromatase gene. *J. Comp. Neurol.* **2005**, 485, 304-320. doi:10.1002/cne.20497.
45. Lassiter, C.S., Linney, E. Embryonic expression and steroid regulation of brain aromatase cyp19a1b in zebrafish (Danio rerio). *Zebrafish* **2007**, 4, 49-57. doi:10.1089/zeb.2006.9995.
46. Nelson, E.R., Habibi, H.R. Estrogen receptor function and regulation in fish and other vertebrates. *Gen. Comp. Endocrinol.* **2013**, 192, 15-24. doi:10.1016/j.ygcen.2013.03.032.
47. Park, C.G.; Singh, N.; Ryu, C.S.; Yoon, J.Y.; Esterhuizen, M., Kim, Y.J. Species Differences in Response to Binding Interactions of Bisphenol A and its Analogs with the Modeled Estrogen Receptor 1 and In Vitro Reporter Gene Assay in Human and Zebrafish. *Environ. Toxicol. Chem.* **2022**, 41, 2431-2443. doi:10.1002/etc.5433.
48. Ekena, K.; Weis, K.E.; Katzenellenbogen, J.A., Katzenellenbogen, B.S. Identification of amino acids in the hormone binding domain of the human estrogen receptor important in estrogen binding. *J. Biol. Chem.* **1996**, 271, 20053-20059. doi:10.1074/jbc.271.33.20053.
49. Helsen, C.; Dubois, V.; Verfaillie, A.; Young, J.; Trekels, M.; Vancraenenbroeck, R.; De Maeyer, M., Claessens, F. Evidence for DNA-binding domain--ligand-binding domain communications in the androgen receptor. *Mol. Cell. Biol.* **2012**, 32, 3033-3043. doi:10.1128/mcb.00151-12.
50. Nadal, M.; Prekovic, S.; Gallastegui, N.; Helsen, C.; Abella, M.; Zielinska, K.; Gay, M.; Vilaseca, M.; Taulès, M.; Houtsmuller, A.B.; et al. Structure of the homodimeric androgen receptor ligand-binding domain. *Nat. Commun.* **2017**, 8, 14388. doi:10.1038/ncomms14388.
51. Gonzalez, T.L.; Rae, J.M.; Colacino, J.A., Richardson, R.J. Homology models of mouse and rat estrogen receptor-α ligand-binding domain created by in silico mutagenesis of a human template: molecular docking with 17ß-estradiol, diethylstilbestrol, and paraben analogs. *Comput. Toxicol.* **2019**, 10, 1-16. doi:10.1016/j.comtox.2018.11.003.
52. Margiotta-Casaluci, L.; Courant, F.; Antignac, J.P.; Le Bizec, B., Sumpter, J.P. Identification and quantification of 5α-dihydrotestosterone in the teleost fathead minnow (Pimephales promelas) by gas chromatography-tandem mass spectrometry. *Gen. Comp. Endocrinol.* **2013**, 191, 202-209. doi:10.1016/j.ygcen.2013.06.017.
53. Lee, M.R.; Loux-Turner, J.R., Oliveira, K. Evaluation of the 5α-reductase inhibitor finasteride on reproduction and gonadal development in medaka, Oryzias latipes. *Gen. Comp. Endocrinol.* **2015**, 216,

64-76. doi:10.1016/j.ygcen.2015.04.008.

54. Sperry, T.S., Thomas, P. Identification of two nuclear androgen receptors in kelp bass (Paralabrax clathratus) and their binding affinities for xenobiotics: comparison with Atlantic croaker (Micropogonias undulatus) androgen receptors. *Biol. Reprod.* **1999**, 61, 1152-1161. doi:10.1095/biolreprod61.4.1152.
55. Flouriot, G.; Pakdel, F., Valotaire, Y. Transcriptional and post-transcriptional regulation of rainbow trout estrogen receptor and vitellogenin gene expression. *Mol. Cell. Endocrinol.* **1996**, 124, 173-183. doi:10.1016/s0303-7207(96)03960-3.
56. Kim, B.H.; Takemura, A.; Kim, S.J., Lee, Y.D. Vitellogenin synthesis via androgens in primary cultures of tilapia hepatocytes. *Gen. Comp. Endocrinol.* **2003**, 132, 248-255. doi:10.1016/s0016-6480(03)00091-1.
57. Le Menn, F.; Rochefort, H., Garcia, M. Effect of androgen mediated by the estrogen receptor of fish liver: vitellogenin accumulation. *Steroids* **1980**, 35, 315-328. doi:10.1016/0039-128x(80)90044-6.
58. Riley, L.G.; Hirano, T., Grau, E.G. Estradiol-17beta and dihydrotestosterone differentially regulate vitellogenin and insulin-like growth factor-I production in primary hepatocytes of the tilapia Oreochromis mossambicus. *Comp. Biochem. Physiol. C Toxicol. Pharmacol.* **2004**, 138, 177-186. doi:10.1016/j.cca.2004.07.009.

4.9 Supporting information

Table S4. 17β-estradiol (E2), dihydrotestosterone (DHT), and dutasteride binding free energies after docking with zebrafish estrogen receptor alpha (zfERα) and androgen receptor (zfAR).

Receptor	Ligand	Interacting residues	Binding free energy (Vina/CDOCKER) (Kcal/mol)	Hydrogen bond interaction		Hydrophobic interaction		Van der Waals interaction		Other interactions	
				No.	Amino acids	No.	Amino acids	No.	Amino acids	No.	Amino acids
zfERα	E2	20	-10.6/ -49.8	3	GLU321, ARG362, HIS492	10	LEU314, ALA318, LEU352, LEU355, MET356, LEU359, PHE372, MET389, ILE392, LEU493	7	MET311, THR315, MET317, PHE393, LEU396, GLY489, MET496	-	-
	Dutasteride	15	-9.8/ -56.4	2	VAL295, LYS417	3	PRO292, MET325, ARG362	9	ALA294, GLU291, HIS324, TRP328, VAL354, LEU355, TRP361, GLN374, PHE413	1	GLU321 (Halogen)
zfAR	DHT	22	-9.6/ -43.2	3	ASN655, ARG702, THR825	7	LEU654, TRP691, MET692, MET695, PHE714, MET730, PHE824	12	LEU651, LEU657, GLY658, GLN661, VAL696, LEU699, MET737, LEU821, LEU828, PHE841, ILE845, ILE849	-	-
	Dutasteride	20	-9.8/ -86.07	1	ASN655	8	LEU654, LEU657, MET695, VAL696, ALA698, PHE714, MET730, LEU821	9	LEU657, GLY658, GLN661, MET692, MET737, PHE824, LEU828, PHE841, ILE849,	2	LEU651 (Halogen), ARG702 (Halogen)

Chapter 5. SRD5A inhibition and steroid hormone profiling

Contribution

As accepted in: **Hyunki Cho**, Young Jun Kim, and Chang Seon Ryu

(This study is in preparation for publication).

Authorship contributions

Hyunki Cho: Writing– original draft and review & editing, Validation, Investigation, Formal analysis, Data curation. Young Jun Kim: Writing – review & editing, Supervision, Project administration, Funding acquisition. Chang Seon Ryu: Writing–original draft and review & editing, draft, Visualization, Validation, Supervision, Methodology, Conceptualization.

Relation to the thesis

Chapter 5 investigates the impact of the 5α-reductase (SRD5A) inhibitors, dutasteride and finasteride, on steroid hormone profiling in H295R cells, offering a comprehensive analysis of steroidogenic disruptions beyond testosterone (T) and 17β-estradiol (E2). By employing a GC-MS/MS-based approach for the quantification 14 steroid hormones, this chapter addresses the limitations of traditional steroidogenesis assays, such as the OECD TG 456, which primarily focus on T and E2. The extended profiling facilities the detection of subtle alterations across steroidogenic pathways, including mineralocorticoids, glucocorticoids, progestins, and androgens, thereby providing a broader understanding of the systemic impacts of SRD5A inhibition.

The findings contribute to the thesis by highlighting the significance of alternative androgen pathways, such as the backdoor pathways, in compensating for the reduction in DHT levels. Furthermore, the application of product-to-substrate ratios, such as the E2/T, progesterone/pregnenolone, and corticosterone/11-deoxycorticosterone, demonstrates the potential to identify indirect disruptions that may not be evident from individual hormone levels alone. This chapter enhances the mechanistic understanding of SRD5A inhibition and its broader effects on steroidogenic pathways, offering valuable data for the development of AOPs related to SRD5A inhibition.

5.1 Abstract

Human adrenocortical H295R cells are a well-established *in vitro* model for detecting chemicals that disrupt steroidogenesis, as validated by the OECD Test Guideline 456, which primarily assesses testosterone (T) and 17β-estradiol (E2) biosynthesis. This study employed a novel GC-MS/MS-based approach to investigate the impact of 5α-reductase (SRD5A) inhibitors, finasteride and dutasteride, on steroidogenesis. By quantifying 14 steroid hormones, the study expanded profiling beyond T and E2 to include progestins, mineralocorticoids, glucocorticoids, androgens, and estrogens, enabling a more comprehensive assessment of steroidogenic disruption. The extended steroid profiling revealed widespread disruptions across steroidogenic pathways, highlighting the broader effects of SRD5A inhibition. Exposure to finasteride and dutasteride significantly reduced E2 levels and showed a decreasing trend in progestins, glucocorticoids, and mineralocorticoids. Although DHT was undetectable in H295R cells, the findings suggest that its reduction may trigger alternative androgen pathways, such as the backdoor pathways, as a compensatory response. Additionally, product-to-substrate ratios—including E2/T, progesterone/pregnenolone, and corticosterone/11-deoxycorticosterone—were used to evaluate CYP19A1, 3β-HSD, and CYP11B activity, providing insights into enzymatic disruptions that may not be apparent from individual metabolite levels alone. These findings demonstrate that extended steroid profiling, combined with product-to-substrate ratio analysis, enhances the detection of chemical-induced perturbations in steroidogenesis, offering deeper insights into the mechanisms of endocrine-disrupting chemicals. This approach facilitates the classification of chemicals based on their mode of action and supports the prioritization of further toxicological research, ultimately advancing chemical safety assessments.

5.2 Introduction

Steroid hormones are essential regulators of various physiological processes, including metabolism, homeostasis, and sexual development. These hormones are synthesized in the gonads and adrenal glands through a series of enzymatic reactions collectively known as steroidogenesis, with cholesterol serving as the precursor [1]. Concerns have been raised regarding potential disruptions to this pathway caused by endocrine-disrupting chemicals (EDCs) due to their capacity to interfere with hormonal systems through mechanisms such as enzyme inhibition, receptor modulation, and post-translational modifications [2; 3]. Among EDCs, 5α-reductase (SRD5A) inhibitors, such as finasteride and dutasteride, have gained attention for their therapeutic applications in treating androgenetic alopecia and benign prostatic hyperplasia by inhibiting the conversion of testosterone (T) to dihydrotestosterone (DHT), a potent androgen [4-8]. Recent studies investigating the adverse outcome pathway (AOP) 289 have outlined the mechanistic consequences of SRD5A inhibition. The molecular initiating event in AOP289 is the inhibition of SRD5A, which leads to reduced DHT levels. This decrease in DHT is linked to a subsequent reduction in 17β-estradiol (E2) levels, causing reduced vitellogenin (VTG) levels and ultimately impairing reproduction. While AOP289 provides a clear framework for understanding these disruptions,

the mechanistic relationship between decreased DHT and reduced E2 remains poorly understood, necessitating further investigation into this critical connection.

The human H295R adrenocortical carcinoma cell line has emerged as a robust *in vitro* model for studying the effects of EDCs, including SRD5A inhibitors [9; 10]. This cell line expresses the majority of key enzymes involved in steroidogenesis and closely mimics the functionality of the human adrenal cortex, enabling comprehensive investigation into chemical effects on steroid hormone biosynthesis [11; 12]. Recognizing its value, the Organization for Economic Cooperation and Development (OECD) Test Guideline (TG) 456 [10], in collaboration with the United States Environmental Protection Agency (USEPA) Endocrine Disruptor Screening Program (EDSP), has validated the H295R cell line as a reliable system to assess the impact of chemicals on steroid hormone production, particularly focusing on T and E2 [13; 14; 10]. Despite its widespread adoption, TG 456 presents notable limitations. The guideline does not define specific analytical methods for hormone quantification, permitting the use of antibody-based approaches that are prone to cross-reactivity and overestimation, which may reduce data reliability [15; 9; 16]. Furthermore, the primary focus on T and E2 disregards disruptions in other crucial steroidogenic pathways, including those involving progestins, glucocorticoids, mineralocorticoids, and adrenal androgens, thus limiting its scope in detecting broader endocrine effects [16].

Advancements in analytical techniques, particularly gas chromatography-tandem mass spectrometry (GC-MS/MS), have significantly addressed the limitations of traditional methods. The employment GC-MS/MS enables the simultaneous quantification of multiple steroid hormones with high sensitivity and selectivity, facilitating expanded analyses of steroidogenic pathways and providing deeper insights into the effects of EDCs on hormone production [17-20]. In addition, modifications to the OECD TG 456 method, such as the incorporation of forskolin (FSK) to stimulate steroidogenesis, have optimized the assay as a broader tool for EDC screening. By increasing steroid hormone production, this adjustment supports the detection of antagonistic effects across multiple steroidogenic pathways, thereby enhancing its utility in EDC research [21-24].

This study investigates the impact of SRD5A inhibitors on steroidogenesis in FSK-stimulated H295R cells. A targeted metabolomic approach was employed, utilizing a GC-MS/MS method to quantify 14 steroid hormones. This method enables a comprehensive evaluation of the impact of SRD5A inhibition on steroidogenic pathways. By investigating the mechanisms underlying SRD5A inhibition, this study offers the potential for deeper insights into EDC-mediated disruptions in steroidogenesis. The findings aim to advance high-throughput screening methods for EDC detection and establish a robust framework for prioritizing chemicals for further toxicological evaluation.

5.3 Materials and methods

5.3.1 Chemicals and reagents

Dutasteride (Cas No. 164656-23-9), finasteride (Cas No. 98319-26-7), dehydroepiandrosterone (Cas No. 53-43-0), androstenedione (Cas No. 63-05-8), T (Cas No. 58-22-0), estrone (Cas No. 53-16-7), E2 (Cas

No. 50-28-2), E2-13C3 (Cas No. 1261254-48-1), progesterone (Cas No. 57-83-0), 17α-hydroxypregnenolone (Cas No. 387-79-1), 17α-hydroxyprogesterone (Cas No. 68-96-2), 11-deoxycortisol (Cas No. 641-77-0), 11-deoxycorticosterone (Cas No. 64-85-7), cortisone (Cas no. 53-06-5), corticosterone (Cas no. 50-22-6), cortisol (Cas No. 50-23-7), cortisol-d4 (Cas No. 73565-87-4), prochloraz (PCZ; Cas No. 67747-09-5), and N-Methyl-N-trimethylsilyltrifluoroacetamide (MSTFA) activated I reagent were purchased from Sigma-Aldrich (Steinheim, Germany). T-13C3 (Cas No. 27048-83-9) and pregnenolone (Cas No. 145-13-1) were purchased from LGC Standards GmbH (Wesel, Germany). Pregnenolone-13C2-d2 was purchased from BIOZOL Diagnostica Vertrieb GmbH (Eching, Germany). FSK (Cas No. 66575-29-9) was purchased from Biomol GmbH (Hamburg, Germany). Stock solutions was prepared in dimethyl sulfoxide (DMSO) (Sigma-Aldrich).

5.3.2 Cell culture and chemical treatment

The experimental procedures were conducted in accordance with OECD TG 456 [10] [1] and a prior study [21]. NCI-H295R cells (ATCC, Manassas, VA, USA) were cultured in DMEM/F12 supplemented with 1% ITS+ Premix (Cat. 354352, Corning), 2.5% Nu-Serum (Cat. 355100, Corning), 100 units/mL penicillin, and 100 µg/mL streptomycin at 37°C with 5% CO_2. Cells were maintained on a 2-3 day passage cycle, and passages 4 to 9 were used for experiments. For optimization, cells were seeded in 24-well plates at 20×10^4, 25×10^4, or 30×10^4 cells/mL and incubated for 24 hours. The medium was then replaced with 10 µM forskolin or 0.1% DMSO (control) and incubated for 48 hours, after which the culture medium was collected to compare basal and FSK-stimulated hormone levels. Subsequently, diluted finasteride, dutasteride,1 µM PCZ or fresh medium with 0.1% DMSO was added, followed by another 48-hour incubation for steroid hormone quantification.

5.3.3 Quantification of steroid hormones

5.3.3.1 Sample preparation

The methods that were modified by Patt et al. (2020); Teubel et al. (2018) was used for sample preparation. 800 µL of collected culture medium was spiked with T-13C3, E2-13C3, pregnenolone-13C2-d2, and cortisol-d4 as a internal standard (Final concentration: 14.4, 2.7, 15.8, and 18.1 ng/mL). The sample were extracted using a Strata-X 33 µm Polymeric Reversed Phase cartridge (30 mg/3 mL, Phenomenex, Inc., Aschaffenburg, Germany). The cartridge was conditioned with methanol and Milli-Q water, and the sample was loaded. Next, the cartridge was washed by sequentially adding 2 mL of Milli-Q water and 1 mL of methanol/water (1:9, v/v). Steroid hormones were eluted by adding 800 µL of methanol, then were dried under a stream of nitrogen. After drying, 40 µL of MSTFA reagent was added to each tube, incubated at 60 °C for 40 minutes, and the derivatized steroid hormone was analyzed using GC-MS/MS.

5.3.3.2 GC-MS/MS analysis

14 steroid hormones were quantitated on a TRACE 1310 GC (Thermo Fisher Scientific, Waltham, MA, USA) equipped with TriPlus RSH autosampler (Thermo Scientific,) and TSQ9000 triple quadrupole mass spectrometer (Thermo Scientific). A 2 µL sample was injected in split mode (1:6 ratio) at 280 ℃ and separated via a RESTEK MXT-1 capillary column (30 m × 0.25 mm i.d., 0.25 µm film thickness) under the constant flow of 0.8 mL/min helium carrier gas. The oven ramping and instrument conditions followed a previously study [19]. The oven temperature program was as follows: initially raised at a rate of 20 °C/min to 230 °C and held for 2 min, then raised at a rate of 2 °C/min to 250 °C and held for 2 min, and finally raised at a rate of 30 °C/min to 310 °C and held for 2 min. The GC-MS/MS instrument was configured with the following parameters: transfer line temperature of 320 °C, ion source temperature of 230 °C, electron energy of 70 eV, and selected reaction monitoring (SRM) mode for quantitation. Chromeleon software (version 7.2.8, Thermo Scientific) was used for data acquisition and analysis. A representative chromatogram and calibration curves for the 14 steroid hormones are shown in Figure S1.1. The optimized SRM parameters are detailed in Table S1.

5.3.4 Statistical analysis

All results were obtained from at least three independent experiments. Statistical analysis was performed using GraphPad Prism software (version 9.5.1; GraphPad Software, San Diego, CA, USA). The normality of data was confirmed using the Shapiro-Wilk test. Statistical differences in each group were determined by one-way analysis of variance (ANOVA) followed by Tukey's honestly significant difference test.

5.4 Results

5.4.1 Steroid hormone level in H295R cells in the basal and FSK stimulated state

The concentrations of 14 steroid hormones were quantified in H295R cells under basal conditions and following FSK stimulation (Figure 5.1). In the basal state, the production of most hormones was relatively low across all seeding densities, although measurable hormone synthesis responses were observed. At seeding densities of 20×10^4, 25×10^4, and 30×10^4 cells/mL, T levels were 2.12 ± 0.34, 3.05 ± 0.42, and 3.53 ± 0.38 nM, respectively. E2 levels at the same densities were 0.37 ± 0.01, 0.65 ± 0.01, and 0.85 ± 0.06 nM, respectively. E2 level at the same condition was 0.37 ± 0.01, 0.65 ±0.01, and 0.85 ± 0.06 nM, respectively. FSK stimulation significantly increased the synthesis of most measured steroid hormones. Specifically, T levels increased by 2.4, 2.2, and 2.0 times relative to basal levels at seeding densities of 20×10^4, 25×10^4, and 30×10^4 cells/mL, respectively. Similarly, E2 levels increased by 8.8, 6.6, and 6.2 times compared to basal levels under the same FSK stimulation conditions.

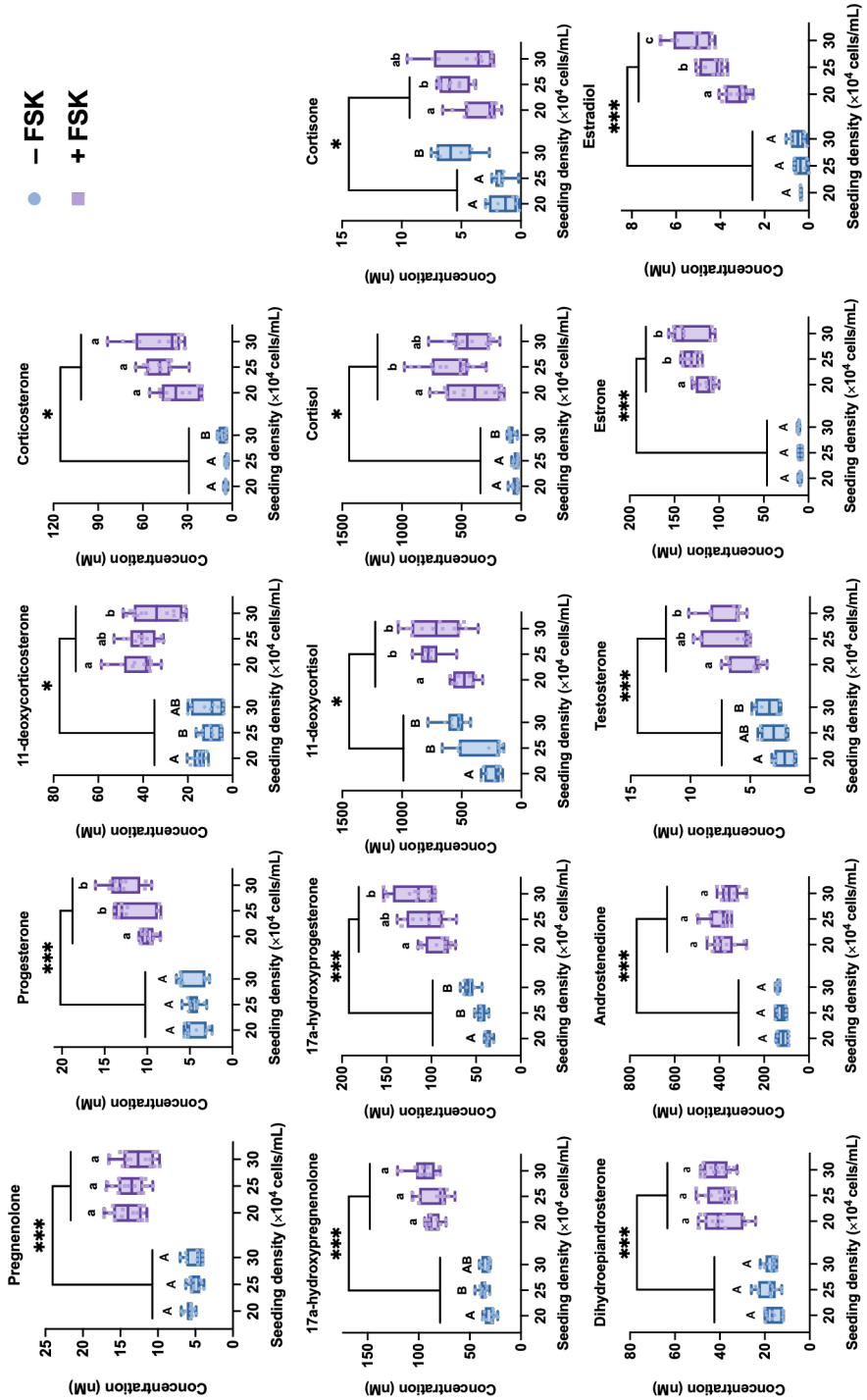

Figure5.1. Steroid hormone levels in H295R cells under basal and FSK-stimulated conditions at different cell densities (20, 25, and 30×10^4 cells/mL). Comparisons between the basal and forskolin-stimulated states for each cell density were performed using a Two-tailed Student's *t*-test ($*p < 0.05$ and $***p < 0.001$). One-way ANOVA followed by Tukey's multiple comparison test was used to compare hormone levels across cell densities within each group (basal and forskolin-stimulated states). Different letters indicate significant differences between cell densities within the same group at $p < 0.05$. Data are presented as MEAN ± SEM from at least three independent experiments ($n \geq 3$).

5.4.2 Steroid hormone level in H295R cells exposed to dutasteride and finasteride

Finasteride and dutasteride exposure demonstrated a tendency to decrease the levels of most steroid hormones (Figure 5.2a). Specifically, E2 levels were significantly reduced following exposure to 5.0 μM finasteride and across all exposures to dutasteride at concentrations ranging from 0.1 to 1.0 μM. Androgen levels showed a tendency to increase with both finasteride and dutasteride exposure; however, these changes were not statistically significant. Progestins, glucocorticoids, and mineralocorticoids generally exhibited a decreasing trend upon exposure to finasteride and dutasteride. Notably, pregnenolone, progesterone, cortisone, and cortisol levels were significantly reduced, while the levels of 11-deoxycorticosterone and corticosterone were significantly decreased with exposure to 5.0 μM finasteride. The impact of dutasteride and finasteride on aromatase enzymatic activity was evaluated using the ratio of the product (estrone or E2) to the substrate (androstenedione or T, respectively) (Figure 5.2b). 3β-hydroxysteroid dehydrogenase (3β-HSD) and steroid 11β-hydroxylase (CYP11B1) activities, assessed through precursor/product ratio under exposure to dutasteride and finasteride also expressed on Figure S5.4. Aromatase (CYP19A1) activity, as measured by the E2/T ratio, was significantly reduced by exposure to 5.0 μM finasteride and 0.5 μM dutasteride.

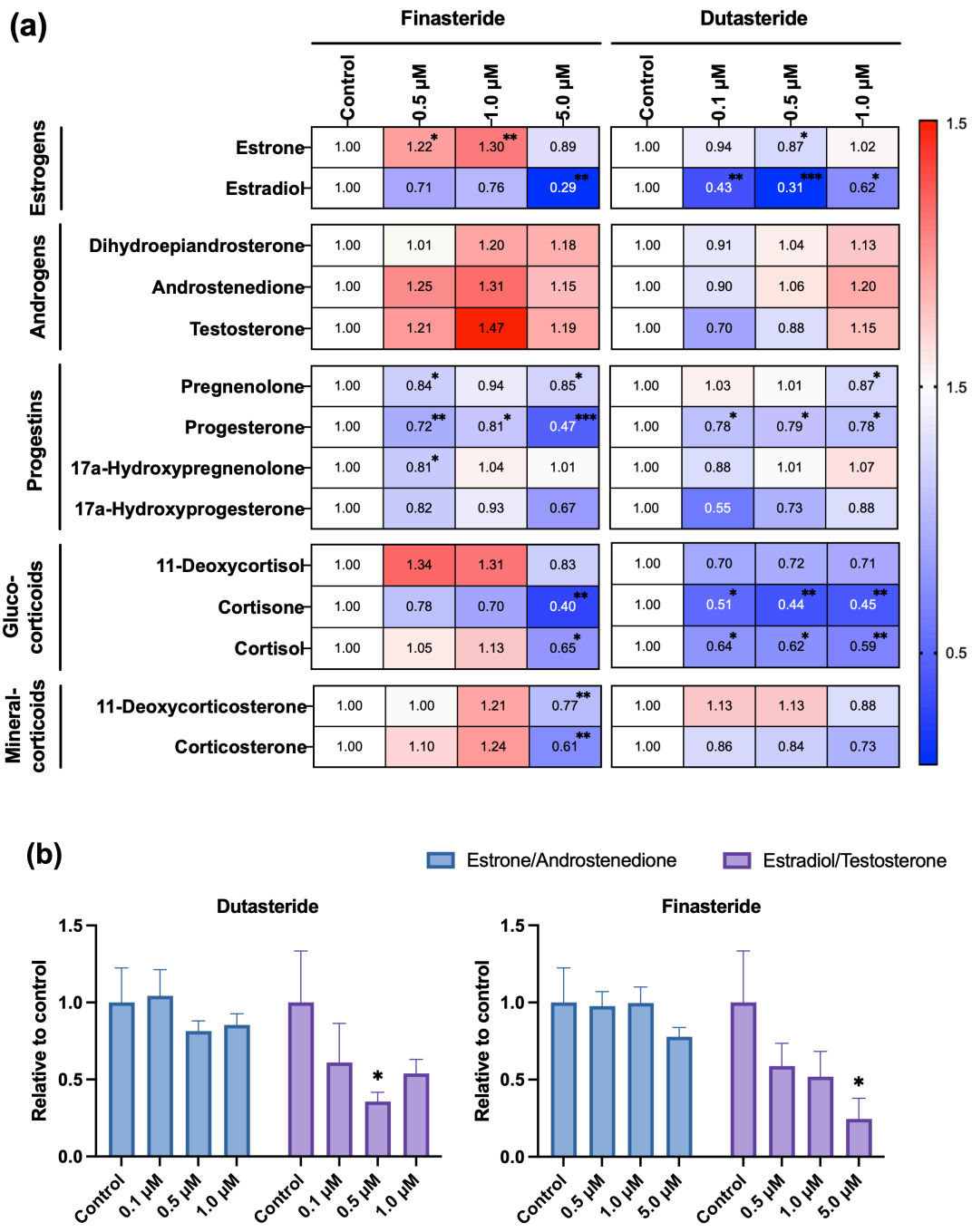

Figure 5.2. Effects of finasteride and dutasteride on steroidogenesis in FSK-stimulated H295R cells. (a) Heat map showing the relative levels of 14 steroid hormones in FSK-stimulated H295R cells treated with varying concentrations of dutasteride and finasteride, with values normalized to the control (set to 1). The red and blue coloring represents changes in steroid hormone levels relative to the control, with red indicating an increase and blue indicating a decrease. The intensity of the color reflects the magnitude of these changes. Steroid hormone levels are categorized by their respective steroidogenic pathways: estrogens, androgens, progestins, glucocorticoids, and mineralocorticoids. (b) Estimated inhibition of aromatase activity, assessed through estrone/androstenedione and E2/T ratios under exposure to dutasteride and finasteride. Data are expressed as mean ± SD from at least three independent experiments ($n \geq 3$). Statistical significance relative to the control is indicated by *$p < 0.05$, **$p < 0.01$, and ***$p < 0.001$.

5.5 Discussion

This study utilized a GC-MS/MS-based quantification method with MSTFA derivatization to broaden the assessment of steroidogenesis pathways, addressing the limitations of traditional assays that focus exclusively on T and E2 levels and commonly employ ELISA for quantification [10]. By incorporating this advanced analytical approach, the study developed a quantitative method to measure 14 steroid hormones spanning five steroid groups: progestins, glucocorticoids, mineralocorticoids, androgens, and estrogens, including T and E2, which are covered by the existing OECD TG 456. This expanded profiling provides critical insights into how chemical exposures impact steroidogenic pathways, capturing disruptions that might not be detectable when focusing solely on testosterone and estradiol levels.

OECD TG 456 establishes performance criteria for quality control, requiring T and E2 levels to increase by at least 1.5 and 7.5 times, respectively, compared to the solvent control under 10 μM FSK-stimulated conditions, and to decrease to less than 0.5 times the solvent control level with 1 μM PCZ exposure. In alignment with these criteria, this study evaluated T and E2 production across varying cell densities (20×10^4, 25×10^4, and 30×10^4 cells/mL). Under FSK-stimulated conditions, T levels increased by 2.4 ± 0.4, 2.2 ± 0.4, and 2.0 ± 0.3 times, respectively, compared to basal levels, while E2 levels increased by 8.8 ± 0.5, 12.0 ± 3.8, and 10.2 ± 2.6 times. When normalized for cell density, most steroid hormone levels were consistent across groups; however, pregnenolone, 11-deoxycorticosterone, 17α-hydroxypregnenolone, dehydroepiandrosterone, androstenedione, and estrone levels were significantly higher at a seeding density of 20×10^4 cells/mL compared to other densities (Figure S5.2). Based on these normalized data, a seeding density of 20×10^4 cells/mL was selected for subsequent chemical exposure experiments. Exposure to 1 μM PCZ significantly inhibited the production of both T and E2 (Figure S5.3). These results confirm that the criteria established by OECD TG 456 were met, validating the assay's performance.

The effects of SRD5A inhibitors, finasteride and dutasteride, were investigated in H295R cells, which express the SRD5A enzyme and androgen receptor, both integral to androgenic signaling [27]. This suggests the potential involvement of a DHT-mediated signaling pathway in these cells. However, DHT levels remained undetectable, even under FSK-stimulated conditions, likely due to low DHT production. Despite this, given the potency of DHT, the possibility of signaling through its metabolites cannot be disregarded. While both finasteride and dutasteride inhibit SRD5A, they differ in potency and isoform selectivity. Finasteride primarily inhibits SRD5A2 but also exhibits inhibitory activity against SRD5A1, though with comparatively lower potency [28]. In contrast, dutasteride effectively inhibits both SRD5A1 and SRD5A2 with greater efficacy, leading to a more substantial reduction in systemic DHT levels. This differential inhibition was also demonstrated in a previous study using overexpressed human SRD5A enzymes [29]. Consequently, dutasteride may induce broader hormonal disruptions than finasteride, including a more pronounced decrease in E2 levels. This trend was observed in the present study, where dutasteride exhibited stronger inhibitory effects on steroidogenesis, particularly in reducing estrogen levels. Consistent with these findings, previous studies have reported that SRD5A inhibition leads to reduced DHT levels, accompanied by a decline in E2 [30; 31]. Furthermore, research suggests that 3β-

androstanediol, a downstream metabolite of DHT, may modulate estrogen receptor (ER) signaling by binding to ERβ and inducing estrogen response element-mediated transcription [32; 33]. This interplay between androgen metabolism and estrogen signaling adds further complexity to the hormonal consequences of SRD5A inhibition.

Recent studies have identified three primary pathways involved in androgen biosynthesis [34-37]. The classical "front-door" pathway synthesizes T *de novo* from cholesterol or converts it from circulating adrenal androgen precursors [37]. The primary backdoor pathway bypasses T as an intermediate and instead synthesizes DHT through intermediates such as progesterone and androstanediol. The secondary backdoor pathway utilizes precursors like dehydroepiandrosterone and androstanedione [36; 37]. Initially, the backdoor pathway was thought to enable local androgen synthesis independently of T precursors [36]. However, both the canonical and backdoor pathways are now recognized as critical routes for androgen biosynthesis from cholesterol. Experimental study, particularly those using LNCaP xenografts, suggested that backdoor androgen synthesis may become dominant following finasteride exposure, as SRD5A inhibition shifts androgen metabolism toward alternative pathways [38]. Furthermore, the effectiveness of finasteride and dutasteride may be compromised by T accumulation or incomplete depletion of intratumoral DHT levels [35; 39; 40]. This insufficient suppression of DHT may result from active SRD5A3 or the recruitment of primary or secondary backdoor pathways, further disrupting steroid hormone homeostasis [41-43]

Another possible explanation for the observed hormonal shifts is the activation of 5β-reduction, a compensatory mechanism triggered by SRD5A inhibition. Unlike 5α-reduction, which produces bioactive androgens, 5β-reduction generates inactive steroid metabolites [44; 45]. This pathway, catalyzed by aldo-keto reductase family 1 member D1 (AKR1D1), diverts progesterone and testosterone into 5β-dihydro metabolites, such as 5β-dihydroprogesterone and 5β-DHT. Although AKR1D1 is primarily expressed in the liver and testes, its expression in the adrenal gland is minimal [46]. These 5β-reduced metabolites lack androgenic activity and serve as terminal products in steroid metabolism. If SRD5A inhibition redirects steroid flux toward 5β-reduction, it may limit precursor availability for androgen and estrogen synthesis, leading to hormonal imbalances.

To further investigate the effects of SRD5A inhibition, product-to-precursor ratios were calculated to estimate key steroidogenic enzyme activity. This analysis revealed significant disruptions across multiple enzymatic pathways [47; 9; 48; 49]. The E2/T ratio, an indicator of aromatase activity, was significantly reduced, suggesting an indirect effect caused by hormonal disruption rather than direct aromatase inhibition. The progesterone/pregnenolone ratio, reflecting 3β-HSD activity, also decreased significantly, indicating upstream disruptions in steroidogenesis. Similarly, the corticosterone/11-deoxycorticosterone ratio, indicative of CYP11B activity, was significantly reduced. The decline in progesterone levels may have impaired corticosterone production, consistent with the observed reduction in corticosterone/11-deoxycorticosterone ratios. These disruptions in 3β-HSD and CYP11B activity suggest that SRD5A inhibition broadly affects steroidogenesis, potentially leading to dysregulated hormone levels.

5.6 Conclusion

This study demonstrated that SRD5A inhibitors, finasteride and dutasteride, significantly disrupted steroidogenesis in H295R cells, leading to a reduction in E2 levels, aligning with previous research on SRD5A inhibition in vertebrate species. While the precise mechanisms underlying these disruptions remain to be fully elucidated, the results suggest that decreased DHT levels may trigger compensatory activation of alternative androgen biosynthetic pathways, such as the backdoor pathways, which could indirectly affect aromatase activity and contribute to reduced E2 synthesis. Beyond the impact on androgens and estrogens, widespread alterations across multiple steroid groups, including progestins, glucocorticoids, and mineralocorticoids, highlight the systemic effects of SRD5A inhibition and the interconnectivity of steroidogenic pathways. Disruptions in 3β-HSD and CYP11B activity, as indicated by significant reductions in progesterone/pregnenolone and corticosterone/11-deoxycorticosterone ratios, suggest that SRD5A inhibition extends beyond androgen metabolism to influence multiple enzymatic processes. The comprehensive steroid profiling employed in this study moves beyond conventional assessments of testosterone and estradiol, offering deeper insights into chemical-induced disruptions in steroidogenesis. These findings underscore the importance of evaluating hormonal perturbations within the broader context of steroidogenic regulation rather than focusing on isolated hormone changes.

5.7 Bibliography

1. Payne, A.H., Hales, D.B. Overview of steroidogenic enzymes in the pathway from cholesterol to active steroid hormones. *Endocr. Rev.* **2004**, 25, 947-970. doi:10.1210/er.2003-0030.
2. Diamanti-Kandarakis, E.; Bourguignon, J.P.; Giudice, L.C.; Hauser, R.; Prins, G.S.; Soto, A.M.; Zoeller, R.T., Gore, A.C. Endocrine-disrupting chemicals: an Endocrine Society scientific statement. *Endocr. Rev.* **2009**, 30, 293-342. doi:10.1210/er.2009-0002.
3. La Merrill, M.A.; Vandenberg, L.N.; Smith, M.T.; Goodson, W.; Browne, P.; Patisaul, H.B.; Guyton, K.Z.; Kortenkamp, A.; Cogliano, V.J.; Woodruff, T.J.; et al. Consensus on the key characteristics of endocrine-disrupting chemicals as a basis for hazard identification. *Nat. Rev. Endocrinol.* **2020**, 16, 45-57. doi:10.1038/s41574-019-0273-8.
4. Choi, S.; Kwon, S.-H.; Sim, W.-Y., Lew, B.-L. Long-term efficacy and safety of dutasteride 0.5 mg in Korean men with androgenetic alopecia: 5-year data demonstrating clinical improvement with sustained efficacy. *J. Dermatol.* **2024**, 51, 684-690. doi:doi.org/10.1111/1346-8138.17138.
5. Kane, S.P. Finasteride. *ClinCalc LLC: [Online]*, February 19, 2022, Available from: https://clincalc.com/DrugStats/Drugs/Finasteride.
6. Kaufman, K.D.; Olsen, E.A.; Whiting, D.; Savin, R.; DeVillez, R.; Bergfeld, W.; Price, V.H.; Van Neste, D.; Roberts, J.L.; Hordinsky, M.; et al. Finasteride in the treatment of men with androgenetic alopecia. Finasteride Male Pattern Hair Loss Study Group. *J. Am. Acad. Dermatol.* **1998**, 39, 578-589. doi:10.1016/s0190-9622(98)70007-6.

7. Sharma, R. Dutasteride Market Research Report 2032. *[Online]*, December 19, 2024, Available from: https://dataintelo.com/report/dutasteride-market-report.
8. Singh, S., Deshmukh, R. Finasteride Market Size, Share, Competitive Landscape and Trend Analysis Report by Application (Benign Prostatic Hyperplasia (BPH), Male pattern baldness), by Type (Branded , Generic), by Distribution Channel (Hospital Pharmacies, Online Providers, Drug Stores and Retail Pharmacies): Global Opportunity Analysis and Industry Forecast, 2021-2031. *[Online]*, February 04, 2023, Available from: https://www.alliedmarketresearch.com/finasteride-market-A14012.
9. Jäger, M.C.; Patt, M.; González-Ruiz, V.; Boccard, J.; Wey, T.; Winter, D.V.; Rudaz, S., Odermatt, A. Extended steroid profiling in H295R cells provides deeper insight into chemical-induced disturbances of steroidogenesis: Exemplified by prochloraz and anabolic steroids. *Mol. Cell. Endocrinol.* **2023**, 570, 111929. doi:10.1016/j.mce.2023.111929.
10. OECD. Test No. 456: H295R Steroidogenesis Assay, OECD Guidelines for the Testing of Chemicals, Section 4. *OECD Publishing* **2023**, Paris. doi:10.1787/9789264122642-en.
11. Gazdar, A.F.; Oie, H.K.; Shackleton, C.H.; Chen, T.R.; Triche, T.J.; Myers, C.E.; Chrousos, G.P.; Brennan, M.F.; Stein, C.A., La Rocca, R.V. Establishment and characterization of a human adrenocortical carcinoma cell line that expresses multiple pathways of steroid biosynthesis. *Cancer Res.* **1990**, 50, 5488-5496.
12. Gracia, T.; Hilscherova, K.; Jones, P.D.; Newsted, J.L.; Zhang, X.; Hecker, M.; Higley, E.B.; Sanderson, J.T.; Yu, R.M.; Wu, R.S.; et al. The H295R system for evaluation of endocrine-disrupting effects. *Ecotoxicol. Environ. Saf.* **2006**, 65, 293-305. doi:10.1016/j.ecoenv.2006.06.012.
13. EPA. Endocrine Disruptor Screening Program Test Guidelines - OPPTS 890.1550: Steroidogenesis (Human Cell line - H295R) [EPA 640-C-09-003], *United States Environmental Protection Agency*, 2009, 1-45. Available from: https://nepis.epa.gov/Exe/ZyPURL.cgi?Dockey=P100SGZ2.txt.
14. Hecker, M.; Hollert, H.; Cooper, R.; Vinggaard, A.M.; Akahori, Y.; Murphy, M.; Nellemann, C.; Higley, E.; Newsted, J.; Laskey, J.; et al. The OECD validation program of the H295R steroidogenesis assay: Phase 3. Final inter-laboratory validation study. *Environ Sci Pollut Res Int* **2011**, 18, 503-515. doi:10.1007/s11356-010-0396-x.
15. Handelsman, D.J., Wartofsky, L. Requirement for mass spectrometry sex steroid assays in the Journal of Clinical Endocrinology and Metabolism. *J. Clin. Endocrinol. Metab.* **2013**, 98, 3971-3973. doi:10.1210/jc.2013-3375.
16. Odermatt, A.; Strajhar, P., Engeli, R.T. Disruption of steroidogenesis: Cell models for mechanistic investigations and as screening tools. *J. Steroid Biochem. Mol. Biol.* **2016**, 158, 9-21. doi:10.1016/j.jsbmb.2016.01.009.
17. Hadef, Y.; Kaloustian, J.; Portugal, H., Nicolay, A. Multivariate optimization of a derivatisation procedure for the simultaneous determination of nine anabolic steroids by gas chromatography coupled with mass spectrometry. *J. Chromatogr. A* **2008**, 1190, 278-285. doi:10.1016/j.chroma.2008.02.100.
18. Junker, J.; Chong, I.; Kamp, F.; Steiner, H.; Giera, M.; Müller, C., Bracher, F. Comparison of Strategies for the Determination of Sterol Sulfates via GC-MS Leading to a Novel Deconjugation-Derivatization Protocol. *Molecules* **2019**, 24. doi:10.3390/molecules24132353.
19. Lee, W.; Lee, H.; Kim, Y.L.; Lee, Y.C.; Chung, B.C., Hong, J. Profiling of Steroid Metabolic Pathways in

Human Plasma by GC-MS/MS Combined with Microwave-Assisted Derivatization for Diagnosis of Gastric Disorders. *Int. J. Mol. Sci.* **2021**, 22. doi:10.3390/ijms22041872.

20. Moon, J.Y.; Jung, H.J.; Moon, M.H.; Chung, B.C., Choi, M.H. Heat-map visualization of gas chromatography-mass spectrometry based quantitative signatures on steroid metabolism. *J. Am. Soc. Mass Spectrom.* **2009**, 20, 1626-1637. doi:10.1016/j.jasms.2009.04.020.
21. Haggard, D.E.; Karmaus, A.L.; Martin, M.T.; Judson, R.S.; Setzer, R.W., Paul Friedman, K. High-Throughput H295R Steroidogenesis Assay: Utility as an Alternative and a Statistical Approach to Characterize Effects on Steroidogenesis. *Toxicol. Sci.* **2018**, 162, 509-534. doi:10.1093/toxsci/kfx274.
22. Karmaus, A.L.; Toole, C.M.; Filer, D.L.; Lewis, K.C., Martin, M.T. High-Throughput Screening of Chemical Effects on Steroidogenesis Using H295R Human Adrenocortical Carcinoma Cells. *Toxicol. Sci.* **2016**, 150, 323-332. doi:10.1093/toxsci/kfw002.
23. Nakano, Y.; Yamashita, T.; Okuno, M.; Fukusaki, E., Bamba, T. In vitro steroid profiling system for the evaluation of endocrine disruptors. *J. Biosci. Bioeng.* **2016**, 122, 370-377. doi:10.1016/j.jbiosc.2016.02.008.
24. Schloms, L.; Storbeck, K.H.; Swart, P.; Gelderblom, W.C., Swart, A.C. The influence of Aspalathus linearis (Rooibos) and dihydrochalcones on adrenal steroidogenesis: quantification of steroid intermediates and end products in H295R cells. *J. Steroid Biochem. Mol. Biol.* **2012**, 128, 128-138. doi:10.1016/j.jsbmb.2011.11.003.
25. Patt, M.; Beck, K.R.; Di Marco, T.; Jäger, M.C.; González-Ruiz, V.; Boccard, J.; Rudaz, S.; Hartmann, R.W.; Salah, M.; van Koppen, C.J.; et al. Profiling of anabolic androgenic steroids and selective androgen receptor modulators for interference with adrenal steroidogenesis. *Biochem. Pharmacol.* **2020**, 172, 113781. doi:10.1016/j.bcp.2019.113781.
26. Teubel, J.; Wüst, B.; Schipke, C.G.; Peters, O., Parr, M.K. Methods in endogenous steroid profiling - A comparison of gas chromatography mass spectrometry (GC-MS) with supercritical fluid chromatography tandem mass spectrometry (SFC-MS/MS). *J. Chromatogr. A* **2018**, 1554, 101-116. doi:10.1016/j.chroma.2018.04.035.
27. Robitaille, C.N.; Rivest, P., Sanderson, J.T. Antiandrogenic mechanisms of pesticides in human LNCaP prostate and H295R adrenocortical carcinoma cells. *Toxicol. Sci.* **2015**, 143, 126-135. doi:10.1093/toxsci/kfu212.
28. Tian, G. In vivo time-dependent inhibition of human steroid 5 alpha-reductase by finasteride. *J. Pharm. Sci.* **1996**, 85, 106-111. doi:10.1021/js950100g.
29. Kim, D.; Cho, H.; Eggers, R.; Kim, S.K.; Ryu, C.S., Kim, Y.J. Development of a Liquid Chromatography/Mass Spectrometry-Based Inhibition Assay for the Screening of Steroid 5-α Reductase in Human and Fish Cell Lines. *Molecules* **2021**, 26. doi:10.3390/molecules26040893.
30. AOP-Wiki Inhibition of 5α-reductase leading to impaired fecundity in female fish. *Society for Advancement of AOPs [Online]*, April 29, 2023, Available from: https://aopwiki.org/aops/289.
31. Cho, H.; Jun, I.; Adnan, K.M.; Park, C.G.; Lee, S.A.; Yoon, J.; Ryu, C.S., Kim, Y.J. Effects of 5α-reductase inhibition by dutasteride on reproductive gene expression and hormonal responses in zebrafish embryos. *Comp. Biochem. Physiol. C Toxicol. Pharmacol.* **2024**, 287, 110048. doi:10.1016/j.cbpc.2024.110048.
32. Pak, T.R.; Chung, W.C.; Hinds, L.R., Handa, R.J. Estrogen receptor-beta mediates dihydrotestosterone-

induced stimulation of the arginine vasopressin promoter in neuronal cells. *Endocrinology* **2007**, 148, 3371-3382. doi:10.1210/en.2007-0086.

33. Pak, T.R.; Chung, W.C.; Lund, T.D.; Hinds, L.R.; Clay, C.M., Handa, R.J. The androgen metabolite, 5alpha-androstane-3beta, 17beta-diol, is a potent modulator of estrogen receptor-beta1-mediated gene transcription in neuronal cells. *Endocrinology* **2005**, 146, 147-155. doi:10.1210/en.2004-0871.
34. Ferraldeschi, R.; Welti, J.; Luo, J.; Attard, G., de Bono, J.S. Targeting the androgen receptor pathway in castration-resistant prostate cancer: progresses and prospects. *Oncogene* **2015**, 34, 1745-1757. doi:10.1038/onc.2014.115.
35. Fiandalo, M.V.; Gewirth, D.T., Mohler, J.L. Potential impact of combined inhibition of 3α-oxidoreductases and 5α-reductases on prostate cancer. *Asian J. Urol.* **2019**, 6, 50-56. doi:10.1016/j.ajur.2018.09.002.
36. Stuchbery, R.; McCoy, P.J.; Hovens, C.M., Corcoran, N.M. Androgen synthesis in prostate cancer: do all roads lead to Rome? *Nat. Rev. Urol.* **2017**, 14, 49-58. doi:10.1038/nrurol.2016.221.
37. Zhou, J.; Wang, Y.; Wu, D.; Wang, S.; Chen, Z.; Xiang, S., Chan, F.L. Orphan nuclear receptors as regulators of intratumoral androgen biosynthesis in castration-resistant prostate cancer. *Oncogene* **2021**, 40, 2625-2634. doi:10.1038/s41388-021-01737-1.
38. Locke, J.A.; Nelson, C.C.; Adomat, H.H.; Hendy, S.C.; Gleave, M.E., Guns, E.S. Steroidogenesis inhibitors alter but do not eliminate androgen synthesis mechanisms during progression to castration-resistance in LNCaP prostate xenografts. *J. Steroid Biochem. Mol. Biol.* **2009**, 115, 126-136. doi:10.1016/j.jsbmb.2009.03.011.
39. Shah, S.K.; Trump, D.L.; Sartor, O.; Tan, W.; Wilding, G.E., Mohler, J.L. Phase II study of Dutasteride for recurrent prostate cancer during androgen deprivation therapy. *J. Urol.* **2009**, 181, 621-626. doi:10.1016/j.juro.2008.10.014.
40. Yamana, K.; Labrie, F., Luu-The, V. Human type 3 5α-reductase is expressed in peripheral tissues at higher levels than types 1 and 2 and its activity is potently inhibited by finasteride and dutasteride. *Horm. Mol. Biol. Clin. Investig.* **2010**, 2, 293-299. doi:10.1515/hmbci.2010.035.
41. Chu, F.M.; Sartor, O.; Gomella, L.; Rudo, T.; Somerville, M.C.; Hereghty, B., Manyak, M.J. A randomised, double-blind study comparing the addition of bicalutamide with or without dutasteride to GnRH analogue therapy in men with non-metastatic castrate-resistant prostate cancer. *Eur. J. Cancer* **2015**, 51, 1555-1569. doi:10.1016/j.ejca.2015.04.028.
42. Titus, M.A.; Schell, M.J.; Lih, F.B.; Tomer, K.B., Mohler, J.L. Testosterone and dihydrotestosterone tissue levels in recurrent prostate cancer. *Clin. Cancer Res.* **2005**, 11, 4653-4657. doi:10.1158/1078-0432.Ccr-05-0525.
43. Uemura, M.; Tamura, K.; Chung, S.; Honma, S.; Okuyama, A.; Nakamura, Y., Nakagawa, H. Novel 5 alpha-steroid reductase (SRD5A3, type-3) is overexpressed in hormone-refractory prostate cancer. *Cancer Sci.* **2008**, 99, 81-86. doi:10.1111/j.1349-7006.2007.00656.x.
44. Barnard, L.; Nikolaou, N.; Louw, C.; Schiffer, L.; Gibson, H.; Gilligan, L.C.; Gangitano, E.; Snoep, J.; Arlt, W.; Tomlinson, J.W.; et al. The A-ring reduction of 11-ketotestosterone is efficiently catalysed by AKR1D1 and SRD5A2 but not SRD5A1. *J. Steroid Biochem. Mol. Biol.* **2020**, 202, 105724. doi:10.1016/j.jsbmb.2020.105724.

45. Chen, M., Penning, T.M. 5β-Reduced steroids and human Δ(4)-3-ketosteroid 5β-reductase (AKR1D1). *Steroids* **2014**, 83, 17-26. doi:10.1016/j.steroids.2014.01.013.
46. Appanna, N.; Gibson, H.; Gangitano, E.; Dempster, N.J.; Morris, K.; George, S.; Arvaniti, A.; Gathercole, L.L.; Keevil, B.; Penning, T.M.; et al. Differential activity and expression of human 5β-reductase (AKR1D1) splice variants. *J. Mol. Endocrinol.* **2021**, 66, 181-194. doi:10.1530/jme-20-0160.
47. Hicks, R.A.; Yee, J.K.; Mao, C.S.; Graham, S.; Kharrazi, M.; Lorey, F., Lee, W.P. Precursor-to-product ratios reflect biochemical phenotype in congenital adrenal hyperplasia. *Metabolomics* **2014**, 10, 123-131. doi:10.1007/s11306-013-0558-1.
48. Medeiros, S.F.; Gil-Junior, A.B.; Barbosa, J.S.; Isaías, E.D., Yamamoto, M.M. New insights into steroidogenesis in normo- and hyperandrogenic polycystic ovary syndrome patients. *Arq. Bras. Endocrinol. Metabol.* **2013**, 57, 437-444. doi:10.1590/s0004-27302013000600005.
49. Trummer, O.; Stern, C.; Reintar, S.; Mayer-Pickel, K.; Cervar-Zivkovic, M.; Dischinger, U.; Kurlbaum, M.; Huppertz, B.; Fluhr, H., Obermayer-Pietsch, B. Steroid Profiles and Precursor-to-Product Ratios Are Altered in Pregnant Women with Preeclampsia. *Int. J. Mol. Sci.* **2024**, 25. doi:10.3390/ijms252312704.

5.8 Supporting information

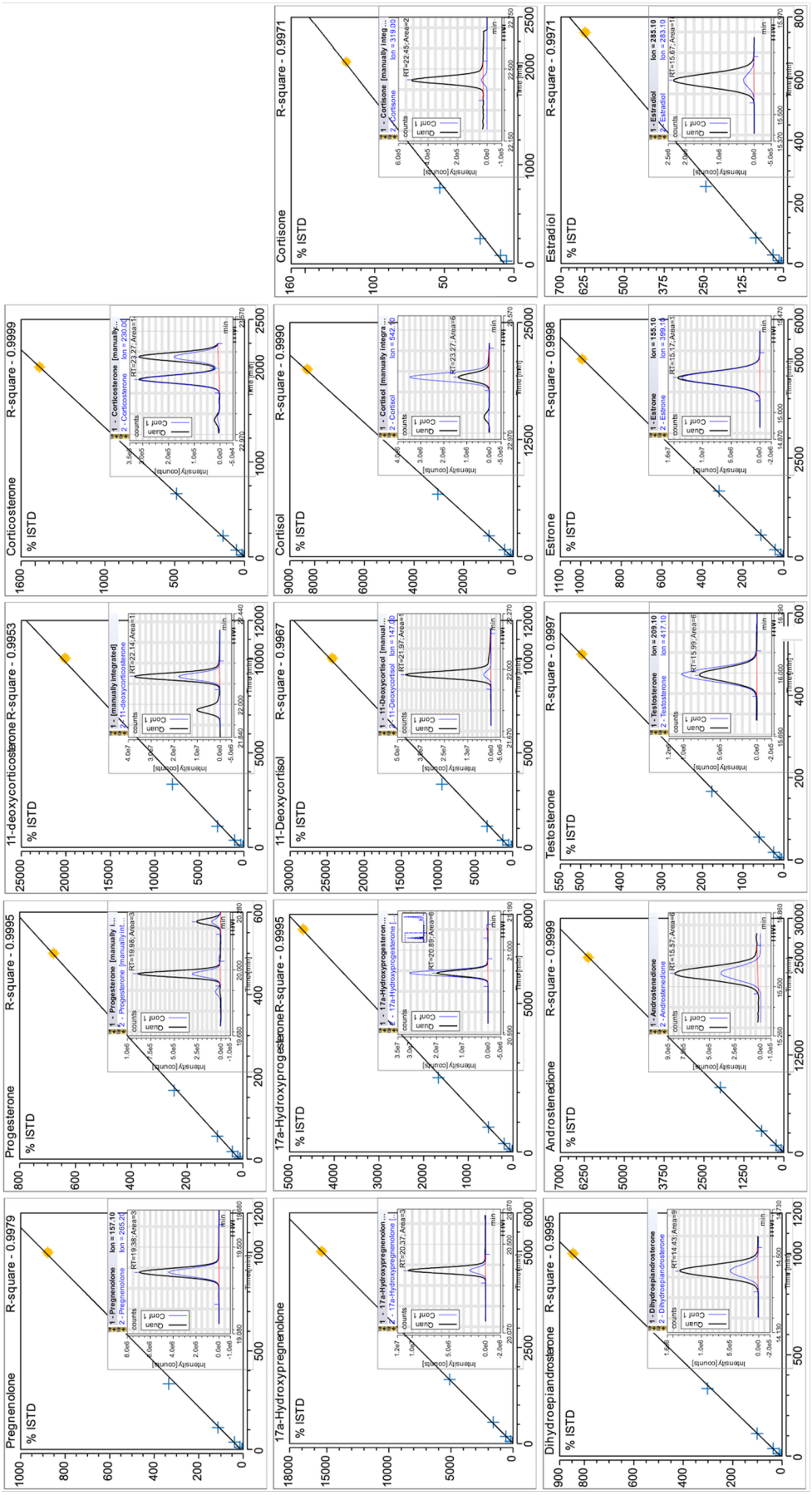

Figure S5.1. Chromatograms of 14 steroid hormones and their corresponding calibration curves.

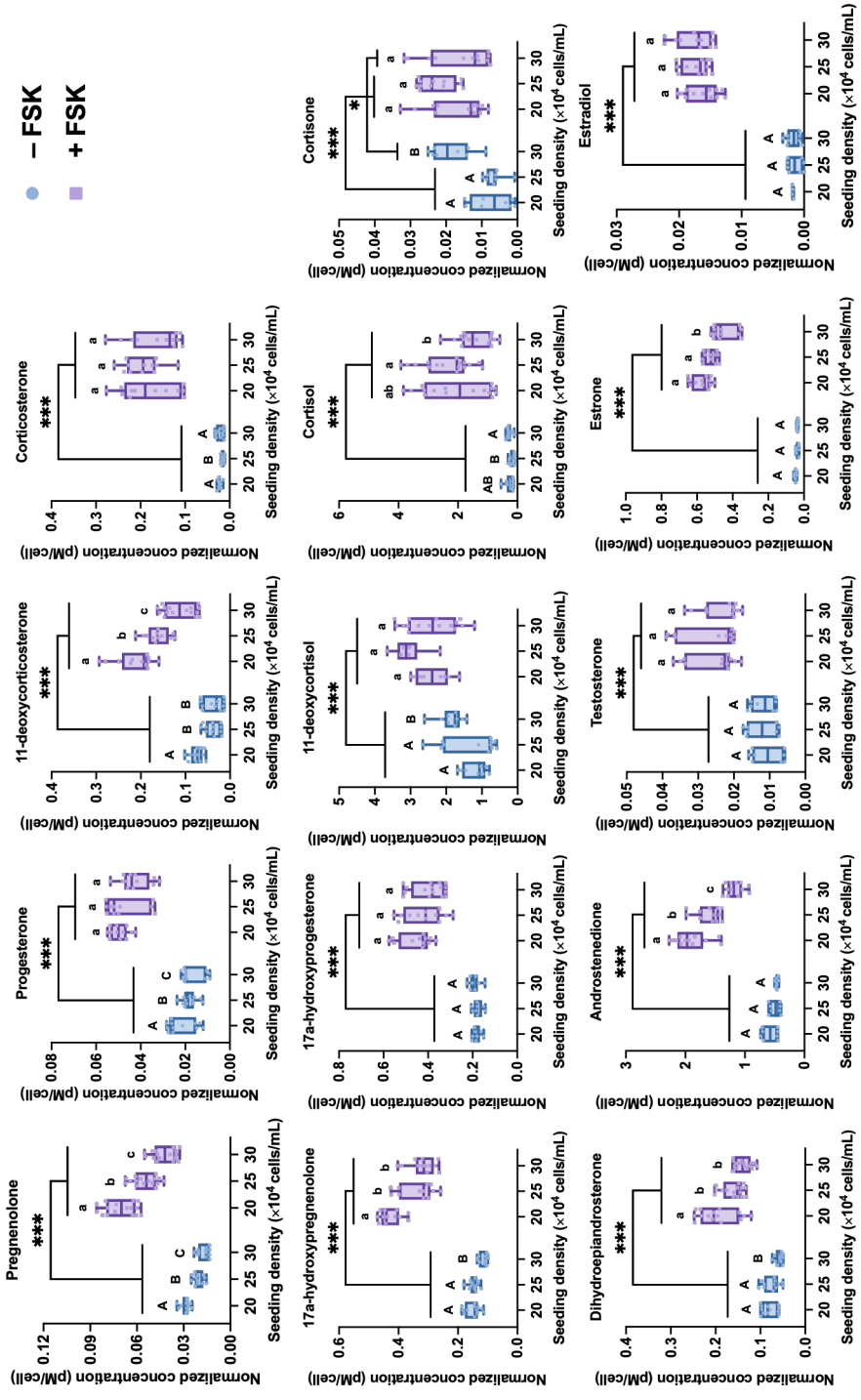

Figure S5.2. Normalized steroid hormone levels by cell number in H295R cells under basal and FSK-stimulated conditions at different cell densities (20, 25, and 30×10^4 cells/mL). Comparisons between the basal and forskolin-stimulated states for each cell density were performed using a Two-tailed Student's *t*-test (*$p <$ 0.05 and ***$p < 0.001$). One-way ANOVA followed by Tukey's multiple comparison test was used to compare hormone levels across cell densities within each group (basal and forskolin-stimulated states). Different letters indicate significant differences between cell densities within the same group at $p < 0.05$. Data are presented as MEAN ± SEM from at least three independent experiments ($n \geq 3$).

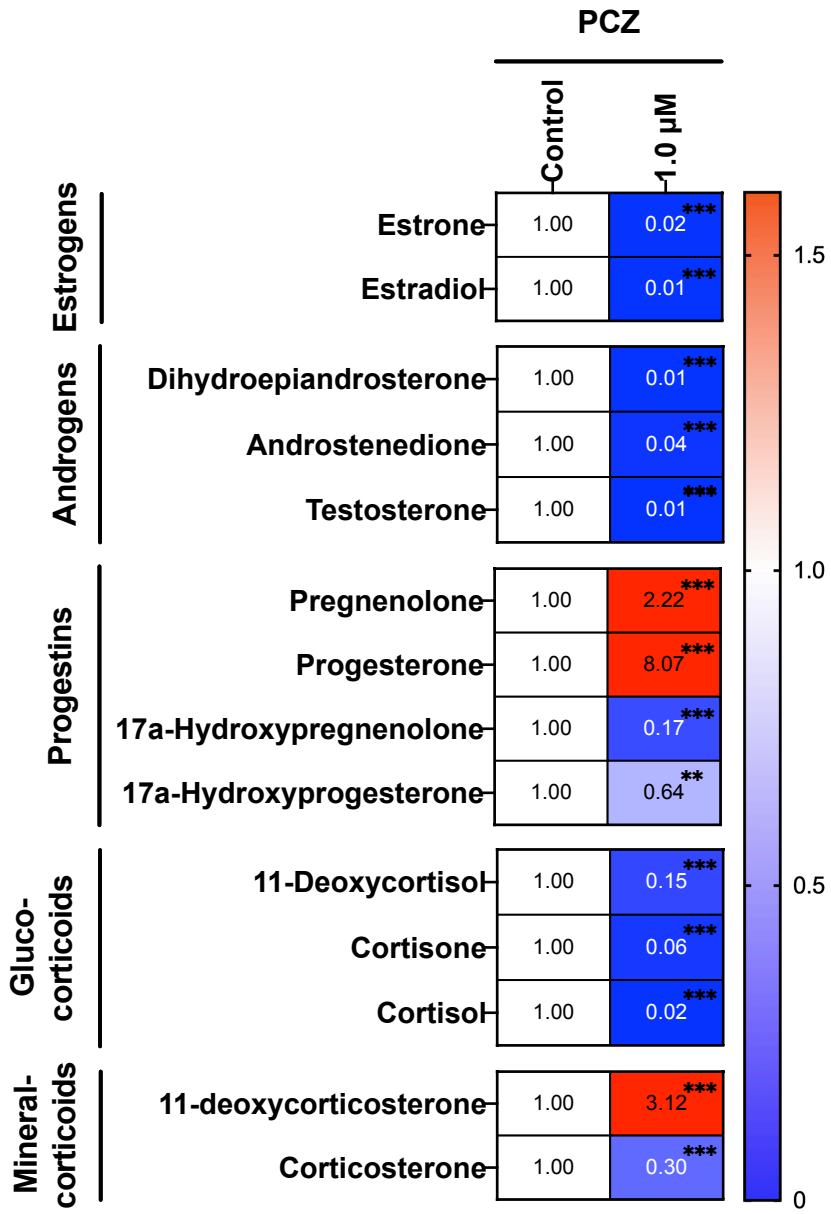

Figure S5.3. Effects of PCZ on steroidogenesis in FSK-stimulated H295R cells. Heat map showing the relative levels of 14 steroid hormones in forskolin-stimulated H295R cells treated, with values normalized to the control (set to 1). The red and blue coloring represents changes in steroid hormone levels relative to the control, with red indicating an increase and blue indicating a decrease. The intensity of the color reflects the magnitude of these changes. Steroid hormone levels are categorized by their respective steroidogenic pathways: estrogens, androgens, progestins, glucocorticoids, and mineralocorticoids. Statistical significance relative to the control is indicated by $^{**}p < 0.01$ and $^{***}p < 0.001$.

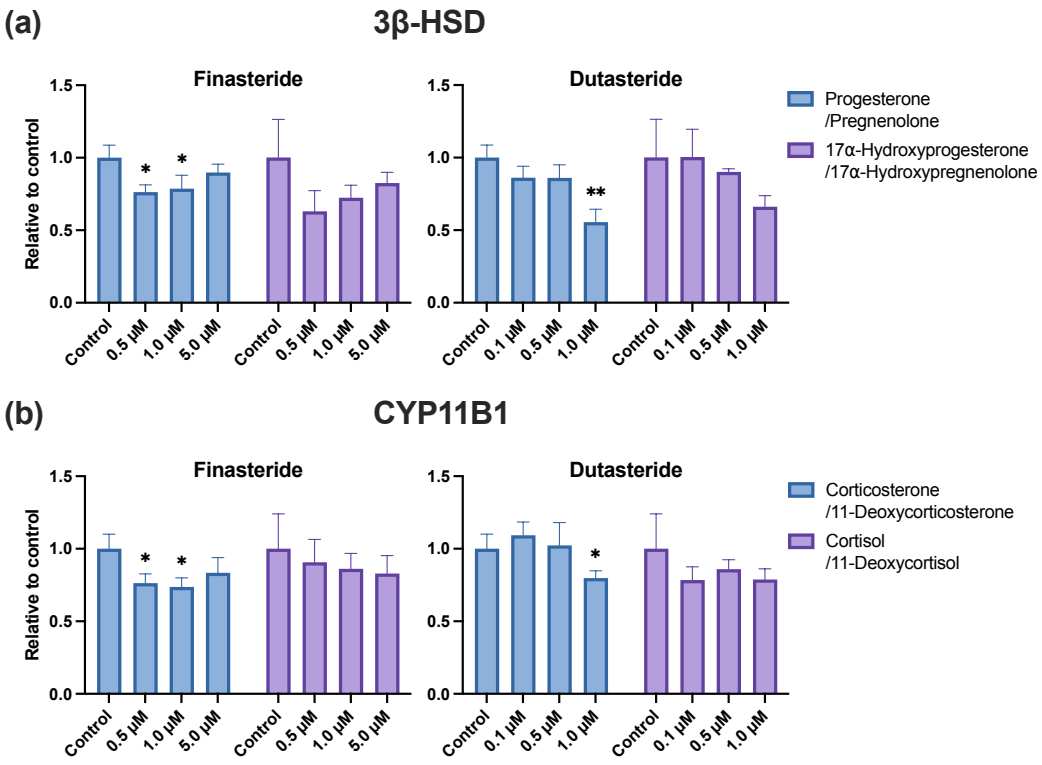

Figure S5.4. Estimated inhibition of 3β-HSD (3β-hydroxysteroid dehydrogenase) and CYP11B1 (steroid 11β-hydroxylase) activities, assessed through precursor/product ratio under exposure to dutasteride and finasteride. Data are expressed as mean ± SD from at least three independent experiments ($n \geq 3$).

Table S1. List of SRM transitions and analytical parameters for steroid hormone analysis

Compound Name	Retention Time (min)	Quantitation ion transition – (Collision energy)	Confirmation ion transition – (Collision energy)	Linear range (nM)	Correlation coefficient (R^2)
Dehydroepiandrosterone	14.43	432.2 > 237.1 (15)	432.2 > 417.1 (10)	0.68-1000	0.9995
Estrone	15.17	414.2 > 155.1 (15)	414.2 > 399.1 (10)	1-5000	0.9998
Androstenedione	15.56	430.2 > 169.1 (20)	430.2 > 405.1 (20)	34.29-25000	0.9999
Estradiol	15.67	416.2 > 285.1 (10)	416.2 > 283.1 (15)	0.68-666	0.9971
Estradiol-13C3	15.67	419.2 > 288.1 (10)	419.2 > 329.2 (10)	-	
Testosterone	15.99	432.1 > 209.1 (15)	432.1 > 417.1 (10)	0.68-500	0.9997
Testosterone-13C3	15.99	435.2 > 420.1 (10)	435.2 > 212.1 (15)	-	
Pregnenolone	19.38	445.2 > 157.1 (15)	445.2 > 265.2 (10)	0.68-1000	0.9979
Pregnenolone-13C2-D2	19.38	449.2 > 269.2 (10)	449.2 > 449.2 (5)	-	
Progesterone	19.98	458.2 > 157.1 (10)	458.2 > 353.1 (15)	0.68-500	0.9995
17a-Hydroxypregnenolone	20.37	548.2 > 548.1 (10)	548.2 > 230.1 (15)	5-5000	0.9998
17a-Hydroxyprogesterone	20.89	546.2 > 314.1 (10)	546.2 > 546.2 (10)	10-7500	0.9995
11-deoxycortisol	21.97	544.2 > 544.0 (10)	544.2 > 147.0 (30)	1-10000	0.9967
11-deoxycorticosterone	22.14	546.2 > 301.1 (20)	546.2 > 546.1 (10)	3-10000	0.9953
Cortisone	22.45	615.2 > 615.0 (15)	615.2 > 319.0 (15)	5-2000	0.9971
Corticosterone	23.27	634.3 > 349.1 (10)	634.3 > 404.1 (20)	7-2000	0.9999
Cortisol	23.27	632.2 > 632.0 (10)	632.2 > 542.0 (10)	10-20000	0.9990
Cortisol-d4	23.68	636.2 > 542.1 (10)	636.2 > 437.1 (10)	-	-

Statistical significance relative to the control is indicated by $*p < 0.05$ and $**p < 0.01$.

Chapter 6. SRD5A inhibitor in *Daphnia magna*

Contribution

As accepted in: **Hyunki Cho**, Si-Eun Sung, Giup Jang, Maranda Esterhuizen, Chang Seon Ryu, Youngsam Kim, Young Jun Kim "Adverse effects of the 5-alpha-reductase inhibitor finasteride on Daphnia magna: Endocrine system and lipid metabolism disruption" *Ecotoxicology and Environmental Safety* 2024, 281:116606, https://doi.org/10.1016/j.ecoenv.2024.116606.

Authorship contributions

Hyunki Cho: Writing–review & editing, Validation, Methodology, Investigation, Formal analysis, Data curation. Si-Eun Sung: Writing – review & editing, Visualization, Validation, Data curation. Giup Jang: Writing–review & editing, Visualization, Validation, Formal analysis, Data curation. Maranda Esterhuizen: Writing–review & editing, Validation, Data curation. Chang Seon Ryu: Writing–review & editing, Validation, Methodology, Investigation, Formal analysis, Data curation, Conceptualization. Youngsam Kim: Writing–original draft and review & editing, Visualization, Validation, Supervision, Methodology, Investigation, Formal analysis, Data curation, Conceptualization. Young Jun Kim: Writing–review & editing, Project administration, Funding acquisition, Conceptualization.

Relation to the thesis

Chapter 6 builds upon the understanding of 5α-reductase's critical role in steroid biosynthesis by exploring its environmental implications in invertebrates, specifically D. magna. The documented presence of a gene in D. magna with functional similarity to vertebrate SRD5A suggests a potential role for this enzyme in ecdysteroidogenesis, which regulates key reproductive and developmental processes in invertebrates. By investigating the adverse effects of the SRD5A inhibitor finasteride on D. magna, this chapter highlights how endocrine-disrupting chemicals designed for vertebrate applications can disrupt invertebrate hormonal pathways. These findings underscore the environmental risks of SRD5A inhibitors and support the development of adverse outcome pathways (AOPs) related to SRD5A inhibition, enhancing their applicability to invertebrate species and informing regulatory toxicology.

6.1 Abstract

Finasteride, a steroid 5-alpha reductase inhibitor, is commonly used for the treatment of benign prostatic hyperplasia and hair loss. However, despite continued use, its environmental implications have not been thoroughly investigated. Thus, we investigated the acute and chronic adverse impacts of finasteride on *Daphnia magna*, a crucial planktonic crustacean in freshwater ecosystems selected as bioindicator organism for understanding the ecotoxicological effects. Chronic exposure (for 23 days) to finasteride negatively affected development and reproduction, leading to reduced fecundity, delayed first brood, reduced growth, and reduced neonate size. Additionally, acute exposure (< 24 h) caused decreased expression levels of genes crucial for reproduction and development, especially *EcR-A/B* (ecdysone receptors), *Jhe* (juvenile hormone esterase), and *Vtg2* (vitellogenin), with oxidative stress-related genes. Untargeted lipidomics/metabolomic analyses revealed lipidomic alteration, including 19 upregulated and 4 downregulated enriched lipid ontology categories, and confirmed downregulation of metabolites. Pathway analysis implicated significant effects on metabolic pathways, including the pentose phosphate pathway, histidine metabolism, beta-alanine metabolism, as well as alanine, aspartate, and glutamate metabolism. This comprehensive study unravels the intricate molecular and metabolic responses of *D. magna* to finasteride exposure, underscoring the multifaceted impacts of this anti-androgenic compound on a keystone species of freshwater ecosystems. The findings emphasize the importance of understanding the environmental repercussions of widely used pharmaceuticals to protect biodiversity in aquatic ecosystems.

6.2 Introduction

Steroid 5α-reductase (5AR; 3-oxo-5alpha-steroid 4-dehydrogenase) is an enzyme found in humans and other mammals, crucial for the conversion of testosterone to 5α-dihydrotestosterone (DHT), a potent androgen. Medications known as 5AR inhibitors, such as finasteride and dutasteride, are frequently prescribed to manage conditions such as benign prostatic hyperplasia (BPH) and androgenetic alopecia (AGA; male pattern baldness) [1]. Their mechanism of action involves suppressing the enzymatic activity of 5AR, subsequently leading to diminished DHT levels. The global finasteride market size is reported to be $362.1 million in 2021 and is expected to grow at a CAGR of 4.2 % until 2031 [2]. Furthermore, in 2020 alone, over 2 million patients were prescribed finasteride, resulting in over 8 million prescriptions in United States [3]. Growing concerns surround the environmental implications of 5AR inhibitors, especially given their increasing use. Despite the inherent persistence of 5AR inhibitors, characterized by their long half-life and high lipophilicity, comprehensive data on their concentrations in diverse environmental settings, ranging from wastewater and surface water to freshwater, seawater, and soil, remain scarce. For instance, finasteride has been detected in the effluent and influent sludge of a domestic sewage treatment plant at concentrations of approximately 0.01 μg/L [4]. The NORMAN Network Database System (https://www.norman-network.com) recorded finasteride concentrations of 0.0064 μg/L

in Ljubljana, Slovenia, and 0.0125 µg/L in Zilina, Slovakia. In the Stockholm region, data from 2020 revealed the presence of finasteride in surface water, with concentrations reaching up to 0.020 µg/L in Sweden's purified wastewater [5]. Additionally, finasteride was also detected in aquatic invertebrate, caddisfly larvae (Hydropsychidae) near Melbourne, Australia [6]. Unfortunately, the environmental concentration of finasteride, particularly in areas with high consumption, is not well-researched. The persistence of the substance, coupled with the increasing demand for AGA treatments, highlights the importance of environmental impacts of 5AR inhibitors.

While several studies have examined for detailed information on the toxicity and side effects of 5AR inhibitors intended for human use, there is a noticeable gap in research on aquatic organisms. Few studies have documented the acute and chronic effects on various aquatic organisms, including fish [7-9], amphibians [10], gastropods [11], and benthic invertebrates [12]. In contrast to research on these species that utilize steroids as hormones, the impact on ecdysteroid-dependent organisms is less understood. Given the pivotal role of these organisms in aquatic ecosystems, their potential susceptibility to drugs such as 5AR inhibitors, and their vulnerability to reproductive disturbances from such drugs, the necessity for such chronic reproductive studies becomes evident [13; 14].

Daphnia magna, a planktonic crustacean found in freshwater environments stands as an ideal subject for this study due to its ecological importance and the role of ecdysteroids in its life cycle [15; 16]. In crustaceans like *D. magna*, ecdysteroids play an important role in growth, development, and maturation [17; 18]. To bridge this knowledge gap and elucidate the broader implications of finasteride, we investigated acute toxicity (immobilization and oxidative stress), acute responses of gene expression (*EcR-A*, *EcR-B*, *neverland*, *Jhe*, *chitinase*, *RXR*, *Hr96*, *Vtg2*, *sod*, *cat*, gpx, and gst) and chronic toxicity endpoints (reproduction and growth as body length) to understand the adverse effects of finasteride on *D. magna*. Furthermore, we explored the comprehensive relationship between metabolic changes in *D. magna* and its acute responses to finasteride exposure, employing high-resolution mass spectrometry (HRMS)-based untargeted metabolomics/lipidomics. To our knowledge, this is the first study assessing the chronic toxicity and molecular biological effects of 5AR inhibitor on daphnia species. The results of this study would provide that a holistic perspective on the impact of finasteride on the ecological dynamics of freshwater ecosystems.

6.3 Materials and methods

6.3.1 Solution preparation

Finasteride (Cas No. 98319–26–7; Y0000090; Merck, Darmstadt, Germany) was dissolved in dimethyl sulfoxide (DMSO) (Sigma-Aldrich, St. Louis, MO, USA) to a concentration of 5000 mg/L as the stock solution. Before addition to the culture media, the stock solution was diluted 100 times for chronic testing. The stock solution was replaced weekly. According to OECD TG 211 and 202 [19; 20], Elendt M4

medium was prepared for the chronic test, and ISO medium IOS. (2012) for the acute test, respectively.

6.3.2 Daphnia magna culture

Ephippia of *D. magna* (Micro Biotests Inc.; Gent, Belgium) were incubated for 72 hours under a 16-hour light/8-hour dark cycle with a light intensity of 7000 lux. This process was conducted in a climate-controlled incubator maintained at a temperature of 20.0 ± 1.0°C. To maintain the *D. magna*, fifteen individuals were placed in a 2 L glass beaker holding 1.5 L of Elendt M4 medium. *D. magna* was fed with Chlorella vulgaris (~1.5 × 10^8cells/mL, 0.1 mg C/*D. magna*/day) daily and yeast, cerophyll, and trout chow (YCT) at a concentration of 0.5 µL/mL was provided three times weekly. To maintain optimal water quality and a favorable environment, the culture media and beakers were refreshed three times weekly, while new neonates were removed on a daily basis. Prior to each replacement and testing, parameters such as pH and dissolved oxygen levels were monitored. Consistent with ISO 6341 Field 18 guidelines, an interlaboratory test using potassium dichromate (Sigma-Aldrich; St. Louis, MO, United States) as a reference substance was routinely conducted to verify the test conditions' reliability.

6.3.3 Physiological, biochemical, and molecular analysis

6.3.3.1 Immobilization and mortality tests

Following the OECD guideline 202 [19], 48 h-acute toxicity tests were conducted. Neonates (< 24 h) from the third brood of *D. magna* culture were exposed to various concentrations of finasteride (50.0, 40.0, 30.0, 27.5, 25.0, 22.5, 20.0, 17.5, 15.0, 10.0, 5.00, 0.50, and 0.10 mg/L), as well as a concurrent control series. The daphnids were placed in exposure groups, each in a specific concentration, and observed for any signs of immobilization or mortality (n = 5). Briefly, the groups consisted of four replicates, each containing five daphnids, for each finasteride concentration in the ISO medium. The exposures were conducted in six-well culture plates, each filled with 10 mL of the solution, and maintained for 48 hours. Immobilization was assessed visually within 15 seconds after gentle agitation. To ensure the reliability of the results, all experimental conditions were replicated three times.

6.3.3.2 Reproduction test

The reproductive tests were slightly modified from OECD TG 211 [20] to meet the criterion that the mean number of offspring per mother should exceed 60 at the end of the test. Briefly, neonates from the third brood of the *D. magna* cultures were randomly pooled. Twenty daphnids were exposed individually to each concentration (specify the concentrations again) versus a control series for 23 days. Each 100 mL

beaker was filled with 60 mL of the designated solution. The medium in the control series contained 0.01 % whatDMSO as the solvent control. *D. magna* was fed daily with algae *C. vulgaris* (~1.5 × 10^8cells/mL, 0.1 mg C/*D. magna*) and supplemented three times a week with YCT (0.5 µL/mL). Neonates from each beaker were counted daily. The solutions and beakers were renewed three times a week.

6.3.3.3 Body length measurement

The lengths of *D. magna* were measured at the end of the reproduction test using an Olympus CKX41 optical microscope (Olympus Inc., Tokyo, Japan). For measurement purposes, daphnids were carefully placed on glass slides, accompanied by a small volume of their respective medium. Using the ImageJ software, the body length was determined, extending from the center of the eye to the base of the apical spine [22]. Furthermore, thirty neonates from the third brood cultured in each group were randomly pooled to measure the size of the neonates following the same procedure. The concentration of 6.0 mg/L was excluded due to the lack of neonates from the third brood.

6.3.3.4 Reactive oxygen species (ROS detection assay)

Samples were obtained from 20 neonates. After exposure for the desired time (6, 24, or 48 hours) and concentrations (1.5, 3.0, 4.5 and 6.0 mg/L) including control (0.01 % DMSO) group, the daphnids were transferred to eppendorf (EP) tubes and rinsed with 1 mM phosphate-buffered saline (PBS, pH 7.4). The samples were thoroughly homogenized in 200 µL of PBS and placed in an ice bath. The EP tubes were centrifuged at 3000 × g at 4°C for 10 min. Protein concentrations were assessed using the bicinchoninic acid kit from Thermo Fisher Scientific (Waltham, MA, USA). For ROS level determination, a cellular ROS assay kit from Abcam (Cambridge, UK) was used. Following the manufacturer's guidelines, these assays involved the use of 20 µL of supernatant from homogenized samples. The obtained fluorescent intensities ($\lambda_{ex/em}$ 495/529 nm) were then normalized against control samples, comprising untreated daphnids.

6.3.3.5 ENA isolation and real-time quantitative reverse transcription PCR (qRT-PCR)

Based on prior studies indicating the potential recovery of gene expression over time [23; 24], two post-treatment timeframes, 6 and 24 hours, were selected for evaluation. Five adult *D. magna*, approximately 17 days old, were subjected to 1.5 and 3.0 mg/L finasteride exposure including control (DMSO) group (n = 3). Subsequently, they were relocated to EP tubes and washed three times with distilled water. Using TRIzol reagent (Thermo Fisher Scientific; Waltham, MA, USA), the samples were homogenized, followed by the isolation of total RNA through a column-based extraction kit from Qiagen (Valencia, CA,

USA). Subsequently, 1000 ng of RNA was subjected to reverse transcription with a high-capacity RNA-to-cDNA kit provided by Applied Biosystems (Foster City, CA, USA). The qRT-PCR assays were conducted with the Fast SYBR Green Master Mix from Applied Biosystems, utilizing the 7500 FAST Real-Time PCR System. The relative expression levels of all genes were determined using the $2^{-\Delta\Delta Ct}$method [25], with *D. magna* actin serving as the endogenous control (*Actin*) for normalization purposes. Details of the primer sequences and their references are listed in Table S6.1.

6.3.4 Lipidomic and metabolomic analyses

6.3.4.1 D. magna lipid sample extraction

Adult *D. magna* (17 days) were exposed in 100 mL beakers containing 50 mL of culture medium diluted with finasteride (1.5 and 3.0 mg/mL) and control group (0.01 % DMSO) for a period of 48 hours ($n \geq 3$). Then, the four daphnids were rinsed with deionized water and transferred to 2 mL microcentrifuge tubes containing beads. The samples were homogenized using a Precellys Evolution homogenizer (Bertin Technologies, France). The samples were dried under nitrogen and weighed, and extractions were conducted using a modified Matyash method [26] with two-phase (polar and nonpolar) fractionation.

6.3.4.2 Untargeted lipidomics and metabolomics

An untargeted approach in lipidomics and metabolomics was employed, utilizing quadrupole time-of-flight (Q-TOF) high-resolution mass spectrometry (HRMS) to explore alterations in lipids and metabolites following finasteride treatment. The analysis of samples was conducted using a Triple TOF 6600+ QTOF mass spectrometer (AB Sciex, Framingham, MA, USA) coupled with an Electrospray ionization (ESI) source and an Exion AD Ultra-High-Performance Liquid Chromatography (UPLC) system (AB Sciex). A positive/negative calibration solution for the ESI source was used to correct the mass during the analysis for every five samples. The lipidomics analysis utilized a liquid chromatography (LC) method, employing an Acquity CSH C18 VanGuard pre-column (5 ×2.1 mm; 1.7 µm; Waters, USA) connected to Acquity UPLC CSH C18 column (100 ×2.1 mm; 1.7 µm), as following the methodology outlined in prior research [27]. All data were acquired using a TOF scan with sequential window acquisition of all theoretical mass spectra (SWATH). For the scan range *m/z* 100–1250, the scanning time was set at 50 ms for TOF and 35 ms for MS2 in 20 windows. Hydrophilic metabolite analysis was performed in hydrophilic interaction chromatography (HILIC) mode, utilizing an Acquity UPLC BEH amide column (150 × 2.1 mm, 1.7 µm) coupled to a VanGuard BEH Amide pre-column (5 × 2.1 mm; 1.7 µm; Waters, USA). The mobile phase and gradient conditions followed the parameters outlined in previous reports [28]. The data were acquired in the scan range of *m/z* 80–1000.

6.3.5 Data analysis

Data analysis for physiological, biochemical and molecular analyses was conducted using OriginPro 9.65 software (OriginLab Corporation, Northampton, MA, USA) GraphPad Prism software (version 10.3.1; San Diego, CA, USA). The EC_{50} values were calculated through nonlinear fitting (dose-response curve with variable Hill slope, Levenberg–Marquardt method), utilizing the immobilization data. For the qRT-PCR data, normality was verified using the Shapiro-Wilk test. Differences between control and exposed groups were statistically evaluated using one-way ANOVA followed by Tukey's multiple comparison tests. Statistically significant differences are denoted by asterisks (*$p < 0.05$, **$p < 0.01$, ***$p < 0.001$).
Lipidomics and metabolomics data analysis was performed using MS-DIAL (version 4.9.2) [29]. Annotated peaks were log-transformed and auto-scaled, followed by multivariate statistical analysis using MetaboAnalyst version 5.0 [30]. A partial least-squares discriminant analysis (PLS-DA) identified influential variables between the treatment and control groups, based on their variable importance in projection (VIP). Statistic differences in lipids and metabolites from untargeted lipidomics and metabolomics were analyzed using one-way analysis of variance (ANOVA), followed by Fisher's LSD (adjusted P-value < 0.05) with a VIP score of > 1. Significant peaks were verified using SCIEX-OS Q to confirm the accurate mass (± 5 ppm) and MS2 fragmentation spectrum. Databases such as the MS-DIAL MSP spectral database (V17), Human Metabolome Database (HMDB) [31], Metlin Database [32], MASS BANK [33], and LIPID MAPS [34] were utilized for the identification of potential metabolite markers.

Lipid classes were identified using typical fragmentations following methodologies described by previous study [28]. Significantly changed lipids were assigned to clusters corresponding to those obtained from hierarchical clustering analysis. Hierarchical clustering was performed based on metabolites that exhibited significant changes. Pearson correlation and Euclidean distance were used, respectively. The pheatmap package (v1.0.12) in R software (v4.2.2) was employed for clustering analysis [35; 36]. Z-score transformation to normalize the value of each sample was used. The Lipid ontology (LION) enrichment analysis was employed for the lipid enrichment analysis in ranking mode [37]. Enrichment analysis for each lipid cluster was performed using the whole dataset as the background. Feature selection, employing a one-way ANOVA F-test, was analyzed to establish the ranking of input identifiers. Peak intensities were normalized through a percentage-based approach, and the Kolmogorov–Smirnov (K-S) test was configured with a two-tailed setting. A bar chart incorporating both upregulated and downregulated metabolites was constructed for visual representation. A mammalian lipidomics analysis tool (BIOPAN), which provides a gene list involved in the activation or suppression of enzymes, was used to identify enzymes involved in changes to lipid metabolites [38]. The correlated enzymes by finasteride exposure in the human homologs of *D. magna* were identified in KEGG [39].

6.4 Results

6.4.1 Acute effects of finasteride on *D. magna* immobility, mortality, and ROS production

To understand the acute toxicity of finasteride to *D. magna* and determine the appropriate concentrations for long-term exposure, acute immobilization tests were conducted. Finasteride was tested across a range of concentrations from 0.10 to 50.0 mg/L. The EC_{50} was determined to be 23.7 mg/L using the fitted dose-response curve (Figure S6.1). Subsequently, a preliminary mortality test (n = 10) at three concentrations (1.0, 5.0, and 10.0 mg/L) was conducted using the same methodology as applied in the chronic test, to determine the appropriate concentrations for the subsequent long-term exposure study. Over 50 % mortality was observed in the 10.0 mg/L group within 10 days. Considering these results and the EC_{50} values, we selected four sublethal concentrations (1.5, 3.0, 4.5, and 6.0 mg/L) for the chronic toxicity test. Additionally, ROS production assays were conducted prior to the chronic test using the selected concentrations to evaluate the potential impact of oxidative stress on chronic parameters. Neonates were exposed to the four sublethal concentrations and the control series at three different time points (6, 24, and 48 h). The result indicated a general increased in ROS levels in a dose-dependent manner across all time points; however, the changes were not statistically significant compared to those of control series (Figure S6.2).

6.4.2 Chronic effects of finasteride on D. magna reproduction

The chronic test duration was extended to 23 days, in accordance with OECD guideline 211 [20], due to insufficient offspring production in the control group by day 21. The control group exhibited a 5 % mortality rate and an average offspring count of 62.1 ± 6.1 neonates per mother at day 23. Finasteride exposure resulted in a significant reduction in reproductive output compared to the control. The average offspring count showed a dose-dependent decrease, with reductions of 37.6 % at 1.5 mg/L (38.8 ± 13.9), 40.8 % at 3.0 mg/L (36.7 ± 9.2), 86.1 % at 4.5 mg/L (8.6 ± 3.3), and 89.9 % at 6.0 mg/L (6.3 ± 4.03) (Figure 6.1a). Furthermore, finasteride exposure notably increased mortality rates and the timing of the first brood. Specifically, the 1.5 and 3.0 mg/L exposure groups had a 15 % mortality rate, while the rates sharply rose to 35 % for the 4.5 mg/L group and 80 % for the 6.0 mg/L group for 23 days. In the control group, the first brood occurred at 10.6 ± 0.5 days. For the finasteride-exposed groups, the 1.5 and 3.0 mg/L concentrations led to first brood timings of 11.6 ± 1.2 days and 11.2 ± 0.3 days, respectively. However, the higher concentrations resulted in more significant delays, with the first brood appearing at 15.1 ± 1.7 days for the 4.5 mg/L group and at 17.0 ± 1.4 days for the 6.0 mg/L group (Figure 6.1b). The first brood timing for the 3.0 mg/L group was slightly shorter than the 1.5 mg/L group, but overall the timing showed a clear dose-dependent delay.

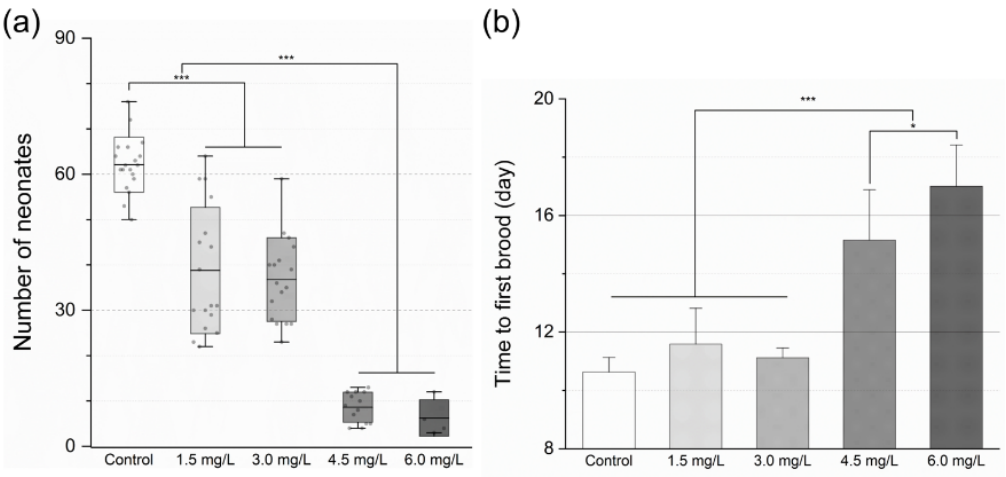

Figure 6.1. (a) Total count of neonates from surviving *D. magna* after a 23-day finasteride exposure period, with boxes showing standard deviation and the central line representing the mean; (b) Average duration until the first brood in response to finasteride exposure, where bars denote the mean and error bars indicate the standard error of mean. Statistical evaluations were conducted using one-way ANOVA and Tukey's multiple comparison tests, with asterisks marking significant differences (*$p < 0.05$ and ***$p < 0.001$).

6.4.3 Chronic effects of finasteride on the size of D. magna adults and neonates

Following chronic exposure, adult *D. magna* body lengths were measured to assess the effects of finasteride on growth. Significant differences were observed between the various exposure levels. The control group had an average length of 3.47 ± 0.11 mm (n = 19) (Figure 6.2a). In comparison, the finasteride-exposed groups showed a decrease in length as follows: 11.5 % decrease to 3.07 ± 0.32 mm for 1.5 mg/L (n = 17), 10.4 % decrease to 3.11 ± 0.30 mm for 3.0 mg/L (n = 18), 40.3 % decrease to 2.07 ± 0.19 mm for 4.5 mg/L (n = 12), and 47.0 % decrease to 1.84 ± 0.50 mm for 6.0 mg/L (n = 4) (Figure 6.2b). Statistical analysis revealed significant reductions in size for the finasteride-treated groups compared to the control. Despite the 1.5 mg/L group having a slightly smaller mean size than the 3.0 mg/L group, a consistent trend was observed.

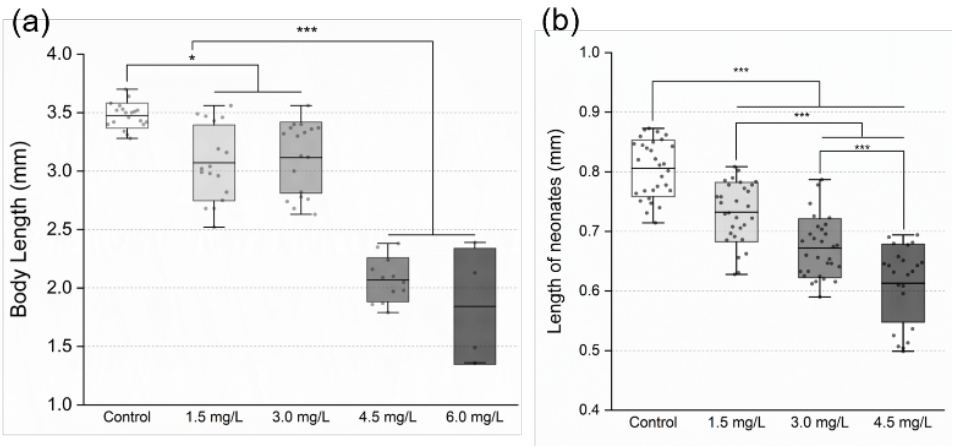

Figure 2. (a) Body length of daphnids in each experimental group at the end of the chronic test, with boxes showing standard deviation and the central line representing the mean; (b) the body length of neonates from the third brood in each experimental group, with boxes for standard deviation and a central line for the mean. Statistical analyses were performed using one-way ANOVA and Tukey's multiple comparison tests, with asterisks highlighting significant differences (*$p < 0.05$ and ***$p < 0.001$).

6.4.4 Transcriptional change

The effect of finasteride exposure on the genomic response of *D. magna* was investigated by examining changes in the mRNA expression levels of genes involved in the ecdysteroid signaling pathway, particularly focusing on key genes associated with reproduction and development (Figure 6.3). The results showed a dose-dependent downregulation of reproductive genes mRNA expression, including juvenile hormone esterase (*Jhe*), vitellogenin 2 (*Vtg2*), ecdysone receptor alpha (*EcR-A*), ecdysone receptor beta (*EcR-B*), *Neverland* and retinoid X receptor (*RXR*) at both time points. Nuclear receptor Hr96 (*Hr96*) expression level decreased only at 6 h exposure. Notably, the expression of *Jhe* was significantly downregulated ($p < 0.001$) at all finasteride concentrations after 24 h of exposure. *Vtg2* expression was also downregulated after 6 h exposure to 3.0 mg/L of finasteride, with this suppression becoming significant after 24 h exposure at both 1.5 and 3.0 mg/L concentration. Conversely, chitinase, associated with developmental processes, was upregulated following finasteride exposure at both time points. Additionally, the transcriptional profiles of oxidative response genes included glutathione S-transferase (*gst*), catalase (*cat*), glutathione peroxidase (*gpx*), and superoxide dismutase (*sod*) were also assessed. Oxidative response genes exhibited a dose-dependent downregulation pattern at both concentrations and time points, except for *sod* at 3 mg/L after 6 hours of exposure.

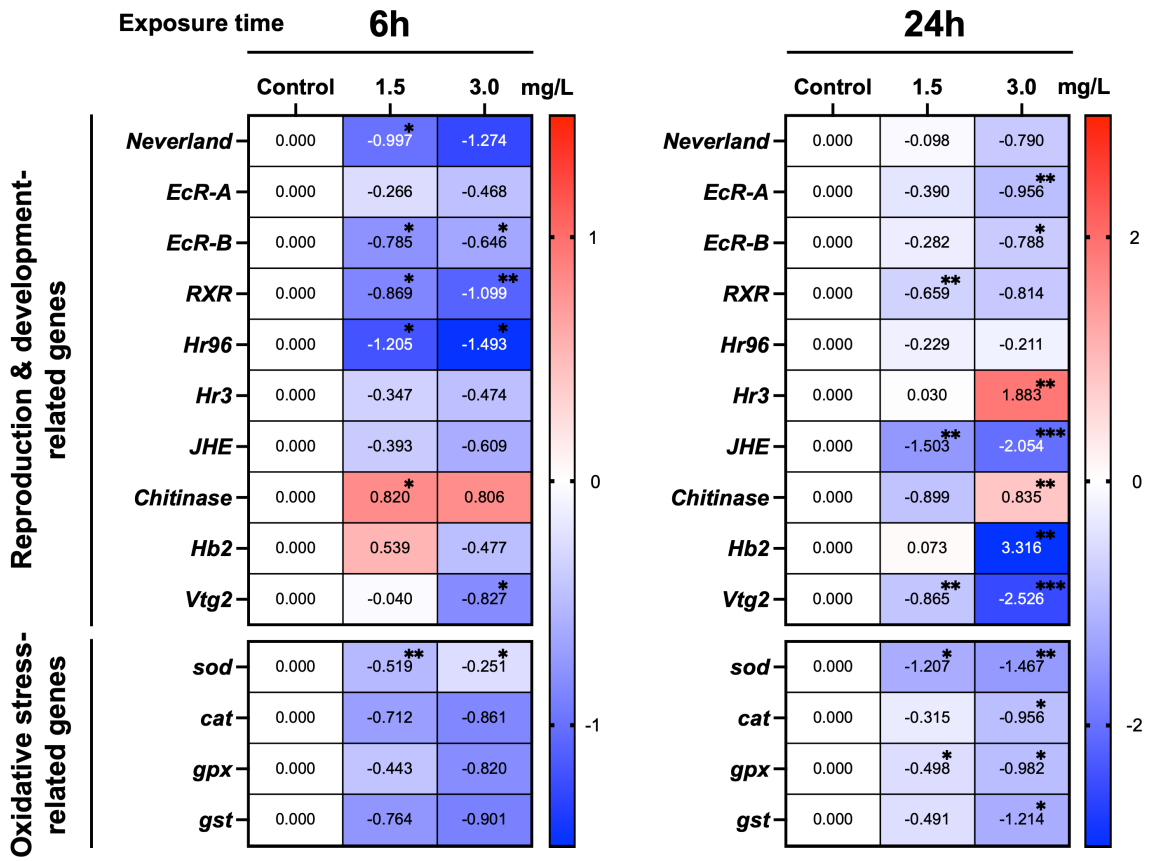

Figure 6.3. Heatmap showing alterations in relative mRNA expression related to development, reproduction, and antioxidant response following exposure to finasteride in 17-day-old *D. magna* adults ($n \geq 3$, each sample comprising at least 3 individuals). Red and blue colors indicate up-regulated and down-regulated levels, respectively. Statistical evaluations were conducted using one-way ANOVA and Tukey's multiple comparison tests, with asterisks denoting significant differences (*$p < 0.05$, **$p < 0.01$, and ***$p < 0.001$).

6.4.5 Effect on lipid contents and metabolites

Untargeted lipidomic and metabolomic analyses identified 445 individual lipids and 22 metabolites that were differently regulated, as depicted in Figure 6.4a and Figure S6.4a, respectively. Following exposure to finasteride in *D. magna*, 14 lipid classes were annotated. The hierarchical analysis of lipid changes is presented in Figure 6.4a as a heatmap, clustering the lipids into three different groups of 344, 75, and 26 lipids (clusters 1, 2, and 3, respectively). These included comparison among lipid classes with detailed distributions provided in Table S6.2. The cluster 1 was composed to triacylglycerol (TG), phosphatidylcholine (PC), diacylglycerol (DG), and ceramide (Cer), and showed the downregulated pattern in finasteride exposure group compared to control group. In the second cluster, differential responses were observed with upregulation at 1.5 mg/L and downregulation at 3.0 mg/L following exposure to finasteride. The third cluster exhibited upregulation pattern in finasteride exposure group compared to control group. Nineteen LION signaling pathways were significantly enriched (FDR q value

< 0.05) indicating a notable upregulation, while four pathways showed significant downregulation (Figure 6.4b). LION-terms such as fatty acid with more than 18 carbons, fatty acid with less than two double bonds, saturated fatty acid, membrane component, high transition temperature, glycerophospholipids, fatty acid with 22–24 carbons, headgroup with positive charge/ zwitter-ion, high bilayer thickness, and neutral intrinsic curvature were upregulated. Conversely, few LION-terms, including plasma membrane, sphingolipids [SP], N-acylsphingosines (ceramides) [SP0201], and DG (34:2) were downregulated. Comprehensive details of the lipids associated with each LION category in the enrichment are available in Table S6.2. Comparisons between control and each finasteride exposure group were presented as network analyses in Figure 6.4c-d. Both exposed groups activated DG to phosphatidylethanolamine (PE) and PC metabolism without suppressing any pathways. Phosphoethanolamine N-methyltransferase (PEMT, KEGG entry 116930291) and choline/ethanolamine phosphotransferase (CEPT1, KEGG entry 116919957) were annotated. Using hydrophilic phase metabolomics, 22 downregulated metabolites were identified (Table S6.3). These metabolites included propionic acid, cytosine, 5,6-dihydro-5-methyluracil, L-leucine, hypoxanthine, glutamine, lysine, guanine, indole-3-carboxylic acid, delta-hydroxylysine, nepsilon, trimethyllysine, theobromine, L-kynurenine, propionylcarnitine, L-carnosine, 1-methyladenosine maltotriose cysteic acid, gluconic acid, carnosine, chrysin, gamma-glutamylleucine, and gamma-glutamyltyrosine. Pathway analysis revealed that the significantly affected metabolic pathways included the pentose phosphate pathway, histidine metabolism, beta-alanine metabolism, and alanine, aspartate, and glutamate metabolism (Figure 6.4.b).

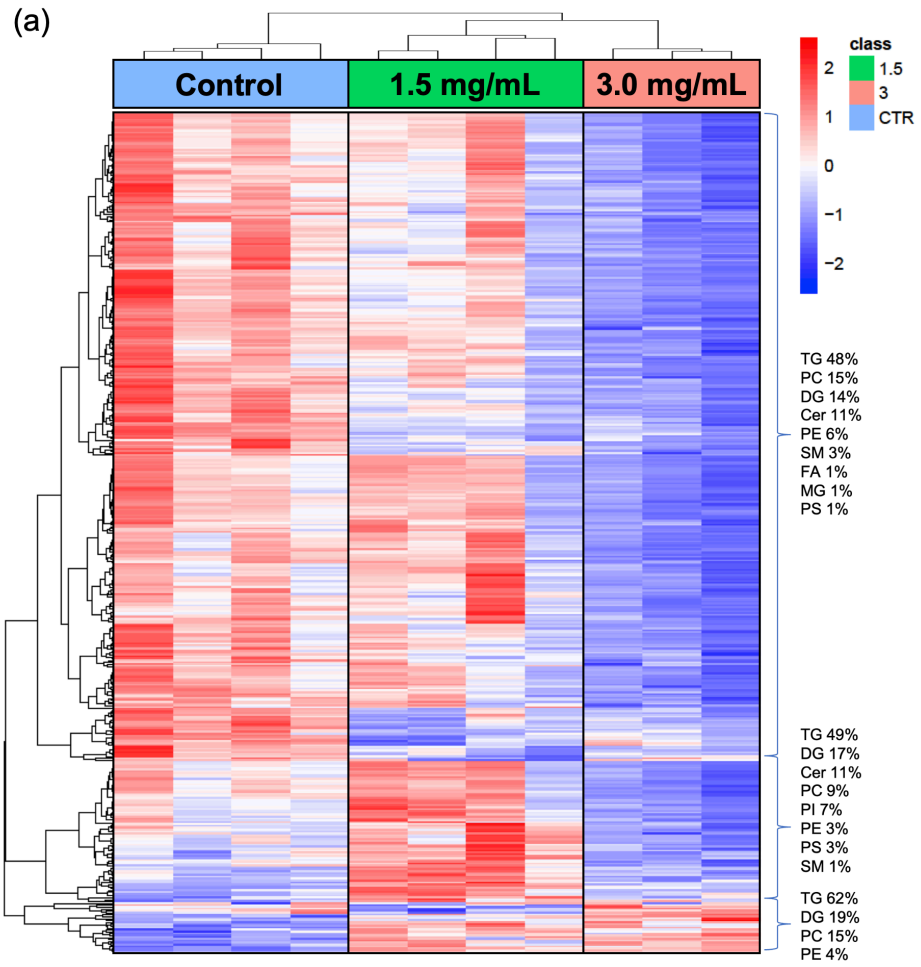
(a)
Control
1.5 mg/mL
3.0 mg/mL
class
1.5
3
CTR
2
1
0
−1
−2
TG 48%
PC 15%
DG 14%
Cer 11%
PE 6%
SM 3%
FA 1%
MG 1%
PS 1%
TG 49%
DG 17%
Cer 11%
PC 9%
PI 7%
PE 3%
PS 3%
SM 1%
TG 62%
DG 19%
PC 15%
PE 4%

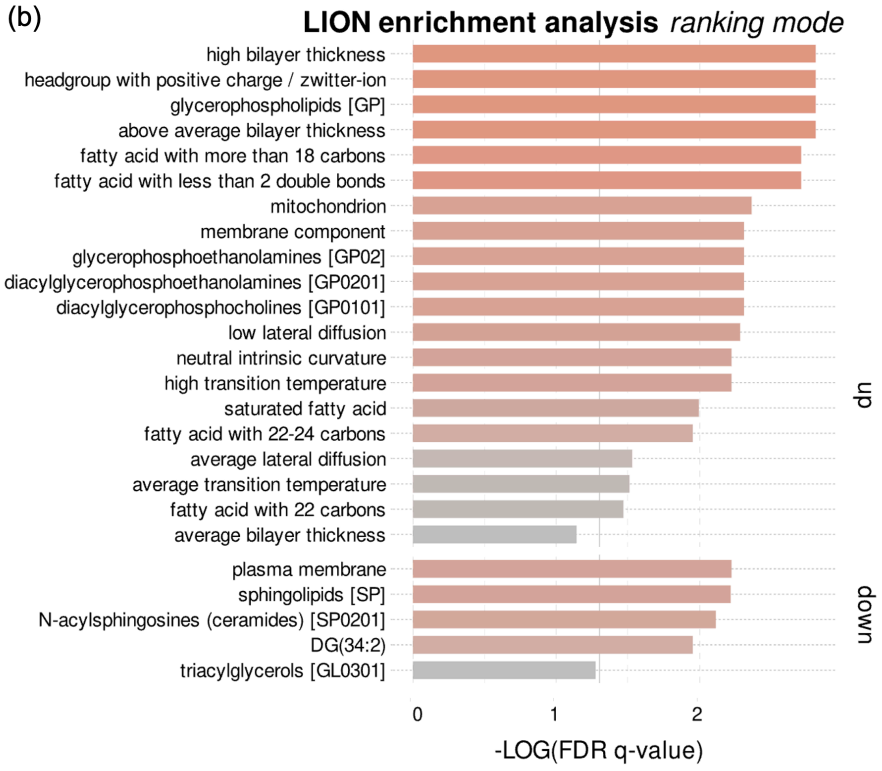
(b)
LION enrichment analysis ranking mode
high bilayer thickness
headgroup with positive charge / zwitter-ion
glycerophospholipids [GP]
above average bilayer thickness
fatty acid with more than 18 carbons
fatty acid with less than 2 double bonds
mitochondrion
membrane component
glycerophosphoethanolamines [GP02]
diacylglycerophosphoethanolamines [GP0201]
diacylglycerophosphocholines [GP0101]
low lateral diffusion
neutral intrinsic curvature
high transition temperature
saturated fatty acid
fatty acid with 22-24 carbons
average lateral diffusion
average transition temperature
fatty acid with 22 carbons
average bilayer thickness
plasma membrane
sphingolipids [SP]
N-acylsphingosines (ceramides) [SP0201]
DG(34:2)
triacylglycerols [GL0301]
up
down
0
1
2
-LOG(FDR q-value)

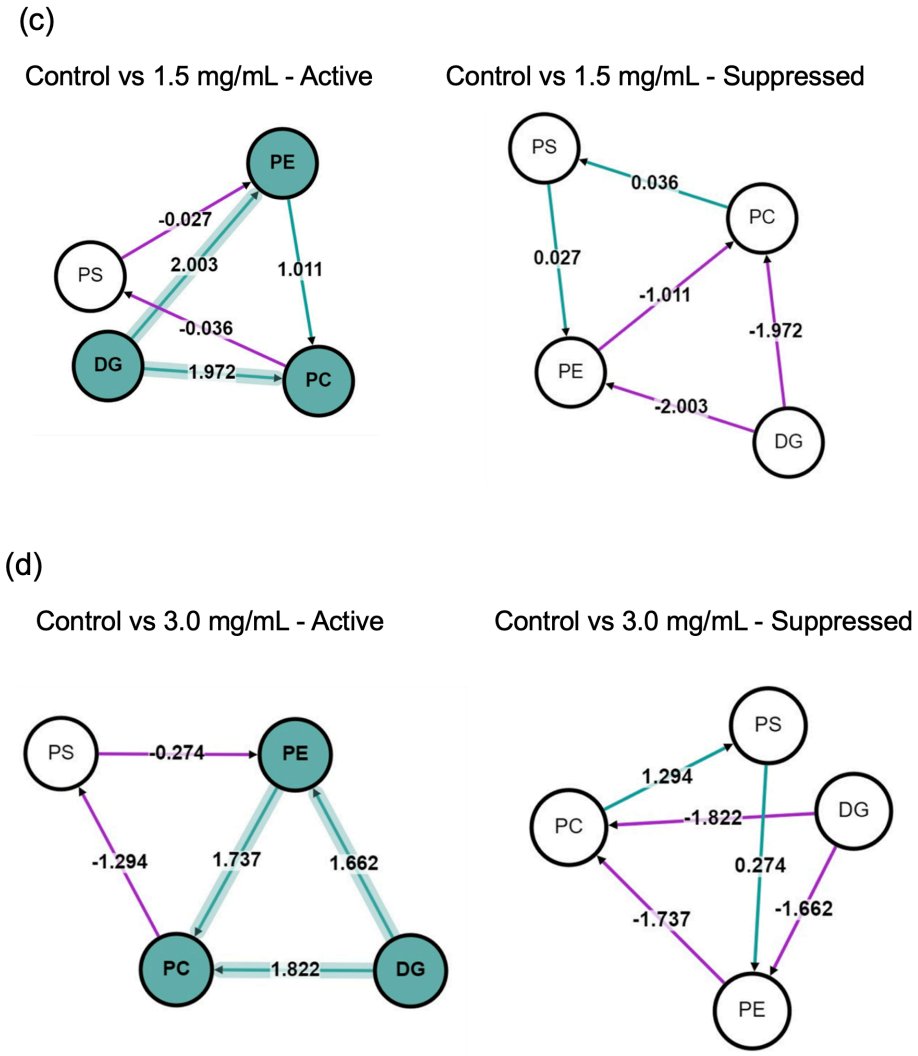

Figure 6.4. (a) Heatmap of the alterations in lipid concentrations in D. magna exposed to 1.5 and 3.0 mg/L finasteride, compared to the untreated group. Red indicates higher metabolites and blue indicates lower metabolites, relative to the average gene metabolite levels. (b) LION enrichment lipid ontology analysis results in ranking mode of comparisons of the untreated group with finasteride (1.5 and 3 mg/mL) exposed groups via one-way ANOVA F-test. Lipid network graphs exported from BioPAN for (c) 1.5 mg/L and (d) 3.0 mg/L finasteride exposure. Green nodes correspond to active lipids, and green shaded arrows correspond to active pathways. Reactions with a positive Z score have green arrows, while negative Z scores are purple colored. Abbreviation: TG, triacylglycerol; PC, phosphatidylcholine; DG, diacylglycerol; Cer, ceramide; PE, phosphatidylethanolamine; PI, Phosphatidylinositol; PS, phosphatidylserine; SM, sphingomyelin; MG, Monoacylglycerols; FA, Fatty acid.

6.5 Discussion

While the mechanism of toxicity in *D. magna* due to exposure to steroid hormones and steroid-related chemicals is less understood compared to their impact on vertebrates [40], previous studies have shown that such exposure impacts invertebrates as evidenced by the anti-ecdysteroidal effects of testosterone in *D. magna* [41] and the antagonistic activities of androstenedione in Drosophila melanogaster *B* (II) cells [42]. Recent studies have explored the effects of 5AR inhibitor exposure in invertebrate species. For instance, pharmaceutical 5AR inhibitors led to observable morphological alterations in gastropods embryos [12]. Considering the signaling pathways centered on ecdysteroids, these findings suggested that steroid-related molecules might have cross-pathway impacts, influencing species with varying hormonal and signaling pathways [43; 14; 44]. In the present study, finasteride exposure had pronounced significant effects on reproductive activities such as reproduction output and the first time to brood. Particularly, the dose-responsive decrease in individual reproduction serve as a key indicator among various parameters for evaluating chronic toxicity of exposure substances in assessing endocrine disrupting effects [45]. Based on these studies and 5AR inhibitor characteristics, which are structural similar to androgens and interfere with the function of androgen receptor signaling, finasteride in *D. magna* may be suggested to act as an endocrine disruptor, particularly affecting ecdysteroid signaling.

Given the close relationship between growth rate and reproduction in *D. magna*, developmental retardation influences the reduction in reproduction. Previous studies investigating the effects of various EDCs in *D. magna* observed simultaneous changes in reproductive output and physiological alterations, confirming significant correlations between these outcomes [46; 41; 47]. The impacts of toxic substances on reproduction and growth differ significantly, with a range of toxicity indicators reflecting the unique interaction of each chemical with organisms [48]. In our result, while the control group exhibited low variability in individual size, the groups exposed to finasteride showed developmental retardation and inter-individual size variation with statistically significant differences. Correspondingly, the size of neonates in each group demonstrated a tendency to decrease with increasing exposure concentrations. The overall decrease in growth and reproduction trends may be not only representative to endocrine disrupting and also related to finasteride exposure affecting the overall metabolism as a toxic mechanism of action [49; 50].

To elucidate the toxicogenomic responses of *D. magna* to finasteride exposure underlying the adverse effects on reproduction through endocrine disruption, we analyzed the expression of key genes associated with development and reproduction including *EcR-A*, *EcR-B*, *neverland, Jhe*, *chitinase*, *RXR*, *Hr96*, *Vtg2*. A marked downregulation of *Vtg2, Jhe*, *EcR-A, EcR-B,* and *RXR* genes was noted in the presence of finasteride. As vitellogenin genes are downstream products in the endocrine signaling pathway, playing a role in orchestrating yolk synthesis and oocyte maturation, their expression levels constitute a critical biomarker for evaluating the reproductive impact in ecotoxicological assessments [51-53]. The dose-responsive decrease in the expression level of *Vtg2* was consistent with the significant reduction in those of *Jhe* observed after 24 hours of exposure. JHE regulates the concentration of juvenile hormone (JH) by

suppressing vitellogenin gene expression. This suggests that the concentration of JH may have become imbalanced in association with the decrease in *Vtg2* [54]. Thus, the reduced *Jhe* levels might impede juvenile hormone degradation, leading to delayed maturation, adult metamorphosis, and reduced reproduction [55]. Considering the interrelationship of these two genes in yolk production and reproduction [56; 55], the significant decrease in these genes following 5AR inhibitor exposure contributed to reduced yolk formation and delayed maturation, resulting in reproductive output decrease. The enzyme Neverland catalyzes the initial steps in the synthesis of ecdysteroids from cholesterol, which then undergo several processes to become active hormones, particularly ecdysone [57]. Subsequently, ecdysteroid interacts with EcR and RXR, binding to the promoters of ecdysone-related genes and exerting downstream effects in regulating reproduction and development, influencing processes such as molting, metamorphosis, and vitellogenesis [58; 59; 54]. Considering particularly relevant in synchronization of reproduction and molting cycles, the decreased expression of EcR and RXR gene ssuggests that ecdysteroid pathways were disrupted [43]. This was accompanied by a notable decrease in the expression of vitellogenin genes, correlating with the observed changes in *EcR* and *Jhe* levels [55; 60]. Thus, finasteride exposure in daphnids led to the suppression of genes linked to ecdysteroid signaling and hormone receptor-mediated pathways, aligning with the noted reductions and retardancy in fecundity. Chitinase gene expression was upregulated after 6 h of exposure and showed a more pronounced increase at 24 h in the 6 mg/L exposure group. A decrease in *Chitinase* expression can induce chronic reproductive effects through a reduction in molting [61]. However, our results, showing an increase in the level of *Chitinase* expression along with a decrease in reproduction, suggest that the exposure to 5AR inhibitors may have a greater impact on disrupting the balance in ecdysteroid and juvenile hormone signaling pathways, rather than regulating metamorphosis [46; 62].

Adaptation to oxidative stress often necessitates the synthesis of antioxidant enzymes, indirectly influencing the levels of antioxidant mRNA [63]. Severe toxicants such as pesticides and heavy metals have been shown to elevate the level of antioxidants and ROS [64; 65]. In this study, the ROS levels did not show a significant increase even though finasteride exposure resulted in the downregulation of antioxidant enzyme genes (Figure 6.3 and S2). Remarkably, there was no observable trend of increment in ROS levels over time. While the response of daphnia at molecular level to environmental stressors is controversial, it is well-recognized that exposure to low-toxic substances causing stress can lead to fluctuations in ROS levels and antioxidant activity [66; 67]. For instance, environmental changes in temperature affect ROS and oxidative stress defense mechanisms in a time-dependent manner; fluctuations were observed up to 24 hours after exposure, stabilizing after 48 hours [68]. While ROS levels showed an increasing trend with time upon exposure to polystyrene nanoplastic, the expression of genes related to antioxidant defenses such as *sod* and *cat* fluctuated over time [69]. Our observations align with phenomena previously reported in the literature. These results suggest that the concentrations of finasteride applied not significantly impact *D. magna* individuals due to cellular toxicity; nevertheless, the adverse effects of the 5AR inhibitor manifested through disruptions in the endocrine signaling pathway.

Lipids serve as essential energy source, significantly influencing the development, growth, and

reproduction of invertebrates [70]. In general, lipid reserves decrease during reproductive phases due to high energy demands and accumulate during non-reproductive periods, reflecting the metabolic costs associated with reproduction [71]. In *D. magna*, female somata showed depletion of nutrients by high maternal investment in reproduction. The cholesterol not only supports eggs development but is also retained at higher levels in somatic tissues [72]. This pattern extends to dietary polyunsaturated fats, which are critical for both asexual and sexual reproduction eggs and lead to significant depletion of fatty acid reserves [73]. The essential role of lipids is further highlighted by the accumulation of glycerophospholipids, necessary for the formation of the new carapace [74]. Additionally, individuals with low TG from eggs develop into smaller individuals that matured late and reproduced late [74; 75]. These studies align with our findings that finasteride exposure leads to downregulation of lipid content, particularly TG (Figure 6.4), and impacts development- and reproduction-related parameters.

As the molecular outcomes of organism's functions, the study by Jordão et al. (2016) reported that the genetic interaction with EcR, RXR, and methyl farnesoate hormone receptors (MfRs) regulated the signaling pathway implicated in lipid storage. This may act similarly to the mechanistic mode of action of the RXR and peroxisome proliferator-activated receptor (PPARγ) signaling pathway, a key regulator of lipid metabolism in vertebrates. The putative MfR is consist of methoprene-tolerant coactivator protein (MET) which is bind to methyl farnesoate and other juvenoid compound, and the steroid receptor coactivator (SRC) [17]. In addition, these molecular results showed to interact through complex crosstalk between ecdysteroids and JHs, which are essential hormones of *D. magna* [43]. In particular, their interaction was hypothesized to antagonistic effect due to the competitive interaction between EcR and MET for binding to SCR, and mixture of ecdysteroids and JHs also negatively affected factors related to lipid storage at the gene response [17; 43; 76]. As another factor, Hr96 is known to regulate several genes involved in energy metabolisms through cholesterol and fatty acid homeostasis through heterodimerization with RXR [77; 78]. These findings may suggest the possibility of interaction between finasteride and this receptor-related signaling pathway, which may suggest a connection the downregulation of between *EcR-A/B*, *Jhe*, *RXR*, and *Hr96* expression levels and lipid metabolites observed in this study (as shown in cluster 1 and 2 in Figure 6.4a).

Specific lipid classes have different regulatory functions across organisms. Lipids, as main components of the cellular membrane, vary across organisms, cell types, organelles, and membrane subdomain levels [79]. In the present study, the LION analysis revealed that lipid bilayer thickness as well as glycerophospholipids was activated due to finasteride exposure. We observed a correlated upregulation of lipid metabolism in the membrane components and mitochondria, while the plasma membrane was downregulated. Phospholipids, particularly PC and PE, are most abundant in the mitochondrial membranes and essential for maintaining the phospholipid composition in the mitochondrial function, structure, and biogenesis [80]. PC not only serves as a vital component of biological membranes and a pulmonary surfactant but also plays a key role in membrane cell signaling [81]. Furthermore, PC is involved in diverse processes, including oxidation, inflammation, endoplasmic reticulum membrane stress, endosome modulation, lipid storage, membrane synthesis, and growth [82]. The biosynthesis of

PE or PC is mediated by CEPT1 (EC:2.7.8.1, KEGG orthology K13644), while the conversion of PE to PC is mediated by PEMT (EC:2.1.1.103, KEGG orthology K05929) through the transfer of three methyl groups from S-adenosylmethionine. Interestingly, finasteride has been reported to inhibit phenylethanolamine N-methyltransferase (PNMT), which is responsible for converting norepinephrine to epinephrine in human [83]. This report suggests that finasteride potentially affects crustacean PEMT including inhibition and compensatory expression. CEPT also mediates the conversion of DG to PE and DG to PC, suggesting crosstalk between PEMT and CEPT under finasteride exposure. Thus, these evidences may explain the results in this study where many lipid metabolites decreased (Figure 6.4a), but metabolism pathways involving DG to PE, DG to PC, and PE to PC (Figure 6.4b-c) were upregulated following finasteride exposure. Sphingolipids, key components of cellular membranes, are significant for the development, growth and reproduction of offspring due to the substantial transfer [84]. Exposure to finasteride led to downregulation of sphingolipids in our study (Figure 6.4b). This disruption in sphingolipid levels could have significant implications for development and reproduction. While the LC-QTOF lipidomics approach in our study did not identify cholesterol and ecdysteroid metabolites, the potential interaction between ecdysteroid and lipids metabolism in daphnia presents a fascinating area for further study. Considering this, future studies should explore the correlation between specific lipids class changes and organelles in reproduction. This is particularly evident in the observed downregulation of lipid metabolism and its potential link to decreased reproduction. Such observations underscore the importance of further investigation to elucidate these complex biochemical relationships.

6.6 Conclusion

In conclusion, our study has revealed significant physiological effects of finasteride on *D. magna*, including a dose-dependent decrease in reproductive output, delayed brood timing, increased mortality, and altered adult size in a dose-response manner. At the molecular level, finasteride exposure led to the downregulation of key genes expression associated with reproduction and development such as *Vtg2*, *Jhe*, *EcR-A/B* and *RXR*, aligning with observed physiological changes. Additionally, lipidomic analyses indicated notable impact on changes in lipid profiles. These findings demonstrate that finasteride acts as an endocrine disruptor in *D. magna*, leading to significant ecotoxicological effects for aquatic ecosystems. Given the rapidly increasing use of finasteride, this study also emphasizes the need for further environmental assessment to understand its potential ecotoxicological effects.

6.7 Acknowledgments

This research was supported by the Nanomaterial Technology Development Program (NRF-2017M3A7B6052455) funded by the South Korean Ministry of Science and by the Korea Institute of Toxicology (KIT), Republic of Korea (1711195881), and Bio-cluster Industry Capacity Enhancement

Project of Jeonbuk Technopark (JBTP).

6.8 Bibliography

1. Salisbury, B.H., Tadi, P. 5-Alpha-Reductase Inhibitors. *StatPearls Publishing LLC [Online]*, October 18, 2023, Available from: https://www.ncbi.nlm.nih.gov/pubmed/32310390.
2. Singh, S., Deshmukh, R. Finasteride Market Size, Share, Competitive Landscape and Trend Analysis Report by Application (Benign Prostatic Hyperplasia (BPH), Male pattern baldness), by Type (Branded , Generic), by Distribution Channel (Hospital Pharmacies, Online Providers, Drug Stores and Retail Pharmacies): Global Opportunity Analysis and Industry Forecast, 2021-2031. *[Online]*, February 04, 2023, Available from: https://www.alliedmarketresearch.com/finasteride-market-A14012.
3. Kane, S.P. Finasteride. *ClinCalc LLC: [Online]*, February 19, 2022, Available from: https://clincalc.com/DrugStats/Drugs/Finasteride.
4. Vieno, N.; Hallgren, P.; Wallberg, P.; Pyhälä, M., Zandaryaa, S. Emerging pollutants in water series, 1, *Pharmaceuticals in the aquatic environment of the Baltic Sea region: a status report*, UNESCO, Paris, 2017, ISBN 978-92-3-100213-7.
5. Health and Medical Care Administration, R.S. Finasteride. *[Online]*, December 27, 2023, Available from: https://janusinfo.se/beslutsstod/lakemedelochmiljo/pharmaceuticalsandenvironment/databaseenven/finasteride.5.30a7505616a041a09b062df5.html#:~:text=Finasteride%20has%20been%20detected%20in,purified%20wastewater%20nationally%20in%20Sweden.
6. Richmond, E.K.; Rosi, E.J.; Walters, D.M.; Fick, J.; Hamilton, S.K.; Brodin, T.; Sundelin, A., Grace, M.R. A diverse suite of pharmaceuticals contaminates stream and riparian food webs. *Nat. Commun.* **2018**, 9, 4491. doi:10.1038/s41467-018-06822-w.
7. García-García, M.; Sánchez-Hernández, M.; García-Hernández, M.P.; García-Ayala, A., Chaves-Pozo, E. Role of 5α-dihydrotestosterone in testicular development of gilthead seabream following finasteride administration. *J. Steroid Biochem. Mol. Biol.* **2017**, 174, 48-55. doi:10.1016/j.jsbmb.2017.07.024.
8. Lee, M.R.; Loux-Turner, J.R., Oliveira, K. Evaluation of the 5α-reductase inhibitor finasteride on reproduction and gonadal development in medaka, Oryzias latipes. *Gen. Comp. Endocrinol.* **2015**, 216, 64-76. doi:10.1016/j.ygcen.2015.04.008.
9. Margiotta-Casaluci, L.; Hannah, R.E., Sumpter, J.P. Mode of action of human pharmaceuticals in fish: the effects of the 5-alpha-reductase inhibitor, dutasteride, on reproduction as a case study. *Aquat. Toxicol.* **2013**, 128-129, 113-123. doi:10.1016/j.aquatox.2012.12.003.
10. Urbatzka, R.; Watermann, B.; Lutz, I., Kloas, W. Exposure of Xenopus laevis tadpoles to finasteride, an inhibitor of 5-alpha reductase activity, impairs spermatogenesis and alters hypophyseal feedback mechanisms. *J. Mol. Endocrinol.* **2009**, 43, 209-219. doi:10.1677/JME-09-0058.
11. Gilroy, E.A.M.; Bartlett, A.J.; Gillis, P.L.; Bendo, N.A.; Salerno, J.; Hedges, A.M.; Brown, L.R.; Holman, E.A.M.; Stock, N.L., de Solla, S.R. Toxicity of the pharmaceuticals finasteride and melengestrol acetate to benthic invertebrates. *Environ Sci Pollut Res Int* **2020**, 27, 41803-41815. doi:10.1007/s11356-020-10121-7.
12. Baynes, A.; Montagut Pino, G.; Duong, G.H.; Lockyer, A.E.; McDougall, C.; Jobling, S., Routledge, E.J.

Early embryonic exposure of freshwater gastropods to pharmaceutical 5-alpha-reductase inhibitors results in a surprising open-coiled "banana-shaped" shell. *Sci. Rep.* **2019**, 9, 16439. doi:10.1038/s41598-019-52850-x.

13. Song, Y.; Rundberget, J.T.; Evenseth, L.M.; Xie, L.; Gomes, T.; Høgåsen, T.; Iguchi, T., Tollefsen, K.E. Whole-Organism Transcriptomic Analysis Provides Mechanistic Insight into the Acute Toxicity of Emamectin Benzoate in Daphnia magna. *Environ. Sci. Technol.* **2016**, 50, 11994-12003. doi:10.1021/acs.est.6b03456.
14. Song, Y.; Villeneuve, D.L.; Toyota, K.; Iguchi, T., Tollefsen, K.E. Ecdysone Receptor Agonism Leading to Lethal Molting Disruption in Arthropods: Review and Adverse Outcome Pathway Development. *Environ. Sci. Technol.* **2017**, 51, 4142-4157. doi:10.1021/acs.est.7b00480.
15. Campioli, E.; Batarseh, A.; Li, J., Papadopoulos, V. The endocrine disruptor mono-(2-ethylhexyl) phthalate affects the differentiation of human liposarcoma cells (SW 872). *PLoS One* **2011**, 6, e28750. doi:10.1371/journal.pone.0028750.
16. Ebert, D. Daphnia as a versatile model system in ecology and evolution. *EvoDevo* **2022**, 13, 16. doi:10.1186/s13227-022-00199-0.
17. Jordão, R.; Campos, B.; Piña, B.; Tauler, R.; Soares, A.M.V.M., Barata, C. Mechanisms of Action of Compounds That Enhance Storage Lipid Accumulation in Daphnia magna. *Environ. Sci. Technol.* **2016**, 50, 13565-13573. doi:10.1021/acs.est.6b04768.
18. LeBlanc, G.A. Crustacean endocrine toxicology: a review. *Ecotoxicol.* **2007**, 16, 61-81. doi:10.1007/s10646-006-0115-z.
19. OECD Test No. 202: Daphnia sp. Acute Immobilisation Test, OECD Guidelines for the Testing of Chemicals, Section 2. *OECD Publishing* **2004**, OECD Guidelines for the Testing of Chemicals, Section 2. doi:10.1787/9789264069947-en.
20. OECD Test No. 211: Daphnia magna Reproduction Test, OECD Guidelines for the Testing of Chemicals, Section 2. *OECD Publishing* **2012**, OECD Guidelines for the Testing of Chemicals, Section 2. doi:10.1787/9789264185203-en.
21. IOS., *Water quality — Determination of the inhibition of the mobility of Daphnia magna Straus (Cladocera, Crustacea) — Acute toxicity test (ISO 6341:2012)*, International Organization for Standardization, Geneve, Switzerland, 2012, ISBN: 978 0 580 69874 3.
22. Schneider, C.A.; Rasband, W.S., Eliceiri, K.W. NIH Image to ImageJ: 25 years of image analysis. *Nat. Methods* **2012**, 9, 671-675. doi:10.1038/nmeth.2089.
23. Bang, S.H.; Ahn, J.-Y.; Hong, N.-H.; Sekhon, S.S.; Kim, Y.-H., Min, J. Acute and chronic toxicity assessment and the gene expression of Dhb, Vtg, Arnt, CYP4, and CYP314 in Daphnia magna exposed to pharmaceuticals. *Mol. Cell. Toxicol.* **2015**, 11, 153-160. doi:https://10.1007/s13273-015-0013-7.
24. Imhof, H.K.; Rusek, J.; Thiel, M.; Wolinska, J., Laforsch, C. Do microplastic particles affect Daphnia magna at the morphological, life history and molecular level? *PLoS One* **2017**, 12, e0187590. doi:10.1371/journal.pone.0187590.
25. Schmittgen, T.D., Livak, K.J. Analyzing real-time PCR data by the comparative CT method. *Nat. Protoc.* **2008**, 3, 1101-1108. doi:10.1038/nprot.2008.73.
26. Sostare, J.; Di Guida, R.; Kirwan, J.; Chalal, K.; Palmer, E.; Dunn, W.B., Viant, M.R. Comparison of

modified Matyash method to conventional solvent systems for polar metabolite and lipid extractions. *Anal. Chim. Acta* **2018**, 1037, 301-315. doi:10.1016/j.aca.2018.03.019.

27. Tsugawa, H.; Cajka, T.; Kind, T.; Ma, Y.; Higgins, B.; Ikeda, K.; Kanazawa, M.; VanderGheynst, J.; Fiehn, O., Arita, M. MS-DIAL: data-independent MS/MS deconvolution for comprehensive metabolome analysis. *Nat. Methods* **2015**, 12, 523-526. doi:10.1038/nmeth.3393.
28. Cho, H.; Seol, Y.; Baik, S.; Sung, B.; Ryu, C.S., Kim, Y.J. Mono(2-ethylhexyl) phthalate modulates lipid accumulation and reproductive signaling in Daphnia magna. *Environ. Sci. Pollut. Res.* **2022**, 29, 55639-55650. doi:10.1007/s11356-022-19701-1.
29. Tsugawa, H.; Ikeda, K.; Takahashi, M.; Satoh, A.; Mori, Y.; Uchino, H.; Okahashi, N.; Yamada, Y.; Tada, I.; Bonini, P.; et al. A lipidome atlas in MS-DIAL 4. *Nat. Biotechnol.* **2020**, 38, 1159-1163. doi:10.1038/s41587-020-0531-2.
30. Pang, Z.; Zhou, G.; Ewald, J.; Chang, L.; Hacariz, O.; Basu, N., Xia, J. Using MetaboAnalyst 5.0 for LC-HRMS spectra processing, multi-omics integration and covariate adjustment of global metabolomics data. *Nat. Protoc.* **2022**, 17, 1735-1761. doi:10.1038/s41596-022-00710-w.
31. Wishart, D.S.; Jewison, T.; Guo, A.C.; Wilson, M.; Knox, C.; Liu, Y.; Djoumbou, Y.; Mandal, R.; Aziat, F.; Dong, E.; et al. HMDB 3.0--The Human Metabolome Database in 2013. *Nucleic Acids Res.* **2013**, 41, D801-807. doi:10.1093/nar/gks1065.
32. Smith, C.A.; O'Maille, G.; Want, E.J.; Qin, C.; Trauger, S.A.; Brandon, T.R.; Custodio, D.E.; Abagyan, R., Siuzdak, G. METLIN: a metabolite mass spectral database. *Ther. Drug Monit.* **2005**, 27, 747-751. doi:10.1097/01.ftd.0000179845.53213.39.
33. Horai, H.; Arita, M.; Kanaya, S.; Nihei, Y.; Ikeda, T.; Suwa, K.; Ojima, Y.; Tanaka, K.; Tanaka, S.; Aoshima, K.; et al. MassBank: a public repository for sharing mass spectral data for life sciences. *J. Mass Spectrom.* **2010**, 45, 703-714. doi:10.1002/jms.1777.
34. Fahy, E.; Sud, M.; Cotter, D., Subramaniam, S. LIPID MAPS online tools for lipid research. *Nucleic Acids Res.* **2007**, 35, W606-612. doi:10.1093/nar/gkm324.
35. Ihaka, R., Gentleman, R. R: A Language for Data Analysis and Graphics. *J. Comput. Graph. Stat.* **1996**, 5, 299-314. doi:10.1080/10618600.1996.10474713.
36. Kolde, R., Kolde, M.R. Package 'pheatmap'. *R package 1* **2015**, 790.
37. Molenaar, M.R.; Jeucken, A.; Wassenaar, T.A.; van de Lest, C.H.A.; Brouwers, J.F., Helms, J.B. LION/web: a web-based ontology enrichment tool for lipidomic data analysis. *Gigascience* **2019**, 8. doi:10.1093/gigascience/giz061.
38. Gaud, C.; B, C.S.; Nguyen, A.; Fedorova, M.; Ni, Z.; O'Donnell, V.B.; Wakelam, M.J.O.; Andrews, S., Lopez-Clavijo, A.F. BioPAN: a web-based tool to explore mammalian lipidome metabolic pathways on LIPID MAPS. *F1000Res* **2021**, 10, 4. doi:10.12688/f1000research.28022.2.
39. Kanehisa, M.; Sato, Y.; Kawashima, M.; Furumichi, M., Tanabe, M. KEGG as a reference resource for gene and protein annotation. *Nucleic Acids Res.* **2016**, 44, D457-462. doi:10.1093/nar/gkv1070.
40. Ojoghoro, J.O.; Scrimshaw, M.D., Sumpter, J.P. Steroid hormones in the aquatic environment. *Sci. Total Environ.* **2021**, 792, 148306. doi:10.1016/j.scitotenv.2021.148306.
41. Mu, X., LeBlanc, G.A. Developmental toxicity of testosterone in the crustacean Daphnia magna involves anti-ecdysteroidal activity. *Gen. Comp. Endocrinol.* **2002**, 129, 127-133. doi:10.1016/s0016-

6480(02)00518-x.

42. Dinan, L.; Bourne, P.; Whiting, P.; Dhadialla, T.S., Hutchinson, T.H. Screening of environmental contaminants for ecdysteroid agonist and antagonist activity using the Drosophila melanogaster B(II) cell in vitro assay. *Environ. Toxicol. Chem.* **2001**, 20, 2038-2046. doi:10.1897/1551-5028(2001)020<2038:soecfe>2.0.co;2.
43. Miyakawa, H.; Sato, T.; Song, Y.; Tollefsen, K.E., Iguchi, T. Ecdysteroid and juvenile hormone biosynthesis, receptors and their signaling in the freshwater microcrustacean Daphnia. *J. Steroid Biochem. Mol. Biol.* **2018**, 184, 62-68. doi:10.1016/j.jsbmb.2017.12.006.
44. Sumiya, E.; Ogino, Y.; Miyakawa, H.; Hiruta, C.; Toyota, K.; Miyagawa, S., Iguchi, T. Roles of ecdysteroids for progression of reproductive cycle in the fresh water crustacean Daphnia magna. *Front. zool.* **2014**, 11, 60. doi:10.1186/s12983-014-0060-2.
45. Tkaczyk, A.; Bownik, A.; Dudka, J.; Kowal, K., Ślaska, B. Daphnia magna model in the toxicity assessment of pharmaceuticals: A review. *Sci. Total Environ.* **2021**, 763, 143038. doi:10.1016/j.scitotenv.2020.143038.
46. Giraudo, M.; Douville, M.; Cottin, G., Houde, M. Transcriptomic, cellular and life-history responses of Daphnia magna chronically exposed to benzotriazoles: Endocrine-disrupting potential and molting effects. *PLoS One* **2017**, 12, e0171763. doi:10.1371/journal.pone.0171763.
47. Oropesa, A.L.; Floro, A.M., Palma, P. Assessment of the effects of the carbamazepine on the endogenous endocrine system of Daphnia magna. *Environ Sci Pollut Res Int* **2016**, 23, 17311-17321. doi:10.1007/s11356-016-6907-7.
48. Knops, M.; Altenburger, R., Segner, H. Alterations of physiological energetics, growth and reproduction of Daphnia magna under toxicant stress. *Aquat. Toxicol.* **2001**, 53, 79-90. doi:10.1016/s0166-445x(00)00170-3.
49. Fuertes, I.; Campos, B.; Rivetti, C.; Piña, B., Barata, C. Effects of Single and Combined Low Concentrations of Neuroactive Drugs on Daphnia magna Reproduction and Transcriptomic Responses. *Environ. Sci. Technol.* **2019**, 53, 11979-11987. doi:10.1021/acs.est.9b03228.
50. Jeong, T.Y., Simpson, M.J. Reproduction stage specific dysregulation of Daphnia magna metabolites as an early indicator of reproductive endocrine disruption. *Water Res.* **2020**, 184, 116107. doi:10.1016/j.watres.2020.116107.
51. Hu, X.L.; Tang, Y.Y.; Kwok, M.L.; Chan, K.M., Chu, K.H. Impact of juvenile hormone analogue insecticides on the water flea Moina macrocopa: Growth, reproduction and transgenerational effect. *Aquat. Toxicol.* **2020**, 220, 105402. doi:10.1016/j.aquatox.2020.105402.
52. LeBoeuf, A.C.; Cohanim, A.B.; Stoffel, C.; Brent, C.S.; Waridel, P.; Privman, E.; Keller, L., Benton, R. Molecular evolution of juvenile hormone esterase-like proteins in a socially exchanged fluid. *Sci. Rep.* **2018**, 8, 17830. doi:10.1038/s41598-018-36048-1.
53. Toyota, K.; Kato, Y.; Miyakawa, H.; Yatsu, R.; Mizutani, T.; Ogino, Y.; Miyagawa, S.; Watanabe, H.; Nishide, H.; Uchiyama, I.; et al. Molecular impact of juvenile hormone agonists on neonatal Daphnia magna. *J. Appl. Toxicol.* **2014**, 34, 537-544. doi:10.1002/jat.2922.
54. Seyoum, A.; Pradhan, A.; Jass, J., Olsson, P.E. Perfluorinated alkyl substances impede growth, reproduction, lipid metabolism and lifespan in Daphnia magna. *Sci. Total Environ.* **2020**, 737, 139682.

doi:10.1016/j.scitotenv.2020.139682.

55. Tokishita, S.; Kato, Y.; Kobayashi, T.; Nakamura, S.; Ohta, T., Yamagata, H. Organization and repression by juvenile hormone of a vitellogenin gene cluster in the crustacean, Daphnia magna. *Biochem. Biophys. Res. Commun.* **2006**, 345, 362-370. doi:10.1016/j.bbrc.2006.04.102.
56. Merzendorfer, H., Zimoch, L. Chitin metabolism in insects: structure, function and regulation of chitin synthases and chitinases. *J. Exp. Biol.* **2003**, 206, 4393-4412. doi:10.1242/jeb.00709.
57. Rewitz, K.F., Gilbert, L.I. Daphnia Halloween genes that encode cytochrome P450s mediating the synthesis of the arthropod molting hormone: evolutionary implications. *BMC Evol. Biol.* **2008**, 8, 60. doi:10.1186/1471-2148-8-60.
58. Abe, R.; Toyota, K.; Miyakawa, H.; Watanabe, H.; Oka, T.; Miyagawa, S.; Nishide, H.; Uchiyama, I.; Tollefsen, K.E.; Iguchi, T.; et al. Diofenolan induces male offspring production through binding to the juvenile hormone receptor in Daphnia magna. *Aquat. Toxicol.* **2015**, 159, 44-51. doi:https://10.1016/j.aquatox.2014.11.015.
59. Dai, T.H.; Sserwadda, A.; Song, K.; Zang, Y.N., Shen, H.S. Cloning and Expression of Ecdysone Receptor and Retinoid X Receptor from Procambarus clarkii: Induction by Eyestalk Ablation. *Int. J. Mol. Sci.* **2016**, 17. doi:10.3390/ijms17101739.
60. Touhara, K.; Soroker, V., Prestwich, G.D. Photoaffinity labeling of juvenile hormone epoxide hydrolase and JH-binding proteins during ovarian and egg development in Manduca sexta. *Insect Biochem. Mol. Biol.* **1994**, 24, 633-640. doi:doi.org/10.1016/0965-1748(94)90100-7.
61. David, R.M.; Dakic, V.; Williams, T.D.; Winter, M.J., Chipman, J.K. Transcriptional responses in neonate and adult Daphnia magna in relation to relative susceptibility to genotoxicants. *Aquat. Toxicol.* **2011**, 104, 192-204. doi:10.1016/j.aquatox.2011.04.016.
62. Poynton, H.C.; Loguinov, A.V.; Varshavsky, J.R.; Chan, S.; Perkins, E.J., Vulpe, C.D. Gene Expression Profiling in Daphnia magna Part I: Concentration-Dependent Profiles Provide Support for the No Observed Transcriptional Effect Level. *Environ. Sci. Technol.* **2008**, 42, 6250-6256. doi:10.1021/es8010783.
63. Kim, H.; Yim, B.; Bae, C., Lee, Y.-M. Acute toxicity and antioxidant responses in the water flea Daphnia magna to xenobiotics (cadmium, lead, mercury, bisphenol A, and 4-nonylphenol). *J. Toxicol. Environ. Health Sci.* **2017**, 9, 41-49. doi:10.1007/s13530-017-0302-8.
64. Fan, W.; Ren, J.; Li, X.; Wei, C.; Xue, F., Zhang, N. Bioaccumulation and oxidative stress in Daphnia magna exposed to arsenite and arsenate. *Environ. Toxicol. Chem.* **2015**, 34, 2629-2635. doi:https://10.1002/etc.3119.
65. Oropesa, A.L.; Novais, S.C.; Lemos, M.F.; Espejo, A.; Gravato, C., Beltrán, F. Oxidative stress responses of Daphnia magna exposed to effluents spiked with emerging contaminants under ozonation and advanced oxidation processes. *Environ Sci Pollut Res Int* **2017**, 24, 1735-1747. doi:10.1007/s11356-016-7881-9.
66. Jemec, A.; Tišler, T.; Erjavec, B., Pintar, A. Antioxidant responses and whole-organism changes in Daphnia magna acutely and chronically exposed to endocrine disruptor bisphenol A. *Ecotoxicol. Environ. Saf.* **2012**, 86, 213-218. doi:10.1016/j.ecoenv.2012.09.016.
67. Yin, J.; Long, Y.; Xiao, W.; Liu, D.; Tian, Q.; Li, Y.; Liu, C.; Chen, L., Pan, Y. Ecotoxicology of microplastics in Daphnia: A review focusing on microplastic properties and multiscale attributes of

Daphnia. *Ecotoxicol. Environ. Saf.* **2023**, 249, 114433. doi:10.1016/j.ecoenv.2022.114433.

68. Becker, D.; Brinkmann, B.F.; Zeis, B., Paul, R.J. Acute changes in temperature or oxygen availability induce ROS fluctuations in Daphnia magna linked with fluctuations of reduced and oxidized glutathione, catalase activity and gene (haemoglobin) expression. *Biol. Cell.* **2011**, 103, 351-363. doi:10.1042/bc20100145.
69. De Felice, B.; Sugni, M.; Casati, L., Parolini, M. Molecular, biochemical and behavioral responses of Daphnia magna under long-term exposure to polystyrene nanoplastics. *Environ. Int.* **2022**, 164, 107264. doi:10.1016/j.envint.2022.107264.
70. Arrese, E.L., Soulages, J.L. Insect fat body: energy, metabolism, and regulation. *Annu. Rev. Entomol.* **2010**, 55, 207-225. doi:10.1146/annurev-ento-112408-085356.
71. Constantinou, J.K.; Southam, A.D.; Kvist, J.; Jones, M.R.; Viant, M.R., Mirbahai, L. Characterisation of the dynamic nature of lipids throughout the lifespan of genetically identical female and male Daphnia magna. *Sci. Rep.* **2020**, 10, 5576. doi:10.1038/s41598-020-62476-z.
72. Martin-Creuzburg, D.; Massier, T., Wacker, A. Sex-Specific Differences in Essential Lipid Requirements of Daphnia magna. *Front. Ecol. Evol.* **2018**, 6. doi:10.3389/fevo.2018.00089.
73. Becker, C., Boersma, M. Differential effects of phosphorus and fatty acids on Daphnia magna growth and reproduction. *Limnol. Oceanogr.* **2005**, 50, 388-397. doi:doi.org/10.4319/lo.2005.50.1.0388.
74. Fuertes, I.; Jordão, R.; Casas, J., Barata, C. Allocation of glycerolipids and glycerophospholipids from adults to eggs in Daphnia magna: Perturbations by compounds that enhance lipid droplet accumulation. *Environ. Pollut.* **2018**, 242, 1702-1710. doi:10.1016/j.envpol.2018.07.102.
75. Jordão, R.; Casas, J.; Fabrias, G.; Campos, B.; Piña, B.; Lemos, M.F.; Soares, A.M.; Tauler, R., Barata, C. Obesogens beyond Vertebrates: Lipid Perturbation by Tributyltin in the Crustacean Daphnia magna. *Environ. Health Perspect.* **2015**, 123, 813-819. doi:10.1289/ehp.1409163.
76. Zhang, Z.; Xu, J.; Sheng, Z.; Sui, Y., Palli, S.R. Steroid receptor co-activator is required for juvenile hormone signal transduction through a bHLH-PAS transcription factor, methoprene tolerant. *J. Biol. Chem.* **2011**, 286, 8437-8447. doi:10.1074/jbc.M110.191684.
77. Karimullina, E.; Li, Y.; Ginjupalli, G.K., Baldwin, W.S. Daphnia HR96 is a promiscuous xenobiotic and endobiotic nuclear receptor. *Aquat. Toxicol.* **2012**, 116-117, 69-78. doi:10.1016/j.aquatox.2012.03.005.
78. Sengupta, N.; Reardon, D.C.; Gerard, P.D., Baldwin, W.S. Exchange of polar lipids from adults to neonates in Daphnia magna: Perturbations in sphingomyelin allocation by dietary lipids and environmental toxicants. *PLoS One* **2017**, 12, e0178131. doi:10.1371/journal.pone.0178131.
79. Harayama, T., Riezman, H. Understanding the diversity of membrane lipid composition. *Nat. Rev. Mol. Cell Biol.* **2018**, 19, 281-296. doi:10.1038/nrm.2017.138.
80. Schenkel, L.C., Bakovic, M. Formation and regulation of mitochondrial membranes. *Int. J. Cell Biol.* **2014**, 2014, 709828. doi:10.1155/2014/709828.
81. Vance, D.E. Physiological roles of phosphatidylethanolamine N-methyltransferase. *Biochim. Biophys. Acta* **2013**, 1831, 626-632. doi:10.1016/j.bbalip.2012.07.017.
82. Kanno, K.; Wu, M.K.; Scapa, E.F.; Roderick, S.L., Cohen, D.E. Structure and function of phosphatidylcholine transfer protein (PC-TP)/StarD2. *Biochim. Biophys. Acta* **2007**, 1771, 654-662. doi:10.1016/j.bbalip.2007.04.003.

83. Giatti, S.; Di Domizio, A.; Diviccaro, S.; Falvo, E.; Caruso, D.; Contini, A., Melcangi, R.C. Three-Dimensional Proteome-Wide Scale Screening for the 5-Alpha Reductase Inhibitor Finasteride: Identification of a Novel Off-Target. *J. Med. Chem.* **2021**, 64, 4553-4566. doi:10.1021/acs.jmedchem.0c02039.
84. Sengupta, N.; Gerard, P.D., Baldwin, W.S. Perturbations in polar lipids, starvation survival and reproduction following exposure to unsaturated fatty acids or environmental toxicants in Daphnia magna. *Chemosphere* **2016**, 144, 2302-2311. doi:10.1016/j.chemosphere.2015.11.015.

6.9 Supporting information

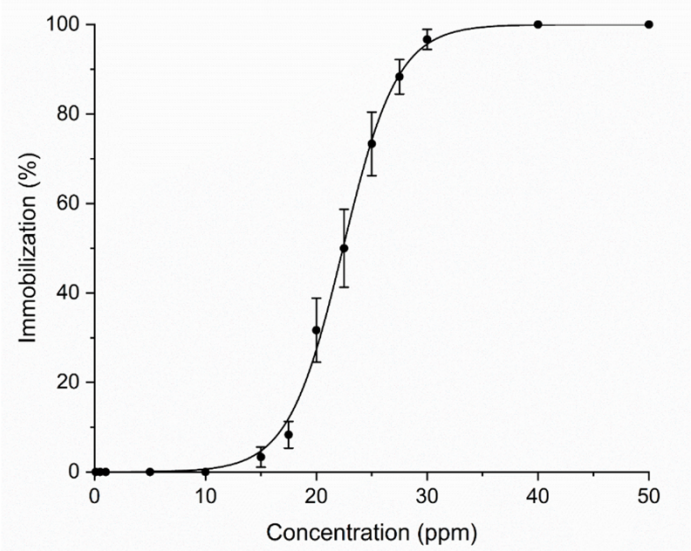

Figure S6.1. Immobilization of daphnids after 48 h exposure to various concentrations of finasteride (0.1 to 5.0 ppm). The graph is expressed as a mean value with SEM.

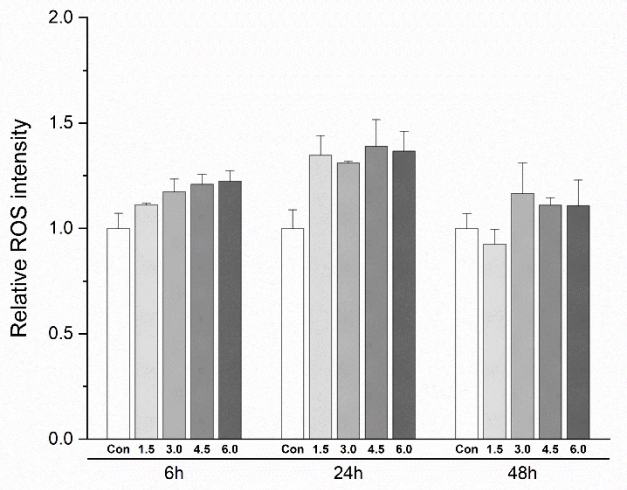

Figure S6.2. Time-dependent relative ROS intensity levels changes during 48 h exposure to various concentrations of finasteride. The graph is expressed as a mean value with SEM (*n*=3, 20 neonates in a group).

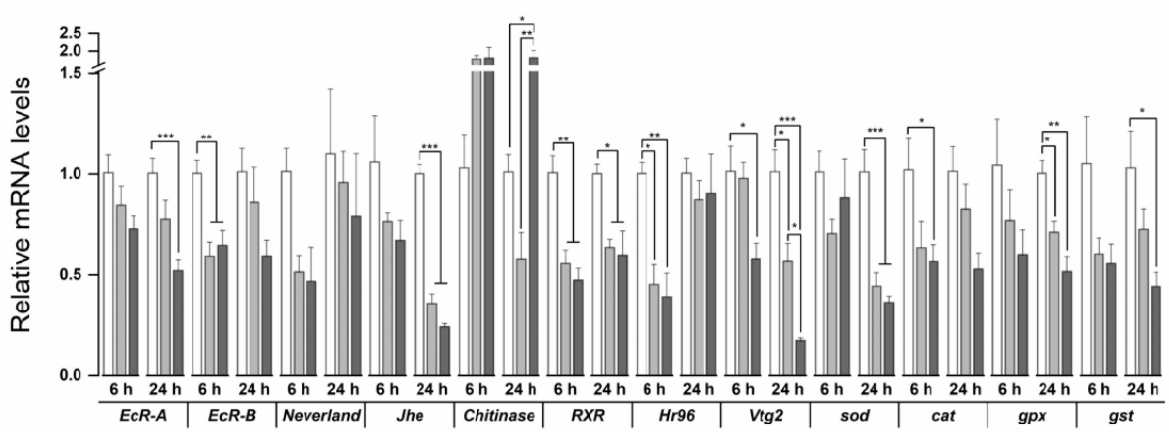

Figure S6.3. Relative mRNA expression following 6 h and 24 h exposure of 17-day-old *D. magna* adults to finasteride. The expression levels of selected reproduction-, development- and antioxidant-related genes. Bars indicate mean values, while error bars represent the standard error of mean ($n \geq 3$, each sample comprising 5 individuals). Statistical evaluations were conducted using one-way ANOVA and Tukey's multiple comparison tests, with asterisks denoting significant differences (*$p < 0.05$, **$p < 0.01$, and ***$p < 0.001$).

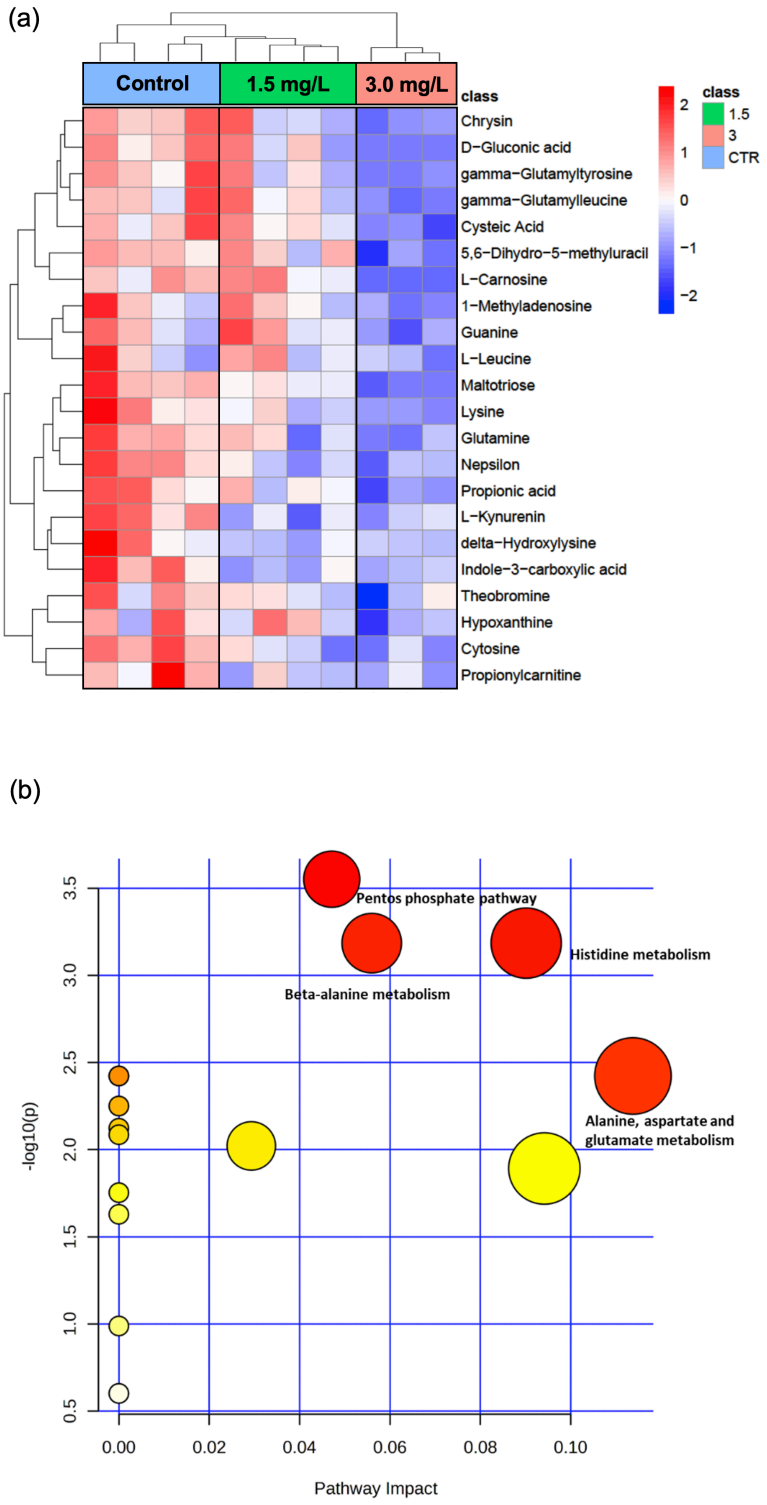

Figure S6.4. (a) Heatmap of metabolites changes from 1.5 mg/L, and 3.0 mg/L finasteride exposed *D. magna* and control with the clustering results. The clustering results are based on Pearson's distance measure and Euclidean distance algorithm. (b) Metabolic pathways analysis results compared control with 3.0 mg/L finasteride exposed *D. magna* using MetaboAnalyst 5.0 shown as circles plotted according to their enrichment score (x-axis) and topology analyses (pathway impact, y-axis).

Table S6.1. Primer sequences of target genes for qRT-PCR.

Gene name	Gene symbol	Forward primer (5′ - 3′) Reverse primer (5′ - 3′)	Reference
Actin	*Actin*	CCTCCACCTCTTTGGAGAAAT CAAGAATGAGGGCTGGAAGAG	Cui et al. (2017)
Ecdysone receptor A	*EcR-A*	CAGGCACATCAACATCAACAAC GGCGACATGGAATCGACA	Kato et al. (2007)
Ecdysone receptor B	*EcR-B*	CACCACAACCAACTGCATTTAC CCATTAATGTCAAGATCCCACA	Kato et al. (2007)
Neverland	*Neverland*	CAAATGAGGGCAATACGCGT GATGCTCTCGGCGAGAACAT	Jordão et al. (2016)
Juvenile hormone esterase	*Jhe*	ATGGAGTTCTCAACGGAACG ATCTCAGGTGTGGGCATTTC	Heckmann et al. (2008)
Chitinase	*Chitinase*	CGAAACCACGTTCAAGATCA CAAGCCGGTGAATTTACGAT	Poynton et al. (2008)
Retinoid X receptor	*RXR*	CTTGCCGTGAAGATCGTCAG ACCGATTTCTCTGGCGTTTG	Talu et al. (2022)
HR96 nuclear hormone receptor	*HR96*	GCGGAGACAAGGCTTTAGGTT AGGGCATTCCGTCTAAAGAAGGCT	Seyoum et al. (2020)
Vitellogenin 2	*Vtg2*	CACTGCCTTCCCAAGAACAT ATCAAGAGGACGGACGAAGA	Hannas et al. (2011)
Superoxide dismutase	*sod*	TGCCGTCGTCTGCTGCTTTGTT TCCGTTGCTGAATACATCGCCGAAT	Cui et al. (2017)
Catalase	*cat*	CTGTTGGCGGAGAAAGCGGTTCA ATCTGGTGTTCCACGGTCGGAGAA	Cui et al. (2017)
Glutathione peroxidase	*gpx*	CGACCTCCTTGCCCTTGACAGAATG GTGCCAGGCTCTTGTGACATGAACT	Cui et al. (2017)
Glutathione-s-transferase	*gst*	CAACGCGTATGGCAAAGATG CTAGACCGAAACGGTGGTAAA	Domínguez et al. (2018)

Table S6.2. The hierarchical clustering of lipid changes into three distinct groups consisting of 344, 75, and 26 lipids, respectively. The lipid names, average mass-to-charge ratios (*m/z*), ionization modes, and retention times (RT) are detailed for each cluster.

Group	Lipid name	Average (*m/z*)	Adduct type	Average RT (min)
Cluster 1	Cer 33:1;2O	506,48917	[M+H-H2O]+	5,66
	Cer 34:0;3O	556,53149	[M+H]+	4,456
	Cer 34:0;3O	556,52979	[M+H]+	5,655
	Cer 34:1;2O	520,50616	[M+H-H2O]+	6,041
	Cer 34:1;2O	520,50494	[M+H-H2O]+	4,742
	Cer 34:1;3O	536,49969	[M+H-H2O]+	5,698
	Cer 35:0;3O	552,53503	[M+H-H2O]+	6,312
	Cer 35:0;3O	570,5448	[M+H]+	4,978
	Cer 35:1;2O	534,51837	[M+H-H2O]+	6,321
	Cer 35:1;3O	550,51697	[M+H-H2O]+	4,802
	Cer 36:1;2O	548,53857	[M+H-H2O]+	6,77
	Cer 37:3;3O	574,51318	[M+H-H2O]+	6,341
	Cer 37:3;3O	592,53607	[M+H]+	10,98
	Cer 38:1;3O	592,56824	[M+H-H2O]+	7,161
	Cer 38:2;2O	574,54999	[M+H-H2O]+	6,798
	Cer 38:3;3O	588,53064	[M+H-H2O]+	6,773

Cer 38:3;3O	606,54852	[M+H]+	11,221
Cer 38:6;3O	600,5047	[M+H]+	6,391
Cer 38:7;3O	598,48981	[M+H]+	4,301
Cer 39:1;3O	606,58356	[M+H-H2O]+	7,521
Cer 39:8;2O	616,45844	[M+Na]+	4,557
Cer 40:1;3O	620,59296	[M+H-H2O]+	7,862
Cer 40:2;2O	602,58917	[M+H-H2O]+	7,538
Cer 40:4;2O	598,55585	[M+H-H2O]+	6,348
Cer 40:8;2O	630,47302	[M+Na]+	4,798
Cer 41:1;3O	634,6131	[M+H-H2O]+	8,181
Cer 42:1;3O	648,62469	[M+H-H2O]+	8,516
Cer 42:4;2	666,56641	[M+Na]+	7,626
Cer 44:8;4O	696,55261	[M+H]+	4,774
Cer 55:9;4O	830,69159	[M+H-H2O]+	8,121
Cer 57:4;4O	886,82111	[M+H]+	11,549
Cer 58:10;4O	870,73438	[M+H-H2O]+	9,961
Cer 58:11;4O	868,73267	[M+H-H2O]+	11,3
Cer 59:9;4O	886,75281	[M+H-H2O]+	9,111
Cer 62:11;4O	924,80554	[M+H-H2O]+	10,867
Cer 63:14;4O	950,7597	[M+H]+	11,62
Cer 63:9;4O	942,83826	[M+H-H2O]+	11,47
DG 31:5	567,4071	[M+Na]+	3,261
DG 32:0	591,49481	[M+Na]+	6,337
DG 32:1	589,4834	[M+Na]+	5,762
DG 32:2	582,50848	[M+NH4]+	6,185
DG 33:1	563,49841	[M-H2O+H]+	11,239
DG 34:0	619,5293	[M+Na]+	7,039
DG 34:1	612,5528	[M+NH4]+	7,407
DG 34:1	617,50757	[M+Na]+	7,394
DG 34:2	610,53955	[M+NH4]+	6,833
DG 34:2	615,49487	[M+Na]+	6,838
DG 34:2	615,49298	[M+Na]+	5,845
DG 34:3	608,5249	[M+NH4]+	6,326
DG 34:3	613,48126	[M+Na]+	5,376
DG 34:3	613,4809	[M+Na]+	6,36
DG 34:4	606,50793	[M+NH4]+	5,762
DG 34:5	585,45544	[M-H]-	5,777
DG 35:2	624,54803	[M+NH4]+	7,177
DG 35:2	629,50757	[M+Na]+	7,171
DG 35:3	622,53485	[M+NH4]+	6,673
DG 35:3	627,49097	[M+Na]+	6,667
DG 35:4	620,5224	[M+NH4]+	6,072
DG 36:1	640,586	[M+NH4]+	8,091
DG 36:1	645,54456	[M+Na]+	7,416
DG 36:2	638,5686	[M+NH4]+	7,514
DG 36:2	643,52789	[M+Na]+	7,483
DG 36:2	643,52618	[M+Na]+	11,56
DG 36:3	641,51038	[M+Na]+	6,937
DG 36:3	641,50989	[M+Na]+	11,44
DG 36:4	634,53796	[M+NH4]+	6,394
DG 36:4	639,49622	[M+Na]+	6,414
DG 36:5	632,52386	[M+NH4]+	5,848
DG 38:4	667,5249	[M+Na]+	7,401
DG 38:4	667,51947	[M+Na]+	7,021
DG 38:6	658,53748	[M+NH4]+	6,266
DG 40:3	673,57617	[M-H]-	7,829
DG 44:11	737,52808	[M+Na]+	6,544
DG 46:10	767,57635	[M+Na]+	6,995
DG 48:13	789,52203	[M+Na]+	4,252
DG 48:9	797,59009	[M+Na]+	5,361
DG 49:6	817,65222	[M+Na]+	6,851
DG 51:12	833,62756	[M+Na]+	6,984
DG 51:14	829,56232	[M+Na]+	5,994
DG 52:7	857,7002	[M+Na]+	8,801
DG O-34:4	592,53424	[M+NH4]+	5,571
DG O-34:5	590,51453	[M+NH4]+	11,273
DG O-34:6	588,49988	[M+NH4]+	10,934
DG O-35:4	606,55292	[M+NH4]+	6,861
DG(32:4-OH)	575,43292	[M-H]-	5,245
FA 22:0;(2OH)	355,32047	[M-H]-	4,485
FA 23:0;(2OH)	369,33618	[M-H]-	4,789
FA 24:0;O	383,35184	[M-H]-	5,169
FA 25:0;O	397,36514	[M-H]-	5,549
FA 26:0;(2OH)	411,38486	[M-H]-	5,929
LDGTS 20:0	530,44135	[M+H]+	3,081

LPE 20:5	500,2767	[M+H]+	5,977
MG O-21:1;O	399,3486	[M-H]-	4,333
MG O-22:1;O	413,36176	[M-H]-	4,637
MG O-23:1;O	427,37604	[M-H]-	4,941
MG(18:0)	341,3064	[M-H2O+H]+	7,492
PC 32:1	732,55273	[M+H]+	5,35
PC 32:2	730,53851	[M+H]+	4,866
PC 32:3	728,52313	[M+H]+	5,442
PC 33:1	746,56342	[M+H]+	6,241
PC 33:1	746,57013	[M+H]+	5,661
PC 34:1	760,58392	[M+H]+	5,996
PC 34:3	756,55334	[M+H]+	5,912
PC 35:1	774,60309	[M+H]+	6,34
PC 35:2	772,58685	[M+H]+	5,781
PC 35:2	772,57922	[M+H]+	6,881
PC 35:3	770,57068	[M+H]+	5,302
PC 35:4	768,55402	[M+H]+	4,797
PC 35:4	768,55011	[M+H]+	6,857
PC 35:5	766,53839	[M+H]+	6,232
PC 36:1	788,61859	[M+H]+	6,733
PC 36:2	786,60095	[M+H]+	6,11
PC 36:3	784,58643	[M+H]+	5,57
PC 36:4	782,56946	[M+H]+	5,082
PC 36:4	782,56732	[M+H]+	5,997
PC 36:5	780,5564	[M+H]+	4,63
PC 37:2	800,61938	[M+H]+	6,409
PC 37:2	800,61139	[M+H]+	5,861
PC 37:3	798,59338	[M+H]+	5,365
PC 37:5	794,56891	[M+H]+	5,793
PC 38:1	816,64508	[M+H]+	6,862
PC 38:1	816,64337	[M+H]+	7,427
PC 38:2	814,63159	[M+H]+	6,785
PC 38:3	812,60516	[M+H]+	6,781
PC 38:3	812,60455	[M+H]+	6,209
PC 38:3	812,61346	[M+H]+	5,822
PC 38:4	810,59723	[M+H]+	5,685
PC 38:4	810,59686	[M+H]+	6,728
PC 38:5	808,58331	[M+H]+	5,182
PC 38:5	808,58313	[M+H]+	6,112
PC 38:8	802,53497	[M+H]+	4,191
PC 40:2	842,65955	[M+H]+	7,497
PC 40:5	836,60828	[M+H]+	5,789
PC 40:6	834,59802	[M+H]+	5,297
PC 40:7	832,5816	[M+H]+	5,229
PC 40:8	830,56647	[M+H]+	4,781
PC 40:8	830,55762	[M+H]+	3,478
PC 40:9	828,56238	[M+H]+	5,995
PC 40:9	828,55066	[M+H]+	4,401
PC 42:10	854,57208	[M+H]+	6,101
PC O-32:0	720,5791	[M+H]+	6,428
PC O-36:2	772,61841	[M+H]+	6,328
PC O-37:2	786,64587	[M+H]+	6,657
PC O-38:1	802,68219	[M+H]+	7,701
PC O-43:9	856,61389	[M+H]+	6,757
PC O-44:6	876,68567	[M+H]+	6,921
PE 32:1	690,5047	[M+H]+	5,485
PE 33:1	704,51929	[M+H]+	5,793
PE 34:1	718,53442	[M+H]+	6,146
PE 34:2	716,52185	[M+H]+	5,604
PE 35:1	732,55273	[M+H]+	6,45
PE 35:1	730,53717	[M-H]-	6,461
PE 35:2	730,5376	[M+H]+	5,91
PE 36:1	746,5661	[M+H]+	6,857
PE 36:1	744,56635	[M-H]-	6,081
PE 36:1	744,56628	[M-H]-	6,005
PE 36:1	744,55255	[M-H]-	6,157
PE 36:2	744,55304	[M+H]+	6,237
PE 36:3	742,53937	[M+H]+	5,692
PE 36:4	740,52368	[M+H]+	5,221
PE 36:5;O	722,51105	[M-H]-	5,549
PE 37:2	756,55518	[M+H]+	6,537
PE 40:8	788,50568	[M-H]-	3,51
PE 42:8;2O	846,52979	[M-H]-	4,181
PE O-43:3	826,65656	[M+H]+	7,816
PE P-36:3	726,53894	[M-H]-	6,178

PG 34:2	745,50409	[M-H]-	5,017
PS 34:1	760,5144	[M-H]-	5,397
PS 36:2	788,54315	[M+H]+	5,549
SM 34:0;3O	721,5863	[M+H]+	4,818
SM 35:1;2O	717,59027	[M+H]+	5,402
SM 36:1;2O	731,60352	[M+H]+	5,842
SM 36:6;2O	721,53992	[M+H]+	4,961
SM 38:2;2O	757,61664	[M+H]+	5,866
SM 40:1;2O	787,66577	[M+H]+	7,345
SM 40:1;3O	803,65216	[M+H]+	7,041
SM 40:2;2O	785,65314	[M+H]+	6,647
SM 40:7;3O	791,56268	[M-H]-	6,081
TG 41:3;1O	736,60144	[M+NH4]+	6,871
TG 41:5	716,58252	[M+NH4]+	7,266
TG 41:6	714,56012	[M+Na]+	6,761
TG 42:1	738,66364	[M+Na]+	9,565
TG 42:6	728,5777	[M+NH4]+	6,681
TG 43:2	755,61414	[M+Na]+	8,316
TG 43:2;1O	766,66248	[M+NH4]+	7,996
TG 43:3;1O	753,60162	[M+Na]+	7,85
TG 43:3;1O	764,6391	[M+NH4]+	7,476
TG 43:6	742,59796	[M+Na]+	7,281
TG 45:7	768,61212	[M+NH4]+	7,639
TG 46:4	793,62665	[M+Na]+	6,961
TG 46:4	793,6286	[M+Na]+	8,499
TG 46:4;1O	804,66779	[M+NH4]+	8,701
TG 46:6	784,64337	[M+Na]+	8,418
TG 46:7	782,63086	[M+Na]+	7,963
TG 46:9	783,55328	[M+Na]+	7,086
TG 47:6	798,6557	[M+NH4]+	8,701
TG 47:7	796,64221	[M+NH4]+	8,261
TG 48:4	821,66394	[M+Na]+	7,519
TG 48:5	819,65094	[M+Na]+	6,881
TG 48:5	819,64911	[M+Na]+	8,571
TG 48:6	812,67432	[M+Na]+	8,986
TG 48:8	808,64221	[M+Na]+	8,03
TG 48:9	806,62732	[M+NH4]+	7,561
TG 49:2	839,70831	[M+Na]+	10,134
TG 49:2	834,75684	[M+NH4]+	10,866
TG 49:5	833,66449	[M+Na]+	8,813
TG 49:6	826,69153	[M+NH4]+	9,225
TG 49:7	824,67328	[M+NH4]+	8,799
TG 49:8	822,66272	[M+NH4]+	8,298
TG 49:9	820,64307	[M+Na]+	7,826
TG 49:9	825,60052	[M+NH4]+	7,825
TG 50:0	857,7583	[M+Na]+	11,142
TG 50:0;2O	884,7749	[M+NH4]+	11,861
TG 50:2	853,73059	[M+Na]+	10,369
TG 50:3	851,71021	[M+Na]+	8,387
TG 50:4	849,69592	[M+Na]+	9,539
TG 50:5	847,6795	[M+Na]+	7,453
TG 50:5;1O	858,71106	[M+NH4]+	8,628
TG 50:6	845,66272	[M+Na]+	8,654
TG 50:6;1O	856,69965	[M+NH4]+	7,538
TG 50:7	843,64502	[M+Na]+	6,745
TG 50:7;1O	854,68402	[M+NH4]+	7,63
TG 50:8	836,67688	[M+NH4]+	8,566
TG 50:8;1O	852,67334	[M+NH4]+	7,981
TG 50:8;3O	884,64764	[M+NH4]+	6,741
TG 50:9	834,66205	[M+NH4]+	8,121
TG 51:1	864,80127	[M+NH4]+	11,63
TG 51:10	851,61298	[M+Na]+	7,434
TG 51:12	847,58197	[M+Na]+	6,551
TG 51:2	862,78461	[M+NH4]+	11,261
TG 51:3	860,76892	[M+NH4]+	10,922
TG 51:4	858,75549	[M+NH4]+	10,535
TG 51:5	856,74127	[M+NH4]+	9,261
TG 51:6	854,72443	[M+NH4]+	9,715
TG 51:7	852,71094	[M+NH4]+	8,426
TG 51:8	850,67798	[M+NH4]+	8,353
TG 51:8	850,69189	[M+NH4]+	8,822
TG 51:8	850,6983	[M+NH4]+	8,014
TG 51:9	853,63251	[M+Na]+	7,917
TG 52:1	878,81427	[M+NH4]+	11,863
TG 52:11	858,65704	[M+NH4]+	7,981

TG 52:3	874,78491	[M+Na]+	11,123
TG 52:3	879,7453	[M+NH4]+	8,847
TG 52:4	872,77179	[M+NH4]+	10,773
TG 52:5	870,75507	[M+NH4]+	10,37
TG 52:6	873,68915	[M+Na]+	7,537
TG 52:6	868,7406	[M+NH4]+	9,974
TG 52:6;3O	916,71033	[M+NH4]+	7,911
TG 52:7	866,7218	[M+Na]+	9,539
TG 52:7	871,68182	[M+NH4]+	7,235
TG 52:7;1O	882,71393	[M+NH4]+	8,177
TG 52:8	864,70563	[M+NH4]+	9,081
TG 52:9	862,69299	[M+NH4]+	8,657
TG 53:10	879,65112	[M+Na]+	7,934
TG 53:4	886,78345	[M+NH4]+	10,961
TG 53:5	884,76782	[M+NH4]+	10,581
TG 53:6	887,69037	[M+Na]+	8,501
TG 53:6	882,75238	[M+NH4]+	10,19
TG 53:6;2O	914,75116	[M+NH4]+	8,381
TG 53:7	880,73669	[M+NH4]+	9,758
TG 53:8;1O	894,72729	[M+NH4]+	10,021
TG 53:9	876,70544	[M+NH4]+	8,89
TG 53:9	876,71051	[M+NH4]+	8,108
TG 54:11	891,6615	[M+Na]+	7,325
TG 54:2	904,82587	[M+NH4]+	11,875
TG 54:2;2O	936,82404	[M+NH4]+	10,897
TG 54:4	900,80298	[M+NH4]+	11,165
TG 54:5	898,78607	[M+Na]+	10,801
TG 54:5	903,72699	[M+NH4]+	10,434
TG 54:6	896,76892	[M+NH4]+	10,411
TG 54:7	894,75513	[M+NH4]+	10,019
TG 54:7;1O	910,74463	[M+NH4]+	8,668
TG 54:8	892,74109	[M+NH4]+	9,581
TG 54:8;1O	908,73328	[M+NH4]+	8,269
TG 54:9	890,72235	[M+NH4]+	9,161
TG 55:10	907,67871	[M+Na]+	8,361
TG 55:14	899,61859	[M+Na]+	7,313
TG 55:3	921,76276	[M+Na]+	10,045
TG 55:3	921,77423	[M+Na]+	11,696
TG 55:5	912,79614	[M+Na]+	10,982
TG 55:6	910,78308	[M+Na]+	10,623
TG 55:6	915,74115	[M+NH4]+	10,621
TG 55:7	908,76233	[M+Na]+	10,222
TG 55:7	913,72089	[M+NH4]+	10,212
TG 56:11	919,65558	[M+Na]+	7,244
TG 56:3	930,84424	[M+NH4]+	11,938
TG 56:4	928,83783	[M+NH4]+	11,591
TG 56:7	922,78119	[M+Na]+	10,486
TG 56:7	927,74072	[M+NH4]+	10,519
TG 57:11	933,69464	[M+Na]+	8,381
TG 57:4	942,84229	[M+NH4]+	11,841
TG 58:2	960,89197	[M+Na]+	12,22
TG 58:2	965,8465	[M+NH4]+	12,208
TG 58:3	958,87274	[M+NH4]+	12,135
TG 59:3	977,84314	[M+Na]+	12,18
TG 60:2	988,92114	[M+NH4]+	12,287
TG 60:2;1O	1004,91003	[M+NH4]+	12,314
TG 60:3	986,9126	[M+NH4]+	12,223
TG 60:4	984,89288	[M+NH4]+	12,146
TG 60:5	982,8739	[M+NH4]+	12,004
TG 61:0;2O	1038,93445	[M+NH4]+	12,236
TG 61:4	998,90247	[M+NH4]+	12,2
TG 61:5	996,8963	[M+NH4]+	12,084
TG 62:3	1014,94165	[M+NH4]+	12,301
TG 62:4	1012,92407	[M+NH4]+	12,236
TG 62:5	1010,90961	[M+Na]+	12,148
TG 62:5	1015,85822	[M+NH4]+	12,144
TG 62:6	1013,85052	[M+Na]+	12,03
TG 62:7	1006,87286	[M+NH4]+	11,788
TG O-33:0	605,51196	[M+Na]+	6,681
TG O-38:2	671,55701	[M+Na]+	6,221
TG O-48:6	803,64069	[M+Na]+	6,501
TG O-50:6	831,67877	[M+Na]+	7,456
TG O-50:6	831,68317	[M+Na]+	8,741
TG O-50:7	829,67133	[M+Na]+	8,267
TG O-51:10	832,69843	[M+NH4]+	8,579

	TG O-51:13	831,60938	[M+Na]+	6,539
	TG O-52:5	861,74182	[M+Na]+	9,041
	TG O-52:9	853,67035	[M+Na]+	6,541
	TG O-53:13	859,6369	[M+Na]+	7,657
	TG O-53:14	857,62488	[M+Na]+	7,217
	TG O-53:8	864,73737	[M+NH4]+	9,081
	TG O-54:12	875,67499	[M+Na]+	6,913
	TG O-54:13	873,65692	[M+Na]+	6,477
	TG O-54:5	889,76428	[M+Na]+	9,481
	TG O-54:9	881,69238	[M+Na]+	8,334
	TG O-55:11	886,74408	[M+NH4]+	7,976
	TG O-55:11	891,69849	[M+Na]+	8,361
	TG O-55:13	887,66888	[M+Na]+	7,427
	TG O-55:13	887,66895	[M+Na]+	7,645
	TG O-55:14	885,65381	[M+Na]+	7,07
	TG O-55:14	885,65393	[M+Na]+	7,752
	TG O-55:7	899,74371	[M+Na]+	11,846
	TG O-56:9	909,72296	[M+Na]+	8,249
	TG O-57:12	917,7243	[M+Na]+	8,381
	TG O-57:13	915,69598	[M+Na]+	7,937
	TG O-57:14	913,68347	[M+Na]+	7,519
	TG O-57:15	911,66724	[M+Na]+	7,231
	TG O-58:11	933,72125	[M+Na]+	7,147
	TG O-58:12	931,71387	[M+Na]+	10,616
	TG O-58:7	941,79071	[M+Na]+	11,426
	TG O-58:9	937,75769	[M+Na]+	8,027
	TG O-59:13	943,73132	[M+Na]+	7,641
	TG O-62:14	983,72705	[M+Na]+	7,534
Cluster 2	Cer 33:6;2O	536,40417	[M+Na]+	2,818
	Cer 34:4;3O	548,47083	[M+H]+	9,841
	Cer 34:6;3O_1	544,44055	[M+H]+	9,881
	Cer 34:6;3O_2	544,44653	[M+H]+	8,491
	Cer 35:2;3O	566,51642	[M+H]+	12,134
	Cer 40:4;3O	614,5592	[M+H-H2O]+	11,56
	Cer 50:7;4O	764,65869	[M+H-H2O]+	9,221
	Cer 54:11;4O	812,65259	[M+H-H2O]+	7,961
	DG 32:3	585,4458	[M+Na]+	10,462
	DG 34:3	613,47711	[M+Na]+	10,862
	DG 36:3	641,51099	[M+Na]+	11,24
	DG 39:0	689,60315	[M+Na]+	12,28
	DG 39:8	673,48157	[M+Na]+	7,309
	DG 41:9	699,49084	[M+Na]+	7,381
	DG 43:11	723,49164	[M+Na]+	7,014
	DG 43:9	727,52753	[M+Na]+	8,001
	DG 45:12	749,50977	[M+Na]+	7,093
	DG 47:12	777,54187	[M+Na]+	7,707
	DG 49:12	805,57275	[M+Na]+	8,383
	DG 52:0	871,80109	[M+Na]+	11,541
	DG 52:4	863,73358	[M+Na]+	11,14
	PC 35:5	766,53375	[M+H]+	4,741
	PC 38:3	812,61475	[M+H]+	5,221
	PC O-38:3	798,63593	[M+H]+	6,433
	PC O-38:4	796,62	[M+H]+	5,922
	PC O-38:9	786,54248	[M+H]+	5,121
	PC O-40:6	820,6134	[M+H]+	6,445
	PC O-40:7	818,60168	[M+H]+	5,906
	PE 22:2	548,33105	[M+H]+	7,096
	PE 33:2	702,50513	[M+H]+	5,284
	PI 32:1	807,50439	[M-H]-	4,713
	PI 32:2	805,48804	[M-H]-	4,333
	PI 32:3	803,47003	[M-H]-	4,029
	PI 33:3	817,48987	[M-H]-	4,257
	PI 34:3	831,50653	[M-H]-	4,409
	PS 34:2	758,50177	[M-H]-	4,941
	PS 34:3	756,48572	[M+H]+	4,561
	SM(d16:1/20:3-2OH(5,6))	755,53125	[M-H]-	5,549
	TG 36:1	654,56793	[M+NH4]+	7,877
	TG 39:3	692,58142	[M+NH4]+	7,691
	TG 40:0	717,59613	[M+Na]+	8,621
	TG 40:1	710,63092	[M+NH4]+	8,986
	TG 40:2	708,61151	[M+NH4]+	8,519
	TG 40:3	711,55322	[M+Na]+	8,006
	TG 41:4	718,59808	[M+NH4]+	7,801
	TG 41:4	723,55206	[M+Na]+	7,772
	TG 42:1	743,61548	[M+NH4]+	8,695

	TG 42:5	735,54877	[M+Na]+	7,623
	TG 44:2	769,63043	[M+Na]+	9,705
	TG 44:3;2O	794,65717	[M+NH4]+	9,321
	TG 44:4	765,60028	[M+Na]+	8,799
	TG 44:5	763,58759	[M+Na]+	8,266
	TG 45:6	770,63165	[M+NH4]+	8,871
	TG 46:2	792,70752	[M+NH4]+	10,19
	TG 46:3	790,69171	[M+NH4]+	9,782
	TG 46:4	788,6759	[M+NH4]+	9,325
	TG 46:5	791,61633	[M+Na]+	8,854
	TG 46:6	789,59821	[M+NH4]+	8,393
	TG 48:1	827,71106	[M+Na]+	10,327
	TG 48:2	825,69592	[M+Na]+	9,906
	TG 48:4	821,66229	[M+Na]+	9,821
	TG 48:5	814,69257	[M+NH4]+	9,413
	TG 48:5	819,64764	[M+Na]+	9,381
	TG 50:3	851,70837	[M+Na]+	10,701
	TG 50:3	846,75409	[M+NH4]+	10,733
	TG 50:4	844,73743	[M+NH4]+	10,322
	TG 50:5	847,6792	[M+Na]+	9,881
	TG 50:6	840,70648	[M+NH4]+	9,498
	TG 50:7	838,69177	[M+NH4]+	9,023
	TG 54:4;1O	916,78003	[M+NH4]+	11,21
	TG O-50:8	827,65649	[M+Na]+	7,091
	TG O-54:3	893,78809	[M+Na]+	11,198
	TG O-55:9	895,71204	[M+Na]+	11,129
	TG O-56:12	903,70105	[M+Na]+	9,301
	TG O-56:7	913,76373	[M+Na]+	10,881
Cluster 3	DG 38:7	661,50067	[M+Na]+	3,228
	DG 49:10	809,60999	[M+Na]+	9,324
	DG 50:9	825,63953	[M+Na]+	10,114
	DG 51:8	841,66656	[M+Na]+	10,641
	DG 51:9	839,65216	[M+Na]+	10,241
	PC 30:0	706,53638	[M+H]+	5,241
	PC 38:6	828,55115	[M+Na]+	4,782
	PC 38:7	826,53461	[M+Na]+	4,534
	PC O-40:5	822,62854	[M+H]+	6,3
	PE 44:4;O	866,63086	[M+H]+	6,309
	TG 27:0	535,40454	[M+Na]+	1,259
	TG 46:3	795,6524	[M+Na]+	9,773
	TG 47:4	807,64508	[M+Na]+	9,675
	TG 47:5	805,6286	[M+Na]+	9,19
	TG 48:3	823,67615	[M+Na]+	10,242
	TG 48:6	817,63104	[M+NH4]+	8,939
	TG 56:13	915,63257	[M+Na]+	6,309
	TG O-49:11	807,58942	[M+Na]+	8,854
	TG O-49:8	813,62921	[M+Na]+	9,781
	TG O-49:9	811,62469	[M+Na]+	9,779
	TG O-51:11	835,61694	[M+Na]+	9,381
	TG O-51:7	843,68127	[M+Na]+	11,036
	TG O-53:13	859,62189	[M+Na]+	8,997
	TG O-53:8	869,6958	[M+Na]+	11,079
	TG O-53:9	867,68433	[M+Na]+	10,699
	TG O-57:14	913,66858	[M+Na]+	9,599

Table S6.3. The 22 hydrophilic phase metabolites that exhibited changes, detailing their names, average mass-to-charge ratios (*m/z*), ionization modes, and retention times (RT).

Metabolite name	Average (*m/z*)	Adduct type	Average Rt(min)
Chrysin	253,05516	[M-H]-	12,304
D-Gluconic acid	195,04739	[M-H]-	12,688
gamma-Glutamyltyrosine	309,10214	[M-H]-	12,15
gamma-Glutamylleucine	259,12372	[M-H]-	11,209
Cysteic Acid	167,9921	[M-H]-	12,604
5,6-Dihydro-5-methyluracil	129,06374	[M+H]+	11,881
L-Carnosine	227,11349	[M+H]+	13,902
1-Methyladenosine	282,11765	[M+H]+	3,64
Guanine	152,05542	[M+H]+	11,752
L-Leucine	132,10094	[M+H]+	9,509
maltotriose	527,1568	[M+Na]+	15,093
Lysine	147,11023	[M+H]+	14,805
Glutamine	147,07611	[M+H]+	11,901
NEPSILON	189,15799	[M+H]+	13,212
Propionic acid	97,02904	[M+Na]+	13,824
L-KYNURENINE	209,09077	[M+H]+	14,895
delta-Hydroxylysine	163,10614	[M+H]+	14,523
Indole-3-carboxylic acid	162,05324	[M+H]+	2,919
Theobromine	203,05052	[M+Na]+	10,466
Hypoxanthine	137,04375	[M+H]+	12,77
Cytosine	112,05067	[M+H]+	14,925
Propionylcarnitine	218,13568	[M+H]+	1,961

Supplementary Bibliography

1. Cui, F.; Chai, T.; Qian, L., Wang, C. Effects of three diamides (chlorantraniliprole, cyantraniliprole and flubendiamide) on life history, embryonic development and oxidative stress biomarkers of Daphnia magna. *Chemosphere* **2017**, 169, 107-116. doi:10.1016/j.chemosphere.2016.11.073.
2. Kato, Y.; Kobayashi, K.; Oda, S.; Tatarazako, N.; Watanabe, H., Iguchi, T. Cloning and characterization of the ecdysone receptor and ultraspiracle protein from the water flea Daphnia magna. *J. Endocrinol.* **2007**, 193, 183-194. doi:10.1677/joe-06-0228.
3. Jordão, R.; Campos, B.; Piña, B.; Tauler, R.; Soares, A.M.V.M., Barata, C. Mechanisms of Action of Compounds That Enhance Storage Lipid Accumulation in Daphnia magna. *Environ. Sci. Technol.* **2016**, 50, 13565-13573. doi:10.1021/acs.est.6b04768.
4. Heckmann, L.H.; Sibly, R.M.; Connon, R.; Hooper, H.L.; Hutchinson, T.H.; Maund, S.J.; Hill, C.J.; Bouetard, A., Callaghan, A. Systems biology meets stress ecology: linking molecular and organismal stress responses in Daphnia magna. *Genome Biol.* **2008**, 9, R40. doi:10.1186/gb-2008-9-2-r40.
5. Poynton, H.C.; Loguinov, A.V.; Varshavsky, J.R.; Chan, S.; Perkins, E.J., Vulpe, C.D. Gene Expression Profiling in Daphnia magna Part I: Concentration-Dependent Profiles Provide Support for the No Observed Transcriptional Effect Level. *Environ. Sci. Technol.* **2008**, 42, 6250-6256. doi:10.1021/es8010783.
6. Talu, M.; Seyoum, A.; Yitayew, B.; AdaneMihret; Aseffa, A.; Jass, J.; Mamo, G., Olsson, P.E. Transcriptional responses of Daphnia magna exposed to Akaki river water. *Environ. Monit. Assess.* **2022**, 194, 349. doi:10.1007/s10661-022-09973-y.
7. Seyoum, A.; Pradhan, A.; Jass, J., Olsson, P.E. Perfluorinated alkyl substances impede growth, reproduction, lipid metabolism and lifespan in Daphnia magna. *Sci. Total Environ.* **2020**, 737, 139682. doi:10.1016/j.scitotenv.2020.139682.
8. Hannas, B.R.; Wang, Y.H.; Thomson, S.; Kwon, G.; Li, H., Leblanc, G.A. Regulation and dysregulation

of vitellogenin mRNA accumulation in daphnids (Daphnia magna). *Aquat. Toxicol.* **2011**, 101, 351-357. doi:10.1016/j.aquatox.2010.11.006.

9. Domínguez, G.A.; Torelli, M.D.; Buchman, J.T.; Haynes, C.L.; Hamers, R.J., Klaper, R.D. Size dependent oxidative stress response of the gut of Daphnia magna to functionalized nanodiamond particles. *Environ. Res.* **2018**, 167, 267-275. doi:10.1016/j.envres.2018.07.024.

Chapter 7. Conclusion

This thesis, titled *Development of Adverse Outcome Pathway for Toxicity Assessment of Environmental Endocrine Disruptors*, presents a comprehensive investigation into the impacts of SRD5A inhibitors on reproduction-related systems across multiple biological models. By utilizing advanced analytical techniques, integrating diverse *in vitro* models, this research addresses critical gaps in understanding the mechanisms and environmental implications of SRD5A inhibition. The findings offer significant insights into the MIEs, KEs, and AOs associated with SRD5A inhibition, thereby contributing to the development of quantitative and broadly applicable AOPs for chemical risk assessment.

The research underscores the pivotal role of SRD5A in the reproductive system and highlights the systemic disruptions caused by its inhibition. Chapter 3 describes the development of a sensitive LC-MS/MS-based method to measure SRD5A activity and evaluate inhibitor potency across human and fish cell lines. Quantitative, dose-dependent data revealed species-specific differences in SRD5A activity and its inhibition by finasteride and dutasteride, establishing a mechanistic link between SRD5A inhibition (MIE) and reduced DHT levels (KE). Building on this understanding, Chapter 4 investigated the downstream effects of SRD5A inhibition in zebrafish embryos. Dutasteride exposure significantly decreased DHT, E2, and VTG levels, with molecular docking analyses suggesting that these effects occurred independently of direct androgen or estrogen receptor interactions. A strong correlation among DHT, E2, and VTG levels supported the hypothesis that DHT plays a critical role in estrogenic signaling, potentially through alternative biosynthetic pathways. These findings provide essential data for linking upstream and downstream KEs within the AOP framework.

Chapter 5 advanced the mechanistic understanding of steroidogenic disruptions by profiling 14 steroid hormones in H295R cells using GC-MS/MS. This extended profiling addressed limitations of existing assays, such as OECD TG 456, which primarily focus on T and E2). The results highlighted nuanced disruptions in progestins, mineralocorticoids, glucocorticoids, androgens, and estrogens, emphasizing the systemic impacts of SRD5A inhibition. While the findings did not directly confirm alternative androgen pathways, such as backdoor pathways, their potential involvement may be suggested in response to reduced DHT levels. The application of product-to-substrate ratios, such as the E2/T ratio, revealed disruptions within steroidogenic pathways and highlighted their interconnected nature. These findings contribute to the development of qAOPs, integrating dose-response relationships and thresholds for chemical risk assessment.

Chapter 6 expanded the scope to invertebrates, specifically D. magna, to investigate the environmental implications of SRD5A inhibitors in non-vertebrate species. The potential presence of an SRD5A-like enzyme in D. magna suggests it may play a role in ecdysteroidogenesis, a process critical for regulating reproduction and development. Chronic exposure to finasteride resulted in significant reproductive impairments, including reduced fecundity, delayed brood timing, and smaller offspring size, along with disruptions in metabolic and lipid pathways. Transcriptional analyses revealed the downregulation of

genes associated with ecdysteroid signaling and oxidative stress responses, highlighting the endocrine-disrupting potential of finasteride in aquatic ecosystems. These findings underscore the environmental risks posed by SRD5A inhibitors and the importance of cross-species evaluations to inform regulatory toxicology and ecosystem protection.

Collectively, this thesis advances the AOP framework as a predictive tool for assessing the impacts of endocrine disruptors by bridging molecular, physiological, and environmental scales. The integration of quantitative data across multiple models enhances the applicability of AOPs to diverse species and ecosystems, facilitating the development of targeted and efficient testing strategies. This work provides robust scientific evidence for developing AOPs related to SRD5A inhibition, offering valuable insights into the risks posed by endocrine disruptors to both human and environmental health. By combining advanced analytical techniques, diverse biological models, and mechanistic frameworks, this thesis addresses emerging challenges in toxicology and regulatory science. As the use of pharmaceuticals like finasteride and dutasteride continues to grow, the findings underscore the urgent need for comprehensive environmental assessments to safeguard biodiversity and promote sustainable chemical management practices.

Chapter 8. Appendix

8.1 Original paper − Screening of SRD5A activity and inhibition

molecules

MDPI

Article

Development of a Liquid Chromatography/Mass Spectrometry-Based Inhibition Assay for the Screening of Steroid 5-α Reductase in Human and Fish Cell Lines

Dahye Kim [1,†], Hyunki Cho [1,†], Ruth Eggers [1], Sang Kyum Kim [2], Chang Seon Ryu [1,*] and Young Jun Kim [1,3]

[1] Environmental Safety Group, Korea Institute of Science and Technology (KIST) Europe Forschungsgesellschaft mbH, 66123 Saarbruecken, Germany; da-hye.kim@daum.net (D.K.); hyunki.cho@kist-europe.de (H.C.); rutheggers@gmx.de (R.E.); youngjunkim@kist-europe.de (Y.J.K.)
[2] College of Pharmacy, Chungnam National University, Daejeon 34134, Korea; sangkim@cnu.ac.kr
[3] Division of Energy & Environment Technology, University of Science and Technology, Daejeon 34113, Korea
* Correspondence: changryu@kist-europe.de; Tel.: +49-681-8382-410; Fax: +49-681-9382-109
† These authors equally contributed to this work.

Abstract: Steroid 5-α reductase (5AR) is responsible for the reduction of steroids to 5-α reduced metabolites, such as the reduction of testosterone to 5-α dihydrotestosterone (DHT). A new adverse outcome pathway (AOP) for 5AR inhibition to reduce female reproduction in fish (AOP 289) is under development to clarify the antiestrogenic effects of 5AR inhibitors in female fish. A sensitive method for the DHT analysis using chemical derivatization and liquid chromatography–tandem mass spectrometry was developed. A cell-based 5AR inhibition assay that utilizes human cell lines, a transient overexpression system, and fish cell lines was developed. The measured IC_{50} values of two well-known 5AR inhibitors, finasteride and dutasteride, were comparable in the different systems. However, the IC_{50} of dutasteride in the fish cell lines was lower than that in the human cell lines. Finasteride showed a higher IC_{50} against the RTG-2 cell line. These results demonstrated that 5ARs inhibition could differ in terms of structural characteristics among species. The assay has high sensitivity and reproducibility and is suitable for the application in 5AR inhibition screening for various endocrine disruption chemicals (EDCs). Future studies will continue to evaluate the quantitative inhibition of 5AR by EDCs to compare the endocrine-disrupting pathway in different species.

Keywords: 5α-reductase inhibitors; dihydrotestosterone; in vitro; dutasteride; finasteride; adverse outcome pathway

check for updates

Citation: Kim, D.; Cho, H.; Eggers, R.; Kim, S.K.; Ryu, C.S.; Kim, Y.J. Development of a Liquid Chromatography/Mass Spectrometry-Based Inhibition Assay for the Screening of Steroid 5-α Reductase in Human and Fish Cell Lines. *Molecules* **2021**, *26*, 893. https://doi.org/10.3390/molecules26040893

Academic Editor: Jorge A. R. Salvador
Received: 11 December 2020
Accepted: 4 February 2021
Published: 8 February 2021

1. Introduction

Steroid 5-α reductase (5AR, EC. 1.3.99.5) is a membrane-bound protein that is responsible for reducing steroids such as testosterone, progesterone, and androstenedione to 5-α reduced metabolites such as 5-α dihydrotestosterone (DHT), 5-α dihydroprogesterone and androstanedione, respectively. There are three isoforms of 5AR in humans: SRD5A1, SRD5A2, and SRD5A3. SRD5A1 and SRD5A2 have functionality for 5-α reduction of steroids in humans. DHT is a more potent androgen than testosterone and has a function in androgen receptor activation [1–3]. The regulation of 5AR is important for the treatment of benign prostate hyperplasia (BPH) and prostate cancer (PC), and 5AR inhibitors have also been used for the treatment of baldness [4–6].

5AR inhibition was suggested as a new molecular initiating event (MIE) in the adverse outcome pathway (AOP) 289 [7]. AOP 289, which is entitled 'Inhibition of 5α-reductase leading to impaired fecundity in female fish', describes the effects of 5AR on reducing estradiol and further decreasing egg production via vitellogenin reduction. 5AR is expressed in both sexes, and DHT is involved in estradiol (E2) level regulation [8]. Even though a lower expression of 5AR was detected in females, its inhibition reduced the fecundity of fish and affected several aspects of reproductive endocrine functions in both sexes of

fathead minnows [9]. For the development of a quantitative AOP for 5AR inhibition, a quantitative structure–activity relationship is required for endocrine disruption chemical (EDC) evaluation. Several methods have been described for screening the pharmacological aspects of 5AR inhibitors, but experimental data are limited in fishes for screening for endocrine disruption.

In practice, 5AR inhibition studies are traditionally conducted using radioactive substrates with thin layer chromatography or high-performance liquid chromatography (HPLC) detection [10,11]. A native substrate method without radiolabeled isotopes that utilizes a spectrophotometric method [12] and a HPLC-UV detection method was also developed [13]. However, these methods have not been extensively applied due to their limitations, which include safety issues with radiometric assays and low sensitivity. The liquid chromatography-tandem mass spectrometry (LC-MS/MS) method can be used for high-throughput screening (HTS) techniques, and combinational chemistry during drug discovery and development has led to a tremendous increase in the number of compounds to be evaluated for potential 5AR inhibition [14,15]. Recently, sensitive chemical derivatization methods for DHT detection in LC-MS/MS were developed [16].

In the present study, using this chemical derivatization technique, a cell incubation method was developed, and the metabolites of the substrates were determined in a single assay using LC-MS/MS for HTS of 5AR inhibition. LNCaP clone FGC (LNCaP) and DU-145 cells that express the SRD5A1 gene, SW-13 cells that express the SRD5A1 and SRD5A2 genes, and HEK-293 cells with transient overexpression of the SRD5A1 and SRD5A2 genes were compared to establish the enzyme inhibition method. In addition, to understand species differences in 5AR between fish and humans, the inhibition of 5AR was compared in the 5AR-expressing zebrafish liver cells (ZFL) and rainbow trout gonad cell lines (RTG-2).

2. Results

2.1. Method Validation

2.1.1. Linearity of the Calibration Curve and LLOQ

The 1/x weighted linear regression calibration curve for DHT was obtained by plotting the MRM peak area ratio (analyte/IS) versus the concentration over the working range 0.01–1000 nM for the assay media. The 1/x weighted linear correlation coefficient (R2) for DHT exceeded 0.995. The LLOQ of this method for DHT was 0.05 nM. Chromatograms of 2-picolinic acid (PA)-derivatized DHT and DHT-d3 are presented in Figure 1.

2.1.2. Accuracy and Precision

The method accuracy and precision that were determined using the low QC, medium QC and high QC samples are presented in Table 1. The inter day accuracies for the low, medium, and high QC samples were 102.3, 104.0, and 95.0%, respectively, and the intraday accuracies for the low, medium, and high QC samples were 101, 98.9, and 95.5%, respectively. The interday precisions were 1.3% for low QC, 0.7% for medium QC, and 1.6% for high QC, and the intraday precisions were 0.9% for low QC, 2.5% for medium QC, and 1.3% for high QC. Acceptable method accuracies and precisions on the QC samples were obtained.

Table 1. Method accuracy and precision (n = 5).

	Low QC	Medium QC	High QC
CV%—inter day [a]	1.3	0.7	1.6
CV%—intra day [b]	0.9	2.5	1.3
Accuracy%—inter day	102.3	104.0	95.0
Accuracy%—intra day	101.0	98.9	95.5

[a] Coefficient of variation within days; [b] Coefficient of variation between 3 consecutive days.

Molecules **2021**, *26*, 893

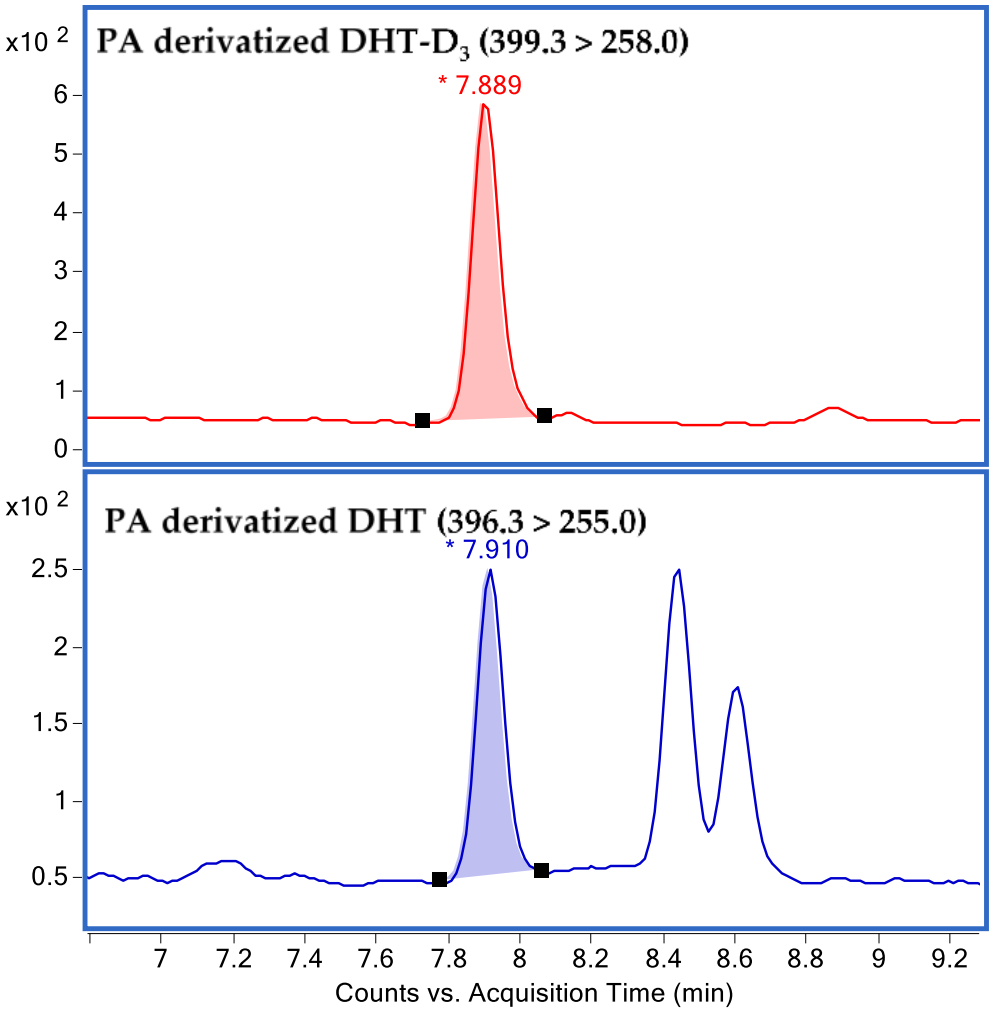

Figure 1. Chromatograms of 2-picolinic acid (PA)-derivatized 5-α dihydrotestosterone (DHT) and DHT-D3.

2.2. Assay Application in Human Cell Lines

The gene expression levels of SRD5A1 and SRD5A2 in LNCaP, DU-145, and SW-13 cells are presented in Figure 2. All cell lines showed SRD5A1 expression, but SRD5A2 expression was identified only for SW-13 cells. For the calculation of K_M, testosterone treatment was applied in increments of 0 to 10 μM in the LNCaP and DU-145 cells and in increments of 0 to 50 μM in the SW-13 cells for 3 h. The de novo synthesized DHT levels were measured (Figure 3a). The calculated values of K_M and V_{max} are presented in Table 2. The V_{max} value of the DU-145 cells was 75.55 nmol/L/h, which exceeded those of the other two cell lines. Based on the calculated K_M value as the substrate concentration, inhibition assays were conducted by treating the cells with a selective SRD5A2 inhibitor, namely, finasteride, and a dual SRD5A1 and SRD5A2 inhibitor, namely, dutasteride (Figure 3b). The IC_{50} value of each inhibitor was calculated and is presented in Table 3.

2.3. Assay Application in SRD5A2-Overexpressing HEK-293 Cells

For the calculation of K_M, testosterone was added in increments of 0 to 50 μM to non-vector- and SRD5A1-HEK293 cells and in increments of 0 to 10 μM to SRD5A2-HEK293 cells 24 h after transfection. The DHT levels were measured (Figure 4a). The calculated K_M and V_{max} values are presented in Table 2. SRD5A2 showed a higher production rate (V_{max} and K_M were 22.52 and 0.36 nM, respectively) due to the higher affinity of the enzyme

for testosterone. Based on the calculated K_M values, inhibition assays were conducted by treating the cells with selective SRD5A2 inhibitor finasteride and the dual SRD5A1 and SRD5A2 inhibitor dutasteride (Figure 4b). The IC_{50} values were calculated (Table 3).

Table 2. V_{max} and K_M value for testosterone in each cell line.

		V_{max} (nmol L^{-1} h^{-1})	K_M (nM)
Human cell lines	LNCaP	38.67 (34.36–45.16) *	15.10 (12.35–19.25)
	DU-145	75.55 (66.61–90.45)	9.15 (7.01–12.81)
	SW-13	29.35 (27.94–30.90)	19.42 (17.31–21.88)
Overexpression lines	Non vector	4.473 (4.29–4.66)	7.56 (6.74–8.46)
	SRD5A1	8.584 (7.86–9.35)	2.29 (1.70–3.09)
	SRD5A2	22.52 (20.01–25.42)	0.36 (0.18–0.65)
Fish cell lines	ZFL	116.60 (106.9–126.9)	0.46 (0.30–0.68)
	RTG-2	13.09 (11.88–14.37)	1.12 (0.78–1.61)

* The values in parentheses are 95% confidence intervals.

Table 3. IC_{50} values of finasteride and dutasteride in each cell line.

		IC_{50} Value	
		Finasteride (nM; 95% CI *)	Dutasteride (nM; 95% CI)
Human cell lines	LNCaP	241.0 (185.8–303.9)	1.26 (1.02–1.57)
	DU-145	308.5 (217.0–415.5)	3.83 (3.10–4.78)
	SW-13	213.5 (180.2–250.7)	4.75 (4.26–5.32)
Overexpression lines	SRD5A1	332.8 (260.9–424.8)	1.27 (0.76–2.06)
	SRD5A2	69.83 (33.65–133.3)	1.19 (0.96–1.47)
Fish cell lines	ZFL	142.4 (121.5–165.7)	7.33 (6.12–8.77)
	RTG-2	2667 (2394–2952)	13.19 (10.73–16.54)

* The values in parentheses are 95% confidence intervals.

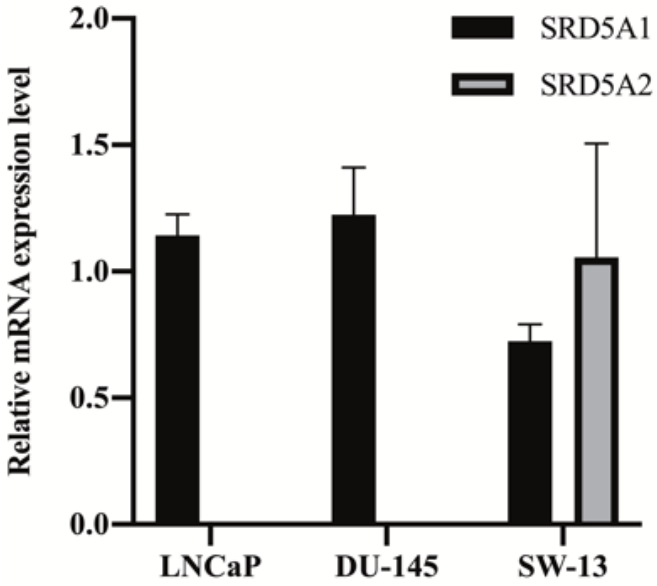

Figure 2. Quantitative PCR analysis for measuring the mRNA expression levels of SRD5A1 and SRD5A2 in the LNCaP, DU-145, and SW-13 cell lines. The data are expressed as the mean ± standard deviation (SD) of three repeated experiments.

Molecules **2021**, *26*, 893

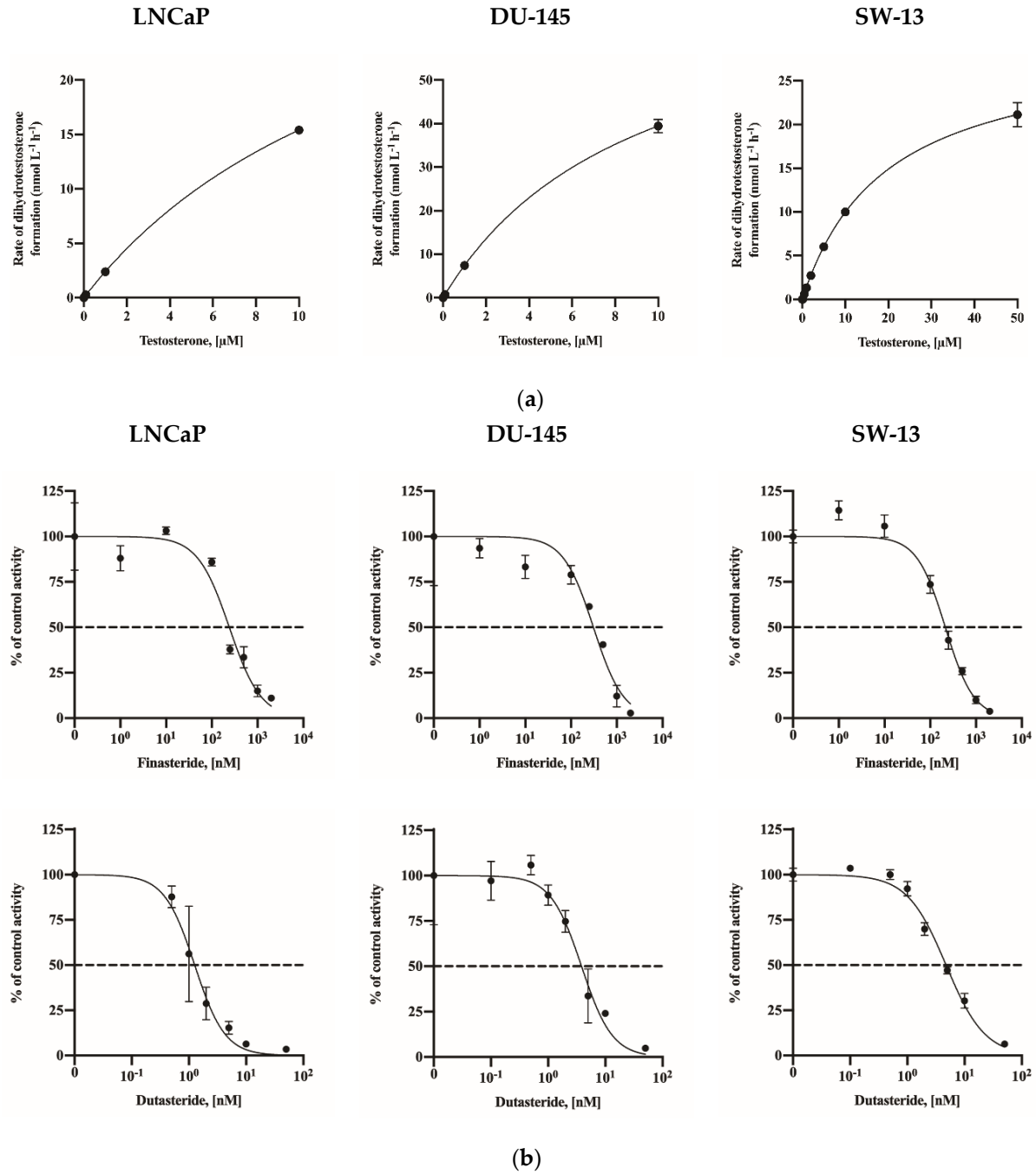

Figure 3. Activity of 5α-reductase (**a**) and inhibitory effects of finasteride and dutasteride (**b**) on LNCaP, DU-145, and SW-13 cells. The data are expressed as the mean ± standard deviation (SD) of three repeated experiments.

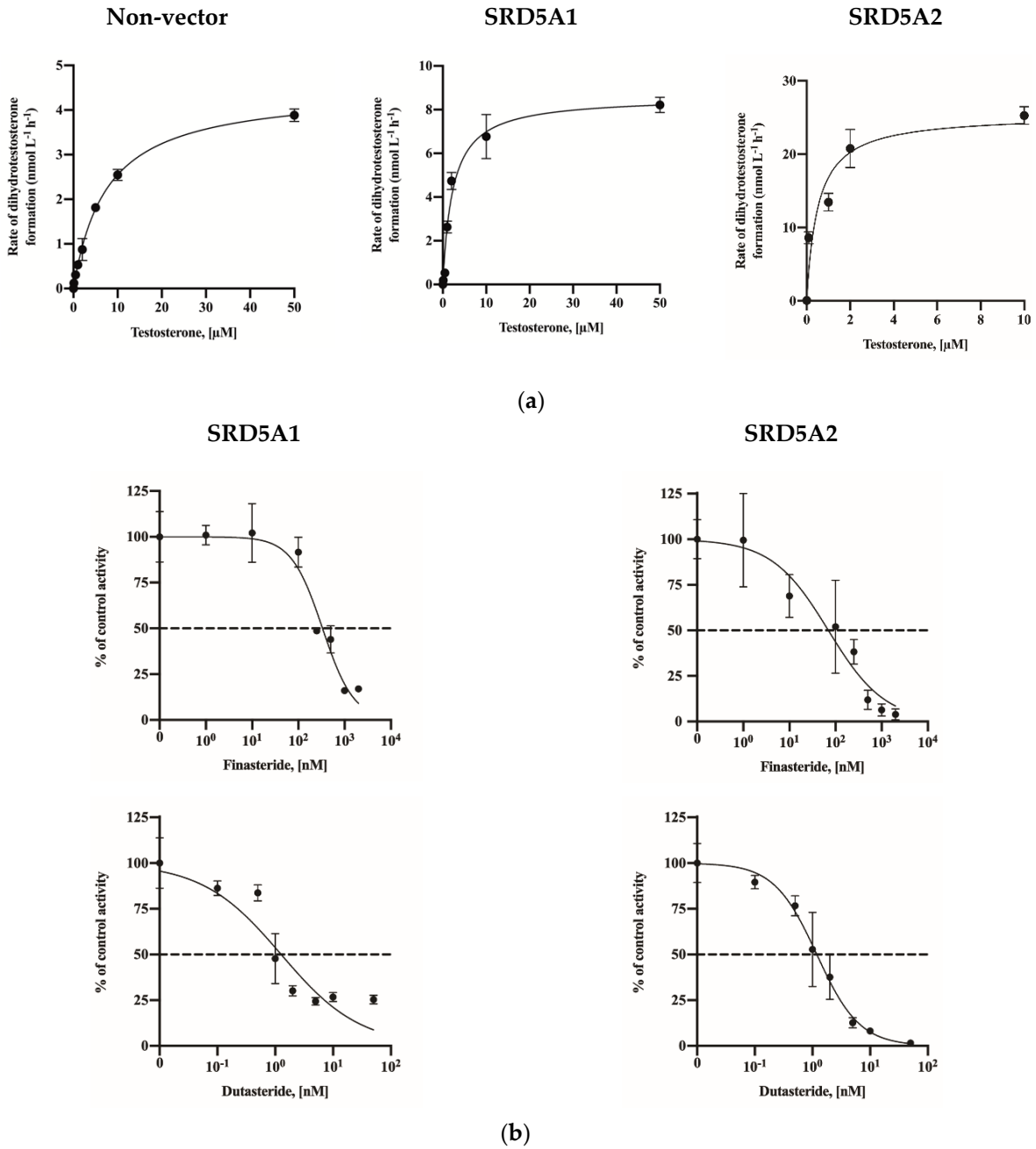

Figure 4. Activity of 5α-reductase (**a**) and inhibitory effects of finasteride and dutasteride (**b**) on transfected HEK-293 cells. The data are expressed as the mean ± standard deviation (SD) of three repeated experiments.

2.4. Assay Application in a Fish Cell Line

For the calculation of K_M for optimized assay conditions, ZFL and RTG-2 cells were treated with testosterone in increments of 0 to 50 µM. The DHT levels were measured (Figure 5a). The calculated K_M and V_{max} values are presented in Table 2. Based on the calculated K_M values, inhibition assays were conducted (Figure 5b). Both the RTG-2 and ZFL cells showed lower K_M values than human cell lines. The V_{max} value of the ZFL cells (116.6 nmol/L/h) substantially exceeded those of the 5AR-overexpressing cell line and the human cell lines (29.35 in LNCaP, 75.55 in DU-145, and 29.35 in SW-13). The

Molecules **2021**, *26*, 893

IC_{50} value of finasteride in the RTG-2 cells was 2459 nM, which exceeded those of the 5AR-overexpressing cell line and the human cell lines (1.27 in SRD5A1 and 1.16 in SRDA2-overexpressing HEK cells). Furthermore, the IC_{50} values of dutasteride in both fish cell lines exceeded those of the 5AR-overexpressing cell line and the human cell lines (Table 3).

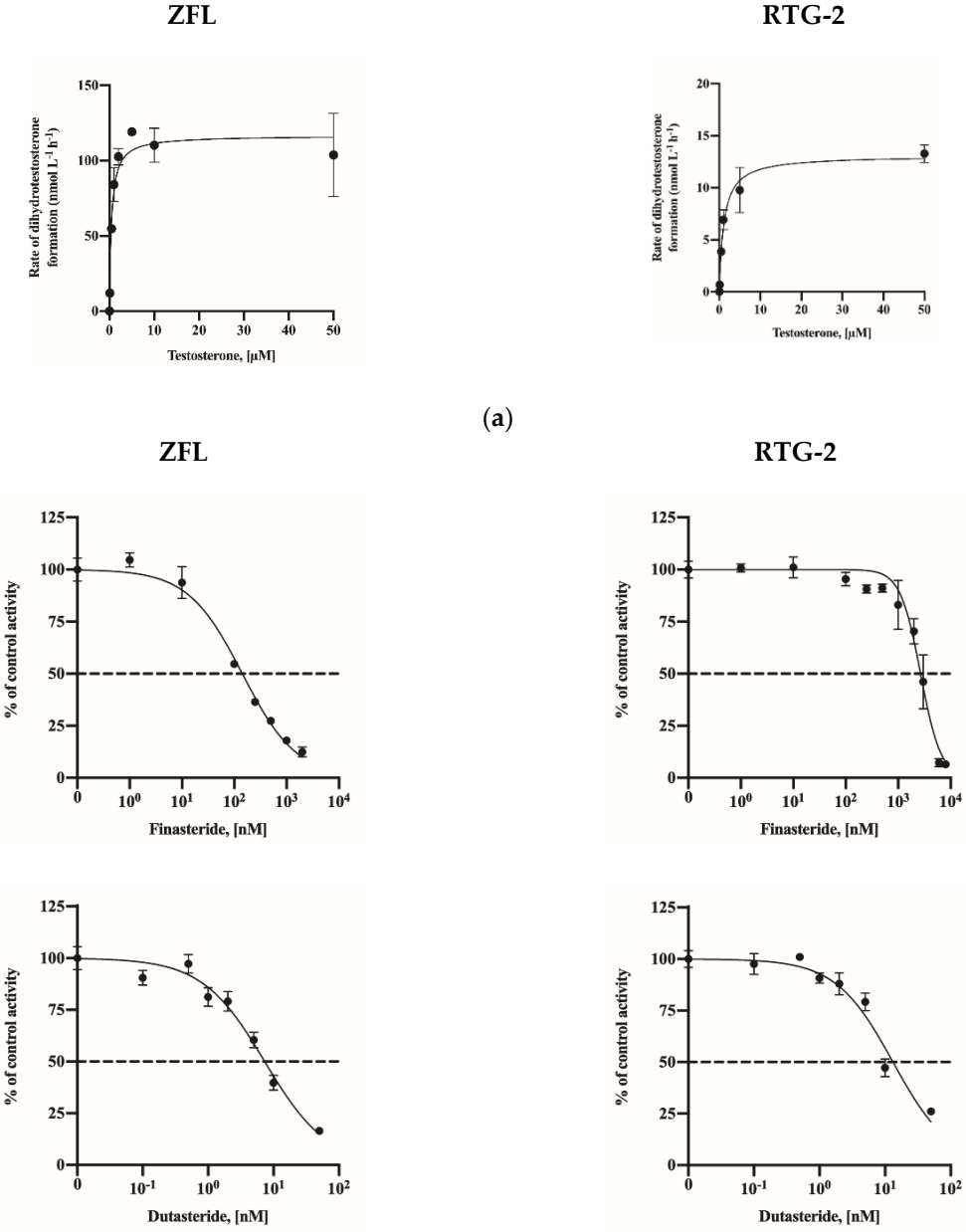

Figure 5. Activity of 5α-reductase (**a**) and inhibitory effects of finasteride and dutasteride (**b**) on and zebrafish liver cells (ZFL) and rainbow trout gonad (RTG-2) cells. The data are expressed as the mean ± standard deviation (SD) of three repeated experiments.

3. Discussion

Fluorinated anhydride acylation methods are widely used for gas chromatography mass spectrometry (GC-MS) for steroid quantification. Similar to the acylation reaction of fluorinated anhydrides and the hydroxyl group of the seventeenth carbon position in the steroid reaction, derivatization using PA showed a higher sensitivity in the detection of 17-OH steroids, such as corticosteroids, in ESI-LC/MS [17]. Recently, LC-MS based quantification methods for androgens such as DHT that utilize various sample sources were developed, and 5AR inhibition studies were conducted [16,18–22]. The method in the present study requires an additional derivatization step compared to the direct measurement. However, compared to these reports, the LLOQ of DHT (14.5 pg/mL) in the present study showed higher sensitivity than hydroxylamine hydrochloride derivatization [18] or direct measurement [19,23] by using LLE after PA derivatization. Also, methods using solid-phase extraction have been developed for the detection of steroids, but these methods are not efficient in time and cost -effective compared with liquid-liquid extraction [16,24,25]. The present study also used 2 times the liquid-liquid extraction step using MTBE after and before derivatization, this process increased the recovery of target compounds from 69 to 74% to 89–108% [16]. The lower limit of quantification of other studies using spectrophotometric method for DHT were from 0.2–10 nM [12,22,26], and other studies using radioactive substrates were range of 25 to 250 ng. The comparison study between immunoassay and LC/MS detection of DHT showed that the variation of detection was relatively more significant in immunoassay than in MS systems [27]. Thus, the method in the present study has an advantage for the detection of DHT than other methods.

A cell-based assay has additional factors that need to optimizing assay condition, but it has more reliability to in vivo system than purified enzyme or centrifuged fraction. Inhibition of 5AR reduced the DHT levels in tissues and can affect the androgen receptor (AR) expression [28–30]. Steroids such as androgens, estrogens and corticosteroids and inhibitors of 5AR are widely utilized in pharmacological applications, and these chemicals may act as EDCs and substantially impact fish and other species that are exposed to the environment [31,32]. We compared the 5AR activities and inhibition rates of 5AR by finasteride and dutasteride between human cell lines and fish cell lines. The V_{max} and K_M values in human cell lines were the largest in the DU-145 cells (Table 2). This result may be related to AR signaling. The LNCaP cell line was AR-positive, whereas the DU-145 cell line was AR-negative. DHT can be metabolized to DHT-glucuronide by the uridine diphosphate-glucuronosyltransferase (UGT) 2B15 and 2B17 enzymes in prostate cells, and these enzymes are modulated by AR [33]. It is possible that the rate of DHT production in AR-negative DU-145 cells exceeds those in other cell lines. The optimal pH of SRD5A1 activity is a broad range from 6.0 to 8.5, and the range for SRD5A2 is from 5.0 to 5.5 [12,33,34]. The steroid affinity of SRD5A2 is 10–20 times higher than that of SRD5A1 under optimal conditions [35].

Under transient transfection conditions, the V_{max} values in HEK-293 cells that were transfected with SRD5A1 and SRD5A2 were approximately 2 times and 5 times larger, respectively, than those of the nontransfected HEK-293 cells. The K_M values in HEK-293 cells that were transfected with SRD5A1 and SRD5A2 were approximately 3.3 times and 21 times smaller, respectively. The transfected cell lines did not show a higher V_{max} compared to human cell lines, but the K_M values decreased; hence, we assume that transient conditions can be used for the comparison of specific enzyme inhibition.

Both fish cell lines were more sensitive to testosterone treatment than human cell lines, and the ZFL cells were more sensitive than the RTG-2 cells. Other studies showed that the activity of 5AR in goldfish (*Carassius auratus*) was high in nonreproductive tissues such as the liver, brain and pituitary tissues, and it was reported that the expression pattern of SRD5A2 in toadfish (*Opsanus tau*) was significantly higher in the liver than in the gonad, in contrast to that in humans [36,37]. In the case of rainbow trout (*Oncorhynchus mykiss*), SRD5A activity was confirmed in the skin of males and females [38,39]. Although we did

not measure the 5AR activity in whole tissue cells, our results demonstrated that fish cell lines are more sensitive to testosterone than human cell lines. The results showed a clear difference in steroid metabolism between the human and fish cell lines. In addition, the activity of 5AR in fish liver cells exceeded that in gonad cells.

The results of the 5AR inhibition assay demonstrated that dutasteride was more potent than finasteride in all cell lines. This is because dutasteride, which is a 5AR dual inhibitor, had a higher 5AR inhibition efficiency, and this tendency was similar to that observed in previous studies [39,40]. However, all the fish cell lines except ZFL on finasteride showed relatively lower sensitivity than human cell lines, and the IC_{50} value of RTG-2 on finasteride was 14 times larger than those on other cell lines. The IC_{50} values of dutasteride in fish cell lines exceeded those in human cell lines.

Similar to our results, other studies also reported that the activity of inhibitors differs among species. The inhibitory effects of finasteride, which mainly inhibits SRD5A2, were similar among dogs, monkeys, and humans, whereas finasteride inhibited both SRD5A1 and SRD5A2 in rats [41,42]. In addition, in a comparison of rat and human IC_{50} values comparisons of finasteride using rat 5α-reductase in prostate microsome were 11 nM, 13 nM, and 237 nM, and IC_{50} values of dutasteride to rat and human 5α-reductase were in the range of 0.2–7 nM [14,43–47]. It was suggested that the difference in amino acid sequences may present a differential response to inhibitors [42]. The amino acid sequence identity of SRD5A1 in humans and fish was approximately 50.2–51.7%, and for SRD5A2 the amino acid identity was detected as 42.4–52.3% (Table 4). Due to the difference in amino acid sequences, the enzymes may differ structurally, and accordingly, the interactions between the substrate or inhibitor and the enzymes can also differ. This suggests that known EDCs may exert various adverse effects on several species through other interactions; thus, future studies are necessary for identifying differences in the impact of EDCs among species.

Table 4. Percentage of amino acid identity of human, zebrafish, and rainbow trout 5ARs.

	Zebrafish srd5a1		**Rainbow Trout** srd5a1
Human srd5a1	51.7		50.2
	Zebrafish		**Rainbow Trout**
	srd5a2a	srd5a2b	srd5a2a
Human srd5a2	52.3	42.4	50.2

Data were compared with human 5ARs amino acid sequence. The percentage of amino acid identity was compared using NCBI's BLAST (http://blast.ncbi.nlm.nih.gov/Blast.cgi, accessed on 4 February 2021) and UniProt (http://www.uniprot.org, accessed on 4 February 2021). The sequences used for analysis are as follows (species, gene_GenBank GI ID): (Human, srd5a1_4507201, srd5a2_39812447); (Zebrafish, srd5a1_11549628, srd5a2a_62955375, srd5a2b_62202806); (Rainbow trout, srd5a1_1211289547, srd5a2_1211257249).

4. Materials and Methods

4.1. Chemicals and Reagents

Fetal bovine serum (FBS), Leibowitz's L-15 medium, the Roswell Park Memorial Institute (RPMI) 1640 medium, Ham's F12 medium, Eagle's minimal essential medium (EMEM), Dulbecco's modified Eagle's medium (DMEM), the Opti-MEM medium, a penicillin/streptomycin solution and trypsin were obtained from GIBCO (Grand Island, NY, USA). Trout serum was purchased from Caisson Laboratories (Smithfield, VA, USA). Mouse epidermal growth factor (EGF) and HEPES were purchased from Thermo Fisher Scientific (Waltham, MA, USA). Sodium bicarbonate, bovine insulin, DHT, DHT-D3 solution, methyl-tertiary-butyl ether (MTBE), trimethylamine (TEA), tetrahydrofuran (THF), 2- PA, 4-(dimethylamino) pyridine (DMAP), 2-methyl-6-nitrobenzoic anhydride (MNBA), and acetic acid were purchased from Sigma-Aldrich (St. Louis, MO, USA), and HPLC-grade formic acid was purchased from Fisher Scientific (Pittsburgh, PA, USA). MS-grade methanol and water were obtained from VWR (Westchester, NY, USA). The stock solution and internal standard were prepared in methanol. The derivatization reagent was prepared

by dissolving 25.0 mg of PA, 10.0 mg of DMAP, and 20.0 mg of MNBA in 1 mL of THF (Yamashita et al., 2009) and vortexing. Then, the mixture was left at room temperature for at least 5 min before the sample pretreatment.

4.2. Cell Culture

HEK-293, LNCaP, DU-145, SW-13, and ZFL cell lines were obtained from the American Type Culture Collection (ATCC; Manassas, VA, USA) and cultured according to their instructions. The HEK-293 cells were cultured in a high-glucose DMEM that contained 10% FBS, 100 units/mL penicillin, and 100 µg/mL streptomycin. The DU-145 cells were cultured in EMEM that contained 10% FBS, 100 units/mL penicillin, and 100 µg/mL streptomycin. The LNCaP cells were cultured in RPMI 1640 that contained 10% FBS, 100 units/mL penicillin, and 100 µg/mL streptomycin at 37 °C in 5% CO_2. SW-13 cells were cultured in Leibovitz's L-15 medium with 10% FBS at 37 °C without CO_2. ZFL cells were cultured in a complete medium that was composed of 50% L-15, 35% DMEM medium, and 15% F12 medium that contained 0.15 g/mL sodium bicarbonate, 15 mM HEPES, 0.01 mg/mL bovine insulin, 50 ng/mL mouse EGF, 5% FBS, and 0.5% trout serum at 28 °C without CO_2. RTG-2 cells were obtained from Prof. Kristin Schirmer (EAWAG, Switzerland) and cultured in the L-15 medium with 5% FBS, 100 units/mL penicillin, and 100 µg/mL streptomycin at 20 °C without CO_2.

4.3. Transient Overexpression

SRD5A1 and SRD5A2 expression vectors were purchased from GenScript (pcDNA3.1+ /C-(K)-DYK-SRD5A1, OHu02727D, and pcDNA3.1+/C-(K)-DYK-SRD5A2, OHu18065D, respectively). Transient overexpression was induced using transfection of cDNA with lipofectamine (Thermo Fisher Scientific, Waltham, MA, USA). HEK-293 cells were seeded in 24-well plates at a density of 10^5 cells per well and incubated at 37 °C in an atmosphere of 5% CO_2. After overnight culture, 500 ng of cDNA and 0.75 µL of the Lipofectamine 3000 reagent were diluted in the Opti-MEM medium and incubated for 15 min for DNA-lipid complex formation. The DNA-lipid complex was added to the wells and incubated for 6 h. After incubation, the sample-treated medium was changed to the complete culture medium and incubated for 18 h.

4.4. Cell Culture Assay Application

All cells were seeded on a 24-well plate. The seeding densities of the DU-145, LNCaP, and SW-13 cells were 0.5×10^5 cells per well. The ZFL and RTG-2 cells were seeded at densities of 1.0×10^5 cells and 2.0×10^5 cells, respectively. After overnight culture, the culture media was aspirated from each well and treated with testosterone that was diluted in the complete medium for 3 h and 6 h. In the case of transiently transfected HEK-293 cells, the testosterone treatment was applied after transient overexpression under the same conditions as other cell lines. The treated media were collected from each well and centrifuged at $3000\times$ *g* for 5 min at 4 °C. The supernatants were stored at −80 °C until needed. A selective SRD5A2 inhibitor, namely, finasteride, and a dual inhibitor of SRD5A1 and SRD5A2, namely, dutasteride, were used as inhibitors of 5-α reductase. The seeding conditions of all cells were the same as those previously described. After overnight culture, the culture medium was aspirated, and the cells were cotreated with a medium that contained testosterone and inhibitors for 3 h. The medium was collected from each well and centrifuged at $3000\times$ *g* for 5 min at 4 °C. The supernatants were stored at −80 °C until analysis.

4.5. qRT PCR

The total RNA was isolated using a column-based kit (Qiagen, Valencia, CA, USA). cDNA was synthesized from 500 ng of the total RNA using a high-capacity RNA-to-cDNA kit (Applied Biosystems, Foster City, CA, USA) according to the manufacturer's instructions. qRT-PCR assays were conducted using a TaqMan gene expression assay

on a 7500 FAST real-time PCR system (Applied Biosystems). The TaqMan assay ID is as follows (Gene, assay ID): RPLO0, Hs00420895_gH; SRD5A1, Hs00165843_m1; SRD5A2, Hs00165843_m1.

4.6. Sample Preparation

A method that was modified by [15] was used for DHT extraction from the samples. Each sample, which included the calibration, QC, and assay medium, was placed in 1.5 mL PP tubes and spiked with a 0.5 ng/mL DHT-D3 internal standard prior to extraction. All sample tubes were vortexed for 5 s, and the samples were extracted using a liquid-liquid extraction (LLE) method via the addition of 600 µL of MTBE. The samples were vortexed and centrifuged at 4500× *g* rpm for 5 min, and the organic phase was transferred into glass tubes. The extraction step was repeated once, and the organic phase extracts were dried under a stream of nitrogen. After the samples were dried, 100 µL of the derivatization reagent and 100 µL of TEA were added for DHT derivatization. The samples were vortexed and incubated at room temperature, and 1 mL of 10% acetic acid was added to stop the reaction after 30 min of incubation. The LLE step, which was conducted before the derivatization step, was repeated twice. The organic phase extracts were collected, dried under a stream of nitrogen, and reconstituted in 50 µL of 80% methanol that contained 0.1% formic acid for LC-MS/MS analysis.

4.7. Instrumental Conditions

The extracts were analyzed for DHT via ultra-performance LC-MS/MS (Agilent 1200/6460C QQQMSD coupled Jet Stream technology electrospray ion (ESI) source; Agilent Technologies, Santa Clara, CA, USA). To separate the analytes, a Kinetex XB-C18 column (2.1 mm × 150 mm, 2.6 µm) that was fitted with a ZORBAX Eclipse Plus C18 guard column (2.1 mm × 5 mm, 1.8 µm) was used. The mobile phase solvents were 0.1% formic acid and methanol, with a flow rate of 300 µL/min for 14 min and a sample injection volume of 10 µL. The gradient started at 5% methanol, was increased to 90% with a 3 min ramp, and was maintained until 5 min. Then, the ramp was increased to 95% methanol until 13 min. At 13.1 min, the ramp was decreased to 5% methanol, which was maintained until 14 min. Mass spectrometry was conducted in the positive ion electrospray mode and multiple reaction mode (MRM) to identify and quantify DHT. The MRM transitions are 396.3 > 255.0 and 273.0 for PA-derivatized DHT and 399.3 > 258.0 and 276.0 for DHT-D3, respectively. The optimized MS conditions are as follows: gas temperature of 350 °C, gas flow of 10 L/min, nebulizer gas pressure of 45 psi, sheath gas temperature of 350 °C, sheath gas flow of 11 L/min, capillary voltage of 3500 V, nozzle voltage of 500 V, and collision energies of 16 V for DHT and 14 V for DHT-D3.

4.8. Calibration Curve and LLOQ

A linear calibration curve was established using a standard solution that consisted of a concentration series of 0.1, 0.5, 1, 5, 10, 50, 100, 500, and 1000 nM DHT with 5 ng/mL DHT-D3. The calibrators for DHT were prepared in an assay medium with a blank (which contained only 5 ng/mL DHT-D3). To evaluate the linearity of the calibration curve, a 1/x weighting linear regression was used. The LLOQ was defined as the lowest concentration of the calibrators at which the signal sensitivity was 3-fold higher than those of the corresponding blank samples.

4.9. Accuracy and Precision

The accuracy and precision of the method were evaluated using intra- and interday quality control (QC) samples. Five replicates each of low QC, medium QC, and high QC samples were prepared by spiking into standard solutions of DHT and DHT-D3 in an assay medium. Their concentrations are 5, 50, and 500 nM, respectively, which represent 100% DHT accuracy of each QC set. The method accuracy was evaluated based on the recoveries (%) that were calculated for each QC spiking level. The precision of the method

was expressed as the coefficient of variation (CV, %). CV was determined by dividing the relative standard deviations of the QC samples by the average DHT concentration of the QC samples. The interday accuracy and precision were determined via three parallel analyses of three sets of QC samples (low, medium, and high). The intraday accuracy and precision were determined via analysis of five replicate samples of each QC set for 3 consecutive days.

4.10. Data Analysis

The LC-MS/MS data were analyzed with the MassHunter quantitative analysis software (Agilent). The DHT inhibition in the presence of inhibitors was expressed as a percentage of the corresponding control value. Each point was expressed as the mean ± S.D. A sigmoid-shaped curve was fitted to the data, and the enzyme kinetic module and inhibition parameter IC_{50} were calculated by fitting the Hill equation to the data using nonlinear regression (least-squares best fit modeling) of the plot of the percent control activity vs. concentration of the test inhibitor using GraphPad Prism 8 (GraphPad Software Inc., San Diego, CA, USA). Control samples (without the inhibitor) were assayed in each analytical run. The amount of metabolite in each sample (relative to the control samples) was plotted vs. the inhibitor concentration.

5. Conclusions

The present study established cell-based 5AR inhibition assay models using quantitative LC-MS/MS analysis. Using this method, all the fish cell lines except the ZFL cell line for finasteride showed significantly higher IC_{50} values for dutasteride and finasteride. This method can be used as a tool for 5AR inhibitor screening in the early stages of drug discovery. In future studies, the inhibitory potency of chemicals will be evaluated for predicting endocrine disruption via a 5AR inhibition assay to develop quantitative AOPs for 5AR inhibition in fishes.

Author Contributions: C.S.R., S.K.K. and Y.J.K. conceived and designed the experiments; D.K., H.C. and R.E. performed the experiments, and analyzed the data; D.K., H.C. and C.S.R. wrote the paper; S.K.K., C.S.R. and Y.J.K. reviewed and edited the entire manuscript. All authors have read and agreed to the published version of the manuscript.

Funding: This research was supported by a National Research Council of Science and Technology (NST) grant by the Korean government (MSIP) (No. CAP-17-01-KIST Europe) and the Korea Institute of Science and Technology Europe basic research program (Project no. 12101).

Data Availability Statement: The datasets generated during and/or analysed during the current study are available from the corresponding author on reasonable request.

Conflicts of Interest: The authors declare no conflict of interest.

Sample Availability: Samples of the compounds are not available from the authors.

References

1. Bruchovsky, N.; Wilson, J.D. The conversion of testosterone to 5α-androstan-17-beta-ol-3-one by rat prostate in vivo and in vitro. *J. Biol. Chem.* **1968**, *243*, 2012–2021. [CrossRef]
2. Russell, D.W.; Wilson, J.D. Steroid 5α-reductase: Two genes/two enzymes. *Annu. Rev. Biochem.* **1994**, *63*, 25–61. [CrossRef]
3. Langlois, V.S.; Zhang, D.; Cooke, G.M.; Trudeau, V.L. Evolution of steroid-5α-reductases and comparison of their function with 5beta-reductase. *Gen. Comp. Endocrinol.* **2010**, *166*, 489–497. [CrossRef] [PubMed]
4. McConnell, J.D.; Wilson, J.D.; George, F.W.; Geller, J.; Pappas, F.; Stoner, E. Finasteride, an inhibitor of 5α-reductase, suppresses prostatic dihydrotestosterone in men with benign prostatic hyperplasia. *J. Clin. Endocrinol. Metab.* **1992**, *74*, 505–508. [CrossRef]
5. Diani, A.R.; Mulholland, M.J.; Shull, K.L.; Kubicek, M.F.; Johnson, G.A.; Schostarez, H.J.; Brunden, M.N.; Buhl, A.E. Hair growth effects of oral administration of finasteride, a steroid 5α-reductase inhibitor, alone and in combination with topical minoxidil in the balding stumptail macaque. *J. Clin. Endocrinol. Metab.* **1992**, *74*, 345–350. [CrossRef] [PubMed]
6. McConnell, J.D.; Roehrborn, C.G.; Bautista, O.M.; Andriole, G.L.; Dixon, C.M.; Kusek, J.W.; Lepor, H.; McVary, K.T.; Nyberg, L.M.; Clarke, H.S.; et al. The long-term effect of doxazosin, finasteride, and combination therapy on the clinical progression of benign prostatic hyperplasia. *N. Engl. J. Med.* **2003**, *349*, 2387–2398. [CrossRef] [PubMed]

7. Ryu, C.S.; Sung, B.; Baik, S.; Kim, Y.J.; Lee, Y. Inhibition of 5α-Reductase Leading to Impaired Fecundity in Female Fish. Available online: https://aopwiki.org/aops/289 (accessed on 11 December 2020).
8. García-García, M.; Sánchez-Hernández, M.; García-Hernández, M.P.; García-Ayala, A.; Chaves-Pozo, E. Role of 5α-dihydrotestosterone in testicular development of gilthead seabream following finasteride administration. *J. Steroid Biochem. Mol. Biol.* **2017**, *174*, 48–55. [CrossRef]
9. Margiotta-Casaluci, L.; Courant, F.; Antignac, J.P.; Le Bizec, B.; Sumpter, J.P. Identification and quantification of 5α-dihydrotestosterone in the teleost fathead minnow (*Pimephales promelas*) by gas chromatography-tandem mass spectrometry. *Gen. Comp. Endocrinol.* **2013**, *191*, 202–209. [CrossRef]
10. Andersson, S.; Bishop, R.W.; Russell, D.W. Expression cloning and regulation of steroid 5α-reductase, an enzyme essential for male sexual differentiation. *J. Biol. Chem.* **1989**, *264*, 16249–16255. [CrossRef]
11. Raynaud, J.P.; Cousse, H.; Martin, P.M. Inhibition of type 1 and type 2 5α-reductase activity by free fatty acids, active ingredients of permixon. *J. Steroid Biochem. Mol. Biol.* **2002**, *82*, 233–239. [CrossRef]
12. Iwai, A.; Yoshimura, T.; Wada, K.; Watabe, S.; Sakamoto, Y.; Ito, E.; Miura, T. Spectrophotometric method for the assay of steroid 5α-reductase activity of rat liver and prostate microsomes. *Anal. Sci.* **2013**, *29*, 455–459. [CrossRef]
13. Matsuda, H.; Sato, N.; Yamazaki, M.; Naruto, S.; Kubo, M. Testosterone 5α-reductase inhibitory active constituents from Anemarrhenae Rhizoma. *Biol. Pharm. Bull.* **2001**, *24*, 586–587. [CrossRef]
14. Mitamura, K.; Narukawa, H.; Mizuguchi, T.; Shimada, K. Degradation of estrogen conjugates using titanium dioxide as a photocatalyst. *Anal. Sci.* **2004**, *20*, 3–4. [CrossRef]
15. Abe, M.; Ito, Y.; Oyunzul, L.; Oki-Fujino, T.; Yamada, S. Pharmacologically relevant receptor binding characteristics and 5α-reductase inhibitory activity of free fatty acids contained in saw palmetto extract. *Biol. Pharm. Bull.* **2009**, *32*, 646–650. [CrossRef]
16. Gorityala, S.; Yang, S.; Montano, M.M.; Xu, Y. Simultaneous determination of dihydrotestosterone and its metabolites in mouse sera by LC-MS/MS with chemical derivatization. *J. Chromatogr. B* **2018**, *1090*, 22–35. [CrossRef]
17. Yamashita, K.; Takahashi, M.; Tsukamoto, S.; Numazawa, M.; Okuyama, M.; Honma, S. Use of novel picolinoyl derivatization for simultaneous quantification of six corticosteroids by liquid chromatography-electrospray ionization tandem mass spectrometry. *J. Chromatogr. A* **2007**, *1173*, 120–128. [CrossRef]
18. Srivilai, J.; Rabgay, K.; Khorana, N.; Waranuch, N.; Nuengchamnong, N.; Ingkaninan, K. A new label-free screen for steroid 5α-reductase inhibitors using LC-MS. *Steroids* **2016**, *116*, 67–75. [CrossRef] [PubMed]
19. Cao, Z.; Lu, Y.; Cong, Y.; Liu, Y.; Li, Y.; Wang, H.; Zhang, Q.; Huang, W.; Liu, J.; Dong, Y.; et al. Simultaneous quantitation of four androgens and 17-hydroxyprogesterone in polycystic ovarian syndrome patients by LC-MS/MS. *J. Clin. Lab. Anal.* **2020**, *34*, 23539. [CrossRef] [PubMed]
20. Tan, J.J.Y.; Pan, J.; Sun, L.; Zhang, J.; Wu, C.; Kang, L. Bioactives in Chinese proprietary medicine modulates 5α-reductase activity and gene expression associated with androgenetic alopecia. *Front. Pharmacol.* **2017**, *8*, 194. [CrossRef] [PubMed]
21. Wang, D.; Zhang, M. Rapid quantitation of testosterone hydroxyl metabolites by ultra-performance liquid chromatography and mass spectrometry. *J. Chromatogr. B* **2007**, *855*, 290–294. [CrossRef]
22. Jain, R.; Monthakantirat, O.; Tengamnuay, P.; De-Eknamkul, W. Identification of a new plant extract for androgenic alopecia treatment using a non-radioactive human hair dermal papilla cell-based assay. *BMC Complementary Altern. Med.* **2015**, *16*, 18. [CrossRef]
23. Nouri, M.-Z.; Kroll, K.J.; Webb, M.; Denslow, N.D. Quantification of steroid hormones in low volume plasma and tissue homogenates of fish using LC-MS/MS. *Gen. Comp. Endocrinol.* **2020**, *296*, 113543. [CrossRef] [PubMed]
24. Licea-Perez, H.; Wang, S.; Szapacs, M.E.; Yang, E. Development of a highly sensitive and selective UPLC/MS/MS method for the simultaneous determination of testosterone and 5α-dihydrotestosterone in human serum to support testosterone re-placement therapy for hypogonadism. *Steroids* **2008**, *73*, 601–610. [CrossRef]
25. Yamashita, K.; Miyashiro, Y.; Maekubo, H.; Okuyama, M.; Honma, S.; Takahashi, M.; Numazawa, M. Development of highly sensitive quantification method for testosterone and dihydrotestosterone in human serum and prostate tissue by liquid chromatography-electrospray ionization tandem mass spectrometry. *Steroids* **2009**, *74*, 920–926. [CrossRef] [PubMed]
26. Koseki, J.; Matsumoto, T.; Matsubara, Y.; Tsuchiya, K.; Mizuhara, Y.; Sekiguchi, K.; Nishimura, H.; Watanabe, J.; Kaneko, A.; Hattori, T.; et al. Inhibition of Rat 5α-Reductase activity and testosterone-induced sebum synthesis in hamster sebocytes by an extract of Quercus acutissima Cortex. *Evid. Based Complementary Altern. Med.* **2015**, *2015*, 853846. [CrossRef] [PubMed]
27. Dorgan, J.F.; Fears, T.R.; McMahon, R.P.; Friedman, L.A.; Patterson, B.H.; Greenhut, S.F. Measurement of steroid sex hormones in serum: A comparison of radioimmunoassay and mass spectrometry. *Steroids* **2002**, *67*, 151–158. [CrossRef]
28. Bauman, T.M.; Sehgal, P.D.; Johnson, K.A.; Pier, T.; Bruskewitz, R.C.; Ricke, W.A.; Huang, W. Finasteride treatment alters tissue specific androgen receptor expression in prostate tissues. *Prostate* **2014**, *74*, 923–932. [CrossRef] [PubMed]
29. Wang, L.G.; Liu, X.M.; Kreis, W.; Budman, D.R. Down-regulation of prostate-specific antigen expression by finasteride through inhibition of complex formation between androgen receptor and steroid receptor-binding consensus in the promoter of the PSA gene in LNCaP cells. *Cancer Res.* **1997**, *57*, 714–719.
30. Audet-Walsh, É.; Yee, T.; Tam, I.S.; Giguère, V. Inverse regulation of DHT synthesis enzymes 5α-reductase Types 1 and 2 by the androgen receptor in prostate cancer. *Endocrinology* **2017**, *158*, 1015–1021. [CrossRef]

31. Chang, H.; Wan, Y.; Hu, J. Determination and source apportionment of five classes of steroid hormones in urban rivers. *Environ. Sci. Technol.* **2009**, *43*, 7691–7698. [CrossRef]
32. Schmid, S.; Willi, R.A.; Fent, K. Effects of environmental steroid mixtures are regulated by individual steroid receptor signaling. *Aquat. Toxicol.* **2020**, *226*, 105562. [CrossRef] [PubMed]
33. Bao, B.-Y.; Chuang, B.-F.; Wang, Q.; Sartor, O.; Balk, S.P.; Brown, M.; Kantoff, P.W.; Lee, G.-S.M. Androgen receptor mediates the expression of UDP-glucuronosyltransferase 2 B15 and B17 genes. *Prostate* **2008**, *68*, 839–848. [CrossRef]
34. Span, P.N.; Smals, A.G.; Sweep, C.G.; Benraad, T.J. Rat steroid 5α-reductase kinetic characteristics: Extreme pH-dependency of the type II isozyme in prostate and epididymis homogenates. *J. Steroid. Biochem. Mol. Biol.* **1995**, *54*, 185–192. [CrossRef]
35. Normington, K.; Russell, D.W. Tissue distribution and kinetic characteristics of rat steroid 5α-reductase isozymes. Evidence for distinct physiological functions. *J. Biol. Chem.* **1992**, *267*, 19548–19554. [CrossRef]
36. Martyniuk, C.J.; Bissegger, S.; Langlois, V.S. Current perspectives on the androgen 5α-dihydrotestosterone (DHT) and 5 α-reductases in teleost fishes and amphibians. *Gen. Comp. Endocrinol.* **2013**, *194*, 264–274. [CrossRef] [PubMed]
37. Pasmanik, M.; Schlinger, B.A.; Callard, G.V. In Vivo steroid regulation of aromatase and 5α-reductase in goldfish brain and pituitary. *Gen. Comp. Endocrinol.* **1988**, *71*, 175–182. [CrossRef]
38. Latz, M.; Reinboth, R. Androgen metabolism in the skin of the rainbow trout (*Oncorhynchus mykiss*). *Fish Physiol. Biochem.* **1993**, *11*, 281–286. [CrossRef]
39. Bramson, H.N.; Hermann, D.; Batchelor, K.W.; Lee, F.W.; James, M.K.; Frye, S.V. Unique preclinical characteristics of GG745, a potent dual inhibitor of 5AR. *J. Pharmacol. Exp. Ther.* **1997**, *282*, 1496–1502.
40. Tian, G.; Mook, R.; Moss, M.L.; Frye, S.V. Mechanism of time-dependent inhibition of 5α-reductases by. DELTA.1-4-Azasteroids: Toward perfection of rates of time-dependent inhibition by using ligand-binding energies. *Biochemistry* **1995**, *34*, 13453–13459. [CrossRef]
41. Azzolina, B.; Ellsworth, K.; Andersson, S.; Geissler, W.; Bull, H.G.; Harris, G.S. Inhibition of rat alpha-reductases by finasteride: Evidence for isozyme differences in the mechanism of inhibition. *J. Steroid. Biochem. Mol. Biol.* **1997**, *61*, 55–64. [CrossRef]
42. Levy, M.A.; Brandt, M.; Sheedy, K.M.; Holt, D.A.; Heaslip, J.I.; Trill, J.J.; Ryan, P.J.; Morris, R.A.; Garrison, L.M.; Bergsma, D.J. Cloning, expression and functional characterization of type 1 and type 2 steroid 5α-reductases from cynomolgus monkey: Comparisons with human and rat isoenzymes. *J. Steroid Biochem. Mol. Biol.* **1995**, *52*, 307–319. [CrossRef]
43. Häußler, A.; Allegrini, P.; Biollaz, M.; Batzl, C.; Scheidegger, E.; Bhatnagar, A. CGP 53153: A new potent inhibitor of 5α-reductase. *J. Steroid Biochem. Mol. Biol.* **1996**, *57*, 187–195. [CrossRef]
44. Hirosumi, J.; Nakayama, O.; Fagan, T.; Sawada, K.; Chida, N.; Inami, M.; Takahashi, S.; Kojo, H.; Notsu, Y.; Okuhara, M. FK143, a novel nonsteroidal inhibitor of steroid 5α-reductase: (1) In vitro effects on human and animal prostatic enzymes. *J. Steroid Biochem. Mol. Biol.* **1995**, *52*, 357–363. [CrossRef]
45. Di Salle, E.; Giudici, D.; Radice, A.; Zaccheo, T.; Ornati, G.; Nesi, M.; Panzeri, A.; Delos, S.; Martin, P. PNU 157706, a novel dual type I and II5α-reductase inhibitor. *J. Steroid Biochem. Mol. Biol.* **1998**, *64*, 179–186. [CrossRef]
46. Xu, Y.; Dalrymple, S.L.; Becker, R.E.; Denmeade, S.R.; Isaacs, J.T. Pharmacologic basis for the enhanced efficacy of dutasteride against prostatic cancers. *Clin. Cancer Res.* **2006**, *12*, 4072–4079. [CrossRef]
47. Mitamura, K.; Ogasawara, C.; Shiozawa, A.; Terayama, E.; Shimada, K. Determination method for steroid 5α-reductase activity using liquid chromatography/atmospheric pressure chemical ionization-mass spectrometry. *Anal. Sci.* **2005**, *21*, 1241–1244. [CrossRef] [PubMed]

8.2 Original paper − SRD5A inhibition on zebrafish embryo

Comparative Biochemistry and Physiology, Part C 287 (2025) 110048

Contents lists available at ScienceDirect

Comparative Biochemistry and Physiology, Part C

journal homepage: www.elsevier.com/locate/cbpc

Effects of 5α-reductase inhibition by dutasteride on reproductive gene expression and hormonal responses in zebrafish embryos

Hyunki Cho [a,b,1], Indong Jun [a,1], Karim Md Adnan [a], Chang Gyun Park [a,c], Sang-Ah Lee [a,d], Juyong Yoon [a], Chang Seon Ryu [a,*], Young Jun Kim [a,e,*]

[a] Environmental Safety Group, Korea Institute of Science & Technology Europe (KIST-EUROPE), 66123 Saarbrücken, Germany
[b] Department of Pharmacy, Saarland University, 66123 Saarbrücken, Germany
[c] Division of Experimental Neurosurgery, Department of Neurosurgery, Heidelberg University Hospital, 69120 Heidelberg, Germany
[d] Faculty of Biotechnology, College of Applied Life Sciences, Jeju National University, 102 Jejudaehak-Ro, Jeju 63243, Republic of Korea
[e] Division of Energy & Environment Technology, University of Science & Technology, 34113 Daejeon, Republic of Korea

ARTICLE INFO

Edited by Martin Grosell

Keywords:
5α-reductase inhibition
Dutasteride
Dihydrotestosterone
Reproductive toxicity
Zebrafish embryo
Adverse outcome pathway

ABSTRACT

Steroid 5α-reductase (SRD5A) is a crucial enzyme involved in steroid metabolism, primarily converting testosterone to dihydrotestosterone (DHT). Dutasteride, an inhibitor of SRD5A types 1 and 2, is widely used for treating benign prostatic hyperplasia. An adverse outcome pathway (AOP) has been documented wherein SRD5A inhibition decreases DHT synthesis, leading to reduced levels of 17β-estradiol (E2) and vitellogenin (VTG), subsequently impairing fecundity in fish (AOP 289). However, the molecular and cellular mechanisms underlying these effects remain poorly understood. In this study, we assessed the impact of SRD5A inhibition on zebrafish embryos *(Danio rerio)*. Exposure to dutasteride resulted in decreased DHT, E2, and VTG levels, showing a positive correlation. Dutasteride also downregulated the expression of reproduction-related *genes (srd5a2, cyp19a1, esr1, esr2a, esr2b,* and *vtg*), with interrelated reductions observed across these levels. Docking studies suggested that dutasteride's effects may operate independently of androgen receptor (AR) and estrogen receptor (ER) interactions. Furthermore, co-exposure of dutasteride (0.5 or 2 μM) with 0.5 μM DHT revealed gene expression levels comparable to the control group. These findings underscore DHT's pivotal role in modulating estrogenic function and the interplay between estrogenic and androgenic responses in vertebrates. Our proposed AOP model offers insights into mechanistic gaps, thereby enhancing current understanding and bridging knowledge disparities.

1. Introduction

Dihydrotestosterone (DHT) is recognized as a potent androgen found in various classes of vertebrates, including mammals, birds, reptiles, and amphibians (Martyniuk et al., 2014). DHT is converted from testosterone (T) by steroid 5α-reductase (SRD5A). Although 11-ketotestosterone (11KT) is generally considered the major androgen in teleosts, DHT also plays a role in development of the male reproductive organs and is involved in the transition from the mitotic to the meiotic stage of spermatogenesis (Margiotta-Casaluci et al., 2013a; Margiotta-Casaluci and Sumpter, 2011; González et al., 2015; García-García et al., 2017). Exposure to DHT (200 ng/L) in male juvenile fathead minnows (*Pimephales promelas*) induces spermatogenesis, whereas, in females, it disrupts ovarian development and functions, leading to the development of spermatogenic tissue (Margiotta-Casaluci and Sumpter, 2011). Additionally, studies have reported that exposure to SRD5A inhibitors in teleost fish results in histological alterations of the ovary, decreased proportion of vitellogenic oocytes, and fluctuations in the expression levels of reproduction-related genes and serum steroid hormone levels (Margiotta-Casaluci et al., 2013a; García-García et al., 2017). These findings suggest a key regulatory role of DHT in reproduction of teleost fishes.

Given the importance of understanding biological mechanisms, zebrafish (*Danio rerio*) serves as an ideal sentinel for assessing aquatic toxicity across vertebrates and has become a popular model system in aquatic ecotoxicology (Spitsbergen and Kent, 2003; McGrath and Li,

* Corresponding authors.
E-mail addresses: changryu@kist-europe.de (C.S. Ryu), youngjunkim@kist-europe.de (Y.J. Kim).
[1] These authors contributed equally to this work

https://doi.org/10.1016/j.cbpc.2024.110048
Received 15 July 2024; Received in revised form 16 September 2024; Accepted 19 September 2024
Available online 21 September 2024

2008). Many studies have demonstrated that the zebrafish model offers excellent versatility for applications ranging from acute systemic toxicity to chronic toxicity, teratogenicity, and endocrine disruption (Volz et al., 2011; Selderslaghs et al., 2009; He et al., 2014). The OECD Test Guideline 236, an acute toxicity test for fish embryos, has facilitated the use of fish embryos in toxicity studies due to advantages such as reduced ethical concerns compared to tests on adult fish, lower costs, and faster results (OECD, 2013).

In recent years, regulatory toxicology has embraced the 3Rs concept (replacement, reduction, and refinement of animal experiments) (Bradbury et al., 2004) to develop alternative approaches to conventional vertebrate toxicity testing. Understanding toxicological effects and accumulating toxicity data are essential to support this approach. Adverse outcome pathways (AOPs) provide highly structured conceptual frameworks for describing toxicological processes (Ankley et al., 2010). AOPs organize knowledge about the progression of toxicity from molecular initiating events (MIEs) through subsequent key events (KEs) to adverse outcomes (AOs), providing mechanistic evidence to predict potential hazards by linking events across different organismal levels. Current AOP formulations have focused on initiating or early-stage events of toxicological responses for their cost- and time-efficient applications (Ankley et al., 2010; Villeneuve et al., 2014). Particularly, AOPs are crucial for transitioning from animal testing to mechanistic-based toxicity assessments using in vivo and in vitro models.

Building on the AOP-Wiki related to impaired fecundity in fish, we organized the present study using AOP 289, which is currently under development (AOP-Wiki, 2022). AOP 289 describes that inhibition of SRD5A (as the MIE) decreases DHT synthesis, sequentially leading to decreased plasma 17β-estradiol (E2) and vitellogenin (VTG) levels, reduced spawning and egg production in zebrafish, and ultimately decreased population levels as the AO. However, a detailed understanding at the molecular level, particularly elucidating the anti-estrogen effects of SRD5A inhibition in fish, is currently lacking. This study aimed to understand the transition from MIE to KEs by evaluating estrogenic effects following SRD5A inhibition in zebrafish embryos. Dutasteride, an inhibitor of SRD5A1 and 2, was used as the MIE, and the relationships between each KE were evaluated at the level of reproductive factors and gene expression. These results can help fill knowledge gaps in AOPs regarding the biological mechanisms of SRD5A inhibition in zebrafish embryos.

2. Materials and methods

2.1. Chemicals and reagents

Dutasteride (CAS No. 164656-23-9), DHT (CAS No. 521-18-6), and T (CAS No. 58-22-0) were purchased from Sigma-Aldrich (Steinheim, Germany). The stock solutions of dutasteride, T, and DHT were dissolved in dimethyl sulfoxide (DMSO) at 20, 100, and 100 mM, respectively. The solvent was limited to 0.01 % DMSO (*v*/v) or less in the zebrafish embryo experiment. All the other chemicals were of analytical grade.

2.2. Zebrafish maintenance

Adult wild-type zebrafish were obtained from the European Zebrafish Resource Center (EZRC; Karlsruhe, Germany). Fish maintenance, breeding conditions, and egg production were performed under internationally accepted standards in an aerated aquarium system (temperature 28.0 ± 0.5 °C and 16/8 h dark/light cycle) with E3 medium (5 mM sodium chloride, 0.17 mM potassium chloride, 0.33 mM calcium chloride, 0.33 mM magnesium sulfate, and 0.01 % methylene blue). The fish were fed a commercial flake diet (JBL, Germany) supplemented with freshly hatched brine shrimp (Artemia).

2.3. Maximum tolerated concentration (MTC)

Zebrafish eggs were collected approximately 60 min after natural mating and rinsed in E3 medium. Unfertilized or injured eggs were discarded. To determine the MTC, fertilized eggs were randomly selected and carefully distributed in a 6-well plate, filled with 6 mL of different concentrations of dutasteride (0.005, 0.05, 0.1, 0.5, 1, and 2 μM) or negative (E3 medium containing 0.01 % DMSO). The test was performed in a climate chamber at 28.0 ± 0.5 °C and 16/8 h dark/light cycle until 120 h post-fertilization (hpf). No food or aeration was provided during the experiment. Embryonic development was assessed at 24, 48, 72, 96, and 120 hpf using a stereomicroscope (SteREO Discovery V8; Carl Zeiss, Zena, Germany). The distinction between normal and abnormal embryo development in terms of phenotypic changes (i.e. skeletal deformity) was established according to the descriptions of zebrafish development reported by Kimmel et al. (1995). In addition, survival (egg coagulation, somite formation, and heartbeat) and hatching rates were observed and reported.

2.4. Zebrafish SRD5A (zfSRD5A) isoforms activity and inhibition assays

HEK-293 cell line (ATCC CRL-1573, Manassas, VA, USA) was cultured in DMEM containing 10 % fetal bovine serum (FBS). Transient overexpression was performed by transfecting the cDNA (GeneScript, Cat. #ODa35277, pcDNA3.1+/C-(K)-DYK-srd5a1; GeneScript, Cat. #ODa35277; pcDNA3.1+/C-(K)-DYK-srd5a2a, GeneScript Cat. #ODa35087, pcDNA3.1+/C-(K)-DYK-srd5a2b; GeneScript Cat. #ODa00115, pcDNA3.1+/C-(K)-DYK-srd5a3) using lipofectamine 3000 reagent (Thermo Fisher Scientific, Waltham, MA, USA). HEK293 cells were seeded in a 24-well plate at a density of 1.0×10^5 cells per well. After overnight culture, 500 ng of cDNA and 0.75 μg of Lipofectamine 3000 reagent diluted in Opti-MEM were treated into each well and incubated for 24 h. For the measurement of SRD5A kinetics, T (0.1, 0.33, 1, 33, 10, and 33 μM) was treated into each well for 24 h. For the measurement of SRD5A inhibition, dutasteride (0.1, 0.5, 1, 2, 5, 10, 50, and 100 nM) and T (Km value) were co-treated for 24 h. The culture medium was then collected and analyzed using LC-MS/MS for the quantification of DHT. DHT concentrations were measured using LC-MS/MS as described previously (Kim et al., 2021). Briefly, DHT was extracted by the liquid-liquid extraction (LLE) method using methyl tert-butyl ether, then the extract was derivatized with picolic acid. After the LLE step, the samples were dried under the nitrogen stream concentrator, the extract was reconstituted and analyzed.

2.5. Exposure experimental procedures on zebrafish embryo

2.5.1. Dutasteride exposure

A schematic diagram of the study is presented in Fig. 1. Zebrafish embryos were placed into 1 L aquarium filled E3 medium and maintained at 28.0 ± 0.5 °C and 16/8 h dark/light cycle until 72 hpf. 20 zebrafish embryos were then placed into each well of 6-well plates filled with 10 mL of each exposure medium, negative control (0.01 % DMSO), and dutasteride (0.005, 0.05, 0.5, and 2 μM), and incubated until 120 hpf. The test solution was changed daily to prevent concentration by uptake and bioaccumulation of the compound in zebrafish embryos.

2.5.2. Steroid hormone extraction and measurement

DHT and E2 levels were measured using ELISA kits (Cat. #KA1886; Abnova, Heidelberg, Germany; Cat. #501890; Cayman, Hamburg, Germany). 200 embryos from 10 wells were collected into a tube for steroid hormone extraction according to the manufacturer's instructions. The embryos were washed with distilled water and dried under a stream of nitrogen. Methanol (1 mL) was added to each tube, and embryos were homogenized using the TissueLyser bead LT (Qiagen, Hilden, Germany). After centrifugation at 10,000 ×*g* and 4 °C for 10 min, the supernatant was dried under a nitrogen stream. The extracted steroids were

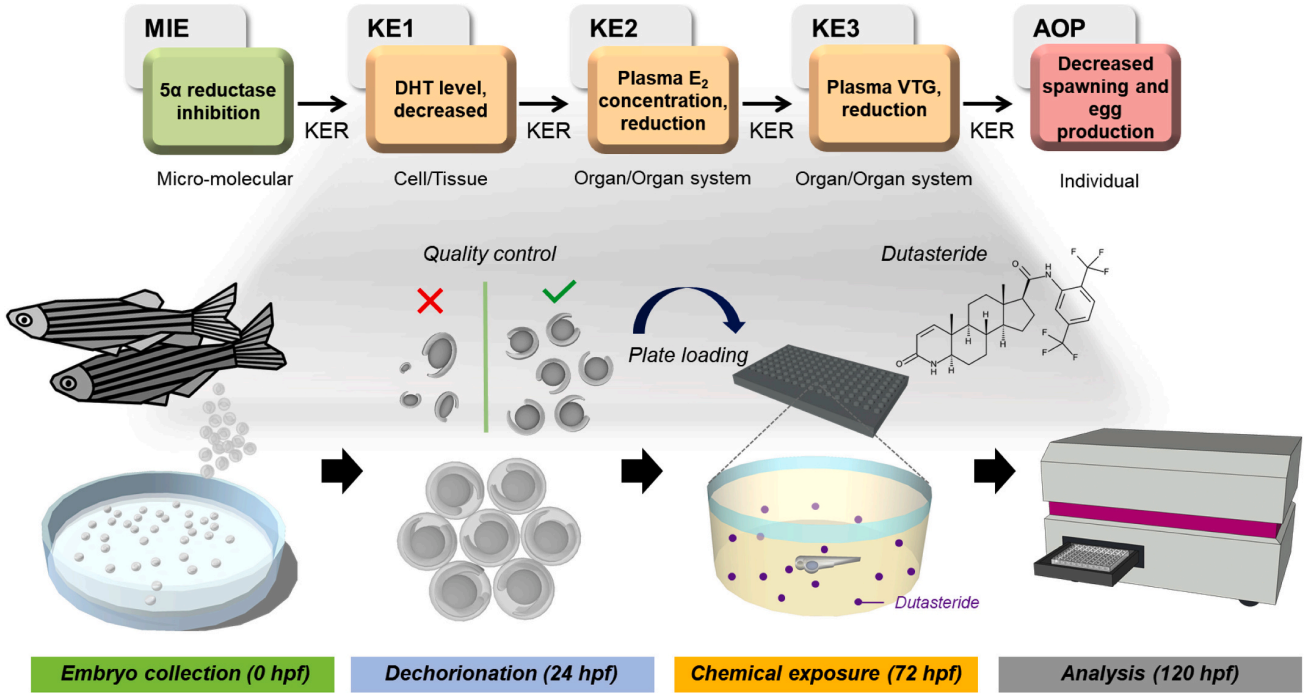

Fig. 1. AOP 289 and schematic diagram representing the assessment of zebrafish embryos exposed to dutasteride. Fertilized eggs were collected and maintained on a 16 h light/8 h dark cycle at 28 °C ± 0.5 °C and unfertilized eggs were separated. Dutasteride was exposed to zebrafish embryos at 72 h post fertilization (hpf). The embryos were collected at 120 hpf and utilized for subsequent assays.

reconstituted with 500 uL of the assay buffer supplied in the kit. The samples were stored at −80 °C until analysis. Each tube was considered a sample, and at least five replicate samples from each condition were prepared from independent cultures ($n \geq 5$). Measurement was performed by a Spark multimode microplate reader (Tecan, Männedorf, Switzerland) at the absorbance of 450 nm. The protein concentration for normalization was determined using the BCA protein assay (Thermo Scientific, Karlsruhe, Germany).

2.5.3. VTG measurement

VTG levels were measured using an ELISA kit (Cat. #10004995; Cayman) according to the manufacturer's instructions. 200 embryos from 10 wells were collected into a tube and washed with distilled water. Cold RIPA buffer was added to each tube and the samples were homogenized by vortexing for 2 min. The homogenates were centrifuged at 14,000 ×*g* and 4 °C for 10 min. Finally, the supernatants were transferred to new tubes and were stored at −80 °C until analysis. Each tube was considered a sample, and at least five replicate samples from each condition were prepared from independent cultures ($n \geq 5$). Measurement was performed by a Spark multimode microplate reader (Tecan) at the absorbance of 492 nm. The protein concentration for normalization was determined using the BCA protein assay (Thermo Scientific, Karlsruhe, Germany).

2.5.4. mRNA expression level measurement

40 embryos from 2 wells were collected into a tube and washed with distilled water. The TRIzol reagent (Invitrogen, Carlsbad, CA, USA) was added to each tube and homogenized with beads. Total RNA was isolated using a column-based kit (cat. #74136; Qiagen). cDNA was synthesized from 500 ng of total RNA using a High-Capacity RNA-to-cDNA Kit (Applied Biosystems, Waltham, MA, USA) according to the manufacturer's instructions. qRT-PCR assays were performed using a TaqMan™ Fast Advanced Master Mix and a Fast SYBR™ Green Master Mix on a 7500 FAST real-time PCR system (Applied Biosystems). The PCR reaction cycles for the SYBR Green assay were as follows: initial denaturation at 95 °C for 20 s, followed by 40 amplification cycles of 95 °C for 3 s and 60 °C for 30 s. For the TaqMan assay, the reaction cycles were: initial denaturation at 90 °C for 20 s, followed by 40 amplification cycles of 95 °C for 3 s and 60 °C for 30 s. Relative mRNA expression of *srd5a2* (Dr03128500_m1; Thermo Scientific), *cyp19a1* (PPZ00217A; Qiagen), *esr1* (Dr03093579_m1; Thermo Scientific), *esr2a* (Dr03074408_m1; Thermo Scientific), *esr2b* (Dr03150586_m1; Thermo Scientific), and *vtg2* (PPZ10052A; Qiagen) was calculated using $2^{-\Delta\Delta Ct}$ method with the endogenous control *eef1a1la* (Dr03432748_m1; Thermo Scientific) and *g6pd* (PPZ12949A; Qiagen) for normalization (Schmittgen and Livak, 2008). Each tube was considered a sample, and at least four replicate samples from each condition were prepared from independent cultures ($n \geq 4$).

2.6. Homology modeling and molecular docking

For the preparations of zebrafish estrogen receptor alpha (zfERα) and zebrafish androgen receptor (zfAR), we downloaded the crystal structures of human ER (hER) and AR (hAR) (Protein Data Bank [PDB] code: 2YJA for hERα and 2 AM9 for hAR) were downloaded from the PDB (http://www.rcsb.org/) and used as template structures. MODELLER 9.25 (https://salilab.org/modeller/9.25/release.html) was used to generate homology models of zfER and zfAR. MODELLER uses a comparative modeling approach to compare the sequence alignment quality of the target protein sequence with that of one or more known template 1protein structures (Webb and Sali, 2016). Ten models were generated for both the zfER and zfAR protein sequences, among which only one structure with the lowest discrete optimized protein energy (DOPE) score was selected as the target receptor for molecular docking experiments (Shen and Sali, 2006). For the molecular docking process, crystallographic water molecules were removed from the crystal structures, and charges and hydrogen atoms were added. The ligand structures were prepared from the PubChem database (ligand, PubChem CID: E2, 5757; DHT, 10635; dutasteride, 6918296). Each structure was saved in SDF format, and the geometry was optimized using the MM2 method

of energy minimization. Eventually, the prepared files were converted to PDB format using Discovery Studio Visualizer 2016 (Accelrys Software). The ligand structures were applied to AutoDock 4.2 (Scripps Research Institute, California). Docking simulations and visualizations were performed using CDOCKER (Wu et al., 2003) and AutoDock 4.2 (Trott and Olson, 2010) software. Standard docking was performed using flexible ligands docked onto rigid proteins. We performed five independent runs per ligand and used grid conditions of 40, 40, and 40 points in the x-, y-, and z-directions, respectively, with grid spacing of 1.0 Å. An energy map was constructed using a distance-dependent function of the dielectric constant. All other parameters were set to default values. Docking sites were calculated based on their ranking and binding free energies. The docked positions were analyzed for hydrogen bonding and hydrophobic, van der Waals, and halogen interactions using Discovery Studio Visualizer 2019.

2.7. Construction of ARE reporter cell line and response activity

HEK293 cells were used as transfection hosts and maintained in DMEM containing 10 % FBS at 37 °C and 5 % CO_2 condition. HEK293-ARE-zfAR cells were constructed using lentiviral transduction for androgen receptor element (ARE, CS-GS241B-mCHER-Lv207-01;

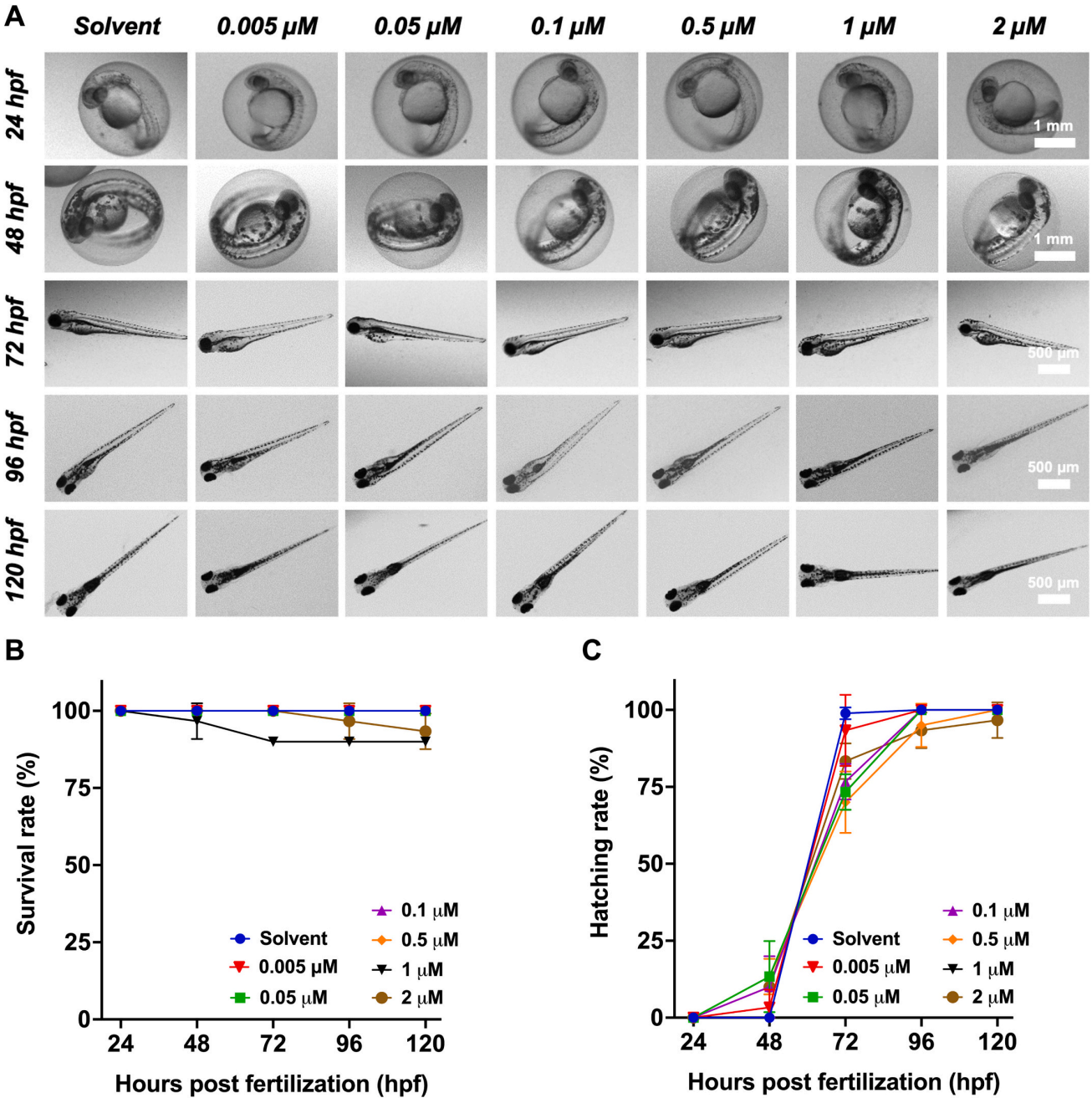

Fig. 2. MTC and toxic effects of dutasteride exposure in zebrafish embryos at various developmental stages. Phenotypes, mortality, and hatching rate were measured from 1 to 120 hpf. (A) Representative images of the embryos. (B) The survival rate and (C) the hatching rate in zebrafish embryos exposed to dutasteride ($n = 20$). Data are expressed as mean ± SD.

Labomics S.A., Nivelles, Belgium) (Azeem et al., 2017) and the PiggyBac transposon system for zfAR (pPB-Puro-CAG > zAR; VectorBuilder Inc., Chicago, IL, USA), according to the manufacturer's instructions. After that, HEK293-ARE-zfAR cells were then maintained in a complete medium with hygromycin (10 μg/mL) and puromycin (2 μg/mL). For the measurement of ARE-zfAR response activity, HEK293-ARE-zfAR cells were seeded on black 96 well plates at a density of 1.0×10^5 cells/mL in an androgen-free medium containing charcoal-stripped FBS. After 24 h, each well was treated with DHT, flutamide as an antagonist (Park et al., 2024), or dutasteride for 48 h. Fluorescence intensity was measured using a Spark multimode microplate reader (Tecan) at excitation and emission wavelengths of 485 and 528 nm for eGFP and 590 and 645 nm for mCherry signals, respectively.

2.8. Statistical analysis

All results were obtained from at least three independent experiments. Data are expressed as the mean ± standard deviation. Statistical differences in each group were determined by one-way analysis of variance (ANOVA) followed by Tukey's honestly significant difference test using GraphPad Prism software (version 9.5.1; GraphPad Software, San Diego, CA, USA). Correlation analysis was performed using the "psych" package in R to investigate the relationship between each group (https://cran.r-project.org/web/packages/psych/psych.pdf). Before calculating each correlation coefficient, the dataset was subjected to the Shapiro-Wilk test using the basic function in the R open-source software. All test groups followed a Gaussian distribution ($p > 0.05$).

3. Results

3.1. MTC and toxicity of dutasteride in zebrafish embryos

The survival and hatching rate of zebrafish embryos exposed to dutasteride (0.005, 0.05, 0.1, 0.5, 1, and 2 μM) were evaluated. Due to the low solubility of dutasteride, the highest concentration was 2 μM. Up to 2 μM dutasteride exposure, no morphologic abnormalities were observed (Fig. 2A). There was no difference in the survival rate up to 2 μM exposure compared to the control (Fig. 2B). The hatching rate was similar to the survival rate (Fig. 2C). Up to 2 μM exposure, the hatching rates were approximately 75 % at 72 hpf and >90 % hatching rate at 96 hpf.

3.2. Measurement of zf5SRD5A activity and inhibitory effect of dutasteride

For the calculation of Km, T was treated to different concentration (0.1, 0.33, 1, 3.3, 10, and 33 μM) for 24 h, and Michaelis-Menten model was used for curve fitting of measured DHT level (Fig. 3A). The calculated Km values for the zfSRD5A isoforms (SRD5A1, SRD5A2a, SRD5A2b, and SRD5A3) were 35.24, 25.88, 12.40, and 22.53 μM, respectively. Based on the calculated Km value, an inhibition assay was conducted by co-treating the cells with different concentrations of dutasteride (0.1, 0.5, 1, 2, 5, 10, 50, and 100 nM) and T (Fig. 3B). The half-maximal inhibitory concentrations (IC_{50}) of each isoform (SRD5A1, SRD5A2a, SRD5A2b, and SRD5A3) were 28.85, 43.17, 2.76, and 10.84 nM, respectively.

3.3. Measurement of DHT, E2, and VTG levels

The exposure of zebrafish embryos to dutasteride significantly decreased DHT, E2, and VTG levels in a concentration-dependent manner. Significant decreases in DHT, E2 and VTG levels were observed at 0.05, 0.005, and 0.005 μM dutasteride exposure, respectively (Fig. 4A-C). A correlation analysis between DHT, E2, and VTG levels in each group was performed (Fig. 4D). The analysis involved the Pearson's correlation coefficient between individual expression levels and a scatter plot of each dataset. Strong positive correlations were observed between DHT-VTG ($r_p = 0.81$, $p < 0.001$) and E2-VTG ($r_p = 0.84$, $p < 0.001$). The correlation coefficient between the DHT and VTG was 0.66 ($p < 0.001$).

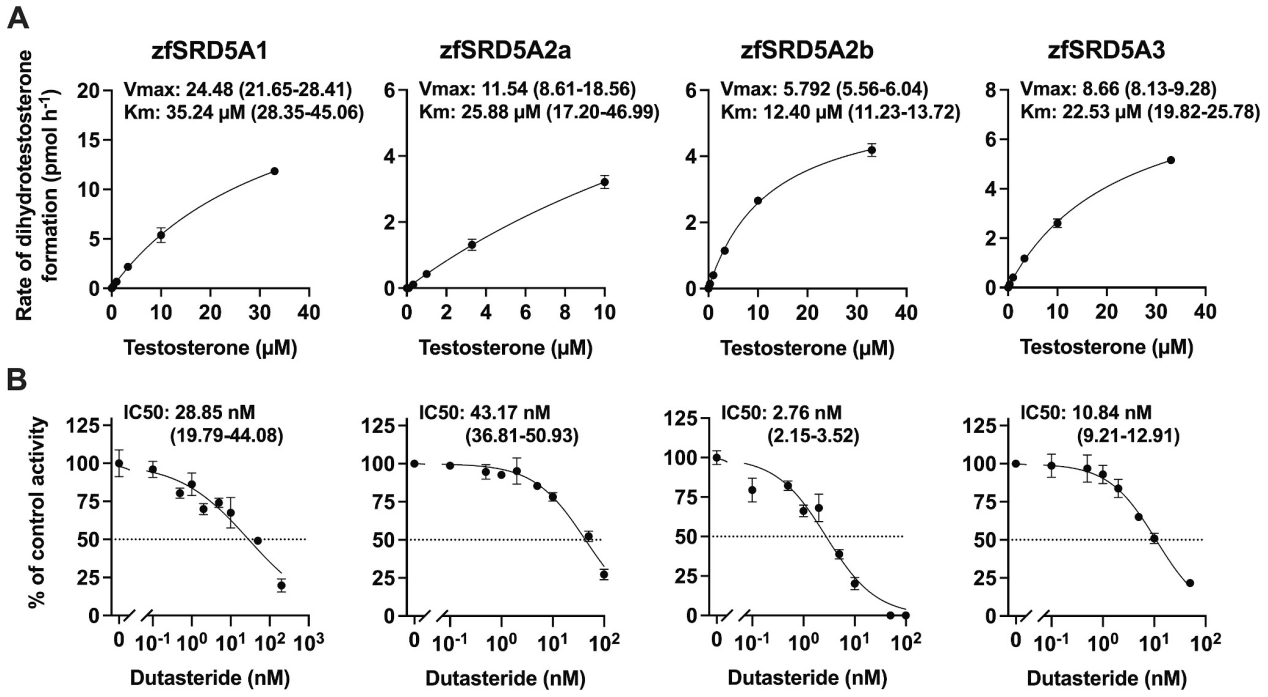

Fig. 3. (A) Activity of zebrafish SRD5A isoforms and (B) inhibitory effect of dutasteride on transiently transfected HEK293 cells. In the fig. (A and B), the order of the isoforms is zfSRD5A1, zfSRD5A2a, zfSRD5A2b, and zfSRD5A3, respectively. Data are expressed as mean ± SD of three repeated experiments ($n \geq 3$). Vmax, Km, and IC_{50} values were presented as 95 % confidence intervals in parentheses.

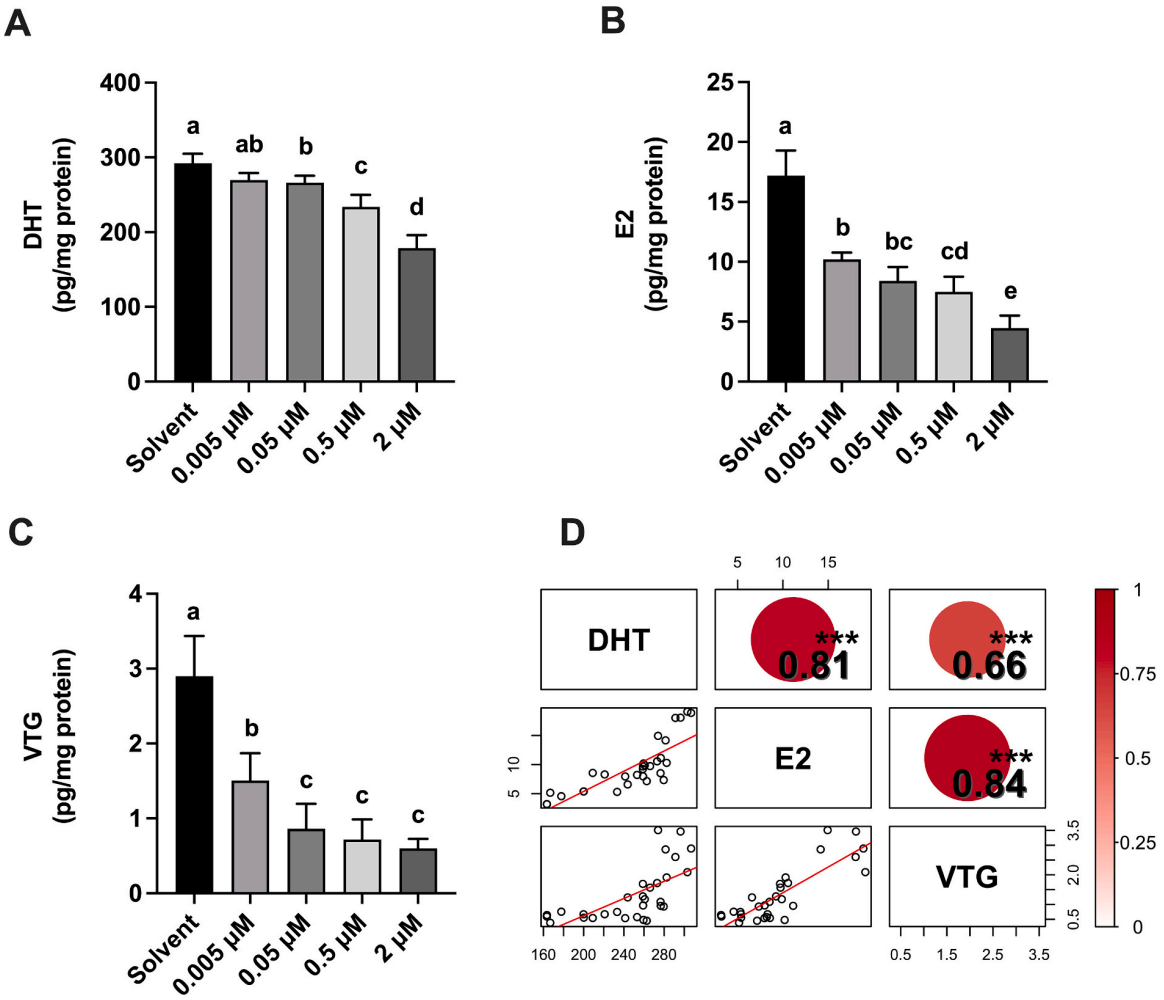

Fig. 4. The level of steroid hormones (DHT and E2) and VTG in zebrafish embryos exposed to dutasteride from 72 to 120 hpf. (A) DHT, (B) E2, and (C) VTG levels were measured by ELISA ($n \geq 5$). Data are expressed as mean ± SD. Different letter for a single substance indicates a significant difference at $p < 0.05$, according to ANOVA with Tukey's multiple comparison tests. (D) Correlation matrix between DHT, E2, and VTG levels. The upper displays Pearson's correlation coefficients (r_p). The color intensity indicates the strength of the correlation. The lower displays scatter plots of each data set with linear regression lines.

3.4. Gene expression level of zebrafish embryos exposed to dutasteride

To investigate changes at the molecular level caused by dutasteride exposure, the expression levels of reproductive-related genes (*srd5a2*, *cyp19a1*, *esr1*, *esr2a*, *esr2b*, and *vtg*) were measured (Fig. 5A-F). The expression levels of *srd5a2* decreased from 0.05 μM and *cyp19a1* decreased in a concentration-dependent manner after 0.005 μM exposure (Fig. 5A-B). Among the three subtype genes encoding ER, the expression level of *esr1* was significantly decreased after 0.005 μM dutasteride exposure, *esr2a* was decreased after dutasteride 2 μM exposure, *esr2b* was decreased after 0.5 and 2 μM dutasteride exposure (Fig. 5C-E). The expression level of *vtg* decreased in a concentration-dependent manner after 0.05 to 2 μM exposure (Fig. 5F). To verify the correlation between reproductive factors and gene expression levels, a correlation analysis between the expression levels of each group was performed (Fig. 5G). The analysis involved Pearson's correlation coefficient between individual expression levels and a scatter plot of each dataset. The strong positive correlations >0.7 were shown at the *srd5a2-esr1* ($p < 0.001$), *-esr2b* ($p < 0.001$), and *-vtg* ($p < 0.001$), *cyp19a1-esr1* ($p < 0.001$), *-vtg* ($p < 0.001$), *esr1-esr2b* ($p < 0.001$), and *-vtg* ($p < 0.001$), *esr2a-esr2b* ($p < 0.001$), and *esr2b-vtg* ($p < 0.001$). The correlation coefficient for the other groups ranged from 0.48 to 0.68, indicating a moderate positive correlation ($p < 0.001$).

3.5. Molecular docking for zfER and zfAR with dutasteride and response activity of ARE-zfAR

Docking simulations between the receptors and chemicals revealed multiple docking poses for each ligand-binding site. The best pose for each docking simulation is shown in Fig. 6A, and the number of interactions and binding free energies are listed in Table S1. For zfERα, the docking complex with E2 showed 20 interactions, including 3 hydrogen bonds, 10 hydrophobic interactions, and 7 Van der Waals interactions. The binding free energies were −10.6 (Vina) and −49.8 (CDOCKER) Kcal/mol, respectively. Dutasteride was docked to zfERα, revealing a binding affinity of −9.8 (Vina) and −56.4 (CDOCKER) Kcal/mol, along with 2 hydrogen bonds, 3 hydrophobic interactions, 9 van der Waals interactions, and 1 halogen interaction. In zfAR, the docking complex with DHT exhibited 22 interactions, including 3 hydrogen bonds, 7 hydrophobic interactions, and 12 van der Waals interactions, with a binding free energy of −9.6 (Vina) and −43.2 (CDOCKER) kcal/mol. The docking of dutasteride to zfAR showed a binding affinity of −9.8 (Vina) and −86.07 (CDOCKER) Kcal/mol, accompanied by 1 hydrogen bond, 8 hydrophobic interactions, 9 van der Waals interactions, and 2

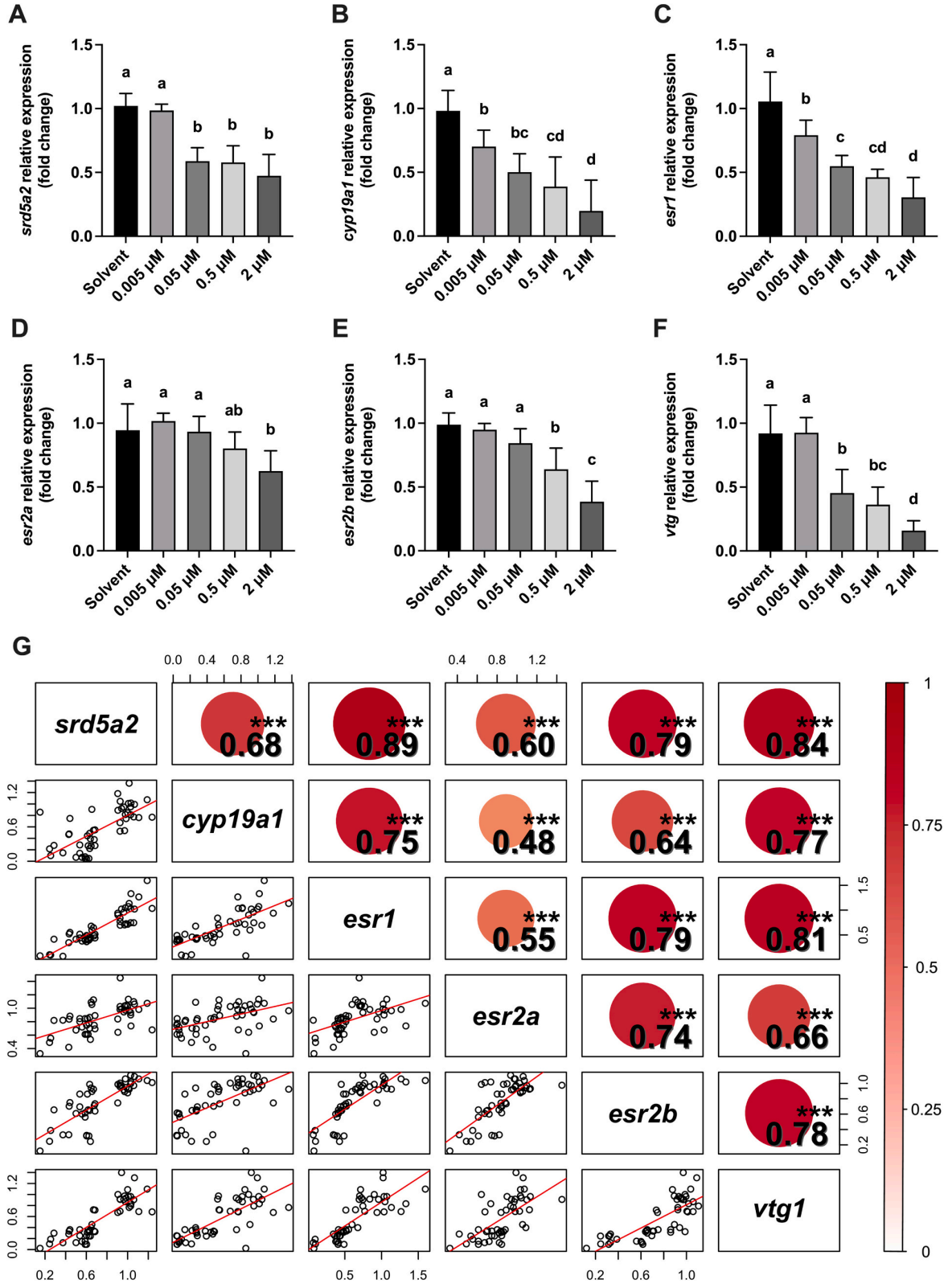

Fig. 5. Relative expression levels of genes in zebrafish embryos exposed to dutasteride from 72 to 120 hpf. The expression levels of (A) *srd5a2*, (B) *cyp19a1* (C) *esr1*, (D) *esr2a*, (E) *esr2b*, (C), and (F) *vtg* were quantified by RT-qPCR ($n \geq 5$). Data are expressed as mean ± SD. Different letter for a single substance indicates a significant difference at $p < 0.05$, according to ANOVA with Tukey's multiple comparison tests. (G) Correlation matrix between gene expression levels. The upper triangle displays Pearson's correlation coefficients (r_p). The color intensity indicates the strength of the correlation. Lower triangle displays scatter plots of each data set with linear regression lines.

halogen interactions.

ARE-zfAR response activity was measured to confirm the molecular docking results. The mCherry fluorescent signal activity showed a dose-dependent increase in the ARE reporter response following treatment with DHT (Fig. 6B-C). Treatment with flutamide, an AR antagonist, resulted in a dose-dependent decrease in the mCherry signal (Fig. 6C). Dutasteride did not significantly decrease the mCherry signal up to the maximum concentration (50 nM).

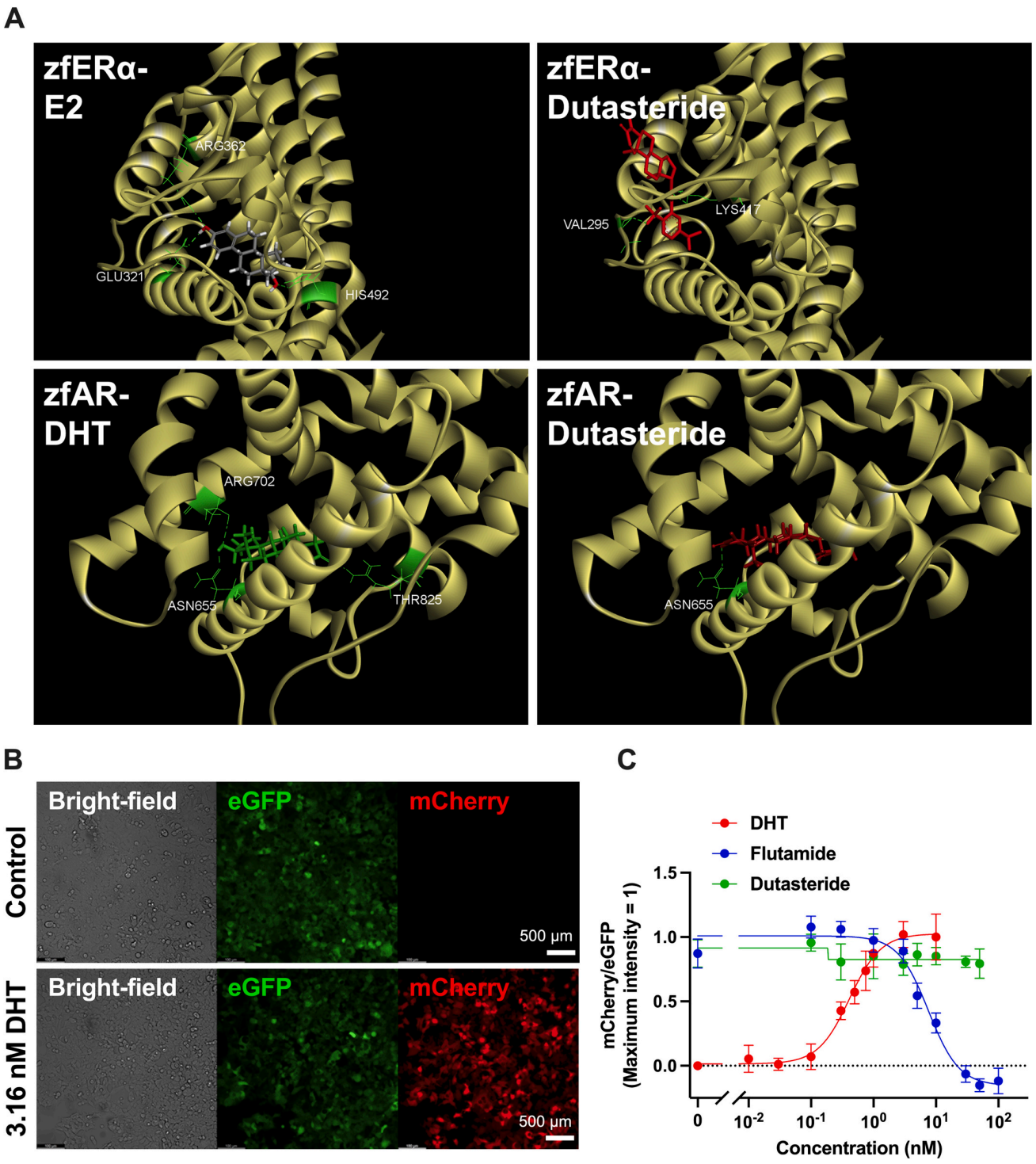

Fig. 6. Representative molecular docking images of (A) E2 and dutasteride with zfERα and DHT and dutasteride with zfAR. The green color indicates the residues interacting with ligands via hydrogen bonds. (B) Fluorescence image on HEK293-ARE-zfAR treated to 0.1 % DMSO (control) and 3.16 nM DHT. (C) ARE-zfAR response activities to DHT, flutamide, and dutasteride. Data are expressed as mean ± SD ($n \geq 4$).

3.6. Gene expression level of zebrafish embryos co-exposed to dutasteride and/or DHT

It was necessary to determine whether the change in molecular signaling under reduced DHT concentrations in zebrafish embryos could be restored by SRD5A inhibition. This study investigated the effect of DHT treatment on reproduction-related gene expression in the presence and absence of dutasteride. DHT exposure was at a concentration of 0.5 μM, and the exposure concentration of dutasteride was selected at 0.5 and 2 μM, based on previous experiments that demonstrated a significant reduction in expression levels. The exposure to 0.5 μM DHT significantly increased the expression levels of *srd5a2*, *cyp19a1*, *esr1*, *esr2a*, *esr2b*, and *vtg* in comparison to the control (Fig. 7). In contrast to the findings presented in Fig. 5A-F, which indicate a reduction in gene expression, the levels of *srd5a2*, *cyp19a1*, *esr1*, *esr2a*, *esr2b*, and *vtg* expression in the DHT with dutasteride co-exposure group were not significantly different from those in the control group (Fig. 7).

4. Discussion

Previously, we developed an AOP that demonstrated that SRD5A inhibitors led to impaired fecundity in female fish (AOP-Wiki, 2022). In this AOP, inhibition of SRD5A was identified as the MIE. This inhibition results in decreased expression of DHT (KE1), which subsequently downregulates androgen signaling. Downregulation of androgen signaling leads to decreased E2 (KE2). The reduction in E2 levels caused a decline in VTG protein production (KE3), ultimately leading to decreased fertility (AO) (Fig. 1). However, the key event relationship (KER) linking decreased DHT and decreased E2 levels remains incompletely understood, and evidence involved in this relationship is needed to clarify the mechanisms. In this study, we investigated a series of pathways involving DHT by measuring the sequential relationship of each KE, such as reproduction-related factors including hormone levels (DHT and E2), VTG levels, and gene expression levels in zebrafish embryos. For the inhibition of SRD5A, dutasteride was employed due to its broad-spectrum inhibition, allowing for a more comprehensive reduction in DHT levels.

The MTC on phenotype image, mortality, and hatching rate confirmed the absence of toxicity, including morphological abnormalities up to 2 μM exposure of dutasteride on zebrafish embryos. SRD5A inhibition is known to decrease DHT levels with a high correlation. This finding is supported by García-García et al. who observed a significant decline in the expression of *srd5a* and DHT in gilthead seabream (*Sparus aurata*) following finasteride exposure. Additionally, our previous study demonstrated the inhibitory effect of dutasteride on zebrafish liver cells, with an IC_{50} value of 7.33 nM (Kim et al., 2021). This study confirmed

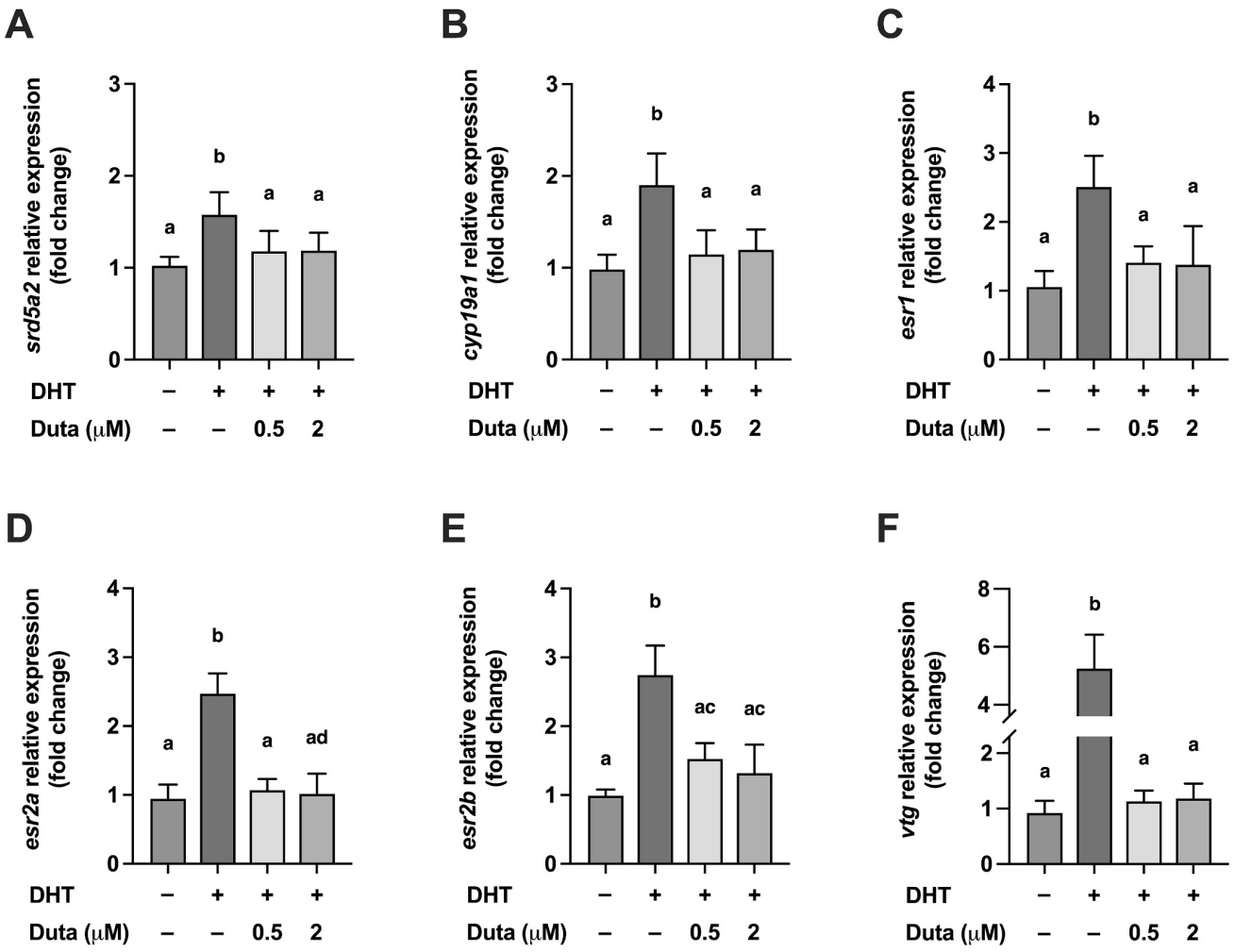

Fig. 7. Relative expression levels of genes in zebrafish embryos exposed dutasteride and/or 0.5 μM DHT from 72 to 120 hpf. The expression levels of (A) *srd5a2*, (B) *cyp19a1* (C) *esr1*, (D) *esr2a*, (E) *esr2b*, (C), and (F) *vtg* were quantified by RT-qPCR ($n \geq 4$). Data are expressed as mean ± SD. A different letter for single substance indicates a significant difference at the $p < 0.05$, according to ANOVA with Tukey's multiple comparison tests.

the inhibitory effects of dutasteride on zfSRD5A isoforms (SRD5A1, SRD5A2a, SRD5A2b, and SRD5A3) in a transiently transfected cell line with IC_{50}. The values for the isoforms ranged from 2.76 to 43.17 nM (Fig. 3), and a concentration-dependent decrease in DHT levels was observed in zebrafish embryos following exposure to up to 2 μM dutasteride (Fig. 4A). However, even exposure to high concentrations of dutasteride which sufficiently inhibited SRD5A, reduced DHT levels by approximately 69 %. This may be attributed to the relatively high basal levels of DHT in the eggs or yolks received from the mother. Alternatively, there are three potential biosynthetic pathways for DHT: the front-door pathway and two back-door pathways (Cai et al., 2011). The front-door pathway, a classical pathway, is involved in the conversion of T to DHT. Two non-canonical backdoor pathways are involved in the production of DHT by utilizing intermediate substrates, including progesterone, androsterone, androstanediol, dehydroepiandrosterone, androstenedione, and androstenedione (Zhou et al., 2021). In humans, clinical deficiency of SRD5A type 2 has been associated with increased expression of enzymes responsible for DHT production via backdoor pathways, as well as enhanced activity of chemical transformation of the relevant steroidogenic enzymes, which involve alternative DHT synthesis pathways (Zhou et al., 2021; Auchus, 2004; Mostaghel, 2014). Although the evidence is not yet clear in fish, it has been suggested that the upregulation of alternative signaling pathways compensates for the downregulation of the classic DHT synthesis pathway upon exposure to dutasteride.

Zebrafish embryos hatch approximately 72 h hpf, exhibiting anatomical development and the ability to express genes such as aromatase and ERs, which are crucial for the synthesis of endogenous E2 (von Hellfeld et al., 2020; Cohen et al., 2022; Sawyer et al., 2006; Trant et al., 2001). Similarly, *srd5a* isoforms are expressed at an early stage of development in fathead minnow embryos (Martyniuk et al., 2014). With regard to gene regulation, the *srd5a2* regulates prostate genes by establishing a feedback loop (Zager and Barton, 2012). In rats, DHT administration upregulates the expression of SRD5A. This increase in expression enhances transcriptional activity through a feed-forward mechanism in which DHT promotes its own biosynthesis (Torres et al., 2003). Conversely, the administration of finasteride in rats resulted in a reduction in DHT levels, which in turn led to the downregulation of SRD5A genes in a DHT-dependent manner (George et al., 1991). Furthermore, DHT can be converted to 5α-androstane-3β,17β-diol (3βAdiol), an androgen metabolite, through the actions of two key enzymes, 17β-hydroxysteroid dehydrogenase (17β-HSD) and 3β-hydroxysteroid dehydrogenase (3β-HSD) (Handa et al., 2008). 3βAdiol may bind to ERβ1 and induce ERE-mediated transcription by recruiting coactivators from ERα and ERβ2 (Pak et al., 2007; Pak et al., 2005).

Ishikawa et al. also suggested the possibility that SRD5A inhibitor could reduce the conversion of DHT into estrogenic steroid like 3βAdiol. Similarly, our finding demonstrated that dutasteride exposure led to the down-regulation of both androgenic and estrogenic factors. Specifically, the positive correlation between DHT and E2 (Fig. 4D), as well as between *srd5a2* and other reproductive gene expression levels (Fig. 5G), suggests a potential link between DHT level and estrogenic signalings. This evidence raises the posibility that DHT might function as a source of estrogen or play a role in estrogen signaling (Ishikawa et al., 2006). Aromatase (encoded by *cyp19a1a* and *cyp19a1b*, which are specifically expressed in the gonads and brain, respectively) is an important factor in sex differentiation in fish (Chiang et al., 2001). The *cyp19a1b* promoter contains estrogen and androgen response elements (ERE and ARE) (Mouriec et al., 2009). Several studies have demonstrated that aromatase is positively regulated by estrogen in fish. However, the effects of androgens are poorly understood (Menuet et al., 2005; Le Page et al., 2008; Le Page et al., 2006). Some studies have demonstrated that DHT is an effective activator of aromatase expression in zebrafish and stimulated expression of the aromatase gene has been observed following exposure to DHT (Mouriec et al., 2009; Lassiter and Linney, 2007). This indicates that androgens may regulate aromatase expression in the same manner as estrogens. ERs (encoded by *esr1*, *esr2a*, and *esr2b* in zebrafish) are known to be induced by estrogens, and their activation is highly related to vitellogenesis (Nelson and Habibi, 2013). Conversely, this implies that ER transcription and, by extension, VTG transcription can be regulated by estrogen. Although studies have suggested that DHT may regulate androgenic and estrogenic signaling, the specific relationship between DHT and estrogenic effects remains challenging to determine.

The molecular docking interactions between zfERα and E2 were consistent with those observed in a previous study (Park et al., 2022). Similarly, our previous work identified hydrogen bond interactions between ASN705, ARG752, and THR877 in the hAR-DHT complex (Park et al., 2024). Furthermore, critical poses of amino acid residues for ligand recognition in the hAR and hERα receptors have been reported in prior studies, highlighting the key roles of residues in the ligand-binding pocket (LBP) in transactivation (Ekena et al., 1996; Helsen et al., 2012; Nadal et al., 2017). The previously conducted docking simulations of E2 yielded results consistent with those of the current study (Gonzalez et al., 2019). In our study, dutasteride was docked into the LBP of zfERα, though different docking sites were observed compared to the E2-zfERα complex. For zfAR, dutasteride interacted in a position similar to that of DHT near the LBP site. However, assessment of ARE-zfAR response activity indicated that dutasteride did not have an antagonistic effect on zfAR binding (Fig. 6C). Despite the presence of a hydrogen bond in the zfAR-dutasteride complex aligning with the zfAR-DHT complex (ASN655, ARG702, and THR825), this suggests that dutasteride does not impact zfAR-DHT binding interactions. These findings imply dutasteride does not act like antagonistic chemicals in zfERα and zfAR, respectively.

The present study demonstrated that dutasteride decreased DHT, E2, and VTG levels in zebrafish embryos, an effect that was independent of interactions with ER and AR as well as the gene expression levels associated with these signals. These findings suggest that dutasteride-induced DHT levels play a crucial role in steroid hormone signaling. This hypothesis is supported by the present results (Fig. 7). DHT has received little attention in fish owing to its dominant androgens (T and 11-KT) and 12- and 20-fold lower levels of DHT compared to T in male and female fathead minnow, respectively (Martyniuk et al., 2014; Margiotta-Casaluci et al., 2013b). Nevertheless, despite its low levels, DHT not only exhibits a high affinity for AR binding but also demonstrates unexpected responses to the steroid hormone biosynthetic pathway and androgenic signaling (Lee et al., 2015; Sperry and Thomas, 1999). Previous studies have demonstrated that DHT regulates VTG synthesis by binding to the ER in the liver of black goby (*Gobius niger*). This estrogenic effect is more pronounced in female and E2-treated male hepatocytes than in untreated male hepatocytes (Le Menn et al., 1980; Kim et al., 2003; Flouriot et al., 1996). Riley et al. (2004) demonstrated that exposure to 5 μM DHT for 48 h in female tilapia (*Oreochromis mossambicus*) hepatocytes increased VTG release, while co-treatment of DHT with tamoxifen inhibited VTG production. These findings provide evidence that DHT may be involved in the estrogenic signaling pathway, suggesting that the level of DHT is important for signaling associated with reproduction. These findings are consistent with the results of the present study, which demonstrated that DHT treatment resulted in increased gene expression levels and that dutasteride treatment with DHT led to the recovery of these levels (Fig. 7).

5. Conclusion

The present study demonstrated that dutasteride inhibited SRD5A activity in zebrafish, resulting in a reduction in E2 and VTG levels, as well as gene expression levels (*srd5a2a*, *cyp19a1*, *esr1*, *esr2a*, *esr2b*, and *vtg*). Furthermore, the inhibitory effect of dutasteride was independent of ER and AR interactions. The positive correlations observed between DHT and -E2 and -VTG, and between *srd5a2* and other genes (*cyp19a1*, *esr1*, *esr2a*, *esr2b*, and *vtg*) suggest a close relationship between them, providing valuable insights into the response-response relationship for

the development of quantitative AOP (qAOP) from downstream to upstream key events. The results of the co-treatment experiment with dutasteride and DHT showed that the decreased gene expression levels after exposure to dutasteride recovered to the control level, which proved that DHT is important in reproductive signaling. This finding supports the hypothesis that DHT levels are important for reproductive signaling. Although our results do not provide evidence of a direct relationship between DHT and E2 levels, the estrogenic effect of DHT was indirectly confirmed by molecular docking and gene expression results. These results provide additional evidence to support the development of qAOP. Consequently, further studies are required to identify alternative pathways for DHT synthesis in fish.

Supplementary data to this article can be found online at https://doi.org/10.1016/j.cbpc.2024.110048.

Funding sources

This research was supported by the Korea Environmental Industry and Technology Institute through the Core Technology Development Project for Environmental Diseases Prevention and Management (2021003310001), funded by the Korea Ministry of Environment and Bio-cluster Industry Capacity Enhancement Project of Jeonbuk Technopark (JBTP).

CRediT authorship contribution statement

Hyunki Cho: Writing – review & editing, Writing – original draft, Validation, Investigation, Formal analysis, Data curation. **Indong Jun:** Writing – review & editing, Writing – original draft, Visualization, Investigation, Data curation. **Karim Md Adnan:** Writing – review & editing, Visualization, Data curation. **Chang Gyun Park:** Writing – review & editing, Visualization, Formal analysis, Data curation. **Sang-Ah Lee:** Writing – review & editing, Visualization, Formal analysis, Data curation. **Juyong Yoon:** Writing – review & editing, Validation, Data curation. **Chang Seon Ryu:** Writing – review & editing, Writing – original draft, Visualization, Validation, Supervision, Methodology, Conceptualization. **Young Jun Kim:** Writing – review & editing, Supervision, Project administration, Funding acquisition.

Declaration of competing interest

The authors declare that they have no known competing financial interests or personal relationships that could have appeared to influence the work reported in this paper.

Data availability

Data will be made available on request.

Acknowledgments

None.

References

Ankley, G.T., Bennett, R.S., Erickson, R.J., Hoff, D.J., Hornung, M.W., Johnson, R.D., Mount, D.R., Nichols, J.W., Russom, C.L., Schmieder, P.K., Serrrano, J.A., Tietge, J. E., Villeneuve, D.L., 2010. Adverse outcome pathways: a conceptual framework to support ecotoxicology research and risk assessment. Environ. Toxicol. Chem. 29, 730–741. https://doi.org/10.1002/etc.34.

AOP-Wiki, 2022. Inhibition of 5α-reductase leading to impaired fecundity in female fish. https://aopwiki.org/aops/289. (Accessed 5 July 2024).

Auchus, R.J., 2004. The backdoor pathway to dihydrotestosterone. Trends Endocrinol. Metab. 15, 432–438. https://doi.org/10.1016/j.tem.2004.09.004.

Azeem, W., Hellem, M.R., Olsen, J.R., Hua, Y., Marvyin, K., Qu, Y., Lin, B., Ke, X., Øyan, A.M., Kalland, K.H., 2017. An androgen response element driven reporter assay for the detection of androgen receptor activity in prostate cells. PloS One 12, e0177861. https://doi.org/10.1371/journal.pone.0177861.

Bradbury, S.P., Feijtel, T.C., Van Leeuwen, C.J., 2004. Meeting the scientific needs of ecological risk assessment in a regulatory context. Environ. Sci. Technol. 38, 463a–470a. https://doi.org/10.1021/es040675s.

Cai, C., Chen, S., Ng, P., Bubley, G.J., Nelson, P.S., Mostaghel, E.A., Marck, B., Matsumoto, A.M., Simon, N.I., Wang, H., Chen, S., Balk, S.P., 2011. Intratumoral de novo steroid synthesis activates androgen receptor in castration-resistant prostate cancer and is upregulated by treatment with CYP17A1 inhibitors. Cancer Res. 71, 6503–6513. https://doi.org/10.1158/0008-5472.Can-11-0532.

Chiang, E.F., Yan, Y.L., Tong, S.K., Hsiao, P.H., Guiguen, Y., Postlethwait, J., Chung, B.C., 2001. Characterization of duplicated zebrafish cyp19 genes. J. Exp. Zool. 290, 709–714. https://doi.org/10.1002/jez.1121.

Cohen, A., Popowitz, J., Delbridge-Perry, M., Rowe, C.J., Connaughton, V.P., 2022. The role of estrogen and thyroid hormones in zebrafish visual system function. Front. Pharmacol. 13, 837687. https://doi.org/10.3389/fphar.2022.837687.

Ekena, K., Weis, K.E., Katzenellenbogen, J.A., Katzenellenbogen, B.S., 1996. Identification of amino acids in the hormone binding domain of the human estrogen receptor important in estrogen binding. J. Biol. Chem. 271, 20053–20059. https://doi.org/10.1074/jbc.271.33.20053.

Flouriot, G., Pakdel, F., Valotaire, Y., 1996. Transcriptional and post-transcriptional regulation of rainbow trout estrogen receptor and vitellogenin gene expression. Mol. Cell. Endocrinol. 124, 173–183. https://doi.org/10.1016/s0303-7207(96)03960-3.

García-García, M., Sánchez-Hernández, M., García-Hernández, M.P., García-Ayala, A., Chaves-Pozo, E., 2017. Role of 5α-dihydrotestosterone in testicular development of gilthead seabream following finasteride administration. J. Steroid Biochem. Mol. Biol. 174, 48–55. https://doi.org/10.1016/j.jsbmb.2017.07.024.

George, F.W., Russell, D.W., Wilson, J.D., 1991. Feed-forward control of prostate growth: dihydrotestosterone induces expression of its own biosynthetic enzyme, steroid 5 alpha-reductase. Proc. Natl. Acad. Sci. U. S. A. 88, 8044–8047. https://doi.org/10.1073/pnas.88.18.8044.

González, A., Fernandino, J.I., Somoza, G.M., 2015. Effects of 5α-dihydrotestosterone on expression of genes related to steroidogenesis and spermatogenesis during the sex determination and differentiation periods of the pejerrey, Odontesthes bonariensis. Comp. Biochem. Physiol. A Mol. Integr. Physiol. 182, 1–7. https://doi.org/10.1016/j.cbpa.2014.12.003.

Gonzalez, T.L., Rae, J.M., Colacino, J.A., Richardson, R.J., 2019. Homology models of mouse and rat estrogen receptor-α ligand-binding domain created by in silico mutagenesis of a human template: molecular docking with 17ß-estradiol, diethylstilbestrol, and paraben analogs. Comput. Toxicol. 10, 1–16. https://doi.org/10.1016/j.comtox.2018.11.003.

Handa, R.J., Pak, T.R., Kudwa, A.E., Lund, T.D., Hinds, L., 2008. An alternate pathway for androgen regulation of brain function: activation of estrogen receptor beta by the metabolite of dihydrotestosterone, 5alpha-androstane-3beta,17beta-diol. Horm. Behav. 53, 741–752. https://doi.org/10.1016/j.yhbeh.2007.09.012.

He, J.H., Gao, J.M., Huang, C.J., Li, C.Q., 2014. Zebrafish models for assessing developmental and reproductive toxicity. Neurotoxicol. Teratol. 42, 35–42. https://doi.org/10.1016/j.ntt.2014.01.006.

Helsen, C., Dubois, V., Verfaillie, A., Young, J., Trekels, M., Vancraenenbroeck, R., De Maeyer, M., Claessens, F., 2012. Evidence for DNA-binding domain–ligand-binding domain communications in the androgen receptor. Mol. Cell. Biol. 32, 3033–3043. https://doi.org/10.1128/mcb.00151-12.

Ishikawa, T., Glidewell-Kenney, C., Jameson, J.L., 2006. Aromatase-independent testosterone conversion into estrogenic steroids is inhibited by a 5 alpha-reductase inhibitor. J. Steroid Biochem. Mol. Biol. 98, 133–138. https://doi.org/10.1016/j.jsbmb.2005.09.004.

Kim, B.H., Takemura, A., Kim, S.J., Lee, Y.D., 2003. Vitellogenin synthesis via androgens in primary cultures of tilapia hepatocytes. Gen. Comp. Endocrinol. 132, 248–255. https://doi.org/10.1016/s0016-6480(03)00091-1.

Kim, D., Cho, H., Eggers, R., Kim, S.K., Ryu, C.S., Kim, Y.J., 2021. Development of a liquid chromatography/mass spectrometry-based inhibition assay for the screening of steroid 5-α reductase in human and fish cell lines. Molecules 26. https://doi.org/10.3390/molecules26040893.

Kimmel, C.B., Ballard, W.W., Kimmel, S.R., Ullmann, B., Schilling, T.F., 1995. Stages of embryonic development of the zebrafish. Dev. Dyn. 203, 253–310. https://doi.org/10.1002/aja.1002030302.

Lassiter, C.S., Linney, E., 2007. Embryonic expression and steroid regulation of brain aromatase cyp19a1b in zebrafish (Danio rerio). Zebrafish 4, 49–57. https://doi.org/10.1089/zeb.2006.9995.

Le Menn, F., Rochefort, H., Garcia, M., 1980. Effect of androgen mediated by the estrogen receptor of fish liver: vitellogenin accumulation. Steroids 35, 315–328. https://doi.org/10.1016/0039-128x(80)90044-6.

Le Page, Y., Scholze, M., Kah, O., Pakdel, F., 2006. Assessment of xenoestrogens using three distinct estrogen receptors and the zebrafish brain aromatase gene in a highly responsive glial cell system. Environ. Health Perspect. 114, 752–758. https://doi.org/10.1289/ehp.8141.

Le Page, Y., Menuet, A., Kah, O., Pakdel, F., 2008. Characterization of a cis-acting element involved in cell-specific expression of the zebrafish brain aromatase gene. Mol. Reprod. Dev. 75, 1549–1557. https://doi.org/10.1002/mrd.20892.

Lee, M.R., Loux-Turner, J.R., Oliveira, K., 2015. Evaluation of the 5α-reductase inhibitor finasteride on reproduction and gonadal development in medaka, Oryzias latipes. Gen. Comp. Endocrinol. 216, 64–76. https://doi.org/10.1016/j.ygcen.2015.04.008.

Margiotta-Casaluci, L., Sumpter, J.P., 2011. 5α-dihydrotestosterone is a potent androgen in the fathead minnow (Pimephales promelas). Gen. Comp. Endocrinol. 171, 309–318. https://doi.org/10.1016/j.ygcen.2011.02.012.

Margiotta-Casaluci, L., Hannah, R.E., Sumpter, J.P., 2013a. Mode of action of human pharmaceuticals in fish: the effects of the 5-alpha-reductase inhibitor, dutasteride,

on reproduction as a case study. Aquat. Toxicol. 128-129, 113–123. https://doi.org/10.1016/j.aquatox.2012.12.003.
Margiotta-Casaluci, L., Courant, F., Antignac, J.P., Le Bizec, B., Sumpter, J.P., 2013b. Identification and quantification of 5α-dihydrotestosterone in the teleost fathead minnow (Pimephales promelas) by gas chromatography-tandem mass spectrometry. Gen. Comp. Endocrinol. 191, 202–209. https://doi.org/10.1016/j.ygcen.2013.06.017.
Martyniuk, C.J., Bissegger, S., Langlois, V.S., 2014. Reprint of "current perspectives on the androgen 5 alpha-dihydrotestosterone (DHT) and 5 alpha-reductases in teleost fishes and amphibians". Gen. Comp. Endocrinol. 203, 10–20. https://doi.org/10.1016/j.ygcen.2014.06.011.
McGrath, P., Li, C.Q., 2008. Zebrafish: a predictive model for assessing drug-induced toxicity. Drug Discov. Today 13, 394–401. https://doi.org/10.1016/j.drudis.2008.03.002.
Menuet, A., Pellegrini, E., Brion, F., Gueguen, M.M., Anglade, I., Pakdel, F., Kah, O., 2005. Expression and estrogen-dependent regulation of the zebrafish brain aromatase gene. J. Comp. Neurol. 485, 304–320. https://doi.org/10.1002/cne.20497.
Mostaghel, E.A., 2014. Beyond T and DHT - novel steroid derivatives capable of wild type androgen receptor activation. Int. J. Biol. Sci. 10, 602–613. https://doi.org/10.7150/ijbs.8844.
Mouriec, K., Gueguen, M.M., Manuel, C., Percevault, F., Thieulant, M.L., Pakdel, F., Kah, O., 2009. Androgens upregulate cyp19a1b (aromatase B) gene expression in the brain of zebrafish (Danio rerio) through estrogen receptors. Biol. Reprod. 80, 889–896. https://doi.org/10.1095/biolreprod.108.073643.
Nadal, M., Prekovic, S., Gallastegui, N., Helsen, C., Abella, M., Zielinska, K., Gay, M., Vilaseca, M., Taulès, M., Houtsmuller, A.B., van Royen, M.E., Claessens, F., Fuentes-Prior, P., Estébanez-Perpiñá, E., 2017. Structure of the homodimeric androgen receptor ligand-binding domain. Nat. Commun. 8, 14388. https://doi.org/10.1038/ncomms14388.
Nelson, E.R., Habibi, H.R., 2013. Estrogen receptor function and regulation in fish and other vertebrates. Gen. Comp. Endocrinol. 192, 15–24. https://doi.org/10.1016/j.ygcen.2013.03.032.
OECD, 2013. Test No. 236: Fish Embryo Acute Toxicity (FET) Test. OECD Publishing, Paris.
Pak, T.R., Chung, W.C., Lund, T.D., Hinds, L.R., Clay, C.M., Handa, R.J., 2005. The androgen metabolite, 5alpha-androstane-3beta, 17beta-diol, is a potent modulator of estrogen receptor-beta1-mediated gene transcription in neuronal cells. Endocrinology 146, 147–155. https://doi.org/10.1210/en.2004-0871.
Pak, T.R., Chung, W.C., Hinds, L.R., Handa, R.J., 2007. Estrogen receptor-beta mediates dihydrotestosterone-induced stimulation of the arginine vasopressin promoter in neuronal cells. Endocrinology 148, 3371–3382. https://doi.org/10.1210/en.2007-0086.
Park, C.G., Singh, N., Ryu, C.S., Yoon, J.Y., Esterhuizen, M., Kim, Y.J., 2022. Species differences in response to binding interactions of bisphenol A and its analogs with the modeled estrogen receptor 1 and in vitro reporter gene assay in human and zebrafish. Environ. Toxicol. Chem. 41, 2431–2443. https://doi.org/10.1002/etc.5433.
Park, C.G., Adnan, K.M., Cho, H., Ryu, C.S., Yoon, J., Kim, Y.J., 2024. A combined in vitro-in silico method for assessing the androgenic activities of bisphenol A and its analogues. Toxicol. In Vitro 98, 105838. https://doi.org/10.1016/j.tiv.2024.105838.
Riley, L.G., Hirano, T., Grau, E.G., 2004. Estradiol-17beta and dihydrotestosterone differentially regulate vitellogenin and insulin-like growth factor-I production in primary hepatocytes of the tilapia Oreochromis mossambicus. Comp. Biochem. Physiol. C Toxicol. Pharmacol. 138, 177–186. https://doi.org/10.1016/j.cca.2004.07.009.
Sawyer, S.J., Gerstner, K.A., Callard, G.V., 2006. Real-time PCR analysis of cytochrome P450 aromatase expression in zebrafish: gene specific tissue distribution, sex differences, developmental programming, and estrogen regulation. Gen. Comp. Endocrinol. 147, 108–117. https://doi.org/10.1016/j.ygcen.2005.12.010.
Schmittgen, T.D., Livak, K.J., 2008. Analyzing real-time PCR data by the comparative C (T) method. Nat. Protoc. 3, 1101–1108. https://doi.org/10.1038/nprot.2008.73.
Selderslaghs, I.W., Van Rompay, A.R., De Coen, W., Witters, H.E., 2009. Development of a screening assay to identify teratogenic and embryotoxic chemicals using the zebrafish embryo. Reprod. Toxicol. 28, 308–320. https://doi.org/10.1016/j.reprotox.2009.05.004.
Shen, M.Y., Sali, A., 2006. Statistical potential for assessment and prediction of protein structures. Protein Sci. 15, 2507–2524. https://doi.org/10.1110/ps.062416606.
Sperry, T.S., Thomas, P., 1999. Identification of two nuclear androgen receptors in kelp bass (Paralabrax clathratus) and their binding affinities for xenobiotics: comparison with Atlantic croaker (Micropogonias undulatus) androgen receptors. Biol. Reprod. 61, 1152–1161. https://doi.org/10.1095/biolreprod61.4.1152.
Spitsbergen, J.M., Kent, M.L., 2003. The state of the art of the zebrafish model for toxicology and toxicologic pathology research–advantages and current limitations. Toxicol. Pathol. 31 (Suppl), 62–87. https://doi.org/10.1080/01926230390174959.
Torres, J.M., Ruiz, E., Ortega, E., 2003. Development of a quantitative RT-PCR method to study 5alpha-reductase mRNA isozymes in rat prostate in different androgen status. Prostate 56, 74–79. https://doi.org/10.1002/pros.10221.
Trant, J.M., Gavasso, S., Ackers, J., Chung, B.C., Place, A.R., 2001. Developmental expression of cytochrome P450 aromatase genes (CYP19a and CYP19b) in zebrafish fry (Danio rerio). J. Exp. Zool. 290, 475–483. https://doi.org/10.1002/jez.1090.
Trott, O., Olson, A.J., 2010. AutoDock Vina: improving the speed and accuracy of docking with a new scoring function, efficient optimization, and multithreading. J. Comput. Chem. 31, 455–461. https://doi.org/10.1002/jcc.21334.
Villeneuve, D.L., Crump, D., Garcia-Reyero, N., Hecker, M., Hutchinson, T.H., LaLone, C. A., Landesmann, B., Lettieri, T., Munn, S., Nepelska, M., Ottinger, M.A., Vergauwen, L., Whelan, M., 2014. Adverse outcome pathway (AOP) development I: strategies and principles. Toxicol. Sci. 142, 312–320. https://doi.org/10.1093/toxsci/kfu199.
Volz, D.C., Belanger, S., Embry, M., Padilla, S., Sanderson, H., Schirmer, K., Scholz, S., Villeneuve, D., 2011. Adverse outcome pathways during early fish development: a conceptual framework for identification of chemical screening and prioritization strategies. Toxicol. Sci. 123, 349–358. https://doi.org/10.1093/toxsci/kfr185.
von Hellfeld, R., Brotzmann, K., Baumann, L., Strecker, R., Braunbeck, T., 2020. Adverse effects in the fish embryo acute toxicity (FET) test: a catalogue of unspecific morphological changes versus more specific effects in zebrafish (Danio rerio) embryos. Environ. Sci. Eur. 32, 122. https://doi.org/10.1186/s12302-020-00398-3.
Webb, B., Sali, A., 2016. Comparative protein structure modeling using MODELLER. Curr. Protoc. Bioinformatics 54, 5.6.1–5.6.37. https://doi.org/10.1002/cpbi.3.
Wu, G., Robertson, D.H., Brooks 3rd, C.L., Vieth, M., 2003. Detailed analysis of grid-based molecular docking: a case study of CDOCKER-A CHARMm-based MD docking algorithm. J. Comput. Chem. 24, 1549–1562. https://doi.org/10.1002/jcc.10306.
Zager, M.G., Barton, H.A., 2012. A multiscale, mechanism-driven, dynamic model for the effects of 5α-reductase inhibition on prostate maintenance. PloS One 7, e44359. https://doi.org/10.1371/journal.pone.0044359.
Zhou, J., Wang, Y., Wu, D., Wang, S., Chen, Z., Xiang, S., Chan, F.L., 2021. Orphan nuclear receptors as regulators of intratumoral androgen biosynthesis in castration-resistant prostate cancer. Oncogene 40, 2625–2634. https://doi.org/10.1038/s41388-021-01737-1.

8.3 Original paper − SRD5A inhibitor in *Daphnia magna*

Ecotoxicology and Environmental Safety 281 (2024) 116606

Contents lists available at ScienceDirect

Ecotoxicology and Environmental Safety

journal homepage: www.elsevier.com/locate/ecoenv

Adverse effects of the 5-alpha-reductase inhibitor finasteride on *Daphnia magna:* Endocrine system and lipid metabolism disruption

Hyunki Cho [a,b], Si-Eun Sung [c], Giup Jang [d], Maranda Esterhuizen [e], Chang Seon Ryu [a,*], Youngsam Kim [a,f,**], Young Jun Kim [a,f]

[a] Environmental Safety Group, KIST Europe Forschungsgesellschaft mbH, Saarbrücken 66123, Germany
[b] Department of Pharmacy, Saarland University, Saarbrücken, Germany
[c] Biologische Experimentalphysik, Saarland University, Saarbrücken, Germany
[d] MetaDx Laboratory, Seoul, South Korea
[e] University of Helsinki, Ecosystems and Environment Research Programme, Faculty of Biological and Environmental Sciences, Lahti, Finland
[f] Division of Energy & Environment Technology, University of Science & Technology, Daejeon 34113, South Korea

ARTICLE INFO

Edited by Dr Yong Liang

Keywords:
Finasteride
5-alpha-reductase inhibitor
D. magna
Endocrine distrusting chemical
Reproductive toxicity
Lipid metabolism

ABSTRACT

Finasteride, a steroid 5-alpha reductase inhibitor, is commonly used for the treatment of benign prostatic hyperplasia and hair loss. However, despite continued use, its environmental implications have not been thoroughly investigated. Thus, we investigated the acute and chronic adverse impacts of finasteride on *Daphnia magna*, a crucial planktonic crustacean in freshwater ecosystems selected as bioindicator organism for understanding the ecotoxicological effects. Chronic exposure (for 23 days) to finasteride negatively affected development and reproduction, leading to reduced fecundity, delayed first brood, reduced growth, and reduced neonate size. Additionally, acute exposure (< 24 h) caused decreased expression levels of genes crucial for reproduction and development, especially *EcR-A/B* (ecdysone receptors), *Jhe* (juvenile hormone esterase), and *Vtg2* (vitellogenin), with oxidative stress-related genes. Untargeted lipidomics/metabolomic analyses revealed lipidomic alteration, including 19 upregulated and 4 downregulated enriched lipid ontology categories, and confirmed downregulation of metabolites. Pathway analysis implicated significant effects on metabolic pathways, including the pentose phosphate pathway, histidine metabolism, beta-alanine metabolism, as well as alanine, aspartate, and glutamate metabolism. This comprehensive study unravels the intricate molecular and metabolic responses of *D. magna* to finasteride exposure, underscoring the multifaceted impacts of this anti-androgenic compound on a keystone species of freshwater ecosystems. The findings emphasize the importance of understanding the environmental repercussions of widely used pharmaceuticals to protect biodiversity in aquatic ecosystems.

1. Introduction

Steroid 5α-reductase (5AR; 3-oxo-5alpha-steroid 4-dehydrogenase) is an enzyme found in humans and other mammals, crucial for the conversion of testosterone to 5α-dihydrotestosterone (DHT), a potent androgen. Medications known as 5AR inhibitors, such as finasteride and dutasteride, are frequently prescribed to manage conditions such as benign prostatic hyperplasia (BPH) and androgenetic alopecia (AGA; male pattern baldness) (Salisbury and Tadi, 2023). Their mechanism of action involves suppressing the enzymatic activity of 5AR, subsequently leading to diminished DHT levels. The global finasteride market size is reported to be $362.1 million in 2021 and is expected to grow at a CAGR of 4.2 % until 2031 (Swapna Singh, 2023). Furthermore, in 2020 alone, over 2 million patients were prescribed finasteride, resulting in over 8 million prescriptions in United States (Kane, 2022). Growing concerns surround the environmental implications of 5AR inhibitors, especially given their increasing use. Despite the inherent persistence of 5AR inhibitors, characterized by their long half-life and high lipophilicity, comprehensive data on their concentrations in diverse environmental settings, ranging from wastewater and surface water to freshwater,

* Corresponding author.
** Corresponding author at: Environmental Safety Group, KIST Europe Forschungsgesellschaft mbH, Saarbrücken 66123, Germany.
E-mail addresses: changryu@kist-europe.de (C.S. Ryu), youngsam.kim@kist-europe.de (Y. Kim).

https://doi.org/10.1016/j.ecoenv.2024.116606
Received 22 February 2024; Received in revised form 5 June 2024; Accepted 14 June 2024

seawater, and soil, remain scarce. For instance, finasteride has been detected in the effluent and influent sludge of a domestic sewage treatment plant at concentrations of approximately 0.01 μg/L (Vieno et al., 2017). The NORMAN Network Database System (https://www.norman-network.com) recorded finasteride concentrations of 0.0064 μg/L in Ljubljana, Slovenia, and 0.0125 μg/L in Zilina, Slovakia. In the Stockholm region, data from 2020 revealed the presence of finasteride in surface water, with concentrations reaching up to 0.020 μg/L in Sweden's purified wastewater (Health and Medical Care Administration, 2023). Additionally, finasteride was also detected in aquatic invertebrate, caddisfly larvae (Hydropsychidae) near Melbourne, Australia (Richmond et al., 2018). Unfortunately, the environmental concentration of finasteride, particularly in areas with high consumption, is not well-researched. The persistence of the substance, coupled with the increasing demand for AGA treatments, highlights the importance of environmental impacts of 5AR inhibitors.

While several studies have examined for detailed information on the toxicity and side effects of 5AR inhibitors intended for human use, there is a noticeable gap in research on aquatic organisms. Few studies have documented the acute and chronic effects on various aquatic organisms, including fish (Garcia-Garcia et al., 2017; Lee et al., 2015; Margiotta-Casaluci et al., 2013), amphibians (Urbatzka et al., 2009), gastropods (Gilroy et al., 2020), and benthic invertebrates (Baynes et al., 2019). In contrast to research on these species that utilize steroids as hormones, the impact on ecdysteroid-dependent organisms is less understood. Given the pivotal role of these organisms in aquatic ecosystems, their potential susceptibility to drugs such as 5AR inhibitors, and their vulnerability to reproductive disturbances from such drugs, the necessity for such chronic reproductive studies becomes evident (Song et al., 2016; Song et al., 2017).

Daphnia magna, a planktonic crustacean found in freshwater environments stands as an ideal subject for this study due to its ecological importance and the role of ecdysteroids in its life cycle (Campioli et al., 2011; Ebert, 2022). In crustaceans like *D. magna*, ecdysteroids play an important role in growth, development, and maturation (Jordão et al., 2016; LeBlanc, 2007). To bridge this knowledge gap and elucidate the broader implications of finasteride, we investigated acute toxicity (immobilization and oxidative stress), acute responses of gene expression (*EcR-A*, *EcR-B*, *neverland*, *Jhe*, *chitinase*, *RXR*, *Hr96*, *Vtg2*, *sod*, *cat*, *gpx*, and *gst*) and chronic toxicity endpoints (reproduction and growth as body length) to understand the adverse effects of finasteride on *D. magna*. Furthermore, we explored the comprehensive relationship between metabolic changes in *D. magna* and its acute responses to finasteride exposure, employing high-resolution mass spectrometry (HRMS)-based untargeted metabolomics/lipidomics. To our knowledge, this is the first study assessing the chronic toxicity and molecular biological effects of 5AR inhibitor on daphnia species. The results of this study would provide that a holistic perspective on the impact of finasteride on the ecological dynamics of freshwater ecosystems.

2. Materials and methods

2.1. Solution preparation

Finasteride (Cas No. 98319–26–7; Y0000090; Merck, Darmstadt, Germany) was dissolved in dimethyl sulfoxide (DMSO) (Sigma-Aldrich, St. Louis, MO, USA) to a concentration of 5000 mg/L as the stock solution. Before addition to the culture media, the stock solution was diluted 100 times for chronic testing. The stock solution was replaced weekly. According to OECD TG 211 and 202 (OECD, 2004; OECD, 2012), Elendt M4 medium was prepared for the chronic test, and ISO medium IOS (6341):(2012) for the acute test, respectively.

2.2. Daphnia magna culture

Ephippia of *D. magna* (Micro Biotests Inc.; Gent, Belgium) were incubated for 72 hours under a 16-hour light/8-hour dark cycle with a light intensity of 7000 lux. This process was conducted in a climate-controlled incubator maintained at a temperature of 20.0 ± 1.0°C. To maintain the *D. magna*, fifteen individuals were placed in a 2 L glass beaker holding 1.5 L of Elendt M4 medium. *D. magna* was fed with *Chlorella vulgaris* (~1.5×10^8 cells/mL, 0.1 mg C/*D. magna*/day) daily and yeast, cerophyll, and trout chow (YCT) at a concentration of 0.5 μL/mL was provided three times weekly. To maintain optimal water quality and a favorable environment, the culture media and beakers were refreshed three times weekly, while new neonates were removed on a daily basis. Prior to each replacement and testing, parameters such as pH and dissolved oxygen levels were monitored. Consistent with ISO 6341 Field 18 guidelines, an interlaboratory test using potassium dichromate (Sigma-Aldrich; St. Louis, MO, United States) as a reference substance was routinely conducted to verify the test conditions' reliability.

2.3. Physiological, biochemical and molecular analyses

2.3.1. Immobilization and mortality tests

Following the OECD guideline 202 (OECD, 2004), 48 h-acute toxicity tests were conducted. Neonates (< 24 h) from the third brood of *D. magna* culture were exposed to various concentrations of finasteride (50.0, 40.0, 30.0, 27.5, 25.0, 22.5, 20.0, 17.5, 15.0, 10.0, 5.00, 0.50, and 0.10 mg/L), as well as a concurrent control series. The daphnids were placed in exposure groups, each in a specific concentration, and observed for any signs of immobilization or mortality ($n = 5$). Briefly, the groups consisted of four replicates, each containing five daphnids, for each finasteride concentration in the ISO medium. The exposures were conducted in six-well culture plates, each filled with 10 mL of the solution, and maintained for 48 hours. Immobilization was assessed visually within 15 seconds after gentle agitation. To ensure the reliability of the results, all experimental conditions were replicated three times.

2.3.2. Reproduction test

The reproductive tests were slightly modified from OECD TG 211 (OECD, 2012) to meet the criterion that the mean number of offspring per mother should exceed 60 at the end of the test. Briefly, neonates from the third brood of the *D. magna* cultures were randomly pooled. Twenty daphnids were exposed individually to each concentration (specify the concentrations again) versus a control series for 23 days. Each 100 mL beaker was filled with 60 mL of the designated solution. The medium in the control series contained 0.01 % DMSO as the solvent control. *D. magna* was fed daily with algae *C. vulgaris* (~1.5×10^8 cells/mL, 0.1 mg C/*D. magna*) and supplemented three times a week with YCT (0.5 μL/mL). Neonates from each beaker were counted daily. The solutions and beakers were renewed three times a week.

2.3.3. Body length measurement

The lengths of *D. magna* were measured at the end of the reproduction test using an Olympus CKX41 optical microscope (Olympus Inc., Tokyo, Japan). For measurement purposes, daphnids were carefully placed on glass slides, accompanied by a small volume of their respective medium. Using the ImageJ software, the body length was determined, extending from the center of the eye to the base of the apical spine (Schneider et al., 2012). Furthermore, thirty neonates from the third brood cultured in each group were randomly pooled to measure the size of the neonates following the same procedure. The concentration of 6.0 mg/L was excluded due to the lack of neonates from the third brood.

2.3.4. Reactive oxygen species (ROS) detection assay

Samples were obtained from 20 neonates. After exposure for the desired time (6, 24, or 48 hours) and concentrations (1.5, 3.0, 4.5 and 6.0 mg/L) including control (0.01 % DMSO) group, the daphnids were transferred to eppendorf (EP) tubes and rinsed with 1 mM phosphate-

buffered saline (PBS, pH 7.4). The samples were thoroughly homogenized in 200 μL of PBS and placed in an ice bath. The EP tubes were centrifuged at 3000 × g at 4°C for 10 min. Protein concentrations were assessed using the bicinchoninic acid kit from Thermo Fisher Scientific (Waltham, MA, USA). For ROS level determination, a cellular ROS assay kit from Abcam (Cambridge, UK) was used. Following the manufacturer's guidelines, these assays involved the use of 20 μL of supernatant from homogenized samples. The obtained fluorescent intensities ($\lambda_{ex/em}$ 495/529 nm) were then normalized against control samples, comprising untreated daphnids.

2.3.5. RNA isolation and real-time quantitative reverse transcription PCR (qRT-PCR)

Based on prior studies indicating the potential recovery of gene expression over time (Bang et al., 2015; Imhof et al., 2017), two post-treatment timeframes, 6 and 24 hours, were selected for evaluation. Five adult *D. magna*, approximately 17 days old, were subjected to 1.5 and 3.0 mg/L finasteride exposure including control (DMSO) group ($n = 3$). Subsequently, they were relocated to EP tubes and washed three times with distilled water. Using TRIzol reagent (Thermo Fisher Scientific; Waltham, MA, USA), the samples were homogenized, followed by the isolation of total RNA through a column-based extraction kit from Qiagen (Valencia, CA, USA). Subsequently, 1000 ng of RNA was subjected to reverse transcription with a high-capacity RNA-to-cDNA kit provided by Applied Biosystems (Foster City, CA, USA). The qRT-PCR assays were conducted with the Fast SYBR Green Master Mix from Applied Biosystems, utilizing the 7500 FAST Real-Time PCR System. The relative expression levels of all genes were determined using the $2^{-\Delta\Delta Ct}$ method (Schmittgen and Livak, 2008), with *D. magna* actin serving as the endogenous control (Actin) for normalization purposes. Details of the primer sequences and their references are listed in Table S1.

2.4. Lipidomic and metabolomic analyses

2.4.1. D. magna lipid sample extraction

Adult *D. magna* (17 days) were exposed in 100 mL beakers containing 50 mL of culture medium diluted with finasteride (1.5 and 3.0 mg/mL) and control group (0.01 % DMSO) for a period of 48 hours ($n \geq 3$). Then, the four daphnids were rinsed with deionized water and transferred to 2 mL microcentrifuge tubes containing beads. The samples were homogenized using a Precellys Evolution homogenizer (Bertin Technologies, France). The samples were dried under nitrogen and weighed, and extractions were conducted using a modified Matyash method (Sostare et al., 2018) with two-phase (polar and nonpolar) fractionation.

2.4.2. Untargeted lipidomics and metabolomics

An untargeted approach in lipidomics and metabolomics was employed, utilizing quadrupole time-of-flight (Q-TOF) high-resolution mass spectrometry (HRMS) to explore alterations in lipids and metabolites following finasteride treatment. The analysis of samples was conducted using a Triple TOF 6600+ QTOF mass spectrometer (AB Sciex, Framingham, MA, USA) coupled with an Electrospray ionization (ESI) source and an Exion AD Ultra-High-Performance Liquid Chromatography (UPLC) system (AB Sciex). A positive/negative calibration solution for the ESI source was used to correct the mass during the analysis for every five samples. The lipidomics analysis utilized a liquid chromatography (LC) method, employing an Acquity CSH C18 VanGuard pre-column (5 ×2.1 mm; 1.7 μm; Waters, USA) connected to Acquity UPLC CSH C18 column (100 ×2.1 mm; 1.7 μm), as following the methodology outlined in prior research (Tsugawa et al., 2015). All data were acquired using a TOF scan with sequential window acquisition of all theoretical mass spectra (SWATH). For the scan range m/z 100–1250, the scanning time was set at 50 ms for TOF and 35 ms for MS2 in 20 windows. Hydrophilic metabolite analysis was performed in hydrophilic interaction chromatography (HILIC) mode, utilizing an Acquity UPLC BEH amide column (150 × 2.1 mm, 1.7 μm) coupled to a VanGuard BEH Amide pre-column (5 × 2.1 mm; 1.7 μm; Waters, USA). The mobile phase and gradient conditions followed the parameters outlined in previous reports (Cho et al., 2022). The data were acquired in the scan range of m/z 80–1000.

2.5. Data analysis

Data analysis for physiological, biochemical and molecular analyses was conducted using OriginPro 9.65 software (OriginLab Corporation, Northampton, MA, USA). The EC_{50} values were calculated through nonlinear fitting (dose-response curve with variable Hill slope, Levenberg–Marquardt method), utilizing the immobilization data. For the qRT-PCR data, normality was verified using the Shapiro-Wilk test. Differences between control and exposed groups were statistically evaluated using one-way ANOVA followed by Tukey's multiple comparison tests. Statistically significant differences are denoted by asterisks ($^*p < 0.05$, $^{**}p < 0.01$, $^{***}p < 0.001$).

Lipidomics and metabolomics data analysis was performed using MS-DIAL (version 4.9.2) (Tsugawa et al., 2020). Annotated peaks were log-transformed and auto-scaled, followed by multivariate statistical analysis using MetaboAnalyst version 5.0 (Pang et al., 2022). A partial least-squares discriminant analysis (PLS-DA) identified influential variables between the treatment and control groups, based on their variable importance in projection (VIP). Statistic differences in lipids and metabolites from untargeted lipidomics and metabolomics were analyzed using one-way analysis of variance (ANOVA), followed by Fisher's LSD (adjusted P-value < 0.05) with a VIP score of > 1. Significant peaks were verified using SCIEX-OS Q to confirm the accurate mass (± 5 ppm) and MS2 fragmentation spectrum. Databases such as the MS-DIAL MSP spectral database (V17), Human Metabolome Database (HMDB) (Wishart et al., 2013), Metlin Database (Smith et al., 2005), MASS BANK (Horai et al., 2010), and LIPID MAPS (Fahy et al., 2007) were utilized for the identification of potential metabolite markers.

Lipid classes were identified using typical fragmentations following methodologies described by previous study (Cho et al., 2022). Significantly changed lipids were assigned to clusters corresponding to those obtained from hierarchical clustering analysis. Hierarchical clustering was performed based on metabolites that exhibited significant changes. Pearson correlation and Euclidean distance were used, respectively. The pheatmap package (v1.0.12) in R software (v4.2.2) was employed for clustering analysis (Ihaka and Gentleman, 1996; Kolde and Kolde, 2015). Z-score transformation to normalize the value of each sample was used. The Lipid ontology (LION) enrichment analysis was employed for the lipid enrichment analysis in ranking mode (Molenaar et al., 2019). Enrichment analysis for each lipid cluster was performed using the whole dataset as the background. Feature selection, employing a one-way ANOVA F-test, was analyzed to establish the ranking of input identifiers. Peak intensities were normalized through a percentage-based approach, and the Kolmogorov–Smirnov (K-S) test was configured with a two-tailed setting. A bar chart incorporating both upregulated and downregulated metabolites was constructed for visual representation. A mammalian lipidomics analysis tool (BIOPAN), which provides a gene list involved in the activation or suppression of enzymes, was used to identify enzymes involved in changes to lipid metabolites (Gaud et al., 2021). The correlated enzymes by finasteride exposure in the human homologs of *D. magna* were identified in KEGG (Kanehisa et al., 2016).

3. Results

3.1. Acute effects of finasteride on D. magna immobility, mortality, and ROS production

To understand the acute toxicity of finasteride to *D. magna* and determine the appropriate concentrations for long-term exposure, acute immobilization tests were conducted. Finasteride was tested across a

range of concentrations from 0.10 to 50.0 mg/L. The EC_{50} was determined to be 23.7 mg/L using the fitted dose-response curve (Figure S1). Subsequently, a preliminary mortality test ($n = 10$) at three concentrations (1.0, 5.0, and 10.0 mg/L) was conducted using the same methodology as applied in the chronic test, to determine the appropriate concentrations for the subsequent long-term exposure study. Over 50 % mortality was observed in the 10.0 mg/L group within 10 days. Considering these results and the EC_{50} values, we selected four sublethal concentrations (1.5, 3.0, 4.5, and 6.0 mg/L) for the chronic toxicity test. Additionally, ROS production assays were conducted prior to the chronic test using the selected concentrations to evaluate the potential impact of oxidative stress on chronic parameters. Neonates were exposed to the four sublethal concentrations and the control series at three different time points (6, 24, and 48 h). The result indicated a general increased in ROS levels in a dose-dependent manner across all time points; however, the changes were not statistically significant compared to those of control series (Figure S2).

3.2. Chronic effects of finasteride on D. magna reproduction

The chronic test duration was extended to 23 days, in accordance with OECD guideline 211 (OECD, 2012), due to insufficient offspring production in the control group by day 21. The control group exhibited a 5 % mortality rate and an average offspring count of 62.1 ± 6.1 neonates per mother at day 23. Finasteride exposure resulted in a significant reduction in reproductive output compared to the control. The average offspring count showed a dose-dependent decrease, with reductions of 37.6 % at 1.5 mg/L (38.8 ± 13.9), 40.8 % at 3.0 mg/L (36.7 ± 9.2), 86.1 % at 4.5 mg/L (8.6 ± 3.3), and 89.9 % at 6.0 mg/L (6.3 ± 4.03) (Fig. 1a). Furthermore, finasteride exposure notably increased mortality rates and the timing of the first brood. Specifically, the 1.5 and 3.0 mg/L exposure groups had a 15 % mortality rate, while the rates sharply rose to 35 % for the 4.5 mg/L group and 80 % for the 6.0 mg/L group for 23 days. In the control group, the first brood occurred at 10.6 ± 0.5 days. For the finasteride-exposed groups, the 1.5 and 3.0 mg/L concentrations led to first brood timings of 11.6 ± 1.2 days and 11.2 ± 0.3 days, respectively. However, the higher concentrations resulted in more significant delays, with the first brood appearing at 15.1 ± 1.7 days for the 4.5 mg/L group and at 17.0 ± 1.4 days for the 6.0 mg/L group (Fig. 1b). The first brood timing for the 3.0 mg/L group was slightly shorter than the 1.5 mg/L group, but overall the timing showed a clear dose-dependent delay.

3.3. Chronic effects of finasteride on the size of D. magna adults and neonates

Following chronic exposure, adult *D. magna* body lengths were measured to assess the effects of finasteride on growth. Significant differences were observed between the various exposure levels. The control group had an average length of 3.47 ± 0.11 mm ($n = 19$) (Fig. 2a). In comparison, the finasteride-exposed groups showed a decrease in length as follows: 11.5 % decrease to 3.07 ± 0.32 mm for 1.5 mg/L ($n = 17$), 10.4 % decrease to 3.11 ± 0.30 mm for 3.0 mg/L ($n = 18$), 40.3 % decrease to 2.07 ± 0.19 mm for 4.5 mg/L ($n = 12$), and 47.0 % decrease to 1.84 ± 0.50 mm for 6.0 mg/L ($n = 4$) (Fig. 2b). Statistical analysis revealed significant reductions in size for the finasteride-treated groups compared to the control. Despite the 1.5 mg/L group having a slightly smaller mean size than the 3.0 mg/L group, a consistent trend was observed.

3.4. Transcriptional change

The effect of finasteride exposure on the genomic response of *D. magna* was investigated by examining changes in the mRNA expression levels of genes involved in the ecdysteroid signaling pathway, particularly focusing on key genes associated with reproduction and development (Fig. 3). The results showed a dose-dependent downregulation of reproductive genes mRNA expression, including juvenile hormone esterase (*Jhe*), vitellogenin 2 (*Vtg2*), ecdysone receptor alpha (*EcR-A*), ecdysone receptor beta (*EcR-B*), *Neverland* and retinoid X receptor (*RXR*) at both time points. Nuclear receptor Hr96 (*Hr96*) expression level decreased only at 6 h exposure. Notably, the expression of *Jhe* was significantly downregulated ($p < 0.001$) at all finasteride concentrations after 24 h of exposure. *Vtg2* expression was also downregulated after 6 h exposure to 3.0 mg/L of finasteride, with this suppression becoming significant after 24 h exposure at both 1.5 and 3.0 mg/L concentration. Conversely, *chitinase*, associated with developmental processes, was upregulated following finasteride exposure at both time points. Additionally, the transcriptional profiles of oxidative response genes included glutathione S-transferase (*gst*), catalase (*cat*), glutathione peroxidase (*gpx*), and superoxide dismutase (*sod*) were also assessed. Oxidative response genes exhibited a dose-dependent downregulation pattern at both concentrations and time points, except for *sod* at 3 mg/L after 6 hours of exposure.

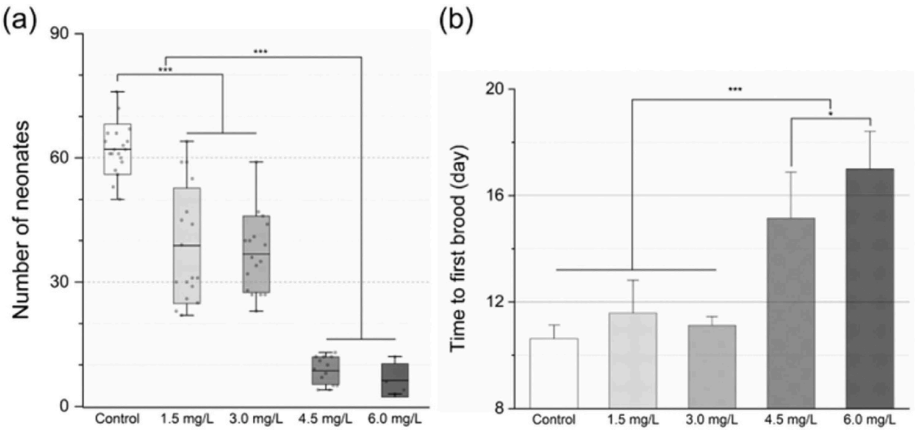

Fig. 1. (a) Total count of neonates from surviving *D. magna* after a 23-day finasteride exposure period, with boxes showing standard deviation and the central line representing the mean; (b) Average duration until the first brood in response to finasteride exposure, where bars denote the mean and error bars indicate the standard error of mean. Statistical evaluations were conducted using one-way ANOVA and Tukey's multiple comparison tests, with asterisks marking significant differences ($*p < 0.05$ and $***p < 0.001$).

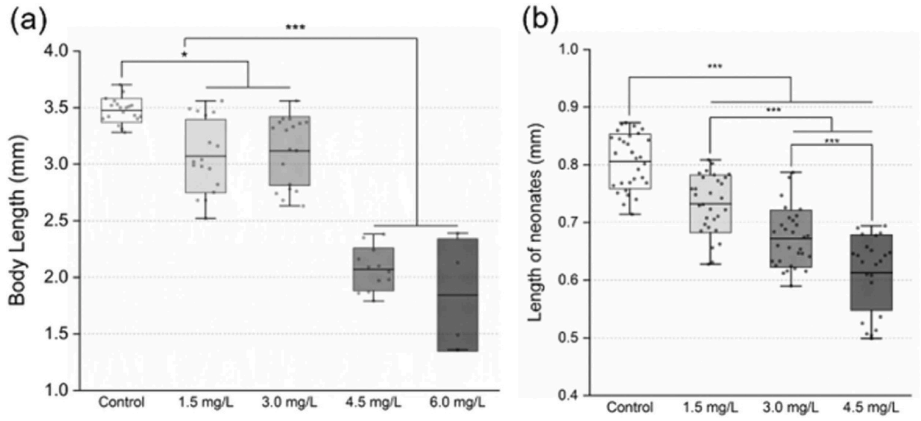

Fig. 2. (a) Body length of daphnids in each experimental group at the end of the chronic test, with boxes showing standard deviation and the central line representing the mean; (b) the body length of neonates from the third brood in each experimental group, with boxes for standard deviation and a central line for the mean. Statistical analyses were performed using one-way ANOVA and Tukey's multiple comparison tests, with asterisks highlighting significant differences (*$p < 0.05$ and ***$p < 0.001$).

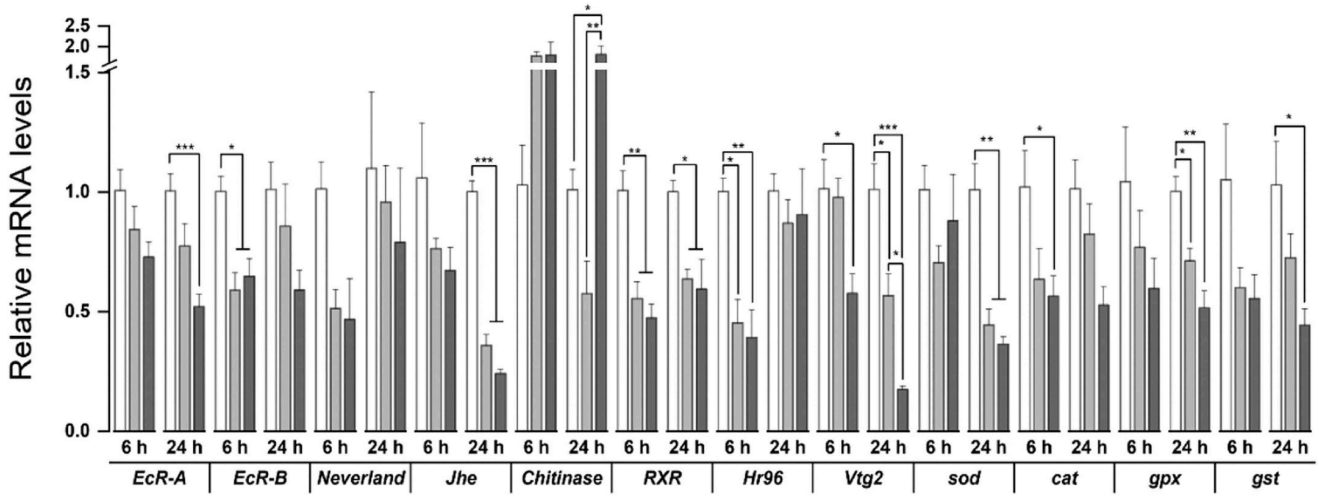

Fig. 3. Relative mRNA expression following 6 h and 24 h exposure of 17-day-old *D. magna* adults to finasteride. The expression levels of selected reproduction-, development- and antioxidant-related genes. Bars indicate mean values, while error bars represent the standard error of mean ($n \geq 3$, each sample comprising 5 individuals). Statistical evaluations were conducted using one-way ANOVA and Tukey's multiple comparison tests, with asterisks denoting significant differences (*$p < 0.05$, **$p < 0.01$, and ***$p < 0.001$).

3.5. Effect on lipid contents and metabolites

Untargeted lipidomic and metabolomic analyses identified 464 individual lipids and 23 metabolites that were differently regulated, as depicted in Fig. 4 and Supplementary data 2 and 3. Following exposure to finasteride in *D. magna*, 14 lipid classes were annotated. The hierarchical analysis of lipid changes is presented in Fig. 4a as a heatmap, clustering the lipids into three different groups of 344, 75, and 26 lipids (clusters 1, 2, and 3, respectively). These included comparison among lipid classes with detailed distributions provided in supplementary data 4. The cluster 1 was composed to triacylglycerol (TG), phosphatidylcholine (PC), diacylglycerol (DG), and ceramide (Cer), and showed the downregulated pattern in finasteride exposure group compared to control group. In the second cluster, differential responses were observed with upregulation at 1.5 mg/L and downregulation at 3.0 mg/L following exposure to finasteride. The third cluster exhibited upregulation pattern in finasteride exposure group compared to control group. Nineteen LION signaling pathways were significantly enriched (FDR q value < 0.05) indicating a notable upregulation, while four pathways showed significant downregulation (Fig. 4b). LION-terms such as fatty acid with more than 18 carbons, fatty acid with less than two double bonds, saturated fatty acid, membrane component, high transition temperature, glycerophospholipids, fatty acid with 22–24 carbons, headgroup with positive charge/ zwitter-ion, high bilayer thickness, and neutral intrinsic curvature were upregulated. Conversely, few LION-terms, including plasma membrane, sphingolipids [SP], N-acylsphingosines (ceramides) [SP0201], and DG (34:2) were downregulated. Comprehensive details of the lipids associated with each LION category in the enrichment are available in supplementary data 4. Comparisons between control and each finasteride exposure group were presented as network analyses in Fig. 4c-d. Both exposed groups activated DG to phosphatidylethanolamine (PE) and PC metabolism without suppressing any pathways. Phosphoethanolamine N-methyltransferase (PEMT, KEGG entry 116930291) and choline/ethanolamine phosphotransferase (CEPT1, KEGG entry 116919957) were annotated. Using hydrophilic phase metabolomics, 22 downregulated metabolites were identified (Figure S3a). These metabolites included propionic acid, cytosine, 5,6-dihydro-5-methyluracil, L-leucine, hypoxanthine,

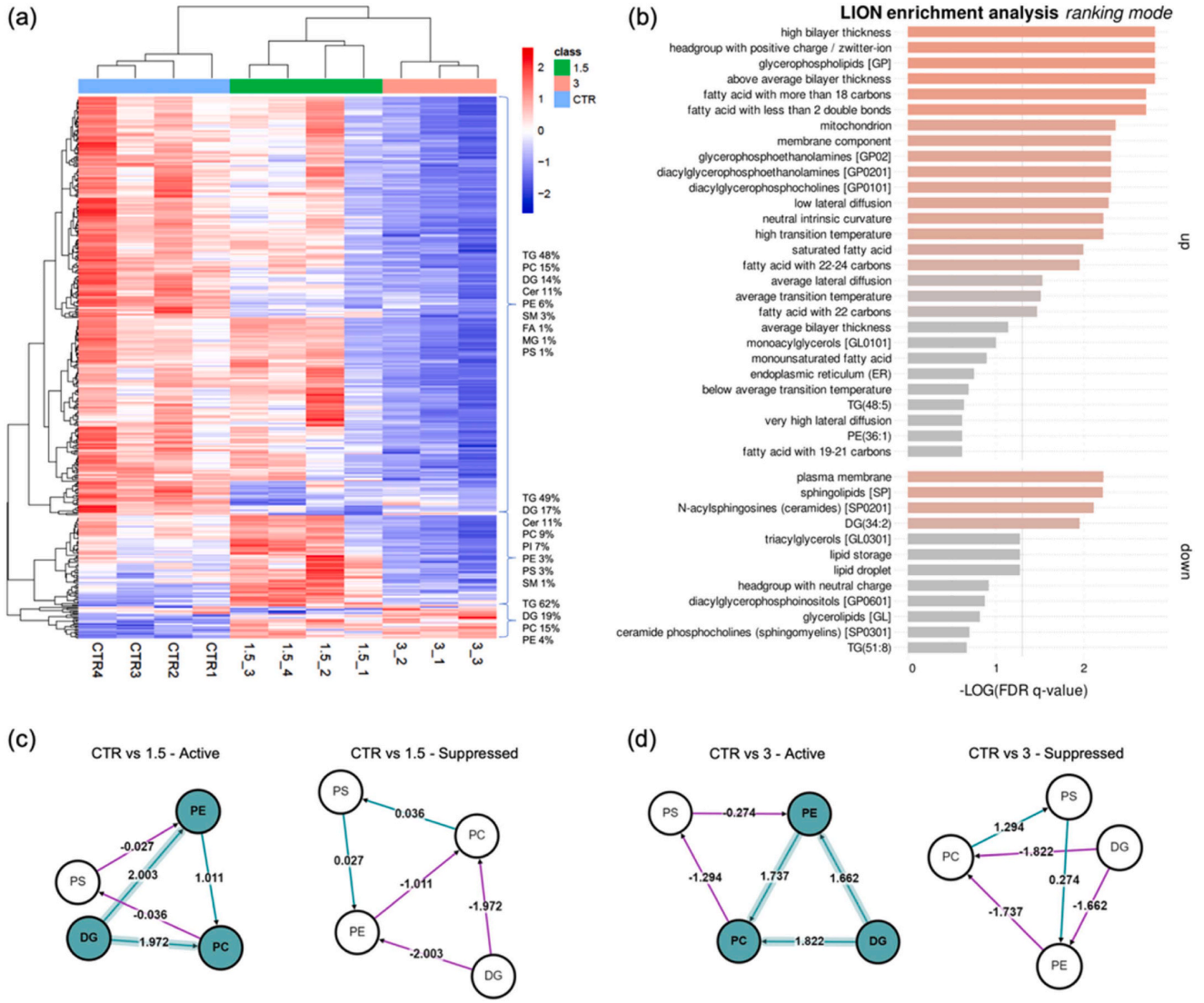

Fig. 4. (a) Heatmap of the alterations in lipid concentrations in *D. magna* exposed to 1.5 and 3.0 mg/L finasteride, compared to the untreated group. Red indicates higher metabolites and blue indicates lower metabolites, relative to the average gene metabolite levels. (b) LION enrichment lipid ontology analysis results in ranking mode of comparisons of the untreated group with finasteride (1.5 and 3 mg/mL) exposed groups via one-way ANOVA F-test. Lipid network graphs exported from BioPAN for (c) 1.5 mg/L and (d) 3.0 mg/L finasteride exposure. Green nodes correspond to active lipids, and green shaded arrows correspond to active pathways. Reactions with a positive Z score have green arrows, while negative Z scores are purple colored. Abbreviation: TG, triacylglycerol; PC, phosphatidylcholine; DG, diacylglycerol; Cer, ceramide; PE, phosphatidylethanolamine; PI, Phosphatidylinositol; PS, phosphatidylserine; SM, sphingomyelin; MG, Monoacylglycerols; FA, Fatty acid.

glutamine, lysine, guanine, indole-3-carboxylic acid, delta-hydroxylysine, nepsilon, trimethyllysine, theobromine, L-kynurenine, propionylcarnitine, L-carnosine, 1-methyladenosine maltotriose cysteic acid, gluconic acid, carnosine, chrysin, gamma-glutamylleucine, and gamma-glutamyltyrosine. Pathway analysis revealed that the significantly affected metabolic pathways included the pentose phosphate pathway, histidine metabolism, beta-alanine metabolism, and alanine, aspartate, and glutamate metabolism (Figure S3b).

4. Discussion

While the mechanism of toxicity in *D. magna* due to exposure to steroid hormones and steroid-related chemicals is less understood compared to their impact on vertebrates (Ojoghoro et al., 2021), previous studies have shown that such exposure impacts invertebrates as evidenced by the anti-ecdysteroidal effects of testosterone in *D. magna* (Mu and LeBlanc, 2002) and the antagonistic activities of androstenedione in *Drosophila melanogaster B* (II) cells (Dinan et al., 2001). Recent studies have explored the effects of 5AR inhibitor exposure in invertebrate species. For instance, pharmaceutical 5AR inhibitors led to observable morphological alterations in gastropods embryos (Baynes et al., 2019). Considering the signaling pathways centered on ecdysteroids, these findings suggested that steroid-related molecules might have cross-pathway impacts, influencing species with varying hormonal and signaling pathways (Miyakawa et al., 2018; Song et al., 2017; Sumiya et al., 2014). In the present study, finasteride exposure had pronounced significant effects on reproductive activities such as reproduction output and the first time to brood. Particularly, the dose-responsive decrease in individual reproduction serve as a key indicator among various parameters for evaluating chronic toxicity of exposure substances in assessing endocrine disrupting effects (Tkaczyk et al., 2021). Based on these studies and 5AR inhibitor characteristics,

which are structural similar to androgens and interfere with the function of androgen receptor signaling, finasteride in *D. magna* may be suggested to act as an endocrine disruptor, particularly affecting ecdysteroid signaling.

Given the close relationship between growth rate and reproduction in *D. magna*, developmental retardation influences the reduction in reproduction. Previous studies investigating the effects of various EDCs in *D. magna* observed simultaneous changes in reproductive output and physiological alterations, confirming significant correlations between these outcomes (Giraudo et al., 2017; Mu and LeBlanc, 2002; Oropesa et al., 2016). The impacts of toxic substances on reproduction and growth differ significantly, with a range of toxicity indicators reflecting the unique interaction of each chemical with organisms (Knops et al., 2001). In our result, while the control group exhibited low variability in individual size, the groups exposed to finasteride showed developmental retardation and inter-individual size variation with statistically significant differences. Correspondingly, the size of neonates in each group demonstrated a tendency to decrease with increasing exposure concentrations. The overall decrease in growth and reproduction trends may be not only representative to endocrine disrupting and also related to finasteride exposure affecting the overall metabolism as a toxic mechanism of action (Fuertes et al., 2019; Jeong and Simpson, 2020).

To elucidate the toxicogenomic responses of *D. magna* to finasteride exposure underlying the adverse effects on reproduction through endocrine disruption, we analyzed the expression of key genes associated with development and reproduction including *EcR-A*, *EcR-B*, *neverland, Jhe*, *chitinase*, *RXR*, *Hr96*, *Vtg2*. A marked downregulation of *Vtg2, Jhe*, *EcR-A, EcR-B,* and *RXR* genes was noted in the presence of finasteride. As vitellogenin genes are downstream products in the endocrine signaling pathway, playing a role in orchestrating yolk synthesis and oocyte maturation, their expression levels constitute a critical biomarker for evaluating the reproductive impact in ecotoxicological assessments (Hu et al., 2020; LeBoeuf et al., 2018; Toyota et al., 2014). The dose-responsive decrease in the expression level of *Vtg2* was consistent with the significant reduction in those of *Jhe* observed after 24 hours of exposure. JHE regulates the concentration of juvenile hormone (JH) by suppressing vitellogenin gene expression. This suggests that the concentration of JH may have become imbalanced in association with the decrease in *Vtg2* (Seyoum et al., 2020). Thus, the reduced *Jhe* levels might impede juvenile hormone degradation, leading to delayed maturation, adult metamorphosis, and reduced reproduction (Tokishita et al., 2006). Considering the interrelationship of these two genes in yolk production and reproduction (Merzendorfer and Zimoch, 2003; Tokishita et al., 2006), the significant decrease in these genes following 5AR inhibitor exposure contributed to reduced yolk formation and delayed maturation, resulting in reproductive output decrease. The enzyme Neverland catalyzes the initial steps in the synthesis of ecdysteroids from cholesterol, which then undergo several processes to become active hormones, particularly ecdysone (Rewitz and Gilbert, 2008). Subsequently, ecdysteroid interacts with EcR and RXR, binding to the promoters of ecdysone-related genes and exerting downstream effects in regulating reproduction and development, influencing processes such as molting, metamorphosis, and vitellogenesis (Abe et al., 2015; Dai et al., 2016; Seyoum et al., 2020). Considering particularly relevant in synchronization of reproduction and molting cycles, the decreased expression of EcR and RXR genes suggests that ecdysteroid pathways were disrupted (Miyakawa et al., 2018). This was accompanied by a notable decrease in the expression of vitellogenin genes, correlating with the observed changes in *EcR* and *Jhe* levels (Tokishita et al., 2006; Touhara et al., 1994). Thus, finasteride exposure in daphnids led to the suppression of genes linked to ecdysteroid signaling and hormone receptor-mediated pathways, aligning with the noted reductions and retardancy in fecundity. Chitinase gene expression was upregulated after 6 h of exposure and showed a more pronounced increase at 24 h in the 6 mg/L exposure group. A decrease in *Chitinase* expression can induce chronic reproductive effects through a reduction in molting (David et al., 2011). However, our results, showing an increase in the level of *Chitinase* expression along with a decrease in reproduction, suggest that the exposure to 5AR inhibitors may have a greater impact on disrupting the balance in ecdysteroid and juvenile hormone signaling pathways, rather than regulating metamorphosis (Giraudo et al., 2017; Poynton et al., 2008).

Adaptation to oxidative stress often necessitates the synthesis of antioxidant enzymes, indirectly influencing the levels of antioxidant mRNA (Kim et al., 2017). Severe toxicants such as pesticides and heavy metals have been shown to elevate the level of antioxidants and ROS (Fan et al., 2015; Oropesa et al., 2017). In this study, the ROS levels did not show a significant increase even though finasteride exposure resulted in the downregulation of antioxidant enzyme genes (Fig. 3 and S2). Remarkably, there was no observable trend of increment in ROS levels over time. While the response of daphnia at molecular level to environmental stressors is controversial, it is well-recognized that exposure to low-toxic substances causing stress can lead to fluctuations in ROS levels and antioxidant activity (Jemec et al., 2012; Yin et al., 2023). For instance, environmental changes in temperature affect ROS and oxidative stress defense mechanisms in a time-dependent manner; fluctuations were observed up to 24 hours after exposure, stabilizing after 48 hours (Becker et al., 2011). While ROS levels showed an increasing trend with time upon exposure to polystyrene nanoplastic, the expression of genes related to antioxidant defenses such as *sod* and *cat* fluctuated over time (De Felice et al., 2022). Our observations align with phenomena previously reported in the literature. These results suggest that the concentrations of finasteride applied not significantly impact *D. magna* individuals due to cellular toxicity; nevertheless, the adverse effects of the 5AR inhibitor manifested through disruptions in the endocrine signaling pathway.

Lipids serve as essential energy source, significantly influencing the development, growth, and reproduction of invertebrates (Arrese and Soulages, 2010). In general, lipid reserves decrease during reproductive phases due to high energy demands and accumulate during non-reproductive periods, reflecting the metabolic costs associated with reproduction (Constantinou et al., 2020). In *D. magna*, female somata showed depletion of nutrients by high maternal investment in reproduction. The cholesterol not only supports eggs development but is also retained at higher levels in somatic tissues (Martin-Creuzburg et al., 2018). This pattern extends to dietary polyunsaturated fats, which are critical for both asexual and sexual reproduction eggs and lead to significant depletion of fatty acid reserves (Becker and Boersma, 2005). The essential role of lipids is further highlighted by the accumulation of glycerophospholipids, necessary for the formation of the new carapace (Fuertes et al., 2018). Additionally, individuals with low TG from eggs develop into smaller individuals that matured late and reproduced late (Fuertes et al., 2018; Jordão et al., 2015). These studies align with our findings that finasteride exposure leads to downregulation of lipid content, particularly TG (Fig. 4a), and impacts development- and reproduction-related parameters.

As the molecular outcomes of organism's functions, the study by Jordão (2016) reported that the genetic interaction with EcR, RXR, and methyl farnesoate hormone receptors (MfRs) regulated the signaling pathway implicated in lipid storage. This may act similarly to the mechanistic mode of action of the RXR and peroxisome proliferator-activated receptor (PPARγ) signaling pathway, a key regulator of lipid metabolism in vertebrates. The putative MfR is consist of methoprene-tolerant coactivator protein (MET) which is bind to methyl farnesoate and other juvenoid compound, and the steroid receptor coactivator (SRC) (Jordão et al., 2016). In addition, these molecular results showed to interact through complex crosstalk between ecdysteroids and JHs, which are essential hormones of *D. magna* (Miyakawa et al., 2018). In particular, their interaction was hypothesized to antagonistic effect due to the competitive interaction between EcR and MET for binding to SCR, and mixture of ecdysteroids and JHs also negatively affected factors related to lipid storage at the gene response (Jordão et al., 2016;

Miyakawa et al., 2018; Zhang et al., 2011). As another factor, Hr96 is known to regulate several genes involved in energy metabolisms through cholesterol and fatty acid homeostasis through heterodimerization with RXR (Karimullina et al., 2012; Sengupta et al., 2017). These findings may suggest the possibility of interaction between finasteride and this receptor-related signaling pathway, which may suggest a connection the downregulation of between *EcR-A/B*, *Jhe*, *RXR*, and *Hr96* expression levels and lipid metabolites observed in this study (as shown in cluster 1 and 2 in Fig. 4a).

Specific lipid classes have different regulatory functions across organisms. Lipids, as main components of the cellular membrane, vary across organisms, cell types, organelles, and membrane subdomain levels (Harayama and Riezman, 2018). In the present study, the LION analysis revealed that lipid bilayer thickness as well as glycerophospholipids was activated due to finasteride exposure. We observed a correlated upregulation of lipid metabolism in the membrane components and mitochondria, while the plasma membrane was downregulated. Phospholipids, particularly PC and PE, are most abundant in the mitochondrial membranes and essential for maintaining the phospholipid composition in the mitochondrial function, structure, and biogenesis (Schenkel and Bakovic, 2014). PC not only serves as a vital component of biological membranes and a pulmonary surfactant but also plays a key role in membrane cell signaling (Vance, 2013). Furthermore, PC is involved in diverse processes, including oxidation, inflammation, endoplasmic reticulum membrane stress, endosome modulation, lipid storage, membrane synthesis, and growth (Kanno et al., 2007). The biosynthesis of PE or PC is mediated by CEPT1 (EC:2.7.8.1, KEGG orthology K13644), while the conversion of PE to PC is mediated by PEMT (EC:2.1.1.103, KEGG orthology K05929) through the transfer of three methyl groups from S-adenosylmethionine. Interestingly, finasteride has been reported to inhibit phenylethanolamine N-methyltransferase (PNMT), which is responsible for converting norepinephrine to epinephrine in human (Giatti et al., 2021). This report suggests that finasteride potentially affects crustacean PEMT including inhibition and compensatory expression. CEPT also mediates the conversion of DG to PE and DG to PC, suggesting crosstalk between PEMT and CEPT under finasteride exposure. Thus, these evidences may explain the results in this study where many lipid metabolites decreased (Fig. 4a), but metabolism pathways involving DG to PE, DG to PC, and PE to PC (Fig. 4b-c) were upregulated following finasteride exposure. Sphingolipids, key components of cellular membranes, are significant for the development, growth and reproduction of offspring due to the substantial transfer (Sengupta et al., 2016). Exposure to finasteride led to downregulation of sphingolipids in our study (Fig. 4b). This disruption in sphingolipid levels could have significant implications for development and reproduction. While the LC-QTOF lipidomics approach in our study did not identify cholesterol and ecdysteroid metabolites, the potential interaction between ecdysteroid and lipids metabolism in daphnia presents a fascinating area for further study. Considering this, future studies should explore the correlation between specific lipids class changes and organelles in reproduction. This is particularly evident in the observed downregulation of lipid metabolism and its potential link to decreased reproduction. Such observations underscore the importance of further investigation to elucidate these complex biochemical relationships.

In conclusion, our study has revealed significant physiological effects of finasteride on *D. magna*, including a dose-dependent decrease in reproductive output, delayed brood timing, increased mortality, and altered adult size in a dose-response manner. At the molecular level, finasteride exposure led to the downregulation of key genes expression associated with reproduction and development such as *Vtg2*, *Jhe*, *EcR-A/B* and *RXR*, aligning with observed physiological changes. Additionally, lipidomic analyses indicated notable impact on changes in lipid profiles. These findings demonstrate that finasteride acts as an endocrine disruptor in *D. magna*, leading to significant ecotoxicological effects for aquatic ecosystems. Given the rapidly increasing use of finasteride, this study also emphasizes the need for further environmental assessment to understand its potential ecotoxicological effects.

Funds

This research was supported by the Nanomaterial Technology Development Program (NRF-2017M3A7B6052455) funded by the South Korean Ministry of Science and by the Korea Institute of Toxicology (KIT), Republic of Korea (1711195881), and Bio-cluster Industry Capacity Enhancement Project of Jeonbuk Technopark (JBTP).

CRediT authorship contribution statement

Hyunki Cho: Writing – review & editing, Validation, Methodology, Investigation, Formal analysis, Data curation. **Si-Eun Sung:** Writing – review & editing, Visualization, Validation, Data curation. **Giup Jang:** Writing – review & editing, Visualization, Validation, Formal analysis, Data curation. **Maranda Esterhuizen:** Writing – review & editing, Validation, Data curation. **Chang Seon Ryu:** Writing – review & editing, Validation, Methodology, Investigation, Formal analysis, Data curation, Conceptualization. **Youngsam Kim:** Writing – review & editing, Writing – original draft, Visualization, Validation, Supervision, Methodology, Investigation, Formal analysis, Data curation, Conceptualization. **Young Jun Kim:** Writing – review & editing, Project administration, Funding acquisition, Conceptualization.

Declaration of Competing Interest

The authors declare that they have no known competing financial interests or personal relationships that could have appeared to influence the work reported in this paper.

Data availability

Data will be made available on request.

Acknowledgements

Special appreciation is extended to Prof. Dr. Albrecht Ott in proofreading.

Appendix A. Supporting information

Supplementary data associated with this article can be found in the online version at doi:10.1016/j.ecoenv.2024.116606.

References

Abe, R., Toyota, K., Miyakawa, H., Watanabe, H., Oka, T., Miyagawa, S., Nishide, H., Uchiyama, I., Tollefsen, K.E., Iguchi, T., Tatarazako, N., 2015. Diofenolan induces male offspring production through binding to the juvenile hormone receptor in Daphnia magna. Aquat. Toxicol. 159, 44–51. https://doi.org/10.1016/j.aquatox.2014.11.015.

Arrese, E.L., Soulages, J.L., 2010. Insect fat body: energy, metabolism, and regulation. Annu. Rev. Entomol. 55, 207–225. https://doi.org/10.1146/annurev-ento-112408-085356.

Bang, S.H., Ahn, J.-Y., Hong, N.-H., Sekhon, S.S., Kim, Y.-H., Min, J., 2015. Acute and chronic toxicity assessment and the gene expression of Dhb, Vtg, Arnt, CYP4, and CYP314 in Daphnia magna exposed to pharmaceuticals. Mol. Cell. Toxicol. 11, 153–160. https://doi.org/10.1007/s13273-015-0013-7.

Baynes, A., Montagut Pino, G., Duong, G.H., Lockyer, A.E., McDougall, C., Jobling, S., Routledge, E.J., 2019. Early embryonic exposure of freshwater gastropods to pharmaceutical 5-alpha-reductase inhibitors results in a surprising open-coiled "banana-shaped" shell. Sci. Rep. 9, 16439 https://10.1038/s41598-019-52850-x.

Becker, C., Boersma, M., 2005. Differential effects of phosphorus and fatty acids on Daphnia magna growth and reproduction. Limnol. Oceanogr. 50, 388–397. https://doi.org/10.4319/lo.2005.50.1.0388.

Becker, D., Brinkmann, B.F., Zeis, B., Paul, R.J., 2011. Acute changes in temperature or oxygen availability induce ROS fluctuations in Daphnia magna linked with fluctuations of reduced and oxidized glutathione, catalase activity and gene

(haemoglobin) expression. Biol. Cell 103, 351–363. https://doi.org/10.1042/bc20100145.
Campioli, E., Batarseh, A., Li, J., Papadopoulos, V., 2011. The endocrine disruptor mono-(2-ethylhexyl) phthalate affects the differentiation of human liposarcoma cells (SW 872). PLoS One 6, e28750. https://doi.org/10.1371/journal.pone.0028750.
Cho, H., Seol, Y., Baik, S., Sung, B., Ryu, C.S., Kim, Y.J., 2022. Mono(2-ethylhexyl) phthalate modulates lipid accumulation and reproductive signaling in Daphnia magna. Environ. Sci. Pollut. Res. Int. 29, 55639–55650. https://doi.org/10.1007/s11356-022-19701-1.
Constantinou, J.K., Southam, A.D., Kvist, J., Jones, M.R., Viant, M.R., Mirbahai, L., 2020. Characterisation of the dynamic nature of lipids throughout the lifespan of genetically identical female and male Daphnia magna. Sci. Rep. 10, 5576. https://doi.org/10.1038/s41598-020-62476-z.
Dai, T.H., Sserwadda, A., Song, K., Zang, Y.N., Shen, H.S., 2016. Cloning and Expression of Ecdysone Receptor and Retinoid X Receptor from Procambarus clarkii: Induction by Eyestalk Ablation. Int. J. Mol. Sci. 17 https://doi.org/10.3390/ijms17101739.
David, R.M., Dakic, V., Williams, T.D., Winter, M.J., Chipman, J.K., 2011. Transcriptional responses in neonate and adult Daphnia magna in relation to relative susceptibility to genotoxicants. Aquat. Toxicol. 104, 192–204. https://doi.org/10.1016/j.aquatox.2011.04.016.
De Felice, B., Sugni, M., Casati, L., Parolini, M., 2022. Molecular, biochemical and behavioral responses of Daphnia magna under long-term exposure to polystyrene nanoplastics. Environ. Int. 164, 107264 https://doi.org/10.1016/j.envint.2022.107264.
Dinan, L., Bourne, P., Whiting, P., Dhadialla, T.S., Hutchinson, T.H., 2001. Screening of environmental contaminants for ecdysteroid agonist and antagonist activity using the Drosophila melanogaster B(II) cell in vitro assay. Environ. Toxicol. Chem. 20, 2038–2046 https://10.1897/1551-5028(2001)020<2038:soecfe>2.0.co;2.
Ebert, D., 2022. Daphnia as a versatile model system in ecology and evolution. EvoDevo 13, 16. https://doi.org/10.1186/s13227-022-00199-0.
Fahy, E., Sud, M., Cotter, D., Subramaniam, S., 2007. LIPID MAPS online tools for lipid research. Nucleic Acids Res. 35, W606–W612. https://doi.org/10.1093/nar/gkm324.
Fan, W., Ren, J., Li, X., Wei, C., Xue, F., Zhang, N., 2015. Bioaccumulation and oxidative stress in Daphnia magna exposed to arsenite and arsenate. Environ. Toxicol. Chem. 34, 2629–2635. https://doi.org/10.1002/etc.3119.
Fuertes, I., Jordão, R., Casas, J., Barata, C., 2018. Allocation of glycerolipids and glycerophospholipids from adults to eggs in Daphnia magna: Perturbations by compounds that enhance lipid droplet accumulation. Environ. Pollut. 242, 1702–1710. https://doi.org/10.1016/j.envpol.2018.07.102.
Fuertes, I., Jordão, R., Piña, B., Barata, C., 2019. Time-dependent transcriptomic responses of Daphnia magna exposed to metabolic disruptors that enhanced storage lipid accumulation. Environ. Pollut. 249, 99–108. https://doi.org/10.1016/j.envpol.2019.02.102.
Garcia-Garcia, M., Sanchez-Hernandez, M., Garcia-Hernandez, M.P., Garcia-Ayala, A., Chaves-Pozo, E., 2017. Role of 5alpha-dihydrotestosterone in testicular development of gilthead seabream following finasteride administration. J. Steroid Biochem. Mol. Biol. 174, 48–55. https://doi.org/10.1016/j.jsbmb.2017.07.024.
Gaud, C., B, C.S., Nguyen, A., Fedorova, M., Ni, Z., O'Donnell, V.B., Wakelam, M.J.O., Andrews, S., Lopez-Clavijo, A.F., 2021. BioPAN: a web-based tool to explore mammalian lipidome metabolic pathways on LIPID MAPS. F1000Res 10, 4. https://doi.org/10.12688/f1000research.28022.2.
Giatti, S., Di Domizio, A., Diviccaro, S., Falvo, E., Caruso, D., Contini, A., Melcangi, R.C., 2021. Three-Dimensional Proteome-Wide Scale Screening for the 5-Alpha Reductase Inhibitor Finasteride: Identification of a Novel Off-Target. J. Med. Chem. 64, 4553–4566 https://10.1021/acs.jmedchem.0c02039.
Gilroy, E.A.M., Bartlett, A.J., Gillis, P.L., Bendo, N.A., Salerno, J., Hedges, A.M., Brown, L.R., Holman, E.A.M., Stock, N.L., de Solla, S.R., 2020. Toxicity of the pharmaceuticals finasteride and melengestrol acetate to benthic invertebrates. Environ. Sci. Pollut. Res. Int. 27, 41803–41815. https://doi.org/10.1007/s11356-020-10121-7.
Giraudo, M., Douville, M., Cottin, G., Houde, M., 2017. Transcriptomic, cellular and life-history responses of Daphnia magna chronically exposed to benzotriazoles: Endocrine-disrupting potential and molting effects. PLoS One 12, e0171763. https://doi.org/10.1371/journal.pone.0171763.
Harayama, T., Riezman, H., 2018. Understanding the diversity of membrane lipid composition. Nat. Rev. Mol. Cell Biol. 19, 281–296. https://doi.org/10.1038/nrm.2017.138.
Health and Medical Care Administration, R.S., 2023. Region Stockholm, Region Stockholm. Finasteride Finasteride.
Horai, H., Arita, M., Kanaya, S., Nihei, Y., Ikeda, T., Suwa, K., Ojima, Y., Tanaka, K., Tanaka, S., Aoshima, K., Oda, Y., Kakazu, Y., Kusano, M., Tohge, T., Matsuda, F., Sawada, Y., Hirai, M.Y., Nakanishi, H., Ikeda, K., Akimoto, N., Maoka, T., Takahashi, H., Ara, T., Sakurai, N., Suzuki, H., Shibata, D., Neumann, S., Iida, T., Tanaka, K., Funatsu, K., Matsuura, F., Soga, T., Taguchi, R., Saito, K., Nishioka, T., 2010. MassBank: a public repository for sharing mass spectral data for life sciences. J. Mass Spectrom. 45, 703–714. https://doi.org/10.1002/jms.1777.
Hu, X.L., Tang, Y.Y., Kwok, M.L., Chan, K.M., Chu, K.H., 2020. Impact of juvenile hormone analogue insecticides on the water flea Moina macrocopa: Growth, reproduction and transgenerational effect. Aquat. Toxicol. 220, 105402 https://doi.org/10.1016/j.aquatox.2020.105402.
Ihaka, R., Gentleman, R., 1996. R: A Language for Data Analysis and Graphics. J. Comput. Graph. Stat. 5, 299–314. https://doi.org/10.1080/10618600.1996.10474713.
Imhof, H.K., Rusek, J., Thiel, M., Wolinska, J., Laforsch, C., 2017. Do microplastic particles affect Daphnia magna at the morphological, life history and molecular level? PLoS One 12, e0187590. https://doi.org/10.1371/journal.pone.0187590.
IOS, 2012. Water quality — Determination of the inhibition of the mobility of Daphnia magna Straus (Cladocera, Crustacea) — Acute toxicity test. International Organization for. Stand., Geneve, Switz. 6341.
Jemec, A., Tišler, T., Erjavec, B., Pintar, A., 2012. Antioxidant responses and whole-organism changes in Daphnia magna acutely and chronically exposed to endocrine disruptor bisphenol A. Ecotoxicol. Environ. Saf. 86, 213–218. https://doi.org/10.1016/j.ecoenv.2012.09.016.
Jeong, T.Y., Simpson, M.J., 2020. Reproduction stage specific dysregulation of Daphnia magna metabolites as an early indicator of reproductive endocrine disruption. Water Res 184, 116107. https://doi.org/10.1016/j.watres.2020.116107.
Jordão, R., Casas, J., Fabrias, G., Campos, B., Piña, B., Lemos Marco, F.L., Soares Amadeu, M.V.M., Tauler, R., Barata, C., 2015. Obesogens beyond Vertebrates: Lipid Perturbation by Tributyltin in the Crustacean Daphnia magna. Environ. Health Perspect. 123, 813–819 https://10.1289/ehp.1409163.
Jordão, R., Campos, B., Piña, B., Tauler, R., Soares, A.M.V.M., Barata, C., 2016. Mechanisms of Action of Compounds That Enhance Storage Lipid Accumulation in Daphnia magna. Environ. Sci. Technol. 50, 13565–13573. https://doi.org/10.1021/acs.est.6b04768.
Kane, S.P., Finasteride. In: V. 2002.08, (Ed.), ClinCalc DrugStats Database:, Vol. 2024. ClinCalc LLC:, 2022.
Kanehisa, M., Sato, Y., Kawashima, M., Furumichi, M., Tanabe, M., 2016. KEGG as a reference resource for gene and protein annotation. Nucleic Acids Res. 44, D457–D462. https://doi.org/10.1093/nar/gkv1070.
Kanno, K., Wu, M.K., Scapa, E.F., Roderick, S.L., Cohen, D.E., 2007. Structure and function of phosphatidylcholine transfer protein (PC-TP)/StarD2. Biochim. Biophys. Acta 1771, 654–662. https://doi.org/10.1016/j.bbalip.2007.04.003.
Karimullina, E., Li, Y., Ginjupalli, G.K., Baldwin, W.S., 2012. Daphnia HR96 is a promiscuous xenobiotic and endobiotic nuclear receptor. Aquat. Toxicol. 116-117, 69–78. https://doi.org/10.1016/j.aquatox.2012.03.005.
Kim, H., Yim, B., Bae, C., Lee, Y.-M., 2017. Acute toxicity and antioxidant responses in the water flea Daphnia magna to xenobiotics (cadmium, lead, mercury, bisphenol A, and 4-nonylphenol). Toxicol. Environ. Health Sci. 9, 41–49. https://doi.org/10.1007/s13530-017-0302-8.
Knops, M., Altenburger, R., Segner, H., 2001. Alterations of physiological energetics, growth and reproduction of Daphnia magna under toxicant stress. Aquat. Toxicol. 53, 79–90. https://doi.org/10.1016/s0166-445x(00)00170-3.
Kolde, R., Kolde, M.R., 2015. Package 'pheatmap'. R. Package 1, 790.
LeBlanc, G.A., 2007. Crustacean endocrine toxicology: a review. Ecotoxicology 16, 61–81. https://doi.org/10.1007/s10646-006-0115-z.
LeBoeuf, A.C., Cohanim, A.B., Stoffel, C., Brent, C.S., Waridel, P., Privman, E., Keller, L., Benton, R., 2018. Molecular evolution of juvenile hormone esterase-like proteins in a socially exchanged fluid. Sci. Rep. 8, 17830. https://doi.org/10.1038/s41598-018-36048-1.
Lee, M.R., Loux-Turner, J.R., Oliveira, K., 2015. Evaluation of the 5alpha-reductase inhibitor finasteride on reproduction and gonadal development in medaka, Oryzias latipes. Gen. Comp. Endocrinol. 216, 64–76. https://doi.org/10.1016/j.ygcen.2015.04.008.
Margiotta-Casaluci, L., Hannah, R.E., Sumpter, J.P., 2013. Mode of action of human pharmaceuticals in fish: the effects of the 5-alpha-reductase inhibitor, dutasteride, on reproduction as a case study. Aquat. Toxicol. 128-129, 113–123. https://doi.org/10.1016/j.aquatox.2012.12.003.
Martin-Creuzburg, D., Massier, T., Wacker, A., 2018. Sex-Specific Differences in Essential Lipid Requirements of Daphnia magna. Front. Ecol. Evol. 6 https://doi.org/10.3389/fevo.2018.00089.
Merzendorfer, H., Zimoch, L., 2003. Chitin metabolism in insects: structure, function and regulation of chitin synthases and chitinases. J. Exp. Biol. 206, 4393–4412. https://doi.org/10.1242/jeb.00709.
Miyakawa, H., Sato, T., Song, Y., Tollefsen, K.E., Iguchi, T., 2018. Ecdysteroid and juvenile hormone biosynthesis, receptors and their signaling in the freshwater microcrustacean Daphnia. J. Steroid Biochem Mol. Biol. 184, 62–68. https://doi.org/10.1016/j.jsbmb.2017.12.006.
Molenaar, M.R., Jeucken, A., Wassenaar, T.A., van de Lest, C.H.A., Brouwers, J.F., Helms, J.B., 2019. LION/web: a web-based ontology enrichment tool for lipidomic data analysis. Gigascience. 8. https://10.1093/gigascience/giz061.
Mu, X., LeBlanc, G.A., 2002. Developmental toxicity of testosterone in the crustacean Daphnia magna involves anti-ecdysteroidal activity. Gen. Comp. Endocrinol. 129, 127–133. https://doi.org/10.1016/s0016-6480(02)00518-x.
OECD, 2004. Test No. 202: Daphnia sp. Acute Immobilisation Test. OECD Publishing, Paris.
OECD, 2012. Test No. 211: Daphnia magna Reproduction Test. OECD Publishing, Paris.
Ojoghoro, J.O., Scrimshaw, M.D., Sumpter, J.P., 2021. Steroid hormones in the aquatic environment. Sci. Total Environ. 792, 148306 https://doi.org/10.1016/j.scitotenv.2021.148306.
Oropesa, A.L., Floro, A.M., Palma, P., 2016. Assessment of the effects of the carbamazepine on the endogenous endocrine system of Daphnia magna. Environ. Sci. Pollut. Res. Int. 23, 17311–17321. https://doi.org/10.1007/s11356-016-6907-7.
Oropesa, A.L., Novais, S.C., Lemos, M.F., Espejo, A., Gravato, C., Beltrán, F., 2017. Oxidative stress responses of Daphnia magna exposed to effluents spiked with emerging contaminants under ozonation and advanced oxidation processes. Environ. Sci. Pollut. Res. Int. 24, 1735–1747. https://doi.org/10.1007/s11356-016-7881-9.
Pang, Z., Zhou, G., Ewald, J., Chang, L., Hacariz, O., Basu, N., Xia, J., 2022. Using MetaboAnalyst 5.0 for LC-HRMS spectra processing, multi-omics integration and

covariate adjustment of global metabolomics data. Nat. Protoc. 17, 1735–1761. https://doi.org/10.1038/s41596-022-00710-w.
Poynton, H.C., Loguinov, A.V., Varshavsky, J.R., Chan, S., Perkins, E.J., Vulpe, C.D., 2008. Gene Expression Profiling in Daphnia magna Part I: Concentration-Dependent Profiles Provide Support for the No Observed Transcriptional Effect Level. Environ. Sci. Technol. 42, 6250–6256. https://doi.org/10.1021/es8010783.
Rewitz, K.F., Gilbert, L.I., 2008. Daphnia Halloween genes that encode cytochrome P450s mediating the synthesis of the arthropod molting hormone: evolutionary implications. BMC Evol. Biol. 8, 60. https://doi.org/10.1186/1471-2148-8-60.
Richmond, E.K., Rosi, E.J., Walters, D.M., Fick, J., Hamilton, S.K., Brodin, T., Sundelin, A., Grace, M.R., 2018. A diverse suite of pharmaceuticals contaminates stream and riparian food webs. Nat. Commun. 9, 4491. https://doi.org/10.1038/s41467-018-06822-w.
Salisbury, B.H., Tadi, P., 5-Alpha-Reductase Inhibitors. 5-Alpha-Reductase Inhibitors. StatPearls Publishing LLC:, Treasure Island (FL), 2023.
Schenkel, L.C., Bakovic, M., 2014. Formation and regulation of mitochondrial membranes. Int. J. Cell Biol. 2014, 709828 https://doi.org/10.1155/2014/709828.
Schmittgen, T.D., Livak, K.J., 2008. Analyzing real-time PCR data by the comparative C (T) method. Nat. Protoc. 3, 1101–1108. https://doi.org/10.1038/nprot.2008.73.
Schneider, C.A., Rasband, W.S., Eliceiri, K.W., 2012. NIH Image to ImageJ: 25 years of image analysis. Nat. Methods 9, 671–675. https://doi.org/10.1038/nmeth.2089.
Sengupta, N., Gerard, P.D., Baldwin, W.S., 2016. Perturbations in polar lipids, starvation survival and reproduction following exposure to unsaturated fatty acids or environmental toxicants in Daphnia magna. Chemosphere 144, 2302–2311. https://doi.org/10.1016/j.chemosphere.2015.11.015.
Sengupta, N., Reardon, D.C., Gerard, P.D., Baldwin, W.S., 2017. Exchange of polar lipids from adults to neonates in Daphnia magna: Perturbations in sphingomyelin allocation by dietary lipids and environmental toxicants. PLoS One 12, e0178131. https://doi.org/10.1371/journal.pone.0178131.
Seyoum, A., Pradhan, A., Jass, J., Olsson, P.E., 2020. Perfluorinated alkyl substances impede growth, reproduction, lipid metabolism and lifespan in Daphnia magna. Sci. Total Environ. 737, 139682 https://doi.org/10.1016/j.scitotenv.2020.139682.
Smith, C.A., O'Maille, G., Want, E.J., Qin, C., Trauger, S.A., Brandon, T.R., Custodio, D. E., Abagyan, R., Siuzdak, G., 2005. METLIN: a metabolite mass spectral database. Ther. Drug Monit. 27, 747–751. https://doi.org/10.1097/01.ftd.0000179845.53213.39.
Song, Y., Rundberget, J.T., Evenseth, L.M., Xie, L., Gomes, T., Høgåsen, T., Iguchi, T., Tollefsen, K.E., 2016. Whole-Organism Transcriptomic Analysis Provides Mechanistic Insight into the Acute Toxicity of Emamectin Benzoate in Daphnia magna. Environ. Sci. Technol. 50, 11994–12003. https://doi.org/10.1021/acs.est.6b03456.
Song, Y., Villeneuve, D.L., Toyota, K., Iguchi, T., Tollefsen, K.E., 2017. Ecdysone Receptor Agonism Leading to Lethal Molting Disruption in Arthropods: Review and Adverse Outcome Pathway Development. Environ. Sci. Technol. 51, 4142–4157. https://doi.org/10.1021/acs.est.7b00480.
Sostare, J., Di Guida, R., Kirwan, J., Chalal, K., Palmer, E., Dunn, W.B., Viant, M.R., 2018. Comparison of modified Matyash method to conventional solvent systems for polar metabolite and lipid extractions. Anal. Chim. Acta 1037, 301–315 https://10.1016/j.aca.2018.03.019.
Sumiya, E., Ogino, Y., Miyakawa, H., Hiruta, C., Toyota, K., Miyagawa, S., Iguchi, T., 2014. Roles of ecdysteroids for progression of reproductive cycle in the fresh water crustacean Daphnia magna. Front. Zool. 11, 60. https://doi.org/10.1186/s12983-014-0060-2.
Swapna Singh, R.D., Finasteride Market Size, Share, Competitive Landscape and Trend Analysis Report by Application (Benign Prostatic Hyperplasia (BPH), Male pattern baldness), by Type (Branded, Generic), by Distribution Channel (Hospital Pharmacies, Online Providers, Drug Stores and Retail Pharmacies): Global Opportunity Analysis and Industry Forecast, 2021-2031. Finasteride Market Size, Share, Competitive Landscape and Trend Analysis Report by Application (Benign Prostatic Hyperplasia (BPH), Male pattern baldness), by Type (Branded, Generic), by Distribution Channel (Hospital Pharmacies, Online Providers, Drug Stores and Retail Pharmacies): Global Opportunity Analysis and Industry Forecast, 2021-2031, 2023.
Tkaczyk, A., Bownik, A., Dudka, J., Kowal, K., Ślaska, B., 2021. Daphnia magna model in the toxicity assessment of pharmaceuticals: A review. Sci. Total Environ. 763, 143038 https://doi.org/10.1016/j.scitotenv.2020.143038.
Tokishita, S., Kato, Y., Kobayashi, T., Nakamura, S., Ohta, T., Yamagata, H., 2006. Organization and repression by juvenile hormone of a vitellogenin gene cluster in the crustacean, Daphnia magna. Biochem Biophys. Res Commun. 345, 362–370. https://doi.org/10.1016/j.bbrc.2006.04.102.
Touhara, K., Soroker, V., Prestwich, G.D., 1994. Photoaffinity labeling of juvenile hormone epoxide hydrolase and JH-binding proteins during ovarian and egg development in Manduca sexta. Insect Biochem. Mol. Biol. 24, 633–640. https://doi.org/10.1016/0965-1748(94)90100-7.
Toyota, K., Kato, Y., Miyakawa, H., Yatsu, R., Mizutani, T., Ogino, Y., Miyagawa, S., Watanabe, H., Nishide, H., Uchiyama, I., Tatarazako, N., Iguchi, T., 2014. Molecular impact of juvenile hormone agonists on neonatal Daphnia magna. J. Appl. Toxicol. 34, 537–544. https://doi.org/10.1002/jat.2922.
Tsugawa, H., Cajka, T., Kind, T., Ma, Y., Higgins, B., Ikeda, K., Kanazawa, M., VanderGheynst, J., Fiehn, O., Arita, M., 2015. MS-DIAL: data-independent MS/MS deconvolution for comprehensive metabolome analysis. Nat. Methods 12, 523–526. https://doi.org/10.1038/nmeth.3393.
Tsugawa, H., Ikeda, K., Takahashi, M., Satoh, A., Mori, Y., Uchino, H., Okahashi, N., Yamada, Y., Tada, I., Bonini, P., Higashi, Y., Okazaki, Y., Zhou, Z., Zhu, Z.J., Koelmel, J., Cajka, T., Fiehn, O., Saito, K., Arita, M., Arita, M., 2020. A lipidome atlas in MS-DIAL 4. Nat. Biotechnol. 38, 1159–1163. https://doi.org/10.1038/s41587-020-0531-2.
Urbatzka, R., Watermann, B., Lutz, I., Kloas, W., 2009. Exposure of Xenopus laevis tadpoles to finasteride, an inhibitor of 5-alpha reductase activity, impairs spermatogenesis and alters hypophyseal feedback mechanisms. J. Mol. Endocrinol. 43, 209–219. https://doi.org/10.1677/JME-09-0058.
Vance, D.E., 2013. Physiological roles of phosphatidylethanolamine N-methyltransferase. Biochim Biophys. Acta 1831, 626–632. https://doi.org/10.1016/j.bbalip.2012.07.017.
Vieno, N., Hallgren, P., Wallberg, P., Pyhälä, M., Zandaryaa, S., 2017. Emerging Pollutants in Water Series. The United Nations Educational, Scientific and Cultural Organization (UNESCO) and HELCOM, Paris.
Wishart, D.S., Jewison, T., Guo, A.C., Wilson, M., Knox, C., Liu, Y., Djoumbou, Y., Mandal, R., Aziat, F., Dong, E., Bouatra, S., Sinelnikov, I., Arndt, D., Xia, J., Liu, P., Yallou, F., Bjorndahl, T., Perez-Pineiro, R., Eisner, R., Allen, F., Neveu, V., Greiner, R., Scalbert, A., 2013. HMDB 3.0–The Human Metabolome Database in 2013. Nucleic Acids Res 41, D801–D807. https://doi.org/10.1093/nar/gks1065.
Yin, J., Long, Y., Xiao, W., Liu, D., Tian, Q., Li, Y., Liu, C., Chen, L., Pan, Y., 2023. Ecotoxicology of microplastics in Daphnia: A review focusing on microplastic properties and multiscale attributes of Daphnia. Ecotoxicol. Environ. Saf. 249, 114433 https://doi.org/10.1016/j.ecoenv.2022.114433.
Zhang, Z., Xu, J., Sheng, Z., Sui, Y., Palli, S.R., 2011. Steroid receptor co-activator is required for juvenile hormone signal transduction through a bHLH-PAS transcription factor, methoprene tolerant. J. Biol. Chem. 286, 8437–8447. https://doi.org/10.1074/jbc.M110.191684.